



University
of Glasgow

Ahmad, Imran (2011) *The role of Wnt signalling in urothelial cell carcinoma*. PhD thesis.

<http://theses.gla.ac.uk/2352/>

Copyright and moral rights for this thesis are retained by the Author

A copy can be downloaded for personal non-commercial research or study, without prior permission or charge

This thesis cannot be reproduced or quoted extensively from without first obtaining permission in writing from the Author

The content must not be changed in any way or sold commercially in any format or medium without the formal permission of the Author

When referring to this work, full bibliographic details including the author, title, awarding institution and date of the thesis must be given

The Role of Wnt signalling in Urothelial Cell Carcinoma

Imran Ahmad

PhD

**Beatson Institute for Cancer Research
Glasgow University Faculty of Medicine
Graduate School**

2011

Table of Contents

Table of Contents of Figures and Tables	6
Declaration	9
Acknowledgements	10
Abbreviations	11
Abstract	15
Chapter 1: Introduction	18
1.1. Urothelial Cell Carcinoma Epidemiology	19
1.2 Pathophysiology of the Urothelium	22
1.3. Classification of Urothelial Cell Carcinoma	23
1.4. Divergent Molecular Pathways of Urothelial Cell Carcinoma	27
1.5. Risk Factors for Urothelial Cell Carcinoma	30
1.5.1. Tobacco Smoking	30
1.5.2. Occupational Exposure to Chemicals	30
1.5.3. External beam radiation therapy	31
1.5.4. Dietary factors	31
1.5.5. Chronic urinary tract infection	32
1.5.6. Gender	32
1.6. Murine Models of Urothelial Cell Carcinoma	33
1.6.1. Chemically induced carcinogenesis	33
1.6.2. Orthotopic Models	34
1.7. Transgenic Models	37
1.7.1. Ras Pathway	40
1.7.2. Receptor Tyrosine Kinases	42
1.7.3. PTEN-PI3K-pAKT	47
1.7.4. p53	49
1.7.5. p21 ^{WAF/CIP1}	52
1.7.6. Retinoblastoma (RB)	53
1.8 The Wnt signalling pathway	56
1.8.1. The Canonical Wnt Signalling Pathway	58
1.8.2. The Role of Wnt Signalling in Cancer	61
1.8.3. The Role of Wnt Signalling in Human UCC	64
1.9. KEGG Pathway of UCC	66

1.10. Research in Progress and Outstanding Research Questions	67
1.11. Thesis Aims	69
Chapter 2: Material and Methods	70
2.1. Statement of Contribution.....	71
2.2. Generation of Mice colonies.....	72
2.2.1. Mouse experiments for Chapter 3 (β -Catenin activation synergises with PTEN loss to cause bladder cancer formation).....	75
2.2.2. Mouse experiments for Chapter 4 (β -Catenin activation synergises with Ras activation to cause bladder cancer formation)	76
2.2.3. Mouse experiments for Chapter 5 (The FGFR3 mutation cooperates with K-Ras and β -catenin mutations to promote skin and lung but not bladder tumour formation) ..	76
2.3. Tissue isolation	77
2.4. Genotyping of mice.....	78
2.4.1. DNA Extraction from tails.....	78
2.4.2. Genotyping of Mice via PCR.....	78
2.4.3. Summary of PCR reactions.....	90
2.5. Rapamycin Treatment.....	92
2.6. Assaying urothelial lesions <i>in vivo</i>	92
2.6.1. Assaying proliferation <i>in vivo</i>	93
2.7. Immunohistochemistry	94
2.7.1. Immunohistochemistry on frozen sections:	94
2.7.2. Immunohistochemistry on paraffin sections:.....	95
2.7.3. Immunohistochemistry for p21:.....	96
2.7.4. Immunohistochemistry for p16:.....	97
2.7.5. Immunohistochemistry for p19:.....	97
2.7.6: β -Catenin Immunohistochemistry:	97
2.7.7. BrdU Immunohistochemistry:	98
2.7.8. p53 Immunohistochemistry:	98
2.7.9. MCM2 Immunohistochemistry:.....	99
2.7.10. Ki67 Immunohistochemistry:	99
2.7.11. PTEN Immunohistochemistry	100
2.7.12. p-AKT (Ser473) Immunohistochemistry	100
2.7.13. p-mTOR (Ser2448) Immunohistochemistry	101
2.7.14. pERK1/2 Immunohistochemistry	101
2.7.15. pMEK1/2 Immunohistochemistry	101

2.7.16. p-S6 Kinase Immunohistochemistry	101
2.7.17. Active-Rac1 Immunohistochemistry	102
2.7.18. GFP Immunohistochemistry	102
2.7.19. Sprouty2 Immunohistochemistry	102
2.7.20. FGFR3 Immunohistochemistry	103
2.8. Imaging	104
2.8.1 Microscopy	104
2.8.2. Ultrasound Scanning.....	104
2.9. Human Tissue Microarray (TMA).....	105
Chapter 3: β -Catenin activation synergises with PTEN loss to cause bladder cancer formation	106
3.1. Introduction.....	107
3.2. Results.....	109
3.2.1 β -catenin overexpression leads to benign hyperproliferation of the urothelium ..	109
3.2.2. The PTEN tumour suppressor pathway is activated in the bladder lesions.....	116
3.2.3. PTEN upregulation acts to block β -catenin driven urothelial proliferation.....	120
3.2.4. PTEN loss cooperates with β -catenin activation to drive UCC formation	127
3.2.5. <i>UroII CRE⁺ β-catenin^{exon3/exon3} Pten^{fl/fl}</i> UCCs are mTOR dependent.....	136
3.2.6. Human UCC demonstrate correlation between Wnt activation and PTEN loss..	140
3.3. Discussion	143
Chapter 4: Ras mutation cooperates with β -catenin activation to drive bladder tumorigenesis	145
4.1. Introduction.....	146
4.2. Results.....	148
4.2.1. Ras activation alone does not lead to UCC in the mouse	148
4.2.2. Ras activation cooperates with β -catenin to drive UCC formation	152
4.2.3. p21 upregulation blocks β -catenin driven UCC.....	158
4.2.4. Human UCC demonstrate correlation between Wnt and Ras activation.....	161
4.3. Discussion	164
Chapter 5: The FGFR3 mutation cooperates with K-Ras and β -Catenin mutations to promote skin and lung but not bladder tumour formation	166
5.1. Introduction.....	167
5.2. Results.....	169
5.2.1. Targeting of the <i>Fgfr3</i> mutations in the bladder	169
5.2.2. <i>Fgfr3</i> mutation alone does not drive tumourigenesis of the bladder	172

5.2.3. Formation of lung tumors in the UroIIICre ⁺ Fgfr3 ^{+/K644E} β-catenin ^{exon3/+} mice	179
5.2.4. Skin Papilloma formation in UroIIICre ⁺ Fgfr3 ^{+/K644E} K-Ras ^{G12D/+} mice	184
5.3. Discussion	191
Chapter 6: Summary and Concluding Remarks.....	195
References.....	200
Appendix 1: Funding Sources.....	218
Appendix 2: Home Office Licenses.....	224
Appendix 3: Publications.....	228

Table of Contents of Figures and Tables

Figure 1.1: Numbers of new cases and age-specific incidence rates, by sex, bladder cancer, UK 2006.....	20
Figure 1.2: Age standardised incidence rates, bladder cancer, by sex, UK, 1975-2006.....	21
Table 1.1: WHO grading in 1973 and in 2004.....	24
Table 1.2: 2002 Tumour, Nodes, Metastases Classification (2002).....	25
Figure 1.3: T Staging of bladder cancer.....	26
Figure 1.4: Important genetic and epigenetic defects that characterise the divergent pathways of UCC.....	28
Figure 1.5: Mutation profile of human UCC.....	29
Figure 1.6: The Cre-LoxP recombination system in transgenic mice.....	39
Figure 1.7: Signalling cascades involved in UCC during FGFR3 and HRAS activation.....	44
Figure 1.8: Collaborative effects between pRb family proteins and p53 in invasive UCC.....	55
Figure 1.9: Canonical Wnt Signaling.....	60
Figure 1.10: KEGG Pathway of UCC.....	66
Figure 1.11: Outline of research.....	69
Table 2.1: Description of transgenes used in this thesis.....	74
Figure 2.1: Apc ^{fl} PCR.....	79
Figure 2.2: β -catenin ^{exon3} PCR.....	80
Figure 2.3: Cre PCR.....	81
Figure 2.4: Fgfr3 K644 PCR.....	82
Figure 2.5: GSK3 α PCR.....	83
Figure 2.6: GSK3 β PCR.....	84
Figure 2.7: Rabbit H-Ras ^{Q61L} PCR.....	85
Figure 2.8: K-Ras G12D PCR.....	86
Figure 2.9: Pten PCR.....	87
Figure 2.10: p21 PCR.....	88
Figure 2.11: Z/EGFP PCR.....	89
Figure 3.1: GFP Expression of <i>UroIIICRE</i> ⁺ <i>Z/EGFP</i> mice.....	110
Figure 3.2: <i>UroIIICRE</i> ⁺ β -catenin ^{exon3/exon3} urothelium demonstrates upregulation of nuclear β -catenin.....	113
Figure 3.3: <i>UroIIICRE</i> ⁺ β -catenin ^{exon3/exon3} urothelium demonstrates upregulation of Wnt target genes and proliferative markers.....	114
Figure 3.4: Box plot of lesion numbers in the wildtype, <i>UroIIICRE</i> ⁺ β -catenin ^{exon3/+} and <i>UroIIICRE</i> ⁺ β -catenin ^{exon3/exon3}	115

Figure 3.5: <i>UroIIICRE</i> ⁺ <i>β-catenin</i> ^{exon3/exon3} urothelium demonstrates upregulation of PTEN, p53, p21 and p19ARF.....	119
Figure 3.6: GFP expression in <i>AhCreER</i> ^T <i>Z/EGFP</i> mice 7 days post induction	121
Figure 3.7: Histology of <i>AhCreER</i> ^T <i>Apc</i> ^{fl/fl} 7 days post induction	122
Figure 3.8: Histology of <i>AhCreER</i> ^T <i>GSK3αβ</i> ^{fl/fl} mice 7 days post induction	123
Figure 3.9: Histology of <i>AhCreER</i> ^T <i>Apc</i> ^{fl/fl} <i>Pten</i> ^{fl/fl}	125
Figure 3.10: Box plot of average number of BrdU positive cells per lesion in both <i>AhCreER</i> ^T <i>Apc</i> ^{fl/fl} and <i>AhCreER</i> ^T <i>Apc</i> ^{fl/fl} <i>Pten</i> ^{fl/fl} mice.	126
Figure 3.11: Histology of <i>UroIIICRE</i> ⁺ <i>Pten</i> ^{fl/fl} mice.....	128
Figure 3.12 Tumour burden of <i>UroIIICRE</i> ⁺ <i>β-catenin</i> ^{exon3/exon3} <i>Pten</i> ^{fl/fl} mice	130
Figure 3.13 Survival of <i>UroIIICRE</i> ⁺ <i>β-catenin</i> ^{exon3/exon3} <i>Pten</i> ^{fl/fl} mice	133
Figure 3.14 Photograph of <i>UroIIICRE</i> ⁺ <i>β-catenin</i> ^{exon3/exon3} <i>Pten</i> ^{fl/fl} bladder tumour	134
Figure 3.15: Histology of a <i>UroIIICRE</i> ⁺ <i>β-catenin</i> ^{exon3/exon3} <i>Pten</i> ^{fl/fl} mice	135
Figure 3.16: <i>UroIIICRE</i> ⁺ <i>β-catenin</i> ^{exon3/exon3} <i>Pten</i> ^{fl/fl} mice treated with Rapamycin	137
Figure 3.17: <i>UroIIICRE</i> ⁺ <i>β-catenin</i> ^{exon3/exon3} <i>Pten</i> ^{fl/fl} mice treated with Rapamycin	138
Figure 3.18: Proliferation of tumours in Rapamycin treated mice versus vehicle control	139
Figure 3.19: Human Bladder UCC TMA	141
Figure 3.20: Correlation between <i>β-catenin</i> and PTEN/pAKT in Human Bladder UCC TMA	142
Figure 4.1: Histology from 12-month-old Wildtype, <i>UroIIICRE</i> + <i>K-Ras</i> ^{G12D/+} and <i>H-Ras</i> ^{Q61L} mice.....	150
Figure 4.2: Histology from 12 month old <i>UroIIICRE</i> ⁺ <i>β-catenin</i> ^{exon3/exon3} mice.	151
Figure 4.3: Kaplan Meier curves of tumour free survival of respective mutant cohorts	153
Figure 4.4: Histology of <i>UroIIICRE</i> + <i>β-catenin</i> ^{exon3/exon3K} - <i>RasG12D/+</i> and <i>UroIIICRE</i> + <i>β-catenin</i> ^{exon3/exon3} <i>H-Ras</i> ^{Q61L} mice:.....	155
Figure 4.5: Boxplot comparing Ki67 positivity between <i>UroIIICRE</i> + <i>β-catenin</i> ^{exon3/exon3} , <i>UroIIICRE</i> + <i>β-catenin</i> ^{exon3/exon3} <i>H-Ras</i> ^{Q61L} and <i>UroIIICRE</i> + <i>β-catenin</i> ^{exon3/exon3} <i>K-Ras</i> mice..	156
Figure 4.6: Boxplot comparing p21 positivity between <i>H-Ras</i> ^{Q61L} and <i>UroIIICRE</i> + <i>β-catenin</i> ^{exon3/exon3} <i>H-Ras</i> ^{Q61L} mice.....	157
Figure 4.7: Kaplan Meier curves of tumour free survival of <i>UroIIICRE</i> ⁺ <i>p21</i> ^{-/-} (U <i>p21</i>) and <i>UroIIICRE</i> ⁺ <i>β-catenin</i> ^{exon3/exon3} <i>p21</i> ^{-/-} (UB <i>p21</i>) cohorts.....	159
Figure 4.8: Histology of <i>UroIIICRE</i> ⁺ <i>β-catenin</i> ^{exon3/exon3} <i>p21</i> ^{-/-} mouse.	160
Figure 4.9: Human Bladder UCC TMA	162
Figure 4.10: Correlation between <i>β-catenin</i> and pERK1/2 in Human Bladder UCC TMA ..	163
Figure 5.1 Cre recombination and expression of <i>Fgfr3</i> in the urothelium.....	170
Figure 5.2 FGFR3 positive cells in 12 month old <i>Wildtype</i> , <i>UroIIICRE</i> + <i>Fgfr3</i> ^{+K644E} and <i>UroIIICRE</i> + <i>Fgfr3</i> ^{+K644M}	171

Figure 5.3 Bladder H&Es from 12 month old Wildtype, <i>UroII CRE⁺ Fgfr3^{+/K644E}</i> and <i>UroII CRE⁺ Fgfr3^{+/K644M}</i> mice.....	173
Figure 5.4 Fgfr3 mutation is not the sole driver of tumourigenesis in the bladder.....	174
Figure 5.5 Further images showing upregulation of pERK1/2 and Sprouty2:	175
Figure 5.6 Role of the AKT-mTOR pathway in mutant models	176
Figure 5.7 Fgfr3 mutation in combination does not lead to tumourigenesis in the bladder ..	178
Figure 5.8 Kaplan-Meier curve of <i>UroII CRE⁺ Fgfr3^{+/K644E} β-catenin^{exon3/+}</i> (Fgfr3 β-Cat) mice	181
Figure 5.9 Formation of lung tumor in the <i>UroII CRE⁺ Fgfr3^{+/K644E} β-catenin^{exon3/+}</i> model ..	182
Figure 5.10 Box plots quantifying immunostaining of pERK1/2, pAKT(Ser473) and Sprouty2 in lung tumors of <i>UroII CRE⁺ β-catenin^{exon3/+} K-Ras^{G12D/+}</i> and <i>UroII CRE⁺ Fgfr3^{+/K644E} β-catenin^{exon3/+}</i> mice	183
Figure 5.11 Kaplan-Meier curve of <i>UroII CRE⁺ Fgfr3^{+/K644E} K-Ras^{G12D/+}</i> (Fgfr3 K-Ras) mice	186
Figure 5.12 Formation of papilloma lesions in the <i>UroII CRE⁺ Fgfr3^{+/K644E} K-Ras^{G12D/+}</i> model	187
Figure 5.13 Formation of papilloma lesions in the <i>UroII CRE⁺ Fgfr3^{+/K644E} K-Ras^{G12D/+}</i> model	189
Figure 5.14 Box plots quantifying immunostaining of pERK1/2 and pAKT(Ser473) in papillomas of <i>UroII CRE⁺ Fgfr3^{+/K644E} K-Ras^{G12D/+}</i> and <i>UroII CRE⁺ K-Ras^{G12D/+} Pten^{fl/+}</i> mice	190
Figure 5.15 Current model of signaling pathways that could contribute to tumour formation in the presence of Fgfr3 mutations in specific organ systems	192

Declaration

I hereby declare that all of the work presented in this thesis is the result of my own independent investigation unless otherwise stated.

No part of this work has been submitted for consideration as part of any other degree or award.

Imran Ahmad

2010

Acknowledgements

During the course of my PhD, I have been lucky enough to be afforded the opportunity to work with some great colleagues, many of whom I would count now as friends. The Beatson institute has been a fabulous place to carry out my PhD.

I would like to thank all members of R8 & 18, both past and present, who have been such a great group of people to work with, and who have truly made this PhD experience enjoyable. In particular I'd like to thank Lukram Babloo Singh (LBS) who double scored my immunohistochemical samples.

I would also like to thank BICR services, biological services unit, and Colin Nixon and his histology department. I am also indebted to "Think Pink" charity for the purchase of the Aperio slide scanner and the Slidepath software.

Of course I will forever be indebted to Hing and Owen, whose patience, guidance and support throughout my PhD has been invaluable.

Many thanks to my family at home for their constant encouragement and loving support throughout the past 3 (31!) years.

Cancer Research UK and the Medical Research Council Fellowships funded this PhD

I Ahmad

January 2011

Abbreviations

APC	Adenomatous Polyposis Coli
<i>APC</i>	<i>Adenomatous Polyposis Coli</i> (human gene)
APC	<i>Adenomatous Polyposis Coli</i> (human protein)
<i>Apc</i>	<i>Adenomatous Polyposis Coli</i> (mouse gene)
Apc	<i>Adenomatous Polyposis Coli</i> (mouse protein)
<i>Apc</i> ^{+/+}	Mouse wild type for <i>Apc</i>
<i>Apc</i> ^{fl/+}	Mouse heterozygous for <i>Apc</i>
<i>Apc</i> ^{fl/fl}	Mouse homozygous for <i>Apc</i>
<i>β-catenin</i> ^{+/+}	Mouse wild type for <i>β-catenin</i>
<i>β-catenin</i> ^{exon3/+}	Mouse heterozygous for <i>β-catenin</i> exon3
<i>β-catenin</i> ^{exon3/exon3}	Mouse homozygous for <i>β-catenin</i> exon3
BBN	<i>N</i> -butyl- <i>N</i> -(4-hydroxybutyl) nitrosamine
BrdU	Bromodeoxyuridine
BSA	Bovine serum albumin
CIS	Carcinoma in situ
COX2	Cyclooxygenase 2
CP	Cytoplasmic
Cre	Cre recombinase
<i>Cre</i>	Cre (mouse transgene)
dH2O	Distilled water
DNA	Deoxyribonucleic acid
E-Cad	E-Cadherin
EDTA	Ethylenediaminetetraacetic acid
EBRT	External Beam Radiotherapy
EC	Extracellular
EGFr	Epidermal Growth Factor Receptor
ERK	Extracellular regulated kinase
ES cells	Embryonic Stem Cells
FANFT	<i>N</i> -[4-(5-nitro-2-furyl)-2-thiazolyl] formamide
FGF	Fibroblast growth factor
<i>FGFR3</i>	Fibroblast growth factor receptor 3 (human gene)

FGFR3	Fibroblast growth factor receptor 3 (human protein)
Fgfr3	Fibroblast growth factor receptor 3 (mouse protein)
<i>Fgfr3</i>	Fibroblast growth factor receptor 3 (mouse gene)
gDNA	Genomic DNA
GFP	Green fluorescence protein
GRB2	Growth factor receptor-bound protein 2
GSK-3α	Glycogen Synthetase kinase 3α
GSK-3β	Glycogen Synthetase kinase 3β
H2O2	hydrogen peroxide
H&E	Haematoxylin and Eosin
HRP	Horseradish peroxidase
IHC	Immunohistochemistry
I.P.	Intra-peritoneal
ISUP	International Society of Urological Pathology
JAK	Janus protein tyrosine kinase
KEGG	Kyoto Encyclopaedia of Genes and Genome
LOH	Loss of Heterozygosity
MMP	Matrix Metalloproteinases
MNU	<i>N</i>-Methyl-<i>N</i>-nitosurea
mRNA	messenger RNA
mTOR	mammalian Target of Rapamycin
NaN₃	Sodium Azide
N-Cad	N-Cadherin
<i>p21^{+/+}</i>	mouse wild type for <i>p21</i>
<i>p21^{+/-}</i>	mouse heterozygous for <i>p21</i>
<i>p21^{-/-}</i>	mouse homozygous/null for <i>p21</i>
PAH	polycyclic aromatic hydrocarbon
PBS	Phosphate Buffered Saline
PCR	Polymerase Chain Reaction
PI3K	Phosphatidylinositol 3-kinase
PTEN	Phosphatase and Tensin Homologue on Chromosome 10 (human protein)

<i>PTEN</i>	Phosphatase and Tensin Homologue on Chromosome 10 (human gene)
Pten	Phosphatase and Tensin Homologue on Chromosome 10 (mouse protein)
<i>Pten</i>	Phosphatase and Tensin Homologue on Chromosome 10 (mouse gene)
<i>Pten</i>^{+/+}	Mouse wild type for <i>Pten</i>
<i>Pten</i>^{fl/+}	Mouse heterozygous for <i>Pten</i>
<i>Pten</i>^{fl/fl}	Mouse homozygous/null for <i>Pten</i>
RB	Retinoblastoma
RNA	Ribonucleic Acid
RTK	Receptor Tyrosine Kinase
Saβgal	Senescence associated β-galactosidase
SB	Sleeping Beauty
SCC	Squamous Cell Carcinoma
SFRP	Secreted Frizzled Related Protein
SHC	SRC-homology-2-domain-containing
SOS	Son of sevenless
SPRY	Sprouty
SV40	Simian virus 40
TBS	Tris Buffered Saline
TBST	Tris Buffered Saline+ Tween
TCC	Transitional Cell Carcinoma
TM	Transmembrane
TMA	Tissue Microarray
TNM	Tumour, Node, Metastasis
Tris	Tris(hydroxymethyl)aminomethane
TSP1	Thrombospondin 1
UCC	Urothelial Cell Carcinoma
UPII	Uroplakin II
<i>UroII</i>Cre⁺	Uroplakin II Cre
US	Ultrasound
VEGF	Vascular Endothelial Growth Factor

WHO

World Health Organisation

WT

Wild type

X-gal

5-Bromo-4-Chloro-3-indolyl- β -D-Galactopyranoside

Abstract

Urothelial cell carcinoma (UCC) of the bladder is a common malignancy worldwide, causing considerable morbidity and mortality. It is unique among epithelial carcinomas in respect of the fact that it has divergent pathways of tumourigenesis. Low-grade papillary tumours which frequently recur, but seldom convert to muscle invasive tumours harbour mutations that activate the MAPK pathways, as a consequence of oncogenic mutations in FGFR3 or HRAS. However, in contrast, the high-grade muscle invasive tumours that readily metastasise have been shown to have defects in the p53 and retinoblastoma (RB) protein pathways

Transgenic mice have allowed us to analyse the molecular basis of initiation, invasion and progression of many human cancers. These mouse models increase our understanding of the disease process as well as providing targets for developing novel therapeutic approaches. In UCC there has been a paucity of models that readily mimic the human disease.

Although deregulation of the Wnt signalling pathway has been implicated in urothelial cell carcinoma (UCC), the functional significance is unknown. Recent studies have demonstrated the importance of this pathway in UCC progression, thus I endeavoured to test its importance both as a “driver” mutation, as well as a “progressor” mutation in more established UCC mutations. Thus I targeted expression of an activated form of β -catenin to the urothelium of transgenic mice using Cre-Lox technology. Expression of this activated form of β -catenin led to the formation of localised hyperproliferative lesions by 3 months, which did not progress to malignancy. Furthermore expression in *UroIIICRE+* β -catenin^{exon3/+} mice showed marked upregulation of the PTEN tumour suppressor protein that appears to be a direct consequence of activating Wnt signalling in the bladder. I therefore combined PTEN deficiency with β -catenin activation, which resulted in rapid formation of papillary UCC by 6 months. These tumours had increased pAKT signalling and were dependent on mTOR. Importantly in human

UCC, there was a significant correlation between high levels of β -catenin and pAKT (and low levels of PTEN) ($p < 0.01$, $n = 80$). Taken together, these data suggest that deregulated Wnt signalling plays a role in driving UCC, and human UCC that have high levels of Wnt and PI3 kinase signalling may be responsive to mTOR inhibition.

I next expressed oncogenic K-Ras or H-Ras in the urothelium alone, and in urothelial cells expressing an activated β -catenin. Although Ras activation was not sufficient to drive tumourigenesis, Ras activation combined with β -catenin activation in *UroIICRE*⁺ *β -catenin*^{exon3/exon3} *K-Ras*^{G12D/+} and *UroIICRE*⁺ *β -catenin*^{exon3/exon3} *H-Ras*^{Q61L} mice rapidly developed UCC. These tumours had upregulation of pERK1/2 with minimal levels of pAKT. Importantly in human UCC, there was a significant correlation between high levels of β -catenin and pERK1/2 ($p < 0.01$, $n = 80$). This data further supports the role of deregulated Wnt signalling and its co-operation with Ras in bladder carcinogenesis.

I observed upregulated p21 expression in our *UroIICRE*⁺ *β -catenin*^{exon3/+} urothelial lesions and thus postulated that p21 may be acting as a block to tumourigenesis in the lesion. It was highly relevant to observe tumour formation in the double mutant *UroIICRE*⁺ *β -catenin*^{exon3/exon3} *p21*^{-/-} mice.

FGFR3 gene is frequently mutated in superficial urothelial cell carcinoma (UCC). To test the functional significance of *FGFR3* mutations as a “driver” of UCC, expression of mutated *Fgfr3* was targeted to the murine urothelium using *UroIICRE*⁺ promoter. These *FGFR3* mutations (K644E and K644M) had no effect on bladder homeostasis or tumourigenesis up to 18 months of ages. Even when these mutations were combined with β -Catenin or Ras activating mutations, no urothelial dysplasia/hyperplasia or UCC was observed. This suggests that other alterations are required that can cooperate with *FGFR3* activation to cause UCC. Interestingly, however, due to sporadic ectopic Cre recombinase expression in the lung and

skin of these mice, FGFR3 mutation caused skin papilloma and promoted lung tumorigenesis in cooperation with K-Ras and β -Catenin activation, respectively. This confirmed that the mutant Fgfr3 was functional and that FGFR3 cooperates with other genetic events involving Ras and Wnt pathways to promote tumorigenesis in a context dependent manner and support the hypothesis that activation of FGFR signaling contributes to human cancer.

Chapter 1: Introduction

1. Introduction to Urothelial Cell Carcinoma

1.1. Urothelial Cell Carcinoma Epidemiology

Urothelial cell carcinoma (UCC) is a significant health problem worldwide, with its prevalence continuing to rise. In the U.K. it is the 4th most common cancer in males, with 7306 new cases in 2006. In comparison, there were only 2957 female cases, making it the 11th most common female cancer. Worldwide there is an estimated 356600 new cases diagnosed yearly, and in terms of overall cancer frequency, it is ranked 9th. (Cancer Research UK - <http://info.cancerresearchuk.org/cancerstats/types/bladder/incidence/index.htm>).

It is a relatively rare disease in under 50s, but the rates rise and peak in the oldest age group, where the male to female ratio becomes 3:1 (Figure 1.1).

The highest incidence rates are found in industrially developed countries, particularly in the West, and in areas associated with endemic schistosomiasis such as Africa and the Middle East.

Marked racial differences have been reported for bladder cancer incidence with higher rates in Caucasian populations (e.g. US rates in caucasians are double those for black men) (National Cancer Institute - http://seer.cancer.gov/csr/1975_2003/).

Looking at the bladder cancer incidence rates over time, it is difficult to interpret because of changes in the classification of muscle invasive disease of the bladder. In spite of this difficulty Cancer Research UK have demonstrated that the age-standardised incidence rates per 100,000 population rose throughout the 1970s and 1980s to reach a peak of 32 in men and 9 in women in the early 1990s and since then have fallen by around a third (Figure 1.2). This fall could be attributed to tighter regulation of occupational factors. This trend will most probably continue since the passing of legislation banning cigarette smoking in public place, reducing active and passive smoking rates.

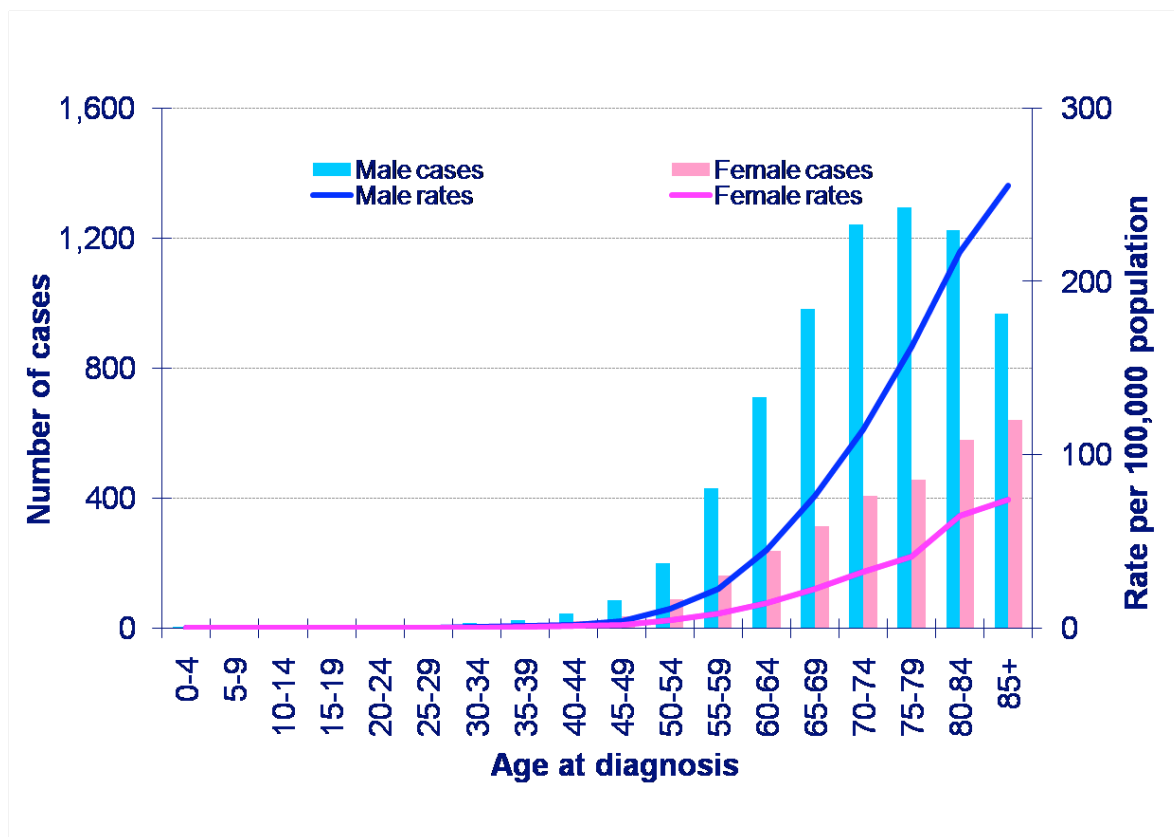


Figure 1.1: Numbers of new cases and age-specific incidence rates, by sex, bladder cancer, UK 2006

(Source Cancer Research UK

<http://info.cancerresearchuk.org/cancerstats/types/bladder/incidence/index.htm>)

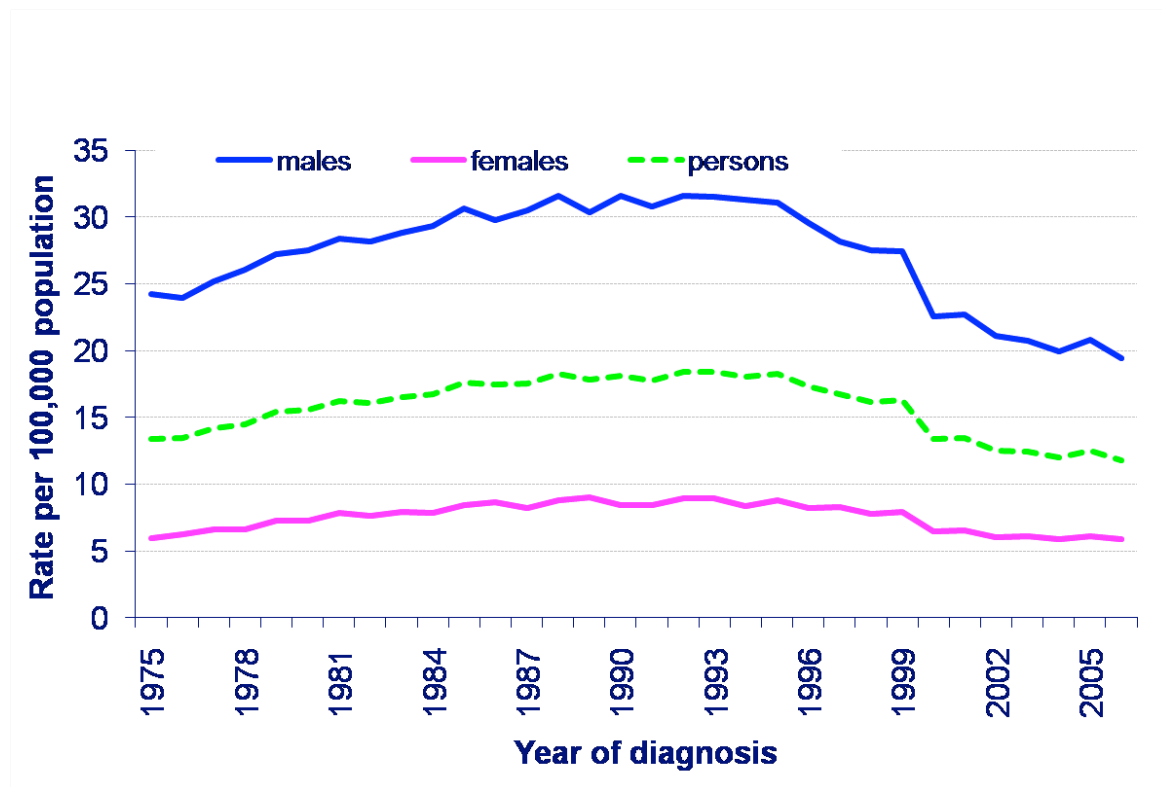


Figure 1.2: Age standardised incidence rates, bladder cancer, by sex, UK, 1975-2006

(Source Cancer Research UK

<http://info.cancerresearchuk.org/cancerstats/types/bladder/incidence/index.htm>)

1.2 Pathophysiology of the Urothelium

Urothelium, from which all UCC arise, is histologically a stratified and polarised epithelium (Khandelwal et al., 2009). It is composed of a single cell type, with differences in layers attributed to degrees of cellular differentiation. It acts as a physiological and mechanical barrier between urine and blood. It acts to protect the underlying tissues from toxic urinary substances, as well as adjusting its surface area during bladder filling (Negrete et al., 1996).

The urothelium is extremely stable, with cells turning over very slowly (turnover rate approximately every 200 days with a tritium-thymidine labelling index of less than 0.01%) (Hicks, 1975, Walker, 1960).

Cells in the basal layer are the smallest in size and least differentiated. This is where the majority of proliferation occurs and where the stem cell niche may reside (Kurzrock et al., 2008). This layer is the only urothelial layer to express appreciable levels of epidermal growth factor (EGF) receptor, but this is protected from the high concentration of EGF in the urine due to the barrier afforded by the superficial urothelial layer (Messing, 1990, Messing, 1992). Similarly, the basal (and presumed stem cells) are well protected from carcinogens, by a differentiated layer of intermediate cells (3-4 layers in humans, single in murine) (Wu et al., 2009).

The superficial urothelial cells facing the bladder lumen, also called umbrella cells, are distinctive large, terminally differentiated, polyhedral and bi-nucleated cells and are thought to be derived from intermediate cells through cell fusion (Koss, 1969). The umbrella cells contribute to form an asymmetrical membrane that lines over 95% of the luminal surface of the urothelium. Within this layer, the four major uroplakins (Ia, Ib, II and IIIa), luminal protein complexes restricted to the urothelium, are expressed (Wu et al., 2009).

1.3. Classification of Urothelial Cell Carcinoma

Clinical and pathological studies have found that development of UCC in humans arise from at least 2 separate mechanisms (Wu, 2005, Koss, 1992). The vast majority of these are transitional cell carcinomas (TCC). About 70% of the incidence is due to papillary, non-invasive tumours (TaT1) (Table 1.1) that despite local excision tend to recur in over 30% of patients but progress to invasive disease in 10-20% of these cases (Knowles, 2001). In 2004, the revised classification of non-invasive urothelial tumours was proposed by the World Health Organization (WHO) and the International Society of Urological Pathology (ISUP) (1998 WHO/ISUP classification) (Eble JN, 2004) (Table 1.1).

Carcinoma *in situ* (CIS) is recognisable as flat, anaplastic epithelium. The urothelium lacks the normal cellular polarity, and cells contain large, irregular hyperchromatic nuclei with prominent nucleoli. CIS may occur either close to or remote from an exophytic lesion or, rarely, it may occur as focal or diffuse lesions in a patient without macroscopic tumours. It has a variable natural history, but many cases progress to invasive disease. In addition, exophytic lesions occurring with CIS are more likely to recur and invade than those without CIS. The frequency of tumour invasion, recurrence, and progression is strongly correlated with tumour grade (Eble JN, 2004).

1973 WHO grading

- Urothelial papilloma
- Grade 1: well differentiated
- Grade 2: moderately differentiated
- Grade 3: poorly differentiated

2004 WHO grading

- Urothelial papilloma
- Papillary urothelial neoplasm of low malignant potential (PUNLMP)
- Low-grade papillary urothelial carcinoma
- High-grade papillary urothelial carcinoma

Table 1.1: WHO grading in 1973 and in 2004

The majority of mortality is associated with patients with non-papillary, muscle invasive TCC (20-30% of all cases). These invasive tumours can penetrate deeply through the muscle wall of the bladder and 50% will relapse with metastases to distant sites despite radical therapy (Williams and Stein, 2004). Treatment fails in 95% of patients with advanced disease, and the 5-year survival rate for metastatic bladder cancer is only 6% (Table 1.2 and Figure 1.3).

T - Primary tumour	
TX	Primary tumour cannot be assessed
T0	No evidence of primary tumour
Ta	Non-invasive papillary carcinoma
Tis	Carcinoma in situ: 'flat tumour'
T1	Tumour invades subepithelial connective tissue
T2	Tumour invades muscle
	T2a Tumour invades superficial muscle (inner half)
	T2b Tumour invades deep muscle (outer half)
T3	Tumour invades perivesical tissue
	T3a Microscopically
	T3b Macroscopically (extravesical mass)
T4	Tumour invades any of the following: prostate, uterus, vagina, pelvic wall, abdominal wall
	T4a Tumour invades prostate, uterus or vagina
	T4b Tumour invades pelvic wall or abdominal wall
N - Lymph nodes	
NX	Regional lymph nodes cannot be assessed
N0	No regional lymph node metastasis
N1	Metastasis in a single lymph node 2 cm or less in greatest dimension
N2	Metastasis in a single lymph node more than 2 cm but not more than 5 cm in greatest dimension, or multiple lymph nodes, none more than 5 cm in greatest dimension
N3	Metastasis in a lymph node more than 5 cm in greatest dimension
M - Distant metastasis	
MX	Distant metastasis cannot be assessed
M0	No distant metastasis
M1	Distant metastasis

Table 1.2: 2002 Tumour, Nodes, Metastases Classification (2002)

The 2002 TNM classification has been approved by the Union Contre le Cancer (UICC)

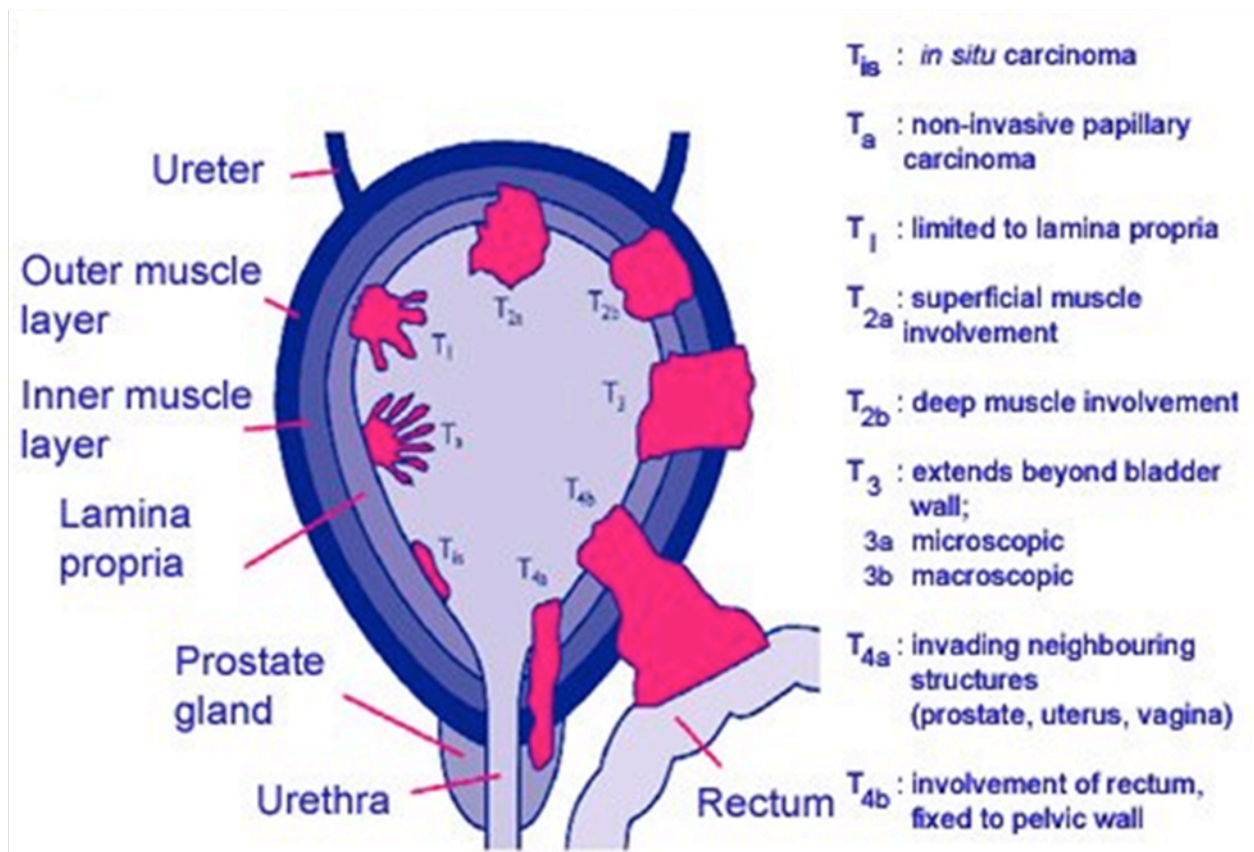


Figure 1.3: T Staging of bladder cancer

(Source Cancer Research UK

<http://info.cancerresearchuk.org/cancerstats/types/bladder/survival/index.htm>)

1.4. Divergent Molecular Pathways of Urothelial Cell Carcinoma

Both clinical and experimental evidence indicate that UCCs arise and progress along two distinctive pathways (Figure 1.4). The low-grade, superficial/papillary UCCs harbour frequent mutations in the *HRAS* gene (30–40%) and fibroblast growth factor receptor 3 (*FGFR3*) gene (~70%), indicating that RTK (Receptor Tyrosine Kinase)–Ras activation has an early and crucial role in this tumorigenesis pathway (Jebar et al., 2005). Deletions in the short arms of chromosomes 8 and 11 (8p– and 11p–) and long arms of chromosomes 13 and 14 (13q– and 14q–) are often associated with the rare cases of progression to the muscle invasive stages of UCC (Wu, 2005).

The high-grade muscle-invasive tumours can either originate from carcinoma *in situ* (CIS) or arise *de novo*. Over 50% of these tumours contain mutations in the tumour suppressors p53 and/or the retinoblastoma protein (RB). Invasion and metastases are promoted by several factors that alter the tumour microenvironment, including the upregulation of N-cadherin (N-Cad) and downregulation of E-cadherin (E-cad), matrix metalloproteinases (MMPs), angiogenic factors (e.g. vascular endothelial growth factor (VEGF)), and antiangiogenic factors (e.g. thrombospondin 1 (TSP1)) and cyclooxygenase 2 (COX2) (Garcia del Muro et al., 2000, Shariat et al., 2001, Popov et al., 2000, Ribeiro-Filho et al., 2002, Zhang et al., 2003, Rieger-Christ et al., 2004, Vihinen and Kahari, 2002, Kanayama, 2001, Izawa et al., 2001, Slaton et al., 2001, Campbell et al., 1998, Grossfeld et al., 1997, Komhoff et al., 2000). Deletion of both arms of chromosome 9 (9p–/9q–) occurs early during urothelial tumorigenesis in both tumour pathways (Chow et al., 2000, Obermann et al., 2003). Further elucidation of the genetic and epigenetic causes of the two distinctive pathways of UCC will have a great impact on the management of this disease condition.

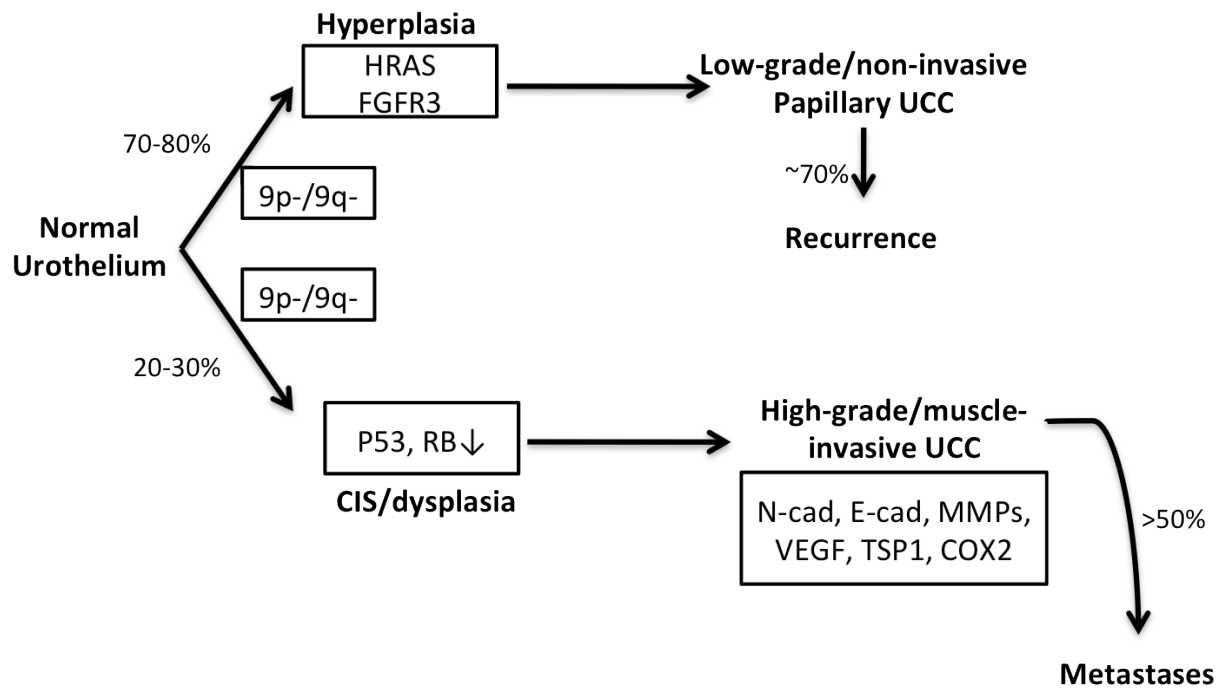
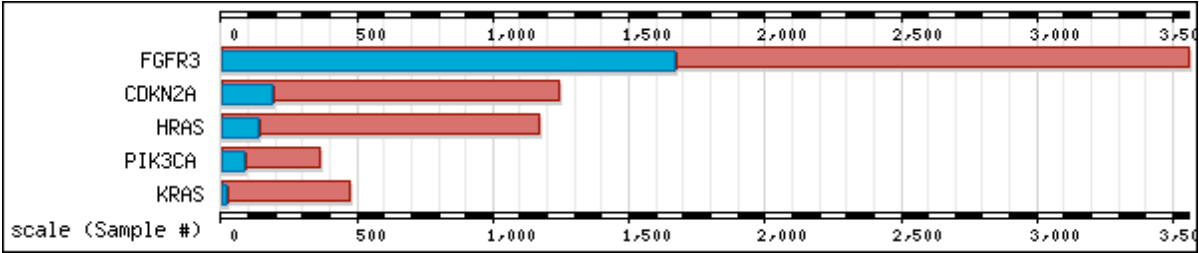


Figure 1.4: Important genetic and epigenetic defects that characterise the divergent pathways of UCC.

Little work has been done on the PTEN and Wnt pathways in bladder cancer, thus their exclusion from this diagram.

(Adapted from Wu, 2005)

Recent sequencing of human UCC by the Sanger institute in Cambridge has confirmed a number of these mutations are indeed present in human UCC (http://www.sanger.ac.uk/perl/genetics/CGP/cosmic?action=byhist&ss=bladder&sn=urinary_t_ract&s=3) (Figure 1.5).



Gene Name	Sample Number	Positive Samples	Percent Mutated
FGFR3	3554	1668	47%
CDKN2A	1241	189	15%
HRAS	1166	135	12%
PIK3CA	361	83	23%
KRAS	470	19	4%

Figure 1.5: Mutation profile of human UCC

Unfortunately these sequenced tumours are a mixture of non-invasive and invasive UCC

1.5. Risk Factors for Urothelial Cell Carcinoma

1.5.1. Tobacco Smoking

Tobacco smoking is the most well established risk factor for bladder cancer, causing about a half of male cases and a third of female cases (Brennan et al., 2000). The carcinogenic contents of tobacco smoke include arylamines (particularly 4-aminobiphenyl), polycyclic aromatic hydrocarbons (PAHs), N-nitroso compounds, heterocyclic amines and a variety of epoxides. The incidence of bladder cancer is related directly to the duration of smoking and number of cigarettes smoked per day (Brennan et al., 2000). There is also a higher risk of bladder cancer in those who start smoking at a young age and those exposed to passive smoking during childhood (Bjerregaard et al., 2006). An immediate decrease in the risk of bladder cancer has been observed in those who quit smoking. This reduction was about 40% within 1-4 years of quitting smoking and reached 60% after 25 years of cessation (Brennan et al., 2000).

1.5.2. Occupational Exposure to Chemicals

Occupational exposure to chemicals is the second most important risk factor for bladder cancer. Work-related cases account for a quarter of all bladder cancer cases in several case series (Pashos et al., 2002, Kogevinas et al., 2003). The substances implicated include benzene derivatives and arylamines (2-naphthylamine, 4-ABP, 4, 4'-methylenedianiline and o-toluidine). At risk professions include those that use dyes, rubbers, textiles, paints, leathers and chemicals (Pashos et al., 2002). However due to the introduction of strict regulations in the West, these chemicals have had minimal contribution to the current incidence of bladder cancer. In fact, there has been a decrease in bladder cancer due to occupational exposure as reported in a pooled analysis of 11 European case control studies on bladder cancer conducted between 1976 and 1996 (Kogevinas et al., 2003). Another source of occupational exposure

are the aromatic amines. A metabolic acetylation pathway can inactivate them and it had been hypothesised that patients with slow acetylation capability were more susceptible to bladder cancer than rapid acetylators. N-acetyltransferase genes 1 and 2 (NAT1 and NAT2) are mapped to the short arm of human chromosome 8, are involved in amine inactivation. The presence of an NAT2 slow acetylation genotype has been related to a higher risk of bladder cancer (Garcia-Closas et al., 2005). Other risk factors include analgesic phenacetin. Some studies have suggested that the risk of bladder cancer due to phenacetin is dose-dependent; however, the data is controversial concerning its metabolite paracetamol (acetaminophen) (Castelao et al., 2000).

1.5.3. External beam radiation therapy

Increased rates of “secondary” bladder carcinomas have been reported in the literature after external beam radiation therapy (EBRT) for gynaecological malignancies (Chrouser et al., 2008, Chrouser et al., 2005). Similarly, in patients treated for prostate cancer by EBRT the rates of bladder malignancy were higher than those subjected to surgery alone (Boorjian et al., 2007).

1.5.4. Dietary factors

To date, there is limited evidence of a causal relationship between bladder cancer and dietary factors. A meta-analysis of 38 articles reporting data on diet and bladder cancer supported the hypothesis that high intake of vegetable and fruit is associated with reduced the risk of bladder cancer (Steinmaus et al., 2000).

1.5.5. Chronic urinary tract infection

Muscle-invasive squamous cell carcinoma (SCC) is directly related to the presence of chronic urinary tract infection. Similarly bladder schistosomiasis has been considered a definitive cause of urinary bladder cancer with an associated five-fold risk. Schistosomiasis is the second most common parasitic infection after malaria, with about 600 million people exposed to the infection in Africa, Asia, South America and the Caribbean (Johansson and Cohen, 1997).

Cyclophosphamide, an alkylating agent, has been correlated with development of posterior muscle-invasive bladder cancer with a latency period of 6 to 13 years. Acrolein is a metabolite of cyclophosphamide and is responsible for an increase in the incidence of bladder cancer and is independent of the occurrence of haemorrhagic cystitis related to the same treatment (Kaldor et al., 1995, Travis et al., 1995).

1.5.6. Gender

Differences in the gender prevalence for bladder cancer may be related to differences in oestrogen and androgen levels between men and women (McGrath et al., 2006).

Interestingly in radical cystectomy patients, it has been demonstrated that women are more likely to be diagnosed with primary muscle-invasive disease than men (85% vs. 51%) (Vaidya et al., 2001). It may be that women are likely to be older than men when diagnosed with a direct effect on their survival. This is however in direct contrast to Cancer Research UK figures (Section 1.1) where UCC is more prevalent in males.

1.6. Murine Models of Urothelial Cell Carcinoma

Until very recently the murine models of UCC have been very limited. One aim of this thesis is to create a better model of UCC. Attempting to elucidate the molecular mechanisms behind UCC in cell lines/tissue culture is hampered by its artificial nature as well as the lack of stroma/microenvironment. Murine models are required to satisfy our desire for increased understanding of the molecular basis of UCC and to explore treatment regimes aimed to improve patient outcome.

Although mice do not spontaneously develop bladder cancer, the murine models of human cancer have provided new tools for the investigation of bladder carcinogenesis. In many other diseases murine models have provided invaluable information regarding pathogenesis and novel disease approaches e.g. cystic fibrosis (Guilbault et al., 2007). In this disease the variety of models reflect that different aspects of the heterogenicity of phenotypes observed in humans; intestinal, pancreatic, hepatobiliary and lung disease as well as ones reflecting the increased susceptibility to respiratory infections.

In the past murine bladder cancer models included the orthotopic approach using primary or genetically altered cell lines derived from localised and metastatic disease and chemical carcinogen techniques.

1.6.1. Chemically induced carcinogenesis

Spontaneous bladder cancers in mice (and rats) are very rare, thus intravesical installation of carcinogens is frequently used. The most commonly used carcinogens are *N*-butyl-*N*-(4-hydroxybutyl) nitrosamine (BBN), *N*-[4-(5-nitro-2-furyl)-2-thiazolyl] formamide (FANFT) and *N*-Methyl-*N*-nitosurea (MNU). They are used particularly for chemoprevention studies,

although novel treatments can be tested and molecular mechanisms elucidated (Black and Dinney, 2007).

BBN is the most widely studied of these agents, since the lesions closely resemble those found in human UCC. Recent work has attempted to profile the gene expression in these murine and rodent tumours and correlate them with human UCC (Williams et al., 2008). They found that many human genes homologous to those differentially expressed in the rodent tumours were also differentially expressed in the human disease and were preferentially associated with progression from non-invasive to muscle invasive disease. They were predominantly cell cycle genes, as well as RAC GTPase-activating protein (*RACGAP1*) and N-*myc* downstream-regulated gene 2 (*NDRG2*). Also interestingly they found that the overall gene expression profiles of rodent tumours corresponded more closely with those of muscle invasive tumours than the non-invasive ones.

Advantages of chemically induced carcinogenesis include that these agents are specific to the urothelium, with 100% of mice developing carcinoma of the bladder. However the process of tumour induction takes 8-14 months and there are safety issues surrounding the exposure of lab/animal unit staff to carcinogens.

1.6.2. Orthotopic Models

There are two forms of orthotopic murine UCC (bladder) models utilised:

1. Orthotopic xenograft models (i.e. implantation of human bladder cancer cells into a nude mouse)
2. Orthotopic syngeneic models (i.e. implantation of murine bladder cancer cells in immunocompetent mice)

1.6.1.1. Orthotopic xenograft models

In these models human TCC cells are implanted into the immunodeficient host mouse. Several TCC cell lines have been used in this fashion including KU7, KU-19, T24 and UM-UC3 cell lines. A major disadvantage of this technique is that the immune response, which is known to be essential to allow treatment with intravesical agents (that is agents instilled directly into the bladder) such as *Bacillus Calmette-Guerine* (BCG) and mitomycin C cannot be assessed in these immuno-compromised mice.

Dinney and colleagues in 1995 established the first reliable orthotopic model of bladder cancer by direct intravesical implantation of the human 253J TCC cells into the bladder of nude mice (Dinney et al., 1995). However many researchers continue to experiment with subcutaneous xenograft models, but as was demonstrated by Perrotte and colleagues results with ectopic tumour inoculation may not reflect what is found with orthotopic models. They used 253J-B-V cells and after 28 days of tumour growth found although tumour size was similar in the ectopic and orthotopic models, however only the orthotopic models developed metastasis to lymph nodes and lung. When these orthotopic models were analysed they found an increase in microvessel density and a corresponding increase in vascular endothelial growth factor (VEGF) and fibroblast growth factor (FGF) expression and MMP-9 activity, demonstrating the importance of microenvironment on tumour cells and their ability to metastasise. Again, however this is limited since the normal microenvironment of the murine bladder may not represent the normal (or indeed abnormal) microenvironment that is found in humans. In these studies single clones of tumours cells are used, when in reality human UCC is indeed a heterogenous condition. Multiple clonal subpopulations arise within the tumour, all of which have differential abilities to invade and metastasise as well as specific responses to treatments.

Further refinements to these models have allowed tagging of these cell lines with either GFP or luciferase technologies for the assessment of tumour burden and ultimately response (Tanaka et al., 2003, Hadaschik et al., 2007).

1.6.1.2. Orthotopic syngeneic models

In these syngenic models, bladder tumours are placed in mice of the same immune status from which the tumours cells were originally derived. The MB49 which contains a mutation in codon 12 of the *K-Ras* gene (from 7,12-dimethylenanthracene-induced bladder tumour in C57BL/6 mouse) and MBT-2 which has lost p53 (from FANFT-induced bladder tumour in C3H/He mouse) cell lines are the most frequently used (Luo et al., 1999, Soloway, 1977, Summerhayes and Franks, 1979, Wada et al., 2001).

One concern with this model (as in any orthotopic model) is that the ‘take’ rate of tumour implantation varies from as low as 30% up to 100% (Chan et al., 2009). Factors influencing tumour ‘take’ include tumourigenicity of tumour cells, number of cells implanted, duration implanted for and pre-treatment methods (e.g. traumatising of urothelial mucosa before inoculation with cells) (Chan et al., 2009). Furthermore multiple passages of these cells either *in vitro* or *in vivo* will result in numerous genetic events occurring in these cell lines.

1.7. Transgenic Models

Transgenic murine bladder models have evolved into important tools for research into UCC, and have been instrumental in elucidating the two pathways of non-invasive (superficial) papillary and muscle invasive bladder cancer (Wu, 2005). The mutations modelled in the mouse are those found in the human disease and have allowed researchers to further study the underlying molecular mechanisms. Such transgenic models allow researchers to study single and/or compound mutational events involving oncogenes and tumour suppressors in an organ specific temporal fashion. There are currently two approaches this can be achieved.

Firstly, the traditional method has been a genome wide knock out of the gene in question (Capecchi, 1994). The major problem is that it does not allow evaluation of the gene function if it results in embryonic lethality or premature death. Also, since the gene is knocked out in all cell types, it is difficult to prove that the abnormal phenotype did not arise from a developmental defect (Copp, 1995). Secondly one may use a conditional gene knock out technique that aims to overcome many of the above limitations. The Cre-loxP recombination is one of these technologies, which allows one to study conditional cell type and tissue specific deletion of genes (Figure 1.5) (Nagy, 2000). The bacterial Cre- (Cre: Cause Recombination) LOXP1 (locus of X-over P1) system has been used in mammalian cells (Sauer and Henderson, 1988). This system relies on a sequence specific DNA cre recombinase which mediates intramolecular recombination and deletion of DNA between loxP sequences. LoxP sequences are small sequences of DNA of 34 base pairs. Using gene targeting LoxP flanked alleles have been generated, allowing deletion of genes upon expression of cre recombinase. To permit gene deletion in the tissue of interest, tissue specific Cre transgenes have been generated so that currently genes can be deleted in nearly every tissue of the mouse, including the bladder urothelium.

In addition invasive tumours that develop metastasis provide an excellent platform for investigating specific genetic events involved in the metastatic phenotype, including the contribution that stromal-epithelial interactions may have.

Limitations include long latency, incomplete penetrance and often the requirement of an artificial promoter (some models use knock-in endogenous alleles which mutate the allele in question, whilst others have overexpression of alleles to non-physiological levels). Tumours developed in transgenic models tend to be less heterogeneous than in human bladder tumours, which may have an impact on tumour progression and distant spread. Given that no model has progressed to bone metastases, some investigators have questioned their relevance to the human cancer.

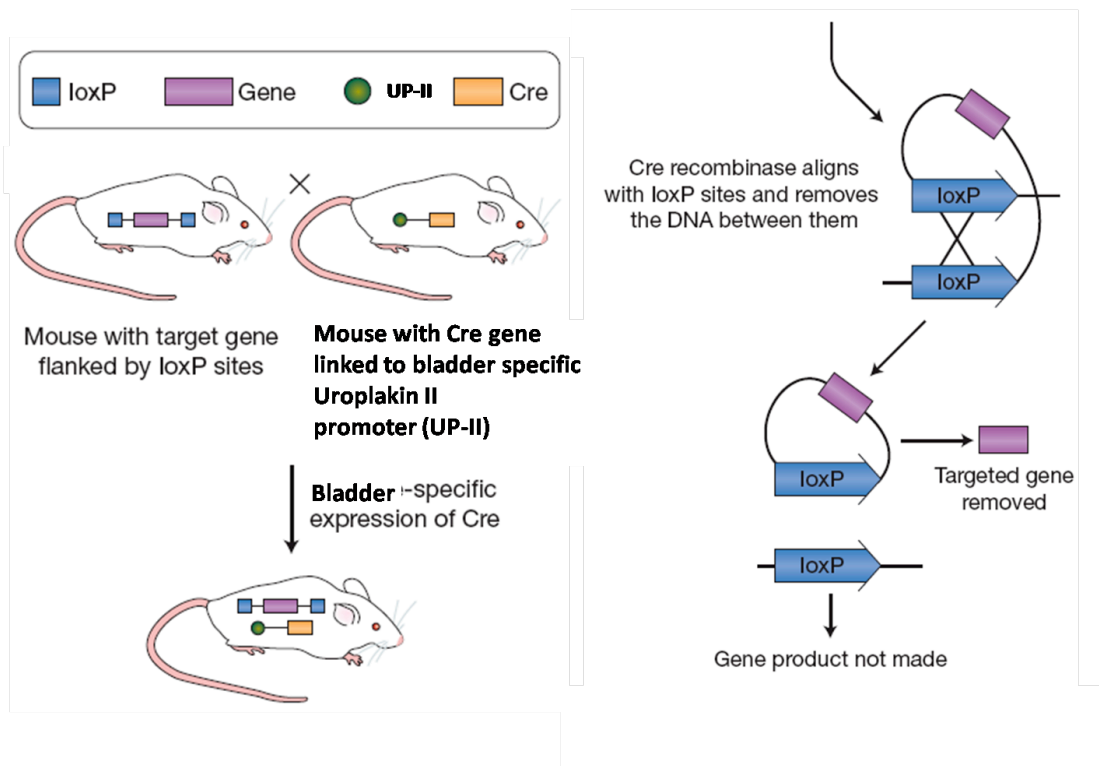


Figure 1.6: The Cre-LoxP recombination system in transgenic mice

The bacterial Cre- (Cre: Cause Recombination) LOXP1 (locus of X-over P1) system relies on a sequence specific DNA cre recombinase which mediates intramolecular recombination and deletion of DNA between loxP sequences. Using gene targeting LoxP flanked alleles have been generated, allowing deletion of genes upon expression of cre recombinase. To permit gene deletion in the urothelium, urothelial specific Cre transgenes have been generated.

[Adapted from (Ahmad et al., 2008)]

1.7.1. Ras Pathway

1.7.1.1. HRAS

This was the first human oncogene isolated in human UCC, being mutated most often at either codon 12, 13 or 61 (Reddy et al., 1982). Mutation allows it to become constitutively active, as well as resulting in overexpression at the protein level (due to alternative splicing of the last intron). Despite the controversy regarding the reported mutation frequency rate recent studies indicate that *HRAS* mutation occurs in approximately in 30-40% of UCC (Bentley et al., 2009, Czerniak et al., 1992).

Transgenic models have provided invaluable information regarding the molecular mechanisms behind H-RAS activation with much of this work largely being carried out by the Wu lab (Department of Urology, New York University School of Medicine) (Wu, 2005). They have utilised the mouse uroplakin II (UPII) promoter, which is expressed in the basal layer of the urothelium, within which the stem cell niche resides (Lin et al., 1995). In the first instance they targeted expression of a constitutively active rabbit *H-Ras*^{Q61L} to the urothelium using this promoter (Zhang et al., 2001). Their rabbit *H-Ras*^{Q61L} mutant had been previously shown to share all the functional characteristics of codon 12 and 13 mutants and to be fully capable of transforming culture NIH 3T3 cells (Zhang et al., 2001).

This induced early onset urothelial hyperplasia, with this hyperplasia progressing to low-grade non-invasive papillary tumours. Interestingly tumour latency depended on transgene number. In the mice that had 1 or 2 copies of the rabbit *H-Ras*^{Q61L} transgene (low-copy), the tumour latency was almost 12 months. Histologically by 3-5 months the urothelial layer has become hyperplastic (from the usual 3 layers to 6-7 layers). At 8 months the urothelium becomes more hyperplastic, forming areas of nodular hyperplasia. From 10-26 months of age 63% of mice developed superficial non-invasive UCC. These lesions remained non-invasive

during the 26-month follow-up period. In contrast mice harbouring “high-copy” numbers of the *HRAS*^{Q61L} *RAS* transgene (30-48 copies) succumbed to death by 5 months of age. The mice had evidence of significantly enlarged bladder and associated bladder outflow obstruction (hydronephrosis and hydroureter). Again these tumours were of a papillary non-invasive histology, with no evidence of muscle invasion or metastases.

This fits with the human literature in which the *Ras* oncogene is shown to be frequently overexpressed. Quantification of the transcripts in paired tumour and adjacent normal tissue identified a 40% overexpression of *H-RAS* (Vageli et al., 1996). Others have found overexpression of *HRAS* at the protein level in more than 50% of bladder tumours (Dunn et al., 1988, Ye et al., 1993). The fact that the bladder tumours in “low-copy” mice developed localised, superficial papillary tumours with a much longer latency, suggests, in the absence of overexpression, *H-Ras*, activation requires a secondary event, either genetic or epigenetic, to fully induce bladder tumours. These mice have been instrumental in showing the *Ras* pathway activation is sufficient to lead to UCC along the low-grade/non-invasive papillary tumourigenesis pathway. They have also suggested that these results indicate urothelial hyperplasia may be an important precursor of papillary UCC.

Subsequently the Wu group found upregulation of the senescent markers *Ink4a/Arf* in the mutant “low copy” *HRAS* urothelium, without histological evidence of senescence (Mo et al., 2007). Surprisingly, when the *Ink4a/Arf* locus in these mice was genetically knocked out, there was no evidence of acceleration of urothelial tumourigenesis.

1.7.2. Receptor Tyrosine Kinases

1.7.2.1. Epidermal Growth Factor Receptor (EGFr)

Epidermal growth factor receptor is overexpressed in 40-60% of human UCC at the mRNA and protein levels (Neal and Mellon, 1992). In addition EGFr overexpression has been implicated in invasive UCC. In chemical carcinogen models EGF significantly increased the frequency of heterotopically transplanted bladder tumours in rats (Fujimoto et al., 1996).

The Wu lab targeted expression of functionally active EGFr (demonstrated auto-phosphorylation and downstream MAPK activation) to the urothelium using the UPII promoter (Cheng et al., 2002). The bladders developed hyperplasia, but did not progress to tumour. When combined with activated *HRAS* transgene there was no synergism in urothelial tumourigenesis, again strengthening the redundancy argument since they are both in the same signal transduction cascade. Interestingly they found that EGFr could potentiate with the SV40 mouse (Simian virus 40, a polyomavirus that interacts SV40 Large T-antigen and SV40 Small T-antigen, leading to defects in RB and p53) to accelerate CIS conversion into high grade UCC.

1.7.2.2. Fibroblast Growth Factor Receptor 3 (FGFR3)

In urothelial tumours, over 70% of low-grade/non-invasive papillary tumours exhibit mutations in *FGFR3*. However only 10-20% of invasive bladder tumours harbour mutations in this same locus, leading researchers to postulate that FGFR3 activation is one of the major genetic events that lead to low-grade/non-invasive papillary tumours (van Rhijn et al., 2004, van Rhijn et al., 2001). Almost all the mutations have been identified as missense mutations. They most frequently involve the receptor's extracellular loop and affect the cysteine residues: either eliminating or creating a cysteine (Wu, 2005). This results in cysteine mis-

pairing, conformational change/misfolding and the failure of the mutated FGFR3 to exit the endoplasmic reticulum. Additionally some FGFR3 mutations are capable of undergoing ligand-independent activation, which lead to autophosphorylation of the intracellular kinase domain (Bakkar et al., 2003, Billerey et al., 2001). These mutated receptors exhibit increased stability and decreased translocation to the lysosomal degradative pathways (Cho et al., 2004, Monsonego-Ornan et al., 2000). All these factors result in increased and prolonged activation of the receptor.

As indicated earlier HRAS and FGFR3 mutations occur in up to 30% and 70% of clinical non-invasive UCC respectively, suggesting that the RTK-Ras pathway is responsible for these types of tumours. Recent studies by the Knowles lab (University of Leeds) suggest that HRAS and FGFR3 mutations are unlikely to co-exist in the same tumours (Jebar et al., 2005). This fits with data from other tumours types such as malignant melanoma, in which components from the same signaling pathway are rarely mutated simultaneously (*NRAS* and *BRAF* in melanoma), presumably since this offers no selective advantage to the tumour cells (Takata and Saida, 2006) (Figure 1.6).

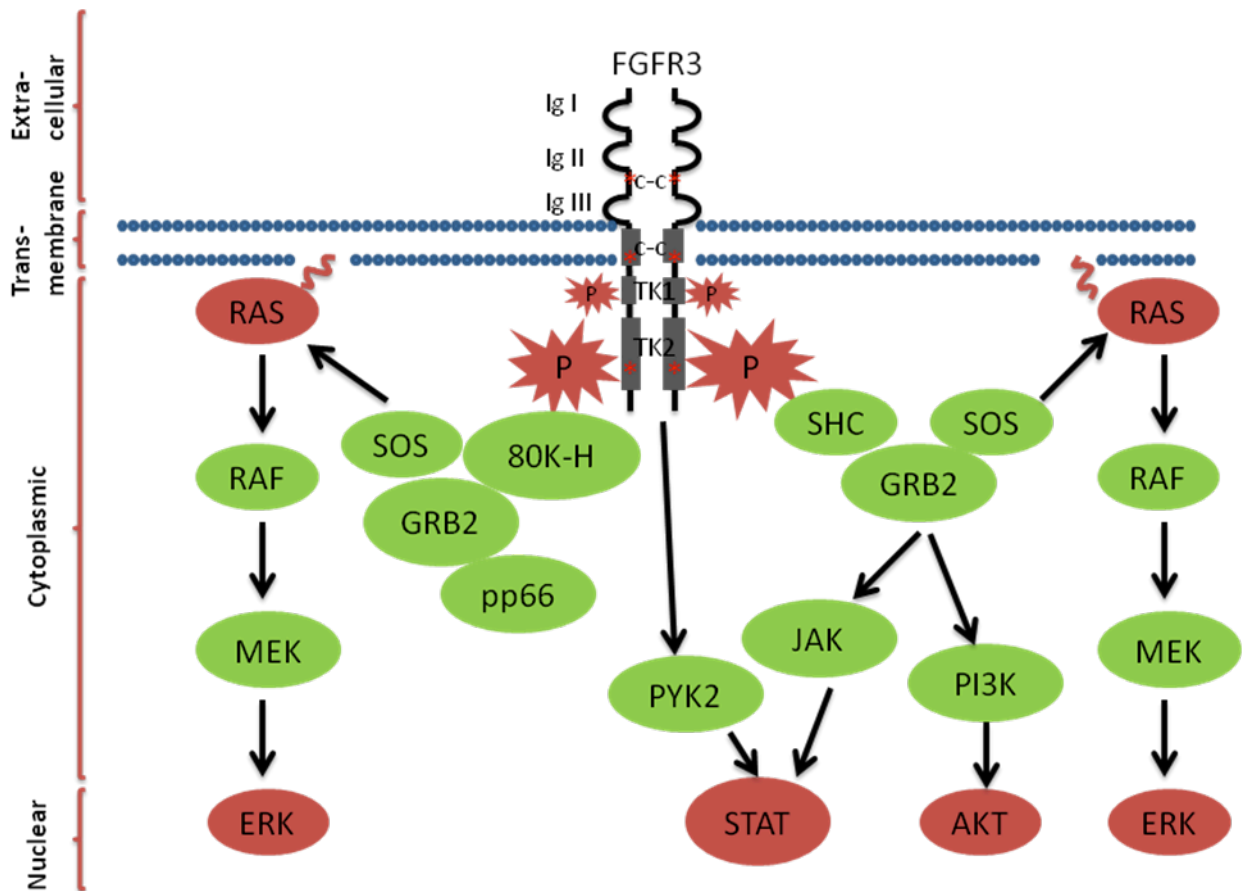


Figure 1.7: Signalling cascades involved in UCC during FGFR3 and HRAS activation

FGFR3 and *HRAS* gene mutation are thought to share the same downstream signalling pathway. *FGFR3* consists of 3 extracellular (EC) immunoglobulin-like domains (IgI–III), a transmembrane domain (TM), and a cytoplasmic (CP) tyrosine kinase domain (TK1 and TK2). Mutations that affect the loop that connects the IgII and IgIII domains account for up to 50-80% of all mutations, whereas those affecting the TM domain account for up to 15-40% and those affecting TK2 account for 5–10%. Loop and TM mutations often create a novel cysteine and might be responsible for receptor dimerization (*C–C*) and autophosphorylation.

FGFR3 phosphorylation triggers several signalling cascades, the most predominant of which is the Mitogen Activated Protein Kinase (MAPK) pathway. Phosphorylated *FGFR3* can activate the phosphatidylinositol 3-kinase (PI3K) and AKT pathway. Lastly, the activated *FGFR3* can directly or indirectly (through Janus-family kinases (JAKs)) trigger the signal

transducer and activator of transcription (STAT) pathway. The activated FGFR3 can also interact directly with proline-rich tyrosine kinase 2 (PYK2), leading to STAT pathway activation (Cappellen et al., 1999, Rieger-Christ et al., 2003, van Rhijn et al., 2004, Bakkar et al., 2003, van Rhijn et al., 2001, Billerey et al., 2001).

Mutational activation of HRAS can trigger similar signalling pathways.

(Adapted from Wu, 2005)

1.7.2.3. Sprouty (SPRY)

SPRY proteins comprises of a family of well-conserved regulators of RTKs. SPRY was originally identified in *Drosophila* as an antagonist of fibroblast growth factor (FGF) mediated signalling (Hacohen et al., 1998). Amongst the four mammalian SPRY orthologues (SPRY1-4), SPRY2 is the closest to *Drosophila* SPRY (dSPRY) and extensively studied as a RTK modulator. SPRY2 has been shown to interact with a number of RTK downstream signalling components such as Grb2, Raf1, Shp2, c-Cbl and GAP1 (Kim and Bar-Sagi, 2004). As a consequence, SPRY2 can regulate both the intensity and duration of RTK mediated signalling. The dSPRY can inhibit both FGF and epidermal growth factor (EGF) mediated signalling (Kramer et al., 1999). However, SPRY2 has been shown to inhibit only FGF mediated signalling. Interestingly, recent evidence indicate that SPRY2 exerts its negative and positive regulatory roles on EGF mediated signalling in a distinctive manner by interfering the trafficking and degradation of epidermal growth factor receptor (EGFR) (Kim and Bar-Sagi, 2004, Rubin et al., 2003, Fong et al., 2003).

Using Oncomine™ (<http://www.oncomine.org/geneModule/differential/filterStore.jsp>) Lindgren and colleagues have demonstrated that in FGFR3 mutant bladder cancer there is a downregulation of Sprouty 2 at the mRNA level ($p=0.015$) (Lindgren *et al.*, 2006). In the same study they find that Sprouty2 mRNA levels are downregulated as the disease progresses from Grade 1 to 3 ($p=0.015$).

1.7.3. PTEN-PI3K-pAKT

1.7.3.1. PTEN

The phosphatase and tensin homology (PTEN), located on human chromosome 10, is a lipid phosphatase that dephosphorylates phosphoinositide-3,4,5-triphosphate (PI3P). As a result of this dephosphorylation, this 55-kDa protein antagonises the activity of PI3 kinase (PI3K), preventing it from activating downstream proliferation and survival signals, especially pAKT, leading to growth inhibition (Dahia, 2000).

The PTEN/pAKT pathway has also been implicated in invasive UCC. Evidence suggests that restoration of PTEN function induces growth arrest in bladder cancer cell lines deficient in PTEN (Tanaka et al., 2000), and inhibition of PI3K may decrease the invasive potential of bladder tumours (Wu et al., 2004).

Also deletion at the *PTEN* locus (3p, 5q, 10q) is rare in non-invasive, but occur frequently in invasive UCC (Puzio-Kuter et al., 2009). The reduction or loss of PTEN protein expression was observed in 42% of non-invasive and 94% of advanced UCC. This reduction in PTEN correlated with stage and grade (Tsuruta et al., 2006).

Unfortunately the transgenic models that exist for *Pten* null mice have been inconsistent, possibly due to use of different *Pten* alleles and promoters, as well as differences in the background strains of the mice.

Yoo and colleagues deleted exon 4-5 of the *Pten* gene using the *Fabp-Cre* system (which directs recombination in all the cell layers of the urothelium by embryonic day 16.5, as well as the intestinal epithelium) and were able to demonstrate urothelial hyperplasia and eventual UCC by 13.5 months of age (Yoo et al., 2006).

Using a similar model, PTEN null mice (*Fabp-Cre Pten^{fl/fl}*) also developed non-invasive UCC in 10% of cases, after a long latency (>40 weeks) (Tsuruta et al., 2006). The long latency and low tumour rate could be because of the slow proliferation rate of the urothelium and/or the requirement of secondary genetic events for urothelial carcinogenesis.

More recently Qian and colleagues investigated the role of PTEN in UCC. In their *Pten* null mice (in this mouse exons 4-5 is flanked by the *loxP* sequences), using the *Ksp-Cre* promoter (expressed in renal tubules, collecting ducts and ureteric bud) they found renal pelvis UCC in 57% of mice at 12 months (Qian et al., 2009). Interestingly they found upregulation of p-mTOR in their tumours, suggesting a role for inhibitors of the pathway (i.e. rapamycin) as therapeutic agents.

Surprisingly, another *Pten^{fl/fl}* bladder model did not have any urological phenotype when aged to 12 months following intravesical administration of the *AdenoCre* (Puzio-Kuter et al., 2009).

1.7.4. p53

p53 is a nuclear phosphoprotein that acts as a key gatekeeper at the G1/S checkpoint of cell cycle progression, integral in controlling urothelial cell growth and maintaining genomic stability (Levine, 1997). Mutation and deletion of the p53 tumour suppressor gene are among the most common genetic changes found in human UCC (Wu, 2005). Usually one allele is mutated and thus non-functional whilst the other is often deleted, suggesting that p53 is non-functional in human UCC. Consistent with these findings, p21 (also known as WAF), an important downstream target of p53, is downregulated in the majority of UCCs that harbour p53 loss/mutation (Lu et al., 2002, Stein et al., 1998). Similar to the p53 data, loss of p21 expression is also associated with disease progression (Stein et al., 1998).

p53 abnormalities are much more prevalent in invasive UCC (>50%) and precursor CIS lesions when compared to the in non-invasive phenotype (Cordon-Cardo et al., 1994, Hartmann et al., 2002, Wagner et al., 1995, Spruck et al., 1994, Orntoft and Wolf, 1998). This suggests that p53 loss/mutation may be responsible for the formation and progression of invasive UCC.

The commonest site of p53 mutation was found in exon 5 and 8 (George et al., 2007). 90% of samples with exon 5 mutations and a substantial proportion of tumours with the exon 8 mutation demonstrate no nuclear p53 accumulation, suggesting loss of the protein and non-functionality of the mutation. The majority of these were point mutations G:C to C:G transversions. Another study found p53 point mutations predominately in codons 280 (Arg to Thr) and 285. These mutations are rare in other epithelial tumours, leading to speculation about the role of urothelial specific carcinogens (Feng et al., 2002, Berggren et al., 2001). Interestingly the association between smoking and UCC did not differ substantially between cases with and without p53 mutations, it was however more strongly associated with CpG

G:C-A:T transitions than with other types of mutations (Spruck et al., 1993, Schroeder et al., 2003). Patients with p53 mutations have a far higher risk of disease progression and death than those without (George et al., 2007, Hartmann et al., 2002, Masters et al., 2003, Cordon-Cardo, 1998).

Nuclear accumulation of p53 (a sign of mutation) is significantly associated with a greater risk of UCC and decreased overall survival in patients with organ confined disease (Esrig et al., 1994). Their multivariate analysis stratified according to grade, pathological stage and lymph node status demonstrated that nuclear p53 accumulation was an independent predictor of recurrence free and overall survival ($p < 0.001$) (Esrig et al., 1994). This is consistent with the theory that with models that promote progression of organ confined UCC have abnormal nuclear p53 function.

However, a meta-analysis based on 43 studies comprising 3764 patients with UCC demonstrated considerable variation in clinical outcome, different immunohistochemistry protocols, patient selection and study design (Schmitz-Drager et al., 2000).

Murine studies of UCC using the Trp53-knockout have been unsatisfactory since these mice develop fatal soft tissue sarcomas and thymic lymphomas by 7 months of age, at which stage the urothelium is still normal (Donehower et al., 1992). The heterozygous Trp53-knockout mice (which live longer) do not develop any urothelial abnormalities.

Interestingly a mouse with dominant negative mutation of p53 (lacks DNA binding domain but retains the tetramerization domain) targeted to the urothelium using the uroplakin promoter develops urothelial hyperplasia and dysplasia without progression to frank carcinoma (Gao et al., 2004). Wu and colleagues studied the expression of activated *H-Ras* (again using the UPII promoter) in the absence of *p53* (Gao et al., 2004). They found absence of *p53* accelerated the formation of the activated *H-Ras* induced high-grade UCC. However

they were unable to prove that these tumours became invasive since the Trp53 null mice died of lymphomas by 7 months of age.

When they repeated the experiment with p53 heterozygous mice they found this acceleration was negated and the mouse phenocopied the activated *H-Ras* mutant.

Using an adenovirus expressing Cre recombinase delivered directly into the bladder, simultaneous p53 and Pten deletion ($p53^{fl/fl} Pten^{fl/fl}$) resulted in bladder tumours with 100% penetrance at 6 months, with metastasis to local lymph nodes and distant sites, including spleen, liver and diaphragm (60% by 4-6 months). (Puzio-Kuter et al., 2009). The histology of these tumours closely resembled that of CIS and invasive tumours found in humans.

Puzio-Kuter found that their $p53^{fl/fl} Pten^{fl/fl}$ mice had highly upregulated p-mTOR, and when rapamycin was given to these mice tumour regression occurred (Puzio-Kuter et al., 2009, Seager et al., 2009). Interestingly when given to mice at the CIS stage, the rapamycin abrogated the progression to frank invasive tumourigenesis.

Currently there are no murine studies looking at the effect of mutant p53 in the formation of UCC.

1.7.5. p21^{WAF/CIP1}

The cyclin-dependent kinase inhibitor p21^{WAF/CIP1} (p21) was originally discovered as a key target of the p53 tumour suppressor gene following DNA damage. Induction of p21 by p53 induced cell cycle arrest by a block in G1 (Deng et al., 1995). p21 has been shown to be induced in a p53 independent fashion, such as through oxidative stress, cytokines, tumour viruses and anti-cancer agents (Abbas and Dutta, 2009). p21 is also implicated in protection from p53-dependent and independent apoptosis (Weiss, 2003, Gartel and Radhakrishnan, 2005), and its overexpression was sufficient to drive tumour cells into senescence (Fang et al., 1999). Moreover, studies have shown that p21 is key in the induction of senescence following treatment with ant-cancer agents (Chang et al., 1999).

p21 is downregulated in the majority of urothelial carcinomas that have p53 loss/mutation (Lu et al., 2002, Stein et al., 1998). Similar to the literature on p53, loss of p21 expression is also associated with a higher recurrence rate and lower survival rate than those tumours with maintained p21 expression levels, irrespective of tumour grade and pathological stage (Stein et al., 1998). It was also noted that maintenance of p21 expression appeared to negate the effects of p53 alterations on UCC progression (Stein et al., 1998).

Similarly, Shariat et al demonstrated that positive p21 expression was independently associated with reduced UCC recurrence and progression in *CIS* (with no muscle-invasive disease), possibly by p53-independent modulation of p21 (Shariat et al., 2003).

Although no models of p21 deletion in the urothelium have been published, Yoo and colleagues observed upregulation of p21 expression in the urothelium in their PTEN null mouse using the urothelial specific *Fabp-Cre* (Yoo et al., 2006). In the urothelium of the

newborn mice, cell proliferation is initially high, but within days is inhibited by p21 induction, suggesting a bladder specific compensatory mechanism.

1.7.6. Retinoblastoma (RB)

Recently it has been noticed that patients with germline mutations of RB1 have a higher risk of developing epithelial carcinoma, particularly UCC (Fletcher et al., 2004). Loss of heterozygosity (LOH) of RB1 is also prevalent in invasive UCC (Cairns et al., 1991). Either there is a lack of RB expression, or overexpression of a hyper-phosphorylated version of the protein (Chatterjee et al., 2004, Logothetis et al., 1992). In these scenarios RB is dysfunctional and cannot inhibit E2F family of transcription factors, leading to an increase in cell proliferation. Transgenic mice with RB1 ablated in all tissues die embryonically (Donehower et al., 1992).

Mutation of both p53 and RB occur in >50% of invasive UCC, with patients having increased rate of recurrence/progression and worse overall survival than patients with single gene mutations (Grossman et al., 1998). Fitting with this, mice with targeted urothelial expression of the simian virus 40 (SV40) large T-antigen, which inactivates both p53 and RB together, develop CIS and subsequent invasive tumours (Zhang et al., 1999, Grippo and Sandgren, 2000). Interestingly the CIS evolved to high-grade papillary UCC before progressing to muscle invasive disease. Whether this is particular to the mouse has yet to be elucidated.

Recently the Wu lab demonstrated that urothelial specific deletion of both copies of RB (UPII Cre) failed to accelerate urothelial proliferation (He et al., 2009). Instead it activated a 'failsafe' signature by profoundly activating the p53 pathway and leading to apoptosis. Deletion of p53 in these RB null urothelial cells may therefore remove the tumourigenesis barrier. However this resulted in nuclear atypia and only 2% of mice progressed to non-

invasive papillary tumours. Interestingly, mice deficient in both RB and p53 become extremely sensitive to chemically induced carcinogenesis (0.01% BBN for 10 weeks) and 50% developed invasive UCC similar to the human condition.

This suggests that loss of both p53 and RB is necessary, but insufficient to initiate UCC along the invasive pathway (Figure 1.7). It is presumed that other genetic alterations are required to trigger invasive UCC.

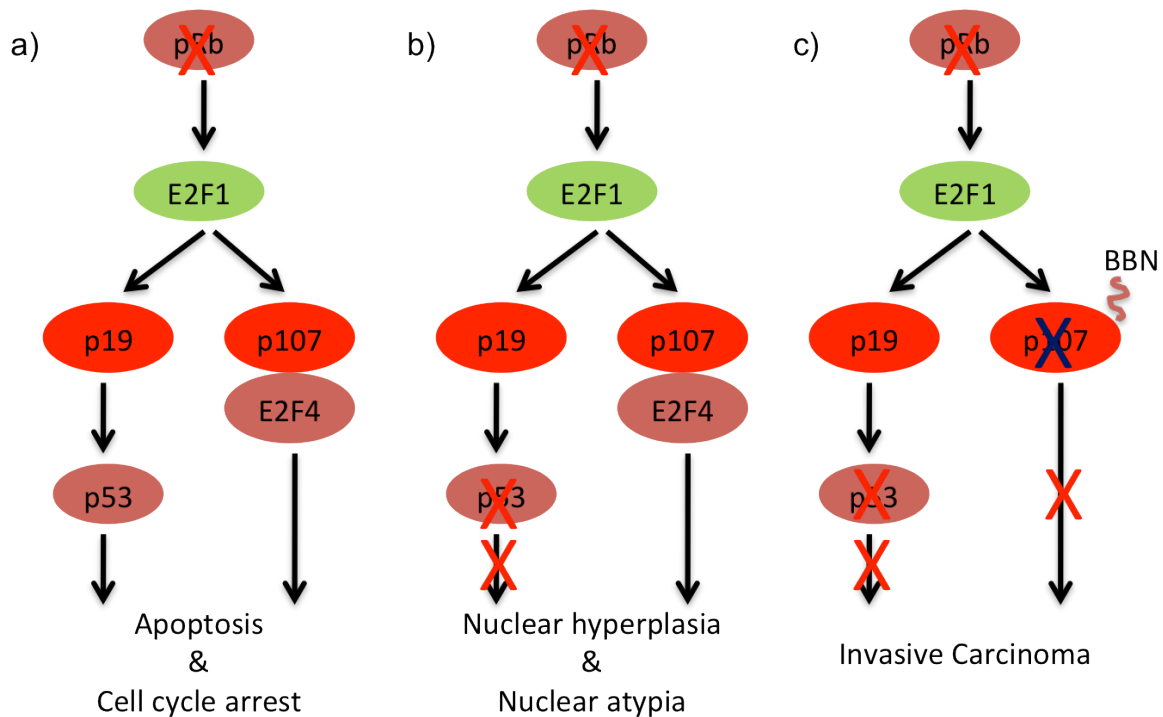


Figure 1.8: Collaborative effects between pRb family proteins and p53 in invasive UCC

a) Ablation of pRb specifically in urothelium leads to E2F1 over-expression that in turn up-regulates the p53 pathway and pRb family member p107 along with transcriptional repressor E2F4. These compensatory urothelial defences cause urothelial cells to undergo cell-cycle arrest and apoptosis.

b) Additional ablation of p53 in urothelial cells lacking pRb effectively blunted apoptotic response, resulting in late-onset hyperplasia and nuclear atypia.

c) Treatment of urothelial cells lacking both pRb and p53 with bladder carcinogen BBN down-regulates p107 and triggers invasive urothelial tumourigenesis. This model emphasizes the collaborative effects among pRb family proteins and p53 in invasive urothelial tumour initiation. (Adapted from He et al., 2009)

1.8 The Wnt signalling pathway

The Wnt pathway is widely conserved throughout many species including *C.elegans*, *Drosophila*, *Xenopus* and mammals. The Wnt pathway was originally discovered in *Drosophila* where the gene *wingless* (*wg*) demonstrated the ability to influence segment polarity during larval development (Nussleinvolhard and Wieschaus, 1980). Murine studies identified a gene called *Wnt1* (originally named *Int-1*) which was shown to be a proto-oncogene in breast tumours induced by the mouse mammary tumour virus (MMTV) (Nusse and Varmus, 1982). Further studies went on to show that *wingless* (*wg*) was a fly homologue of the mouse *Wnt1* gene (Rijsewijk et al., 1987). Thus the name Wnt, a compromise of *wg*, from the *Drosophila* *wingless* gene and *Int*, the mouse homologue.

The Wnt pathway is now known to control many events during embryonic development, and regulates homeostatic self-renewal in a number of adult tissues. As a result, mutations in this pathway are associated with the onset of various cancers, due to the influence of the Wnt pathway has on processes such as proliferation, motility and cell fate at the cellular level (Oving and Clevers, 2002, Polakis, 2000b). Wnt ligands are glycoproteins which interact with a seven-transmembrane frizzled cell surface receptor, leading to Wnt pathway activation. Three different pathways are believed to be activated upon receptor activation (the Wnt/Ca²⁺ pathway, the non-canonical planar cell polarity pathway and the canonical pathway) (Clevers, 2006).

In the planar cell polarity pathway Wnt signalling through frizzled receptors mediates asymmetric cytoskeletal organisation and the polarization of cells by inducing modifications to the actin cytoskeleton. Two independent pathways, which are initiated by dishevelled, trigger the activation of the small GTPases Rho and Rac. Activation of Rho requires Daam-1 and leads in turn to the activation of the Rho-associated kinase ROCK. Rac activation is

independent of Daam-1 and stimulates JNK activity (Huelsenken and Behrens, 2002, Habas and Dawid, 2005).

Wnt signalling via frizzled receptors can also lead to the release of intracellular calcium. Frizzled co-receptors, involved in this pathway include Knypek and Ror2. Other intracellular second messengers associated with this pathway include heterotrimeric G-proteins, phospholipase C (PLC) and protein kinase C (PKC). The exact genes activated by the Wnt/Ca²⁺ pathway are unknown, but NFAT appears to be involved, which is a transcription factor regulated by the calcium/calmodulin-dependent protein phosphatase, calcineurin. The Wnt/Ca²⁺ pathway is important for cell adhesion and cell movements during gastrulation (Habas and Dawid, 2005, Kohn and Moon, 2005).

1.8.1. The Canonical Wnt Signalling Pathway

The canonical Wnt pathway is a ligand dependent system whereby Wnt proteins bind to frizzled and LPR family member receptors at the cell surface. This in turn activates dishevelled family proteins and ultimately results in an increase in the amount of β -catenin that reaches the nucleus (Figure 1.8) (Reya and Clevers, 2005). Consequently β -catenin now complexes with TCF/LEF resulting in the transcriptional activation of Wnt target genes. In the presence of a Wnt ligand, Frizzled (Fz) proteins cooperate with a single pass transmembrane molecule called LRP6 to bind the ligand. Upon this binding, the scaffold protein axin translocates to the membrane where it interacts with the intracellular tail of LRP5. This results in the disassociation of the destruction complex comprising axin, GSK3 β (glycogen synthase kinase), CK1 (casein kinase), Apc, and β -catenin (reviewed in Reya and Clevers, 2005 and Clevers, 2006). Also, by an unknown mechanism, the binding of Wnt to Frizzled results in the hyperphosphorylation of Dishevelled (Dsh), which inhibits the activity of GSK3 β making it unable to phosphorylate β -catenin (Mao et al., 2001, Yanagawa et al., 1995). In its unphosphorylated state, β -catenin is now not recognized by the F-box β -TRCP protein, a component of the E3 ubiquitin ligase and therefore is not degraded. Subsequently, β -catenin is now free to translocate to the nucleus, where it binds to the N terminus of LEF/TCF (lymphoid enhancer factor/T cell factor), and activates transcription of a number of Wnt target genes (Behrens et al., 1996, Molenaar et al., 1996, vandeWetering et al., 1997, Polakis, 2000b), including c-Myc (He et al., 1998), CD44 (Wielenga et al., 1999), TCF-1 (Roose et al., 1999), LEF-1 (Hovanes et al., 2001).

Therefore, during inappropriate Wnt activation, (caused by Apc/ β -catenin mutations), activation of key Wnt target genes such as c-Myc lead to uncontrolled bursts in proliferation. This once again, serves to highlight the important role that Apc plays as a key ‘gate keeper’ in

controlling cell proliferation, particularly in the formation of colorectal cancer (Kinzler and Vogelstein, 1996).

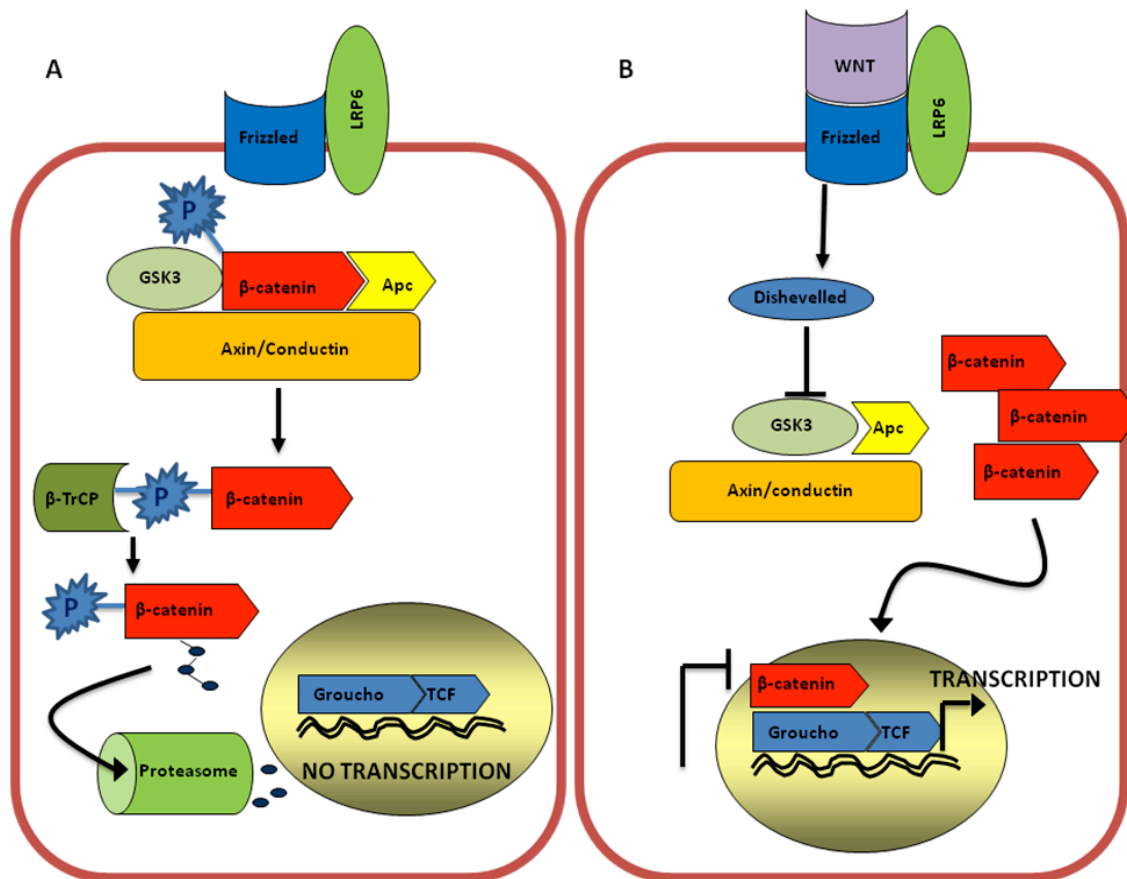


Figure 1.9: Canonical Wnt Signaling

a) In the absence of a WNT signal, the level of free intracellular β -catenin is minimised by sending it for degradation in the proteasome. Free cytoplasmic β -catenin, which is in equilibrium with β -catenin at adherens junctions, is recruited to a 'destruction complex' containing APC, axin/conductin and glycogen synthase kinase 3 β (GSK3 β). GSK3 β phosphorylates β -catenin, allowing it to be recognized by an SCF complex containing the F-box protein β -TrCP. Other proteins in the SCF complex catalyse the addition of a polyubiquitin chain to β -catenin, allowing β -catenin to be recognized and degraded by the proteasome. Consequently, β -catenin cannot reach the nucleus, and cannot co-activate TCF-responsive genes. Groucho, a corepressor, also prevents the activation of TCF/LEF-responsive genes in the absence of β -catenin.

b) In the presence of WNT, its receptor, Frizzled, in complex with LRP6, is activated. This leads to a poorly understood signalling cascade in which Dishevelled activates GBP — an inhibitor of GSK3 β . Consequently, β -catenin cannot be targeted for destruction and is free to diffuse into the nucleus, where it acts as a co-activator for TCF/LEF-responsive genes. [Adapted from (Fodde et al., 2001)]

1.8.2. The Role of Wnt Signalling in Cancer

Germline mutations of the *APC* gene cause Familial adenomatous polyposis (FAP). This is an autosomal dominant disease that affects approximately 1/7000 people and is characterised by the development of hundreds of colorectal adenomas, often arising by the second decade of life (Kinzler and Vogelstein, 1996). As the patient ages, a small proportion of adenomas progress to carcinomas, with 100% of FAP patients developing colorectal cancer by the average age of forty years (Sancho et al., 2004). FAP patients can also develop other intestinal lesions including gastric fundic gland polyposis, duodenal adenomas, and gastric, pancreatic, biliary or distal small intestinal lesions. At much lower frequencies, FAP patients can also develop lesions out with the GI tract such as desmoids of the skin, retinal lesions, osteomas and brain tumours (Kinzler and Vogelstein, 1996).

It has also been discovered that mutations in *APC* occur in the majority of all sporadic colorectal tumours (Miyoshi et al., 1992, Powell et al., 1992). Given the high frequency of mutations in the *APC* gene, it has been proposed that APC acts as a key ‘gatekeeper’ gene of colonic homeostasis, importantly controlling colonic epithelial cell proliferation. Therefore a mutation in this ‘gatekeeper’ gene results in uncontrolled cellular renewal and proliferation (Kinzler and Vogelstein, 1996). Although it is now widely accepted that mutations in *APC* initiate the neoplastic process, it is also known that a sequential series of mutations are necessary for tumour progression,

The *Apc*^{Min+} (Multiple Intestinal Neoplasia) mouse was the first murine model to phenotypically recapitulate FAP (Moser et al., 1990). The mice demonstrated signs of anaemia and were moribund by 120 days. Upon necropsy, multiple adenomas were observed in the small intestine, which occasionally progressed to adenocarcinomas in older mice. Each mouse presented with on average 30 intestinal adenomas, hence the name

Multiple Intestinal Neoplasia (Moser et al., 1990). The mutation in these adenomas was mapped to codon 850 of the murine homologue of the Apc protein, and was similar to those observed in FAP patients (Su et al., 1992). Similar to FAP patients this mutation was characterised as a fully penetrant autosomal dominant disorder (Moser et al., 1990). Despite similar germline mutations, FAP patients predominantly have colorectal adenomas which routinely progress to invasive adenocarcinomas, in contrast to the small intestinal adenomas observed in the *Apc^{Min+}* mouse. This is possibly due to the fact that *Apc^{Min+}* mice present with a high tumour burden, and as a consequence mice need to be sacrificed before tumours are able to progress to adenocarcinomas.

Outwith colorectal cancer, mutations in the *APC* gene are much rarer. In cancer such as hepatocellular carcinoma (HCC) Wnt pathway activation is observed through β -catenin activating mutations or loss of negative regulators such as Axin or Axin2 (Sato et al., 2000, Giles et al., 2003). Similarly activating/stabilising mutations of β -catenin have been observed in melanoma, ovarian carcinomas, childhood hepatoblastomas and medulloblastomas, desmoid tumours and non-ductal solid pancreatic tumours (Giles et al., 2003). Interestingly in these cancers activating mutations of the Wnt pathways are not thought to be initiating event.

Zhou et al proposed a role for Wnt signalling in renal carcinoma, since the key renal tumour suppressor protein (Von Hippel Lindau) VHL, acts through JADE, an E3 ubiquitin ligase to target β -catenin for degradation (Zhou et al., 2005). Therefore, a mutation in VHL results in the stabilisation and activation of the oncogenic β -catenin pathway (Behrens, 2008). This link between the pathways explains why FAP patients, with a germline mutation of *Apc* rarely present with renal cell carcinoma, but mice with a renal specific deletion of *Apc* develop cancer similar to those with VHL mutations (Sansom et al., 2005). In addition, the promoter of the *Apc* gene is hypermethylated in up to 30% of renal carcinomas (Dulaimi et al., 2004),

suggesting *Apc* loss/reduction may play an important role in the progression of renal carcinoma. Indeed using the *AhCre* transgene which yields sporadic constitutive Cre expression within all cell lineages of the kidney, only 1/3 of mice develop renal carcinoma, despite showing the presence of small premalignant lesions from 2 months of age (Sansom et al., 2005). This suggests that *Apc* loss can predispose to renal carcinoma but *Apc* gene loss alone is a very poor initiating event. In contrast deletion of *Apc* within the intestinal epithelium rapidly leads to a marked ‘crypt-progenitor cell-like’ phenotype (Sansom et al., 2004) and moreover, deletion of *Apc* within the LGR5⁺ stem cell zones leads to adenoma formation in as little as 2 weeks, suggesting the importance of the cells that are targeted (Barker et al., 2009).

1.8.3. The Role of Wnt Signalling in Human UCC

Germline and somatic mutations of *APC* are found in the majority of colorectal cancers (Kinzler et al., 1991, Cottrell et al., 1992, Rubinfeld et al., 1993). However, in the case of bladder carcinoma, controversy surrounds the occurrence of somatic mutations in key components of the pathway; *APC* (Miyamoto et al., 1996, Bohm et al., 1997, Stoehr et al., 2002, Urakami et al., 2006a) and β -catenin (Burger et al., 2008, Shiina et al., 2002, Shiina et al., 2001). Miyamoto and colleagues found LOH of the *APC* locus in only 1 of 16 (6%) of UCCs (Miyamoto et al., 1996). However another study reported LOH for the *APC* locus in 50% of the 30 tumours (Bohm et al., 1997). In a larger study Stoehr and colleagues found LOH in 10% of 72 tumours, but no *APC* mutations in 22 tumours and 4 cell lines, apart from a common SNP at codon 1493. All of these studies, however included both non-invasive and invasive tumours, and utilised them as a single entity. Recent human UCC sequencing by the Sanger institute in Cambridge has revealed *APC* mutation in 11 out of 93 (12%) samples (http://www.sanger.ac.uk/perl/genetics/CGP/cosmic?action=bycancer&ln=APC&sn=urinary_tract&ss=bladder).

Many of these studies have demonstrated immunohistochemical upregulation of β -catenin, the key protein in this pathway (Kashibuchi et al., 2006, Nakopoulou et al., 2000, Shimazui et al., 1996, Zhu et al., 2000, Garcia et al., 2000). Urakami and colleagues showed that CpG hypermethylation of Wnt inhibitory factor-1 (*Wif-1*) was a frequent event in bladder tumourigenesis (Urakami et al., 2006b). Most recently Kastiris and colleagues demonstrated *APC* missense (13%) and frameshift (3%) deletions adjacent to the β -catenin binding sites in bladder tumours (Kastiris *et al.*, 2009). They found either *APC* mutations or β -catenin accumulation resulted in shorter disease free interval, and a shorter disease specific survival in multivariate analysis. Similarly, epigenetic silencing of the four secreted frizzled receptor

proteins (SFRP), antagonists of the Wnt signalling pathway, has been demonstrated as an independent predictor of invasive bladder cancer (Marsit *et al.*, 2005). In a cohort of 355 patients, a linear relationship between the magnitude of the risk of invasive disease and the number of SFRP genes methylated was observed ($p < 0.0004$) with a subsequent reduction in overall survival ($p < 0.0003$). Therefore these studies suggest a key role of deregulation of Wnt signalling in bladder cancer, a finding that I tested in this thesis.

1.9. KEGG Pathway of UCC

KEGG (Kyoto Encyclopaedia for Genes and Genome) is a bioinformatics resource that has been developed to attempt to link the common genetic mutations and pathways occurring in human cancer including UCC. The pathways for UCC are reproduced below:

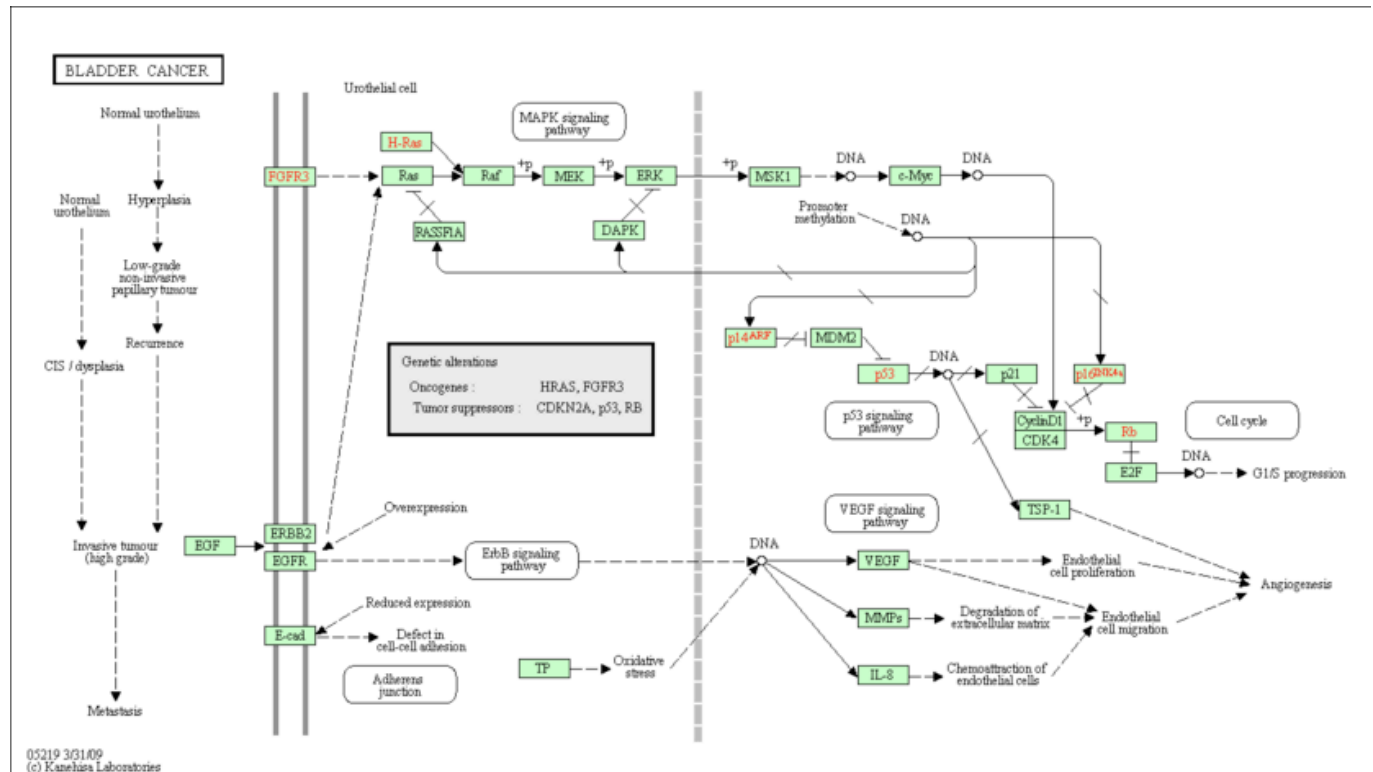


Figure 1.10: KEGG Pathway of UCC

(<http://www.genome.jp/kegg/pathway/hsa/hsa05219.html>)

1.10. Research in Progress and Outstanding Research Questions

The currently available models have provided researchers with a wealth of information regarding potential molecular mechanisms and pathways involved in bladder cancer. However, many limitations still exist. No model as yet demonstrated metastasis to the skeletal system. A transgenic mouse that demonstrates these would be invaluable in preclinical therapeutic models. Why spontaneous osseous lesions have not been achieved remains to be elucidated, but may be due to a variety of reasons including the murine platform representing fundamental pathophysiological differences (e.g. pelvic venous drainage), the inability to accurately detect the metastasis or whether the genetic defects I created in our current models are not sufficient to initiate bone metastasis.

As I have described there are a paucity of publications regarding therapeutic trials in murine models. As further novel genes and markers are identified in the human bladder carcinogenesis, it is essential that we base our murine models on these findings. Newer models will mimic human bladder tumourigenesis more closely and will offer attractive platforms for trials of novel agents.

The *in vivo* imaging of tumours has revolutionised the way researchers now manipulate murine models of cancer. The technology will allow one to follow disease progression as well as the effects of therapeutic interventions in a model system comparable to that of humans (Weissleder, 2002). The two most widely available imaging modalities currently are bioluminescent enzyme firefly luciferase and green fluorescent protein (GFP). GFP provides the benefit that one can directly monitor cells down to the single cell level, whilst luciferase only allows one to view derived pseudo-layered images. GFP allow does not require injection of a substrate. Despite this luciferase is much more sensitive and allows one to simultaneously monitor multiple mice (whereas GFP requires multiple excitation sources for

multiple mice) (Massoud and Gambhir, 2003, Choy et al., 2003). One of the most applied techniques uses bioluminescent imaging to noninvasively monitor the growth of luciferase-expressing carcinoma cells in vivo. In this thesis I plan to utilise both ultrasound and fluorescence based imaging techniques to image bladder tumours and assess their response to treatment.

1.11. Thesis Aims

- To investigate whether Wnt signaling is sufficient to drive tumourigenesis within the bladder urothelium
- To investigate the role of Wnt signaling within the bladder urothelium as a progressor mutation of UCC in the background of mutations to other key oncogenic/tumour suppressors (*PTEN*, *Ras*, *p21*, *FGFR3*)
- To utilise the above transgenic mice to develop better models of UCC

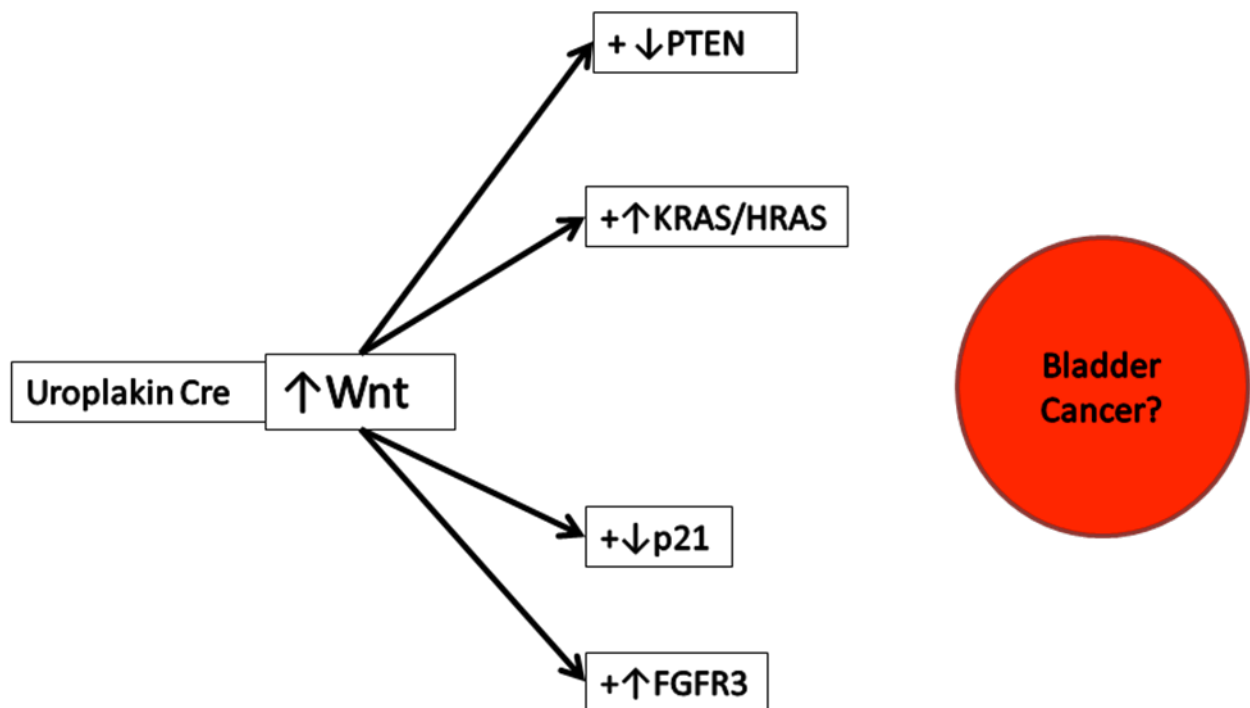


Figure 1.11: Outline of research

Chapter 2: Material and Methods

2.0. Material and Methods

2.1. Statement of Contribution

- Choosing which mice were to be mated to give genotypes required (animal staff physically set up matings, carried out weanings and tail tipplings)
- Tumour surveillance of mice (3 x weekly)
- Drug treatment of all mice
- Harvesting of organs
- Imaging of organs via US and OV100
- All immunohistochemistry
- All counting/scoring (double scored with Lukram Babloo Singh LBS)
- Extracting DNA and carrying out all PCR reactions at least once for each genotype (using published protocols for each mouse strain). When reaction was confirmed as working, gel product sent to Transnetyx, IncTM (TN, USA) to allow them to sequence product and develop qPCR based genotyping assay to outsource any subsequent genotyping.

2.2. Generation of Mice colonies

Mouse Experiments: All experiments were performed under the UK Home Office guidelines (project license 60/3947, personal license 60/11372). All mice were of a mixed background (derived predominantly from FVB/N [*H-Ras*^{Q61L}, *Fgfr3* K644E, *Fgfr3* K644M] and C57BL/6 [*Apc*^{fl/+}, *β-catenin*^{exon3/+}, *GSK3αβ*^{fl/fl}, *K-Ras*^{G12D/+}, *p21*^{-/+}, *Pten*^{fl/+} and *Z/EGFP*] strains) mice) and littermates were used as control mice. All mice were maintained under non-barrier conditions and given a standard diet (Harlan) and water *ad libitum*. The Biological services department at the Beatson Institute provided animal husbandry including setting up matings, weaning pups, and tail tipping for genotyping.

The following cre were used: Uroplakin II (*UroII*CRE⁺) (Zhang *et al.*, 1999) and *AhCreER*^T mice (Kemp *et al.*, 2004).

They were intercrossed with the following alleles in this thesis: *Apc*^{fl/+} (Shibata *et al.*, 1997), *β-catenin*^{exon3/+} (Harada *et al.*, 1999), *Fgfr3* K644E and *Fgfr3* K644M (Iwata *et al.*, 2000, Iwata *et al.*, 2001), *GSK3αβ*^{fl/fl} (Patel *et al.*, 2008, MacAulay *et al.*, 2007), the rabbit *H-Ras*^{Q61L} transgene (Zhang *et al.*, 2001), *K-Ras*^{G12D/+} (Jackson *et al.*, 2001), *p21*^{-/+} (Deng *et al.*, 1995), *Pten*^{fl/+} (Lesche *et al.*, 2002) and the *Z/EGFP* allele (Novak *et al.*, 2000) (Table 2.1).

Transgene	Description	Reference
<i>UroIIICRE⁺</i>	Uroplakin II is a protein expressed throughout the urothelial layers in mice. The 3.6-kb 5'-upstream sequence of mouse <i>Uroplakin II</i> promoter has been reported to successfully drive the expression of proteins including SV40 large T antigen and H-Ras. Previous studies (as well as ours) have shown that the <i>UroIIICRE⁺</i> mice exhibit bladder specific recombination.	(Zhang <i>et al.</i> , 1999)
<i>Ah CreER^T</i>	This is the cytochrome p450 inducible <i>AhCreER^T</i> transgene. Following administration of both β -naphthoflavone and tamoxifen, this yields cre-mediated recombination within the urothelium of the bladder (as well as the intestine and liver).	(Kemp <i>et al.</i> , 2004)
<i>Apc^{fl/+}</i>	<i>loxP</i> sites have been inserted into the introns around <i>Apc</i> exon 14, inducing a frameshift mutation at codon 580, resulting in the mutant allele (<i>Apc^{580S}</i>) being introduced in a Cre specific manner.	(Shibata <i>et al.</i> , 1997)
<i>β-catenin^{exon3/+}</i>	In this transgene the β -catenin gene has its exon3 flanked by <i>loxP</i> sequences. On addition of Cre recombinase, exon3 is deleted. As this exon contains the residues that are phosphorylated by GSK3 β , leading to β -catenin degradation, β -catenin will therefore accumulate to drive Wnt signalling.	(Harada <i>et al.</i> , 1999)
<i>Fgfr3 K644E and K644M</i>	Both lines carry a neomycin resistant gene (<i>neo</i>) flanked by <i>loxP</i> sites in the intron approximate to the exon with the K644 mutations. This <i>neo</i> insertion is known to suppress the expression of <i>Fgfr3</i> mutant allele in the absence of Cre recombination. In the presence of Cre, the <i>neo</i> gene is excised allowing expression of the mutant <i>Fgfr3</i> protein, with a pattern and protein expression level similar to those of the age matched wildtype	(Iwata <i>et al.</i> , 2000, Iwata <i>et al.</i> , 2001)
<i>GSK3$\alpha\beta$^{fl/fl}</i>	<i>GSK3α^{fl/fl}</i> were generated with <i>loxP</i> sites flanking exon2 (by homologous recombination). Cre recombination results in a loss of the protein. <i>GSK3β^{fl/fl}</i> were generated with <i>loxP</i> sites flanking exon2 (by homologous recombination). Cre recombination results in transcription of a non-functional protein form of GSK3 β .	(Patel <i>et al.</i> , 2008, MacAulay <i>et al.</i> , 2007)

<i>H-Ras</i> ^{Q61L}	Constitutively active rabbit <i>H-Ras</i> ^{Q61L} mutant had been previously shown to share all the functional characteristics of codon 12 and 13 mutants and to be fully capable of transforming culture NIH 3T3 cells. Transgene drive by <i>UPII</i> promoter. Low copy number (2 copies) used in this thesis	(Zhang et al., 2001)
<i>K-Ras</i> ^{G12D/+}	A <i>Lox-Stop-Lox K-Ras</i> conditional mouse strain, in which expression of oncogenic K-Ras is controlled by a removable transcriptional termination Stop element. The endogenous K-Ras locus is targeted in the <i>LSL-K-Ras G12D</i> strain and, therefore, endogenous levels of oncogenic K-Ras G12D protein are expressed following removal of the Stop element.	(Jackson et al., 2001)
<i>p21</i> ^{-/+}	This targeting construct <i>p21</i> ^{neo} was used to delete exon 2 of the <i>p21</i> ^{CIP1/WAP1} gene. This exon encodes about 90% of coding sequence of the <i>p21</i> ^{CIP1/WAP1} protein, and Cre recombination results in loss of the protein.	(Deng et al., 1995)
<i>Pten</i> ^{fl/+}	Conditional inactivatable <i>Pten</i> allele (where exon 5 is flanked by <i>loxP</i> sites). This encodes for the phosphatase domain of PTEN in which many tumor-associated mutations have been detected.	(Lesche et al., 2002)
<i>Z/EGFP</i>	The <i>Z/EGFP</i> transgene results in the expression of β -galactosidase by most tissues via a β -geo insert, which is flanked by <i>loxP</i> sites. The presence of Cre recombinase results in the excision of the β -geo, activating the constitutive expression of GFP.	(Novak et al., 2000)

Table 2.1: Description of transgenes used in this thesis

2.2.1. Mouse experiments for Chapter 3 (β -Catenin activation synergises with PTEN loss to cause bladder cancer formation)

To achieve urothelial specific expression of activated β -catenin and PTEN loss, these mice were interbred with mice carrying the uroplakin II (*UroII*CRE+) Cre transgene to generate the following cohorts $UroII$ CRE⁺ β -catenin^{+/+}, $UroII$ CRE⁺ β -catenin^{exon3/+} and $UroII$ CRE⁺ β -catenin^{exon3/exon3}, $UroII$ CRE⁺ *Pten*^{fl/+}, $UroII$ CRE⁺ *Pten*^{fl/fl}, $UroII$ CRE⁺ β -catenin^{exon3/+} *Pten*^{fl/+}, $UroII$ CRE⁺ β -catenin^{exon3/exon3} *Pten*^{fl/+}, $UroII$ CRE⁺ β -catenin^{exon3/exon3} *Pten*^{fl/fl}, β -catenin^{exon3/+} *Pten*^{fl/fl} and $UroII$ CRE⁺ β -catenin^{exon3/+} *Pten*^{fl/+}.

I also bred the *AhCreER*^T mice to *Apc*^{fl/fl}, *Pten*^{fl/fl} and *GSK3 α* ^{fl/fl} mice to generate the following cohorts *AhCreER*^T *Apc*^{fl/fl}, *AhCreER*^T *Apc*^{fl/fl} *Pten*^{fl/fl} and *AhCreER*^T *GSK3 α* ^{fl/fl}.

For Cre induction, *AhCreER*^T mice were given 3 injections intra-peritoneally (IP) of 80mg/kg β -naphthoflavone and Tamoxifen in a single day, which yields nearly 100% constitutive recombination in the murine small intestine (Marsh et al., 2008).

Approximately a quarter of each cohort were also bred with the *Z/EGFP* allele (Novak et al., 2000). This is a double reporter mouse line that expressed enhanced GFP upon Cre-mediated recombination.

Tumourigenic cohorts (n>20 for each genotype) were aged, and examined three times a week by myself for signs of urinary tract disease. These included blood in the urine, hunching, and swollen kidneys; which was investigated through scruffing the mouse and gently feeling for an enlarged kidney, renal pelvis or urinary bladder that was indicative of a tumour. This was the criterion for sacrifice of the animal. Metastatic disease was assessed both at a macroscopic levels in organs (lung, liver, spleen, diaphragm and local lymph nodes) and at a microscopic level by looking at multiple sections through the organ of interest.

2.2.2. Mouse experiments for Chapter 4 (β -Catenin activation synergises with Ras activation to cause bladder cancer formation)

Uroplakin II Cre mouse (*UroIIICRE*⁺) mice were intercrossed with mice harbouring *Z/EGFP*, *β -catenin*^{exon3/+}, *K-Ras*^{G12D/+}, the *H-Ras*^{Q61L} transgene and *p21*^{-/-} in the following combinations *UroIIICRE*⁺*K-Ras*^{G12D/+}, *H-Ras*^{Q61L}, *UroIIICRE*⁺ *β -catenin*^{exon3/exon3} *K-Ras*^{G12D/+}, *UroIIICRE*⁺ *β -catenin*^{exon3/exon3} *H-Ras*^{Q61L}, *UroIIICRE*⁺ *p21*^{-/-} and *UroIIICRE*⁺ *β -catenin*^{exon3/exon3} *p21*^{-/-}.

Approximately a quarter of mice from each cohort were also bred with the *Z/EGFP* allele carrying mice.

Mice were assessed as per 2.2.1.

2.2.3. Mouse experiments for Chapter 5 (The FGFR3 mutation cooperates with K-Ras and β -catenin mutations to promote skin and lung but not bladder tumour formation)

UroIIICre⁺ mice were bred to lines carrying *Fgfr3*^{K644E}, *Fgfr3*^{K644M}, *K-Ras*^{G12D/+} and *β -catenin*^{exon3/+} to generate the following cohorts *UroIIICre*⁺*Fgfr3*^{+K644E} and *UroIIICre*⁺*Fgfr3*^{+K644M} *UroIIICre*⁺*Fgfr3*^{+K644E}*K-Ras*^{G12D/+} and *UroIIICre*⁺*Fgfr3*^{+K644E} *β -catenin*^{exon3/+}.

Approximately a quarter of mice from each cohort were also bred with the *Z/EGFP* allele carrying mice.

Mice were assessed as per 2.2.1.

2.3. Tissue isolation

For the analysis of urothelial cell carcinoma (UCC) cohorts, at the appropriate time, mice were culled and both kidneys, ureters and the urinary bladder were removed and fixed in 4% formalin, overnight at 4°C for no more than 24 hours before processing and were then paraffin embedded. For senescence associated β -galactosidase staining, urinary bladder and kidney were placed on a cork disk and covered in OCT fixative before being submerged into liquid nitrogen.

When urinary bladders were excised they were all emptied of urine. All bladders were processed and cut in the same manner by a single histology technician (Mr. Colin Nixon) to aid standardisation.

2.4. Genotyping of mice

When I started at the Beatson, genotyping was carried out in-house by the Genotyping facility. In 2009 this was outsourced to TransnetyxTM (TN, USA) who genotype based on real time PCR techniques.

2.4.1. DNA Extraction from tails

DNA was extracted from tails using the Puregene DNA Extraction kit. Tails were lysed overnight in 500µl of cell lysis solution (Puregene) and 10µl of proteinase K (20mg/ml, Sigma), shaken at 37°C. Tails were then left to cool at room temperature; 200µl of protein precipitation solution (Puregene) was added to each tube. These were vortexed and centrifuged at top speed for 5 minutes in a microfuge.

The supernatant was removed into a clean tube containing 500µl of isopropanol, vortexed and centrifuged at top speed for 5 minutes. The supernatant was poured off and the DNA pellet was left to dry overnight. DNA was resuspended in 500µl DNA hydration solution (Puregene).

2.4.2. Genotyping of Mice via PCR

Initially all genotyping of mice was done by genomic PCR (Polymerase Chain Reaction) from DNA extracted from tails (2.2.1) by the in-house genotyping facility. All PCR were done in 50µl volumes using 2.5µl of the tail DNA preparation. The groups that created the mice developed these protocols.

Apc^{fl} PCR Protocol

PCR mix

	μ l
5x Colorless GoTaq Flexi Buffer*	10
MgCl ₂ (25mM)	5
dNTPs (10mM)	0.4
Primer (100 μ M)	0.2 (of each)
Go Taq*	0.2

H₂O to final volume of 47.5 μ l

*GoTaq Flexi DNA Polymerase from Promega.

Primers

APC F = 5' GTT CTG TAT CAT GGA AAG ATA GGT GGT C 3'

APC R = 5' CAC TCA AAA CGC TTT TGA GGG TTG 3'

PCR Program: 95°C, 3min (95°C, 30s; 60°C, 30s; 72°C 1min) ₃₀ 72°C, 5min. 4°C, hold.

PCR products were run on a 2% gel.

Bands FLOX = 314bp

WT = 226bp

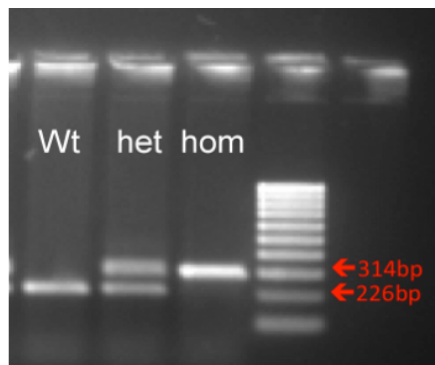


Figure 2.1: Apc^{fl} PCR

β -catenin^{exon3} PCR Protocol

PCR mix

	μ l
5x Colorless GoTaq Flexi Buffer*	10
MgCl ₂ (25mM)	5
dNTPs (10mM)	0.4
Primer (100 μ M)	0.2 (of each)
Go Taq*	0.2

H₂O to final volume of 47.5 μ l

*GoTaq Flexi DNA Polymerase from Promega.

Primers

β -catenin act F = 5' CTG CGT GGA CAA TGG CTA CT 3'

β -catenin act R = 5' TCC ATC AGG TCA GCT GTA AAA A 3'

PCR Program: 94°C, 2.5min (94°C, 30s; 60°C, 30s; 72°C 1min)₃₄ 72°C, 10min. 4°C, hold.

Products run on a 2% gel

Bands WT = 324bp

Dominant stable = ~500bp

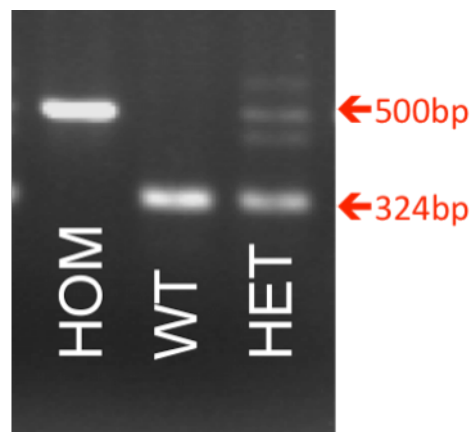


Figure 2.2: β -catenin^{exon3} PCR

Cre PCR Protocol

PCR mix

	μl
5x Colorless GoTaq Flexi Buffer*	10
MgCl ₂ (25mM)	5
dNTPs (10mM)	0.4
Primer (100 μM)	0.2 (of each)
Go Taq*	0.2

H₂O to final volume of 47.5 μl

*GoTaq Flexi DNA Polymerase from Promega.

Primers

CRE F = 5' TGA CCG TAC ACC AAA ATT TG 3'

CRE R = 5' ATT GCC CCT GTT TCA CTA TC 3'

PCR Program: 95°C, 3min (95°C, 30s; 55°C, 30s; 72°C 1min)₃₀, 72°C, 5min. 15°C, hold.

Bands CRE = 1000bp

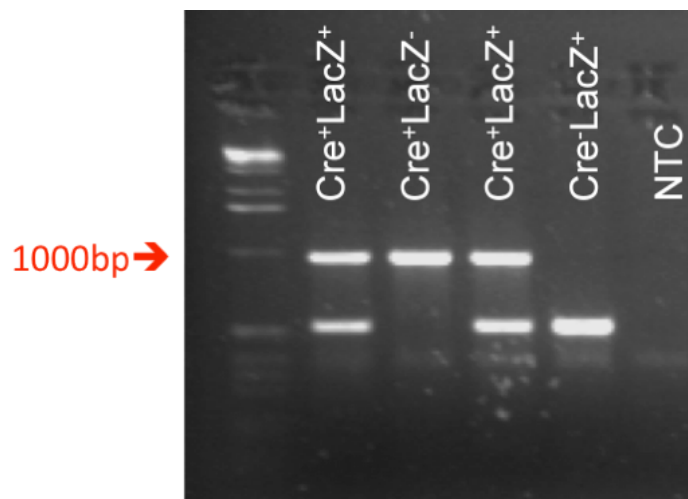


Figure 2.3: Cre PCR

Fgfr3 K644 Protocol

PCR Mix

	μ l
Buffer	5
MgCl ₂ (50mM)	2.5
dNTPs (10mM)	0.4
Primer (100 μ M)	0.1 (of each)
Platinum Taq	0.2
<i>H₂O to final volume of 47.5</i>	

Primers

F = 5' GGG TGA TGC TTT GCC TGA GC 3'

R = 5' TTC AGA TCT CCC TAC CCC CAT 3'

PCR Program: 94°C, 3min (94°C, 1min; 60°C, 1min; 72°C 1min)₃₀, 72°C, 7min. 15°C, hold.

PCR product was digested with *BbsI*

Bands WT = Double band of ~120bp

+/K644 = Two bands of ~120bp and 350bp

K644/K644 =Band of 350bp only

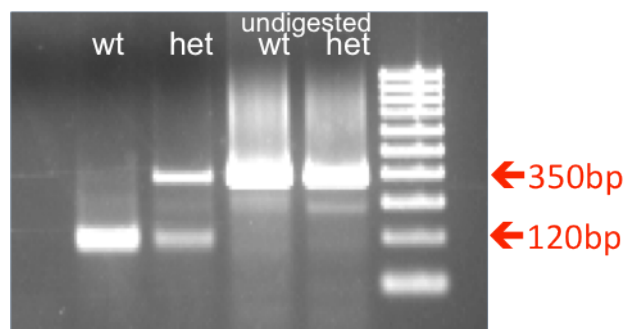


Figure 2.4: Fgfr3 K644 PCR

GSK3 α PCR Protocol

PCR Mix

	μ l
Buffer	10
MgCl ₂ (50mM)	5
dNTPs (10mM)	0.4
Primer (100 μ M)	0.2 (of each)
Go Taq	0.2

H₂O to final volume of 47.5

Primers

GSK3 α F = 5' CCC CCA CCA AGT GAT TTC ACT GCT A 3'

GSK3 α R = 5' AAC ATG AAA TTC CGG GCT CCA ACT CTA T 3'

PCR Program: 94°C 2mins (94°C, 30s;56°C, 30s; 68°C 1min)₃₅, 68°C 7 min; 15°C, hold.

Bands (NULL = 250bp)

WT = 600bp

FLOX= 750bp

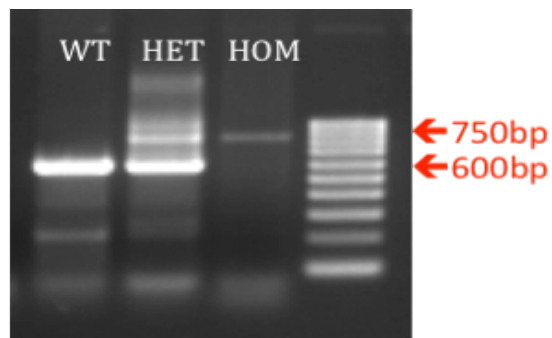


Figure 2.5: GSK3 α PCR

GSK3 β PCR Protocol

PCR Mix

	μ l
Buffer	10
MgCl ₂ (50mM)	5
dNTPs (10mM)	0.4
Primer (100 μ M)	0.2 (of each)
Go Taq	0.2

H₂O to final volume of 47.5

Primers

GSK3 β fl F = 5' GGG GCA ACC TTA ATT TCA TT 3'

GSK3 β fl R = 5' TCT GGG CTA TAG CTA TCT AGT AAC G 3'

PCR Program: 94°C 2mins (94°C, 30s; 56.5°C, 30s; 68°C 1min)₃₅, 68°C 7 min; 15°C, hold.

Bands WT = 600bp

FLOX= 1100bp

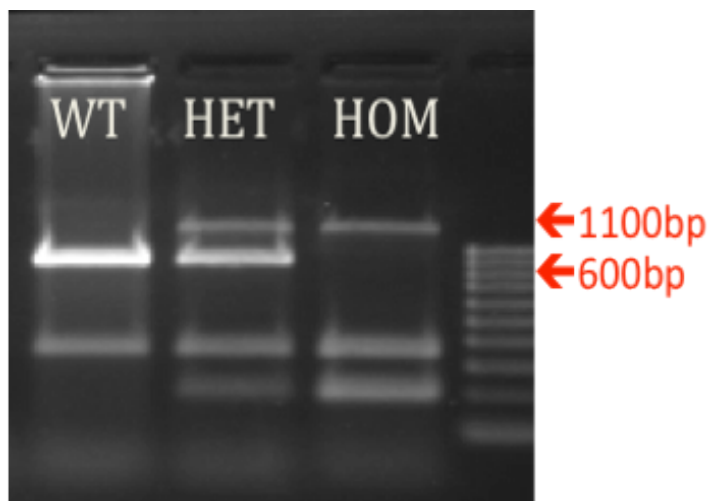


Figure 2.6: GSK3 β PCR

Rabbit H-Ras^{Q61L} Transgene PCR Protocol

PCR mix

	μl
5x Colorless GoTaq Flexi Buffer*	10
MgCl ₂ (25mM)	5
dNTPs (10mM)	0.4
Primer (100 μM)	0.2 (of each)
Go Taq*	0.2

H₂O to final volume of 47.5 μl

*GoTaq Flexi DNA Polymerase from Promega.

Primers

RABBIT HRAS F = 5' CGGCGGTGTAGGCAAGAGCGC 3'

RABBIT HRAS R = 5' TCTTGGCCGAGGTCTCGATA 3'

PCR Program: 94°C, 5min (94°C, 1 min; 64°C, 30s; 72°C 1min)₃₅, 72°C, 8min. 4°C, hold.

Bands RABBIT HRAS = ~500bp

Only HET should have a band here

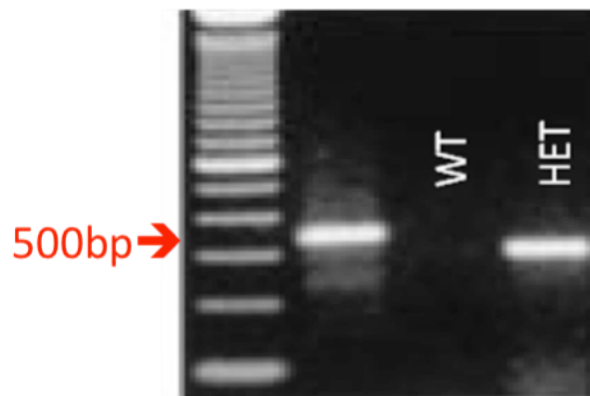


Figure 2.7: Rabbit H-Ras^{Q61L} PCR

K-Ras G12D PCR Protocol (Split PCR)

PCR Mix

	μl
Buffer	5
MgCl ₂ (50mM)	2.5
dNTPs (10mM)	0.4
Primer (100 μM)	0.1 (of each)
Platinum Taq	0.2
<i>H₂O to final volume of 47.5</i>	

Note: This is a duplex PCR

WT Reaction use primers KRasG12D WT and KRasG12D Universal

LSL Reaction use primers KRasG12D Mut and KRasG12D Universal

Primers

KRasG12D WT = 5' GTC GAC AAG CTC ATG CGG GTG 3'

KRasG12D Universal = 5' CCT TTA CAA GCG CAC GCA GAC TGT AGA 3'

KRasG12D Mut = 5' AGC TAG CCA CCA TGG CTT GAG TAA GTC TGC A 3'

PCR Program: 94°C 3min (94°C, 30s; 60°C, 1min 30; 72°C 1min)₃₅, 72°C, 5min. 4°C hold.

Bands WT = 500bp

LSL = 550bp

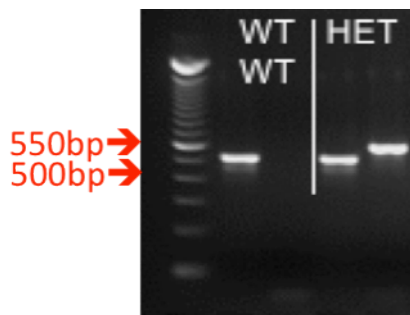


Figure 2.8: K-Ras G12D PCR

Pten^{fl} PCR Protocol

PCR Mix

	μ l
Buffer	5
MgCl ₂ (50mM)	2.5
dNTPs (10mM)	0.4
Primer (100 μ M)	0.1 (of each)
Platinum Taq	0.2

H₂O to final volume of 47.5

Primers

PTEN F1 F = 5' CTC CTC TAC TCC ATT CTT CCC 3'

PTEN F1 R = 5' ACT CCC ACC AAT GAA CAA AC 3'

PCR Program: 95°C, 2min 30s (94°C, 1min; 58°C, 1min; 72°C 1min)₃₅, 72°C, 10min. 15°C, hold.

Bands WT = 228bp

Flox = 335bp

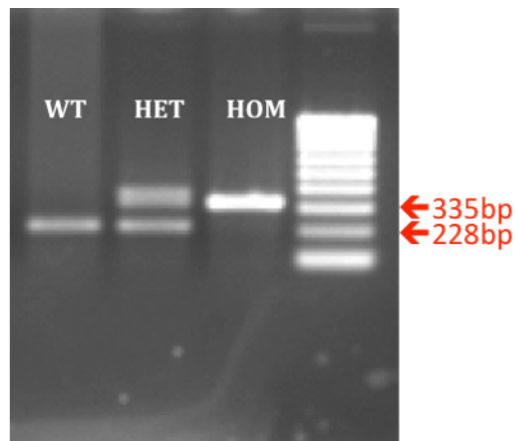


Figure 2.9: Pten PCR

p21 PCR Protocol (Split PCR)

PCR Mix

	μl
Buffer	5
MgCl ₂ (50mM)	2.5
dNTPs (10mM)	0.4
Primer (100 μM)	0.1 (of each)
Platinum Taq	0.2
<i>H₂O to final volume of 47.5</i>	

Note: This is a duplex PCR

WT Reaction use primers p21F and p21R

Mutant Reaction use primers p21-5 and R1N-1A

Primers

P21 F = 5' TCT TGT GTT TCA GCC ACA GGC 3'

P21 R = 5' TGT CAG GCT GGT CTG CCT CC 3'

P21-5. = 5' ATT TTC CAG GGA TCT GAC TC 3'

R1N-1A = 5' CCA GAC TGC CTT GGG AAA AGC 3'

PCR Program: 95°C, 2min (95°C, 30s; 59°C, 30s; 72°C, 1min)₃₅, 72°C, 3min. 4°C hold.

Bands WT = 430bp

NULL = 150bp



Figure 2.10: p21 PCR

Z/EGFP (GFP) PCR Protocol

PCR Mix

	μl
5x Colorless GoTaq Flexi Buffer*	10
MgCl ₂ (25mM)	5
dNTPs (10mM)	0.4
Primer (100 μM)	0.2 (of each)
Go Taq*	0.2
<i>H₂O to final volume of 47.5 μl</i>	

*GoTaq Flexi DNA Polymerase from Promega.

Primers

Bry-GFP F = 5' ACG TAA ACG GCC ACA AGT TC 3'

Bry-GFP R = 5' AAG TCG TGC TGC TTC ATG TG 3'

PCR Program: 95°C, 3min (95°C, 30s; 58°C, 45s; 72°C 1min) ₄₀ 72°C, 5min. 4°C, hold.

Band GFP = 187bp

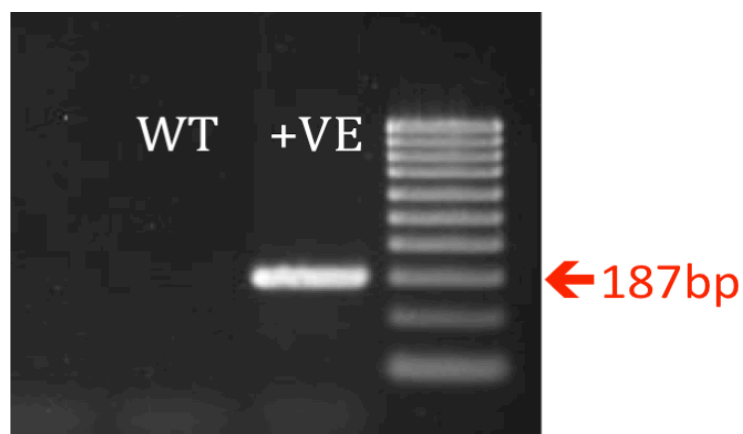


Figure 2.11: Z/EGFP PCR

2.4.3. Summary of PCR reactions

PCR	Primer Sequences (5' to 3')	PCR Program	Expected Products
Apc Flox	APC F = GTT CTG TAT CAT GGA AAG ATA GGT GGT C APC R = CAC TCA AAA CGC TTT TGA GGG TTG ATT C	95°C, 3min (95°C, 30s; 60°C, 30s; 72°C 1min) ³⁰ 72°C, 5min. 4°C, hold.	FLOX = 314bp WT = 226bp
β-catenin exon3	β-catenin F = CTG CGT GGA CAA TGG CTA CT β-catenin R = AAA AAT GTC GAC TGG ACT ACC T	94°C, 2.5min (94°C, 30s; 60°C, 30s; 72°C 1min) ³⁴ 72°C, 10min. 4°C, hold.	WT = 324bp Dominant stable = ~500bp
Cre	CRE F = TGA CCG TAC ACC AAA ATT TG CRE R = ATT GCC CCT GTT TCA CTA TC	95°C, 3min (95°C, 30s; 55°C, 30s; 72°C 1min) ³⁰ 72°C, 5min. 15°C, hold.	CRE = ~1000bp
FGFR3 K644	F = GGG TGA TGC TTT GCC TGA GC R = TTC AGA TCT CCC TAC CCC CAT	94°C, 3min (94°C, 1min; 60°C, 1min; 72°C 1min) ³⁰ 72°C, 7min. 15°C, hold.	Double band of ~120bp +/K644 = Two bands of ~120bp and 350bp K644/K644 = Band of 350bp only
GSK3α null	GSK3α F = CCC CCA CCA AGT GAT TTC ACT GCT A GSK3α R = AAC ATG AAA TTC CGG GCT CCA ACT CTA T	94°C 2mins (94°C, 30s; 56°C, 30s; 68°C 1min) ³⁵ 68°C 7 min	WT = 600bp NULL = 250bp
GSK3βfl	GSK3βflF = GGG GCA ACC TTA ATT TCA TT GSK3βflR = TCT GGG CTA TAG CTA TCT AGT AAC G	94°C, 2min 30s (94°C, 30s; 56.5°C, 30s; 68°C, 1min, 25s) ³⁰ 68°C, 7min.	FLOX = 1100bp WT = 895bp

Rabbit H-Rqw Transgene	RABBIT HRAS F = CGGCGGTGTAGGCAAGAGCGC RABBIT HRAS R = TCTTGGCCGAGGTCTCGATA	94°C, 5min (94°C, 1 min; 64°C, 30s; 72°C 1min) for 35 cycles, 72°C, 8min. 4°C, hold.	RABBIT HRAS = ~500bp
K-Ras^{G12D} (Duplex PCR)	KRasG12D WT = GTC GAC AAG CTC ATG CGG G KRasG12D Universal = CGC AGA CTG TAG AGC AGC G KRasG12D Mut = CCA TGG CTT GAG TAA GTC TGC	94°C, 3min (94°C, 30s; 60°C, 1.5min; 72°C, 1min) 35 72°C, 5min. 4°C hold.	WT = ~500bp LSL = ~550bp
p21 Null (Duplex PCR)	P21 F = TCT TGT GTT TCA GCC ACA GGC P21 R = TGT CAG GCT GGT CTG CCT CC (WT PCR)	95°C, 2min (95°C, 30s; 59°C, 30s; 72°C, 1min) 35 72°C, 3min. 4°C hold.	WT = 430bp
	P21-5. = ATT TTC CAG GGA TCT GAC TC 3' R1N-1A = CCA GAC TGC CTT GGG AAA AGC 3' (P21 interrupted PCR)	95°C, 2min (95°C, 30s; 59°C, 30s; 72°C, 1min) 35 72°C, 3min. 4°C hold.	NULL = 150bp
Pten Flox	PTEN F = CTC CTC TAC TCC ATT CTT CCC PTEN-R = ACT CCC ACC AAT GAA CAA AC	95°C, 2min 30s (94°C, 1min; 58°C, 1min; 72°C 1min) 35 72°C, 10min. 15°C, hold.	WT = 228bp Flox = 335bp
Z/EGFP	GFP F = ACG TAA ACG GCC ACA AGT TC GFP R = AAG TCG TGC TGC TTC ATG TG	95°C, 3min (95°C, 30s; 58°C, 45s; 72°C 1min) 40 72°C, 5min. 4°C, hold.	GFP = 187bp

2.5. Rapamycin Treatment

Mice were also treated with either Rapamycin (LC laboratories, Woburn, MA) or vehicle treatment. This was provided once daily via intraperitoneal (i.p.) at 10mg/kg *in vivo* for 4 weeks. The i.p. solution was prepared as an aqueous solution with a final concentration of 4% ethanol, 5% polyethylene glycol and 5% Tween 80 immediately before injection (Namba et al., 2006).

2.6. Assaying urothelial lesions *in vivo*

At each indicated time point, a minimum of three animals were killed and the urinary bladder was removed. Urine was removed and the bladder was fixed overnight in 4% formalin before processing. Haematoxylin and Eosin (H&E) stained sections were made and the number of lesions were counted using the Olympus BX51 microscope. At least 3 sections were counted from each mouse and the number of lesions was averaged over these 3 slides to give an average lesion count for that mouse. For each genotype, 3 age-matched mice were used. Statistics (Mann Whitney tests) were performed using Minitab v.15. In Boxplots the thick bar represents median, and the box represents the inter-quartile range.

2.6.1. Assaying proliferation *in vivo*

In order to examine levels of proliferation mice were injected with 250ul of bromodeoxyuridine (BrdU) (Amersham) two hours prior to being sacrificed (50mg/kg). Immunohistochemical staining for BrdU was then performed using an anti-BrdU antibody (BD 1:50). At least 3 mice were used for each genotype and timepoint. To examine levels of proliferation, following a two-hour BrdU pulse chase, total numbers of BrdU positive cells per lesion/tumour were counted.

To quantify levels of proliferation between different cohorts of mice, at least 3 mice of each genotype were injected with BrdU two hours prior to being sacrificed. BrdU immunohistochemistry was then performed on paraffin embedded urinary bladder sections of these mice.

Statistics (Mann Whitney tests) were performed using Minitab v.15. In Boxplots the thick bar represents median, and the box represents the inter-quartile range.

2.7. Immunohistochemistry

2.7.1. Immunohistochemistry on frozen sections:

Senescence associated β -galactosidase:

Frozen sections of either kidney or urinary bladder were cut into 3 μ m sections on Poly-L-lysine slides (Sigma). Sections were then thawed at room temperature for 30 minutes. The senescence β -galactosidase staining kit from Cell signalling (# 9860) was used. Slides were then fixed with 1x fixative solution from the kit for 10 minutes at room temperature. Slides were then washed 2x in dH₂O. A 1x staining solution from the kit was then prepared and the pH was adjusted to 5.5. Slides were incubated with the staining solution overnight at 37°C. A small piece of parafilm was applied to each slide to ensure that the staining solution did not evaporate off. The following day excess staining solution was removed from the slides and the slides were counter stained with nuclear fast red for 5 minutes. Slides were then washed in dH₂O for 5 minutes. Slides were mounted using DPX mounting medium.

2.7.2. Immunohistochemistry on paraffin sections:

For all immunohistochemistry on paraffin sections, except for β -catenin, antigen retrieval was performed with citrate buffer either in the microwave or in the water bath (protocols below)

Microwave antigen retrieval:

Solution A (0.1M):

10.5g of Citric Acid (molecular weight 192.12g: $10.5\text{g}/192.12\text{g/mole} = 0.055$ moles)

500 mls dH₂O ($M = 0.055$ moles/ 0.500 L = $0.110\text{M} = 0.1\text{M}$)

Solution B (0.5M):

29.4g Sodium Citrate (molecular weight = 58.44g: $29.4\text{g}/58.44\text{g/mole} = 0.503$ moles)

1 litre dH₂O ($M = 0.503$ moles/ 1.000 L = $0.503\text{M} = 0.5\text{M}$)

To make a 1.5L solution: 27mls of solution A ($[27\text{ml} \times 0.1\text{M}]/1500\text{ml} = 1.8\text{mM}$) was mixed with 123mls of solution B ($[123 \times 0.1\text{M}]/1500\text{ml} = 8.2\text{mM}$) and made up to 1.5L with dH₂O and adjusted to pH 6.0. The 1.5 L solution was placed in a pressure cooker and microwaved for 20 minutes or until the solution was boiling. Slides were added and microwaved until the cooker was pressurised and then boiled for another 3-4 minutes.

The pressure cooker was then removed and placed into a sink filled with cold water. Slides were removed and allowed to cool in solution for 20 minutes.

Water Bath antigen retrieval:

Citrate Buffer (Labvision) was diluted 1/10 in distilled water and 50ml of diluted citrate buffer solution was placed into a glass coplin jar. The coplin jar was immersed into a water bath and pre-heated to 99.9°C. Slides were immersed into a preheated solution and boiled for

20 minutes. The coplin jar was removed from the water bath and allowed to cool for 30 minutes at room temperature in the solution.

2.7.3. Immunohistochemistry for p21:

The staining was done on paraffin embedded, 'quick fixed' samples. This entailed the specimens being placed in a formalin fixative for less than 24 hours. 3µm sections of tissue were cut onto Poly-L-lysine slides (Sigma). Sections were dewaxed by placing into xylene for 20 minutes. They were rehydrated through graded ethanol solutions (absolute alcohol, 70% ethanol) and then into water. Antigen retrieval was performed as per the microwave method. Slides were washed 3x5 minutes in PBS. They were then blocked for 30 minutes with 5% goat serum in PBS. Again they were washed 3x5 minutes with PBS. Slides were then incubated with Santa Cruz anti-p21 (M-19) (rabbit polyclonal) diluted 1/500 in 5% goat serum /PBS for 1 hour at room temperature. After this slides were washed again 3x5 minutes with PBS. Slides were then incubated for 30 minutes with biotinylated secondary antibody from rabbit ABC kit (Vector Laboratories). Slides were washed 3x5 minutes with PBS. Slides were then incubated with ABC solution for 30 minutes; 2 drops of solution A + 2 drops of solution B in 5 ml 5% goat serum/PBS. (made up 30 minutes earlier). DAB reagents were then mixed in the ratio 1ml substrate buffer to 1 drops chromogen. This was applied to slides and incubated for 5-10mins. Slides were wash 3x5 minutes with PBS. Slides were then transferred to dH₂O.

Slides were then counterstained in Haematoxylin for approximately 60 seconds before washing in running tap water for 5 minutes. Slides were dehydrated by washing in increasing concentrations of alcohols (1x5 minute wash in 70% alcohol, 2x5 minute washes in 100%

alcohol) before being placed in xylene for 2x10 minute washes. Slides were then mounted using DPX mounting medium.

2.7.4. Immunohistochemistry for p16:

Immunohistochemistry was performed as in 2.7.3. Exceptions: Slides were incubated with primary antibody to p16 (Santa Cruz M-156) 1/25 in 5% goat serum PBS for 1 hour at room temperature. Slides were then incubated for 30 minutes with biotinylated secondary antibody from rabbit ABC kit (Vector Laboratories).

2.7.5. Immunohistochemistry for p19:

Immunohistochemistry was performed as in 2.7.3. Exceptions: Antigen retrieval was performed as per the water bath method. Slides were incubated with primary antibody p19/ARF 1/300 (Upstate) in 5% goat serum PBS overnight at 4⁰C. Slides were then incubated for 30 minutes with biotinylated secondary antibody from rabbit ABC kit (Vector Laboratories).

2.7.6: β -Catenin Immunohistochemistry:

Slides were cut and rehydrated as in 2.7.3. Slides were blocked for 30-45 minutes in the following block; 1 litre stock = 4.16g citric acid, 10.76g Na₂HPO₄ (DiSodium Hydrogen Phosphate 2 hydrate), 1g NaAz (Sodium Azide); add fresh H₂O₂ to 1.5%. For antigen retrieval, slides were boiled in a water bath for 50 minutes in Tris EDTA; 1 litre stock = 242g Tris, 18.6g EDTA. (10mM Tris Base, 1mM EDTA Solution). For working solution, 30ml stock was diluted in 1500ml dH₂O, adjusted to pH to 8.0 with HCl. Slides were allowed to

cool for 1 hour. Slides were then blocked for 30 minutes in 1% BSA in PBS. Slides were then incubated with β -catenin antibody (mouse monoclonal; C19220, Transduction Laboratories) 1/50 in 1%BSA/PBS for 2 hours at room temperature. Then slides were washed 3x in PBS. Incubate slides with HRP-labelled polymer from Mouse Envision+ system (Dako systems) for 1 hour at room temperature. Washed slides 3x in PBS. Slides were then developed with DAB, rehydrated and mounted as 2.6.3.

2.7.7. BrdU Immunohistochemistry:

Slides were cut and rehydrated as in 2.7.3. Antigen retrieval was performed as per the water bath method for 20 minutes. Slides were allowed to cool for 30 minutes at room temperature in solution. Slides were then rinsed in dH₂O. For prevention of endogenous staining, slides were blocked for 15 minutes in 1.5% H₂O₂ solution in dH₂O. Slides were then blocked for 30 minutes in 1%BSA in PBS. Slides were then incubated with a 1/500 dilution of mouse anti-BrdU (BD:cat N 347 580) diluted in PBS/1%BSA overnight at 4⁰C. Slides were then washed 3x in PBS and incubated with secondary polymer HRP-conjugated Envision+ (Mouse Envision+ system Dako Systems) for 1 hour at room temperature. Slides were then washed 3x 5 minutes in PBS. Slides were then developed with DAB, rehydrated and mounted as in 2.6.3.

2.7.8. p53 Immunohistochemistry:

Slides were cut and rehydrated as in 2.7.3. For epitope retrieval slides were steamed for 40-45 minutes in 10mM sodium citrate (pH 6.0), and cooled slowly at room temperature for 30 minutes. Slides were then incubated in methanol/ H₂O₂ (180 mL meth. /20 mL 30% H₂O₂) for 20 minutes at room temp. They were then rinsed profusely with H₂O. Slides were then blocked for 30 minutes at room temperature in normal serum from VECTASTAIN kit (4

drops serum/10 mL 1X PBS-0.1% Tween-20). Slides were then incubated with primary antibody diluted in blocking solution for 1-2 hours at room temperature (anti-p53 (CM5 from Vector laboratories) at 1:200 dilution), followed by 3x in PBS washes, and then incubated with secondary antibody from Vectastain Universal kit (1 drop/10 mL blocking solution) at room temperature for 30 minutes.

Slides were washed 3x in PBS and then incubated slides with ABC solution for 30 minutes (2 drops of solution A + 2 drops of solution B in 5 ml 5% goat serum/ PBS). Slides were then developed with DAB, rehydrated and mounted as in 2.6.3.

2.7.9. MCM2 Immunohistochemistry:

Slides were cut and rehydrated as in 2.7.3. Antigen retrieval was performed as per the microwave method. Slides were then blocked in 10% H₂O₂ made with dH₂O for 10 minutes at room temperature. Slides were then washed with PBS 3x5 minutes, before being blocked in 5% goat serum PBS for 30 minutes. Incubated slides with MCM2 (Cell signalling # 4007) rabbit polyclonal antibody at 1/200 with 5% goat serum PBS. Incubated overnight at 4°C. Washed slides with PBS 3x 5 minutes. Slides were then incubated with secondary polymer HRP-conjugated Envision+ (Rabbit Envision+ system Dako Systems) for 1 hour at room temperature. Slides were then washed 3x 5 minutes in PBS. Slides were then developed with DAB, rehydrated and mounted as in 2.6.3.

2.7.10. Ki67 Immunohistochemistry:

IHC was performed as per MCM2 IHC. Incubate with primary antibody: (Thermo; RM-9106) 1/250 in 5% goat serum PBS for 1 hour at room temperature. Wash slides with PBS 3x5

minutes. Slides were then incubated with secondary polymer HRP-conjugated Envision+ (Rabbit Envision+ system Dako Systems) for 1 hour at room temperature. Slides were then washed 3x5 minutes in PBS. Slides were then developed with DAB, rehydrated and mounted as in 2.6.3.

2.7.11. PTEN Immunohistochemistry

Slide were cut and rehydrated as per 2.7.3. Antigen retrieval was performed as per the water bath method. Slides were then blocked in 3% H₂O₂ made with dH₂O for 20 minutes at room temperature. Slides were then washed 2x5 minutes in dH₂O, then 1x 5min TBS/T. Slides were then blocked for 45mins in 5% Goat Serum diluted in TBS/T at room temperature, followed by incubation in PTEN (Cell signalling # 9559) rabbit monoclonal antibody at 1/100 with 5% goat serum TBS/T overnight at 4°C. Washed slides with TBS/T 3x5 minutes, and incubated with secondary biotinylated goat anti-rabbit secondary Ab (DAKO) diluted 1/200 in 5% Goat Serum in TBS/T for 30mins at room temperature. Unbound secondary antibodies were washed off by 3x5 minutes TBS/T and signal reported with ABC solution for 30 minutes. Slides were washed slides 3x in PBS. Slides were then developed with DAB, rehydrated and mounted as in 2.6.3.

2.7.12. p-AKT (Ser473) Immunohistochemistry

Immunohistochemistry as per 2.7.10 except slides were then incubated with p-AKT (Ser473) (Cell signalling # 3787) rabbit monoclonal antibody at 1/100 with 5% goat serum TBS/T. Incubated overnight at 4°C.

2.7.13. p-mTOR (Ser2448) Immunohistochemistry

Immunohistochemistry as per 2.7.10 except slides were then incubated with p-mTOR (Ser2448) (Cell signalling # 2976) rabbit polyclonal antibody at 1/100 with 5% goat serum TBS/T. Incubated overnight at 4°C.

2.7.14. pERK1/2 Immunohistochemistry

Immunohistochemistry as per 2.7.10 except slides were then incubated with p-ERK1/2 (Cell signalling # 9001) rabbit polyclonal antibody at 1/100 with 5% goat serum TBS/T. Incubated overnight at 4°C.

2.7.15. pMEK1/2 Immunohistochemistry

Immunohistochemistry as per 2.7.10 except slides were then incubated with p-MEK1/2 (Cell signalling # 2338) rabbit polyclonal antibody at 1/125 with 5% goat serum TBS/T. Incubated overnight at 4°C.

2.7.16. p-S6 Kinase Immunohistochemistry

Immunohistochemistry as per 2.7.10 except slides were then incubated with p-S6 Kinase (Thr421/Ser424) (Cell signalling # 9204) rabbit polyclonal antibody at 1/100 with 5% goat serum TBS/T. Incubated overnight at 4°C.

2.7.17. Active-Rac1 Immunohistochemistry

Immunohistochemistry as per 2.7.10 except slides were then incubated with Active-Rac1 (NewEast Biosciences # 26903) rabbit polyclonal antibody at 1/400 with 5% goat serum TBS/T. Incubated overnight at 4°C.

2.7.18. GFP Immunohistochemistry

Slide were cut and rehydrated as per 2.7.3. Antigen retrieval was performed as per the microwave method. Slides were then blocked in 3% H₂O₂ made with dH₂O for 15 minutes at room temperature. Slides were then washed 3x 5min TBS/T. Slides were then blocked for 1 hour in 5% Goat Serum diluted in TBS/T at room temperature. Slides were then incubated with GFP (AbCam #abcam6556) rabbit polyclonal antibody at 1/1000 with 5% goat serum TBS/T overnight at 37°C humidified. Slides were then washed with TBS/T 3x5 minutes, before being incubated with secondary antibody from Vectastain Universal kit (1 drop/10 mL blocking solution) at room temperature for 30 minutes.

Slides were washed 3x in PBS. Incubated slides with ABC solution for 30 minutes; 2 drops of solution A + 2 drops of solution B in 5 ml 5% goat serum/ PBS. Washed slides 3x in PBS. Slides were then developed with DAB, rehydrated and mounted as in 2.6.3.

2.7.19. Sprouty2 Immunohistochemistry

Immunohistochemistry as per 2.7.15 except slides were then incubated with Sprouty2 (AbCam # ab60719) mouse monoclonal antibody at 1/300 with 1%BSA/PBS overnight at 4°C.

2.7.20. FGFR3 Immunohistochemistry

Slide were cut and rehydrated as per 2.7.3. No antigen retrieval was performed. Slides were then blocked in 3% H₂O₂ made with dH₂O for 20 minutes at room temperature. Slides were then washed 2x in 5min dH₂O, then 1x 5min TBS/T. Slides were then blocked for 45mins in 5% Goat Serum diluted in TBS/T at room temperature. Slides were then incubated with FGFR3 (Santa Cruz c-15) rabbit polyclonal antibody at 1/20 with 5% goat serum TBS/T overnight at 4°C. Slides were then washed with TBS/T 3x5 minutes before being incubated with secondary biotinylated goat anti-rabbit secondary Ab (DAKO) diluted 1/200 in 5% Goat Serum in TBS/T for 30mins at room temperature. Washed 3x 5mins TBS/T. Slides incubated with ABC solution for 30 minutes; 2 drops of solution A + 2 drops of solution B in 5 ml 5% goat serum/ PBS. Slides were then washed 3x in PBS. Slides were then developed with DAB, rehydrated and mounted as in 2.7.3.

2.8. Imaging

2.8.1 Microscopy

Light microscopy was carried out using the Olympus BX51. All images were taken at 20x magnification, unless otherwise stated in the figure legends.

For GFP *in vivo* imaging we used the Olympus OV100 system. Mice were anaesthetised by inhalation anaesthetic, using a mixture of O₂ and isoflurane. Imaging was also performed on mice post-mortem with both skin intact and removed.

2.8.2. Ultrasound Scanning

This was performed on live mice using Visualsonic's Vevo 770 (Visualsonics Inc, Toronto, Canada). For all abdominal imaging mice were anaesthetised using hypnorm(fentanyl)/hypnovel(midazolam) 10ml/kg i.p. To improve resolution an ascites protocol using an i.p. injection of 5ml of PBS was utilised.

2.9. Human Tissue Microarray (TMA)

This was purchased from Folio biosciences (OH, USA) and consists of 60 cancer and 20 benign bladder cancer cases with data on patient sex, age and tumour grade. Slides were scanned using the Aperio slide scanner (Pathology department, Western Infirmary).

Protein expression levels were scored by two independent observers (Imran Ahmad and Lukram Babloo Singh, Research technician, The Beatson Institute for Cancer Research), blinded to clinical parameters, using a weighted histoscore method, also known as the H-score, at magnification $\times 40$. Each cellular location (membranes, cytoplasm, and nuclei) was scored separately. The weighted histoscore method assesses the staining intensity and the percentage of cells stained with that intensity for the full slide. It is calculated by $(1 \times \% \text{ cells staining weakly positive}) + (2 \times \% \text{ cells staining moderately positive}) + (3 \times \% \text{ cells staining strongly positive})$. This provides a semiquantitative classification of staining intensity, with the maximum score being 300 (if 100% of cells stain strongly positive) and minimum score being 0 (if 100% of cells are negative). The weighted histoscore method is a well-established method for scoring tissue that has heterogeneous staining. Inter-observer agreement between the scorers was excellent with interclass correlation scores >0.80 .

I classified upregulation as a score ≥ 100 and downregulation as < 100 (Kirkegaard et al., 2006). Correlation coefficient was calculated using SPSS v.15). Multiple testing was taken into account (Bonferroni principle).

Chapter 3: β -Catenin activation synergises with PTEN loss to cause bladder cancer formation

3.1. Introduction

A number of genetic and epigenetic alterations involved in bladder tumourigenesis have been identified, including activating mutations in *FGFR3*, and *RAS* family genes, amplification of *ERBB2*, and loss of the *TP53*, *RB1* and *PTEN* tumour suppressors (Cordon-Cardo, 2008, Diaz et al., 2008, Luis et al., 2007, Schulz, 2006). However the role of the Wnt pathway in UCC has yet to be resolved.

The Wnt/ β -catenin signalling pathway plays a crucial role in embryogenesis, cell differentiation and tumourigenesis. Wnts are secreted glycoproteins that act as ligands to stimulate receptor-mediated signal transduction pathways in both vertebrates and invertebrates (Moon *et al.*, 2004). In the absence of a Wnt signal, cytoplasmic β -catenin is phosphorylated and degraded in a complex of proteins. The complex which causes the phosphorylation of β -catenin and thus targets it for degradation is a multi-protein scaffolding complex, consisting of adenomatous polyposis coli (APC), glycogen synthase kinase 3 β (GSK-3 β), CK1 (casein kinase 1) and axin. Following Wnt pathway activation (through the binding of a Wnt ligand to the frizzled transmembrane receptor), GSK3 is inactivated and β -catenin is no longer phosphorylated and targeted for degradation. As a result β -catenin accumulates in the cytoplasm and enters the nucleus, where it binds to TCF/LEF family members and transcriptionally regulates Wnt target genes which include cyclin D1 and c-myc (canonical Wnt signalling pathway) (Bienz and Clevers, 2000, He et al., 1998, Tetsu and McCormick, 1999, Polakis, 2000a).

Mutations of the tumour suppressor *PTEN* have been described in many tumours (Salmena *et al.*, 2008), including deletion of the locus in bladder cancers (Aveyard et al., 1999, Teng et al., 1997, Tsuruta et al., 2006). These deletions are absent/rare in superficial tumours, but occur frequently in invasive bladder cancers. Previously published models of inactivation of PTEN

in the murine urothelium have shown widely conflicting phenotypes from benign epithelium to widespread hyperplasia whilst some demonstrate UCC after a long latency and with an incomplete penetrance (Puzio-Kuter et al., 2009, Tsuruta et al., 2006, Yoo et al., 2006, Qian et al., 2009). This may be in part related to the different promoters, PTEN alleles and backgrounds of the mice used. Recently it has been demonstrated that combined deletion of *Pten* and *Trp53* in the murine urothelium results in aggressive UCC, which is dependent on mTOR signalling (Puzio-Kuter *et al.*, 2009).

In this study, I tested whether activation of Wnt signalling pathway may cooperate with loss of PTEN function to drive UCC *in vivo*.

3.2. Results

3.2.1 β -catenin overexpression leads to benign hyperproliferation of the urothelium

In order to drive deregulated Wnt signalling, I used mice that carry a dominant allele of the β -catenin gene in which exon3 is flanked by *loxP* sequences (Harada *et al.*, 1999). On addition of Cre recombinase, exon3 is deleted. As this exon contains the residues that are phosphorylated by GSK3 β , leading to β -catenin degradation, β -catenin will therefore accumulate to drive Wnt signalling (Moon *et al.*, 2004). To achieve urothelial specific expression of activated β -catenin, these mice were interbred with mice carrying an *uroplakin II (UroII) CRE* transgene (He *et al.*, 2009, Mo *et al.*, 2005). UroII is a protein localised at the apical surface of the urothelium and is important for its permeability barrier function (Zhang *et al.*, 1999). It is expressed throughout the urothelial layers in mice (Mo *et al.*, 2005). The *UroII* promoter has been reported to successfully drive the expression of proteins including SV40 large T antigen and H-Ras (Zhang *et al.*, 2001, Mo *et al.*, 2007). Previous studies have shown that the *UroIICRE*⁺ mice exhibit bladder specific recombination (Zhang *et al.*, 1999). To confirm this and to report levels of recombination, *UroIICRE*⁺ mice were intercrossed with mice carrying the *Z/EGFP* reporter transgene (Novak *et al.*, 2000). In the *Z/EGFP* reporter mouse, the *Z/EGFP* transgene results in the expression of β -galactosidase by most tissues via a *β -geo* insert, which is flanked by *lox-P* sites. The presence of Cre recombinase results in the excision of the *β -geo*, activating the constitutive expression of GFP. Both immunohistochemistry and OV100 imaging for GFP shows the expression of eGFP in the urothelial lining of the bladder and ureters (Figure 3.1) (Novak *et al.*, 2000).

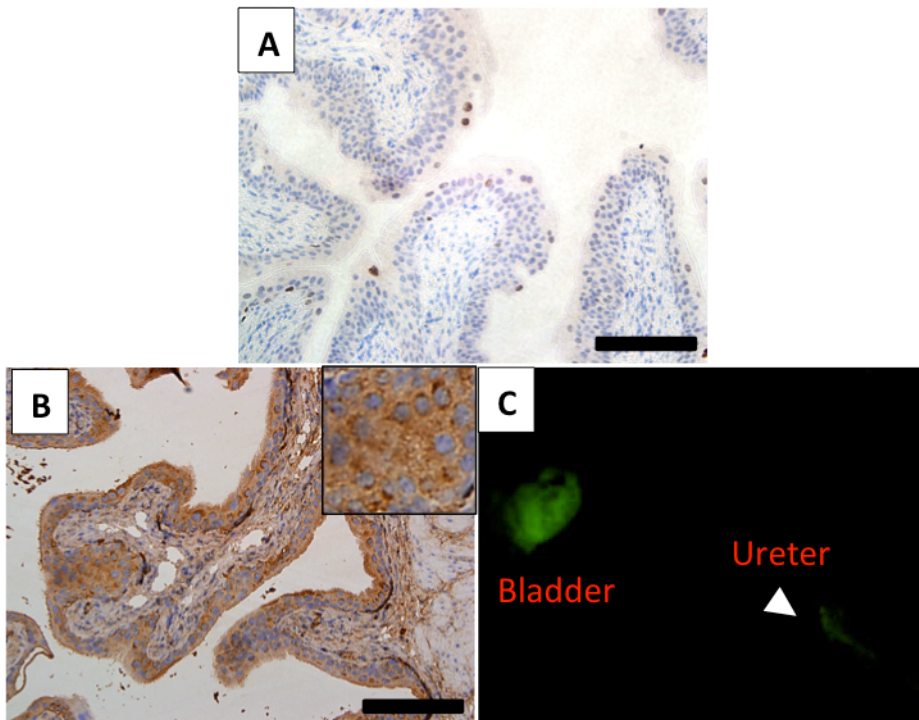


Figure 3.1: GFP Expression of *UroIIICRE*⁺ *Z/EGFP* mice

IHC for Green Fluorescent Protein (GFP) in wildtype (A) and 12-month old *UroIIICre*⁺ *Z/EGFP* bladder (B). Black bar measures 200µm (20x magnification). GFP visualised by OV100 shows evidence of Cre mediated recombination in the urothelium of 12-month old *UroIIICre*⁺ *Z/EGFP* bladder (C). Imaging was performed ex-vivo after urine had been drained. Magnification at 14x.

(At least 3 samples from each cohort stained and representative images are shown above).

Firstly, I used mice carrying one or two copies of the *β-catenin exon3* allele to test whether the amplitude of the Wnt deregulation was important, as levels of deregulated Wnt signalling have been shown to be key in other organs such as the mammary gland (Howe and Brown, 2004). To investigate the phenotype of *β-catenin* activation within the bladder I aged *UroIICRE⁺ β-catenin^{+/+}*, *UroIICRE⁺ β-catenin^{exon3/+}* and *UroIICRE⁺ β-catenin^{exon3/exon3}* mice to 3 months of age. In mice carrying one or two copies of the *β-catenin exon3* allele there was a clear phenotype in the bladder epithelium, with all mice developing areas of urothelial hyperplasia (Figure 3.2 A,C,E). To confirm that this was due to the activation of *β-catenin*, I performed IHC for *β-catenin* and saw a marked upregulated of nuclear *β-catenin* compared to wildtype (Figure 3.2 B,D,F) as well as Wnt target gene c-Myc (Figure 3.3 A,D). To confirm the lesions were hyperproliferative I then stained for the proliferation markers Ki67 and BrdU, both of which I found to be upregulated (Figure 3.3 B,C,E,F). No differences in proliferation as assessed by BrdU positivity were observed in mice carrying either one or two copies of the *β-catenin exon3* allele (data not shown).

Given that mice formed hyperproliferative lesions I wished to test whether these mice developed UCC as they aged. Therefore *UroIICRE⁺ β-catenin^{+/+}*, *UroIICRE⁺ β-catenin^{exon3/+}* and *UroIICRE⁺ β-catenin^{exon3/exon3}* mice were aged to 18 months old. Remarkably, no mice developed UCC within this time course and when bladders from these 18-month-old mice were examined they appeared equivalent to those at 3 months with a number of hyperproliferative lesions that had not progressed to cancer. There was however a small yet significant increase in the numbers of lesions in bladders for each group of aged mice ($p < 0.001$) (Figure 3.4). Interestingly given the paucity of lesions in the mutant bladders this suggests that secondary mutations are required in the recombined cells to allow these lesions to form, whilst the majority of singly *β-catenin* mutant cells that do not possess these additional mutations are being selected against.

The lack of invasive progression among these lesions highlights that β -catenin activation is not sufficient to drive UCC formation and potentially explains why subjects that carry germline mutations of *APC* do not develop UCC. Similarly the lesions are composed of numerous proliferating cells, but never progress to tumours/overrun the urothelium. This suggests that either there is a concordant high rate of apoptosis or the somehow these cells despite exhibiting markers of proliferation are not actually dividing (suggestive by upregulation of markers of senescence (Figure 3.5)).

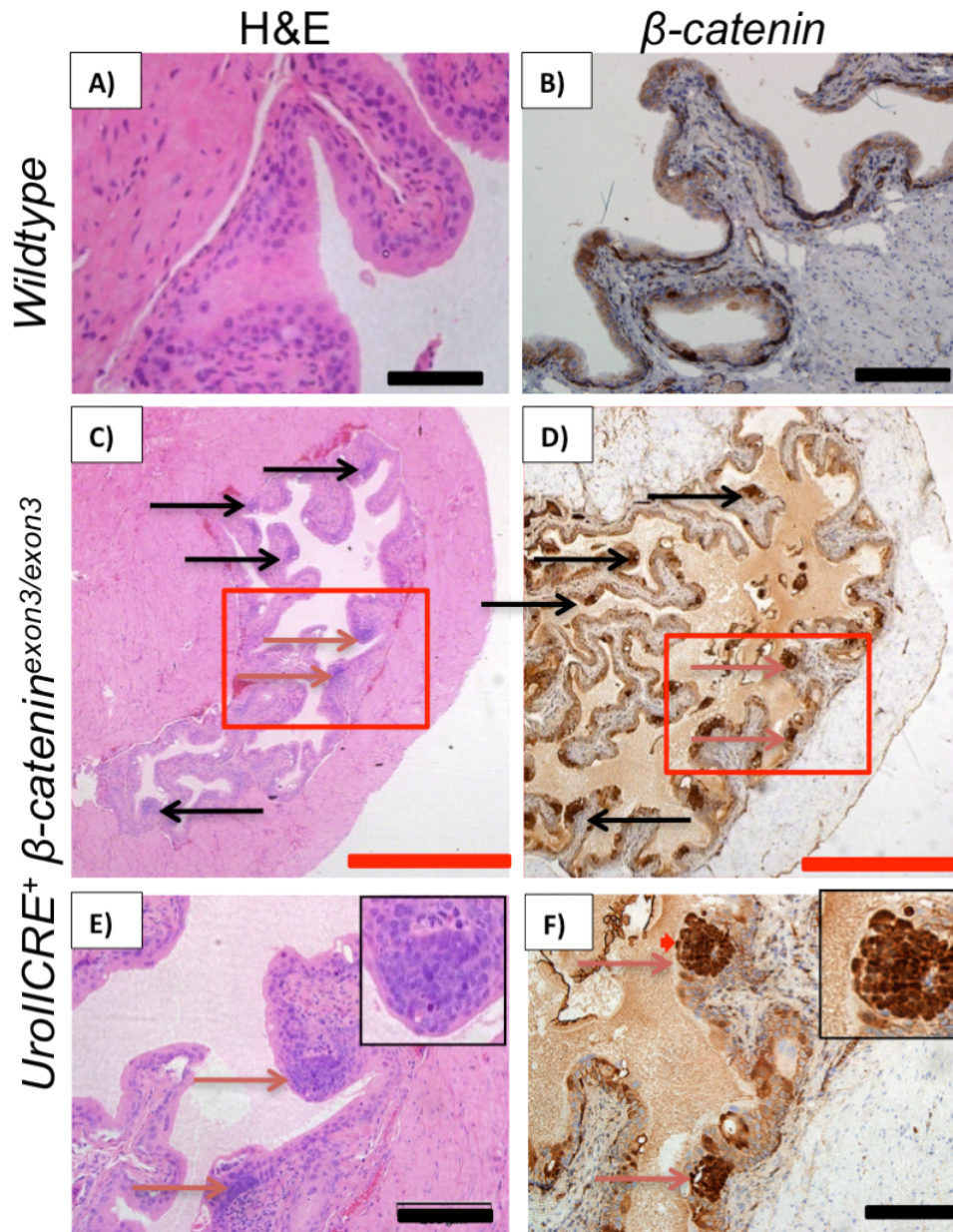


Figure 3.2: *UroII CRE*⁺ *β-catenin*^{exon3/exon3} urothelium demonstrates upregulation of nuclear *β-catenin*

Histology from 12-month-old Wildtype and *UroII CRE*⁺ *β-catenin*^{exon3/exon3} mice. H&E reveals development of hyperplastic lesions in the mutant urothelium (black/red arrows) (A&C), of which a close up (red arrows) is seen in (E). Immunohistochemistry shows strong upregulation of nuclear *β-catenin* (B,D,F) compared to wildtype. Red bar measures 1000 μm (4x magnification), black bar measures 200μm (20x magnification). Red box outline in (A) and (B) highlights the picture for (C) and (D).

(At least 3 samples from each cohort stained and representative images are shown above).

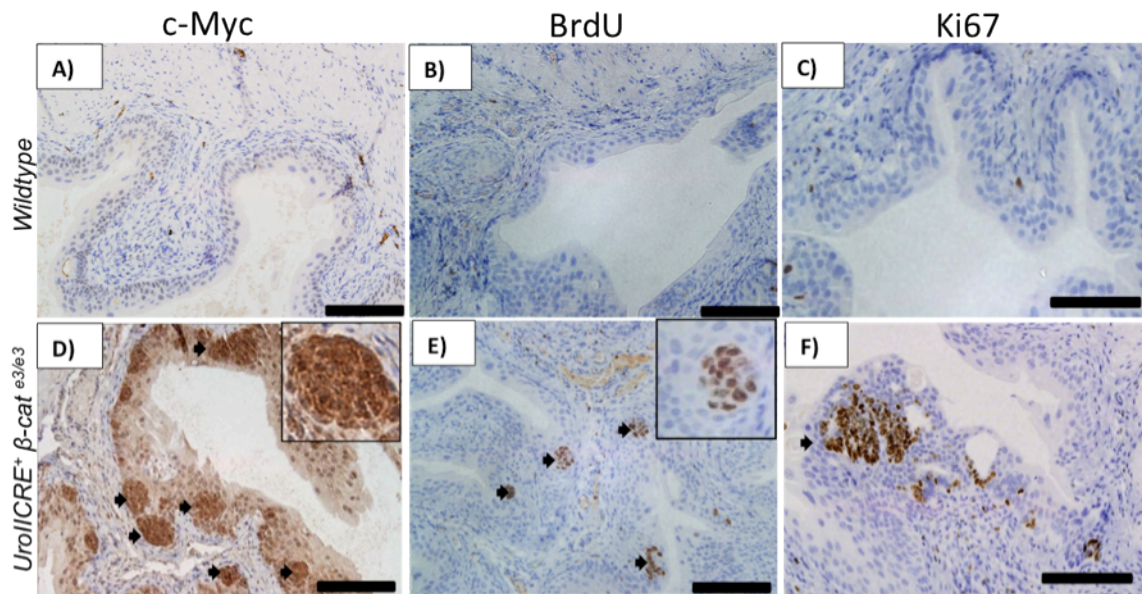


Figure 3.3: *UroII CRE⁺ β-catenin^{exon3/exon3}* urothelium demonstrates upregulation of Wnt target genes and proliferative markers

IHC from 12-month-old Wildtype and *UroII CRE⁺ β-catenin^{exon3/exon3}* urothelium demonstrates strong upregulation Wnt target gene c-Myc (A&D), as well as upregulation of markers of proliferation; BrdU (B&E) and Ki-67 (C&F) in the mutant urothelia. Black bar measures 200μm (20x magnification).

(At least 3 samples from each cohort stained and representative images are shown above).

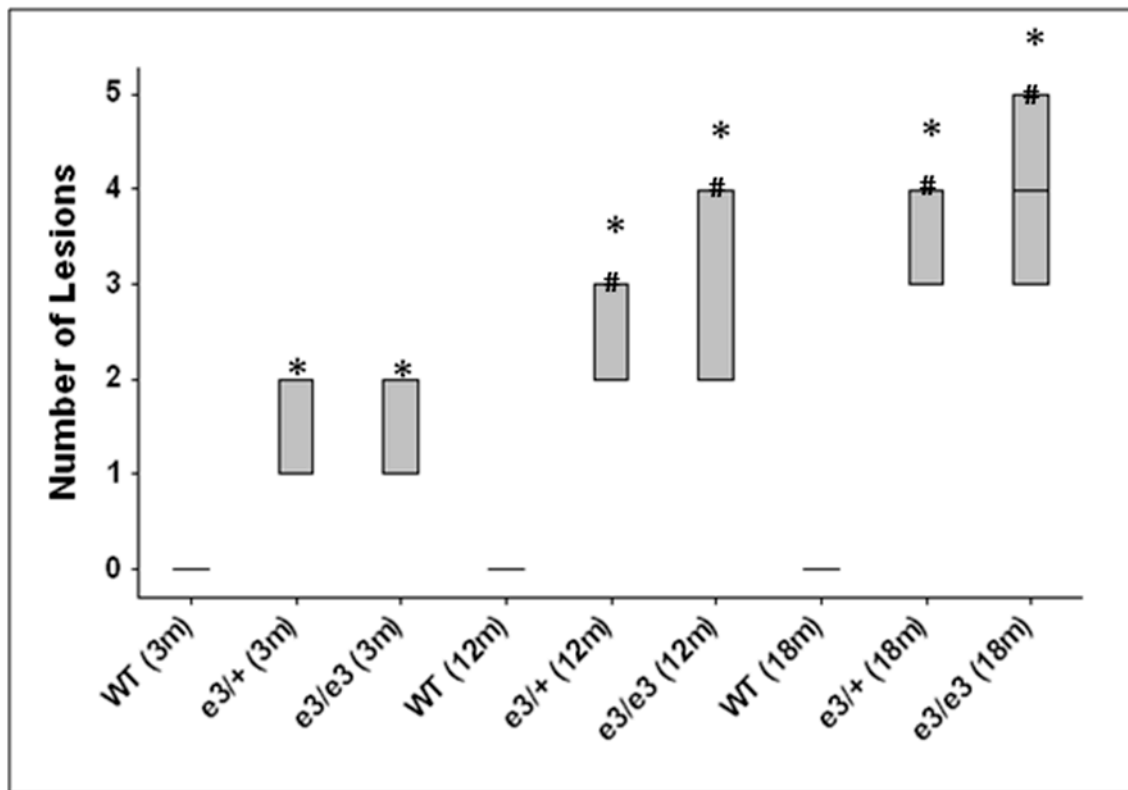
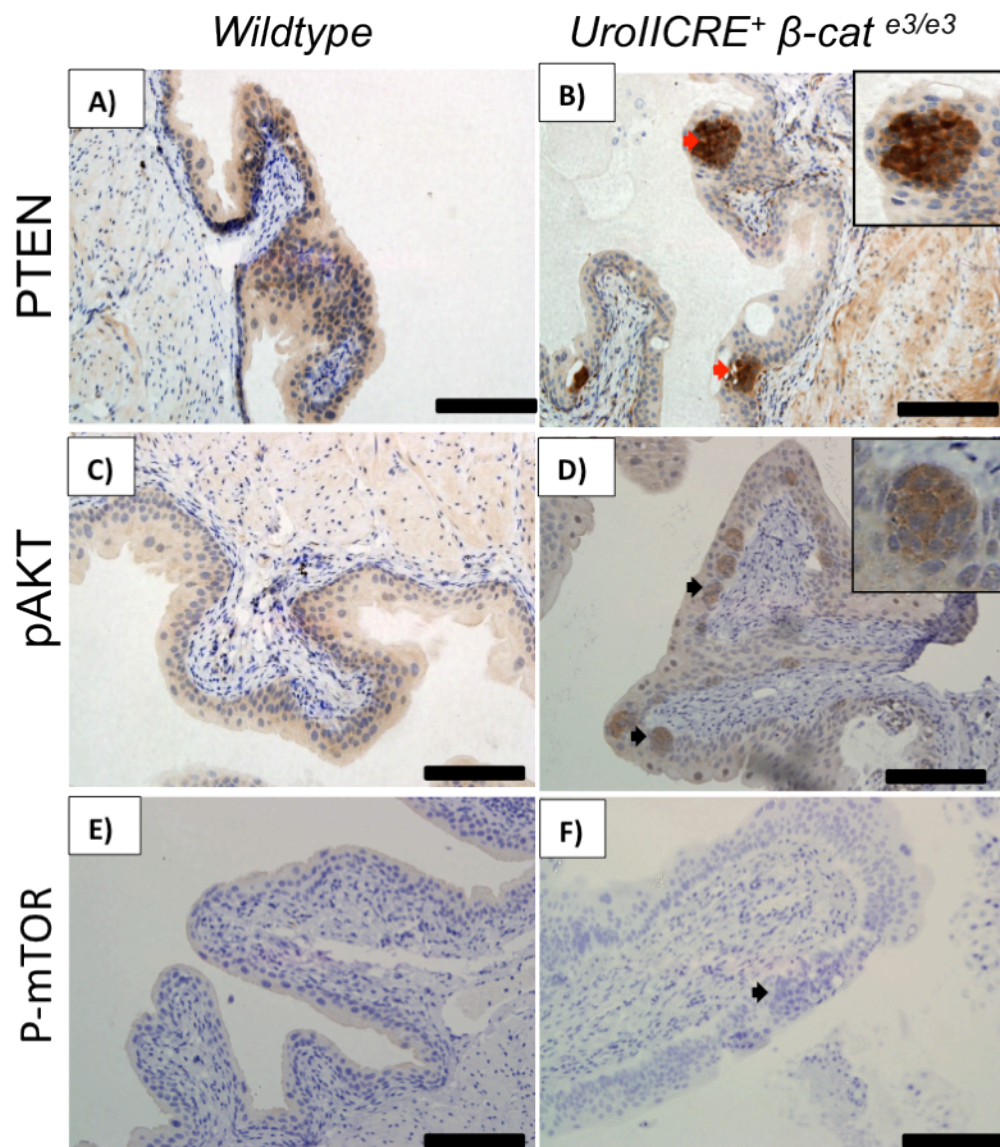


Figure 3.4: Box plot of lesion numbers in the wildtype, *UroII CRE*⁺ *β-catenin*^{exon3/+} and *UroII CRE*⁺ *β-catenin*^{exon3/exon3}

Box plot of lesion numbers in the wildtype, *UroII CRE*⁺ *β-catenin*^{exon3/+} and *UroII CRE*⁺ *β-catenin*^{exon3/exon3} cohorts at 3, 12 and 18 months of age (n=3). I showed that at 3, 12 and 18 months the number of lesions in the *UroII CRE*⁺ *β-catenin*^{exon3/+} (e3/+) and *UroII CRE*⁺ *β-catenin*^{exon3/exon3} (e3/e3) are significantly higher than the corresponding wildtype (WT) time point (*, p<0.001, Mann Whitney Test). Similarly lesions at both 12 and 18 months in the *UroII CRE*⁺ *β-catenin*^{exon3/+} and *UroII CRE*⁺ *β-catenin*^{exon3/exon3} cohorts are significantly higher than the corresponding cohort at 3 months (#, p<0.001, Mann Whitney Test). Thick bar represents median, and the box represents the inter-quartile range.

3.2.2. The PTEN tumour suppressor pathway is activated in the bladder lesions

I next investigated the pathways that were constraining tumour progression within the areas of urothelial hyperplasia. UCC can be broadly separated into two molecular pathways (Luis et al., 2007, Wu, 2005). In one pathway where patients have either *FGFR3* or *HRAS* mutations, they develop superficial papillary disease, which often carries a good prognosis. The other tumour subtype has a more aggressive phenotype, leading to muscle invasion and ultimately metastatic disease. These tumours have often lost p53 and/or have an activation of the PI3-kinase signalling pathway. Indeed, a recent study has shown that low PTEN levels correlate with a poor prognosis in human bladder cancer (Puzio-Kuter *et al.*, 2009). This has recently been modelled in the mouse using adenoviral Cre infections into the bladder. Mice either singly mutant for *Pten* or *Trp53* did not develop tumours, however double knockout mice developed metastatic urothelial cancer. Thus I next investigated the expression of candidate molecules from the p53 and PTEN tumour suppressor pathways within lesions from the *UroIIICRE⁺ β-catenin^{exon3/exon3}* mice. Within the lesions, there were very high levels of the PTEN tumour suppressor protein expression (Figure 3.5 A&B) with associated minimal pAKT, p-mTOR and pS6 Kinase staining (Figure 3.5 D,F,H) suggesting that the PTEN tumour suppressor was potentially blocking tumour progression. In contrast to a large increase in PTEN, there was only a modest increase in the levels of nuclear p53 although one of its targets p21 was highly upregulated within the lesions of the mice (Figure 3.5 J&L). There was strong upregulation of p19^{ARF} (Figure 3.6 N), another p53 related tumour suppressor. Similarly I noticed upregulation of senescence-associated β-galactosidase (Saβgal) (Figure 3.5 P).



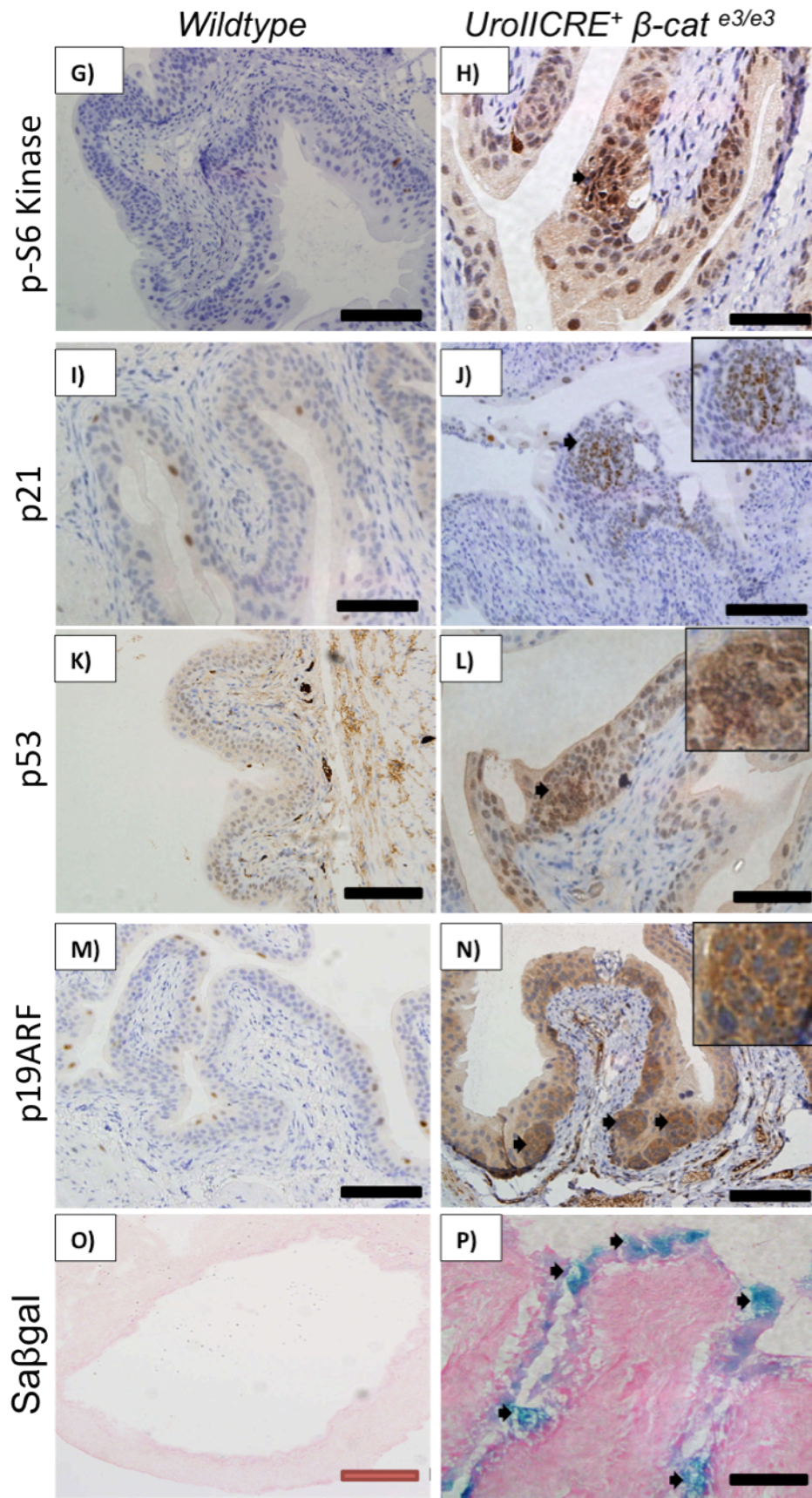


Figure 3.5: *UroII CRE*⁺ *β-catenin*^{exon3/exon3} urothelium demonstrates upregulation of PTEN, p53, p21 and p19ARF

IHC from 12 month old *Wildtype* and *UroII CRE*⁺ *β-catenin*^{exon3/exon3} urothelium demonstrates strong upregulation PTEN (A&B), with minimal pAkt(Ser473) (C&D) and p-mTOR (E&F) signal. I also noticed significant upregulation of p-S6 Kinase, p21, p19ARF, p53 and Saβgal (G-P). Red bar measures 1000 μm (4x magnification), black bar measures 200μm (20x magnification).

(At least 3 samples from each cohort stained and representative images are shown above).

3.2.3. PTEN upregulation acts to block β -catenin driven urothelial proliferation

As the *uroplakin II cre* recombinase is expressed throughout development of the urothelium, it is difficult to assess whether the upregulation of PTEN is a direct consequence of β -catenin accumulation. Therefore I next investigated the consequence of inducibly activating Wnt signaling in the adult urothelium. To do this mice carrying the cytochrome p450 inducible $AhCreER^T$ transgene were used. Following administration of both β -naphthoflavone and tamoxifen, this yields cre-mediated recombination within the urothelium of the bladder (as well as the intestine) (Marsh et al., 2008). Figure 3.6 demonstrate recombination in the bladder as evidenced by GFP signalling identified by OV100 imaging (ex-vivo) and IHC for GFP in $AhCreER^T$ Z/*EGFP* reporter mice 7 days following induction. To investigate the impact of acutely activating Wnt signalling in the adult bladder I intercrossed $AhCreER^T$ mice to mice carrying the inducible knockout *Apc*^{580S} allele (from here on known as *Apc*^{fl}) in which *loxP* sites are inserted into the introns around exon 14 (Shibata et al., 1997). Remarkably, examination of the bladders from $AhCreER^T$ *Apc*^{fl/fl} mice seven days following induction revealed development of urothelial lesions which phenocopied those from our *UroIIICRE*⁺ β -catenin^{exon3/exon3} mice (Figure 3.7 A). Indeed there were more lesions in the $AhCreER^T$ *Apc*^{fl/fl} urothelia suggesting a greater recombination frequency than the *UroIIICRE*⁺. Consistent with the activation of Wnt signalling, lesions demonstrated a high level of nuclear β -catenin and again an upregulation in BrdU incorporation compared to the surrounding urothelium (Figure 3.7 B&C). Importantly, once again very high levels of PTEN were seen within these lesions (Figure 3.7 D) with minimal upregulation of pAKT (Figure 3.7 E). To confirm this was due to increased levels of Wnt signalling, I also activated Wnt signalling by deleting both copies of GSK3 α and GSK3 β . Bladders from induced $AhCreER^T$ *GSK3 α* ^{fl/fl} mice displayed similar lesions to the $AhCreER^T$ *Apc*^{fl/fl} mice, with the accumulation of nuclear β -catenin, BrdU and PTEN (Figure 3.8 A-D) (MacAulay et al., 2007, Patel et al., 2008, Kemp et al., 2004). Using

this induction regime, mice developed hyperplastic intestinal epithelium, which precluded long term tumour experiments, however in mice aged up to 4 months bladder lesions still remained small and did not progress to cancer, suggesting PTEN was once again blocking tumourigenesis.

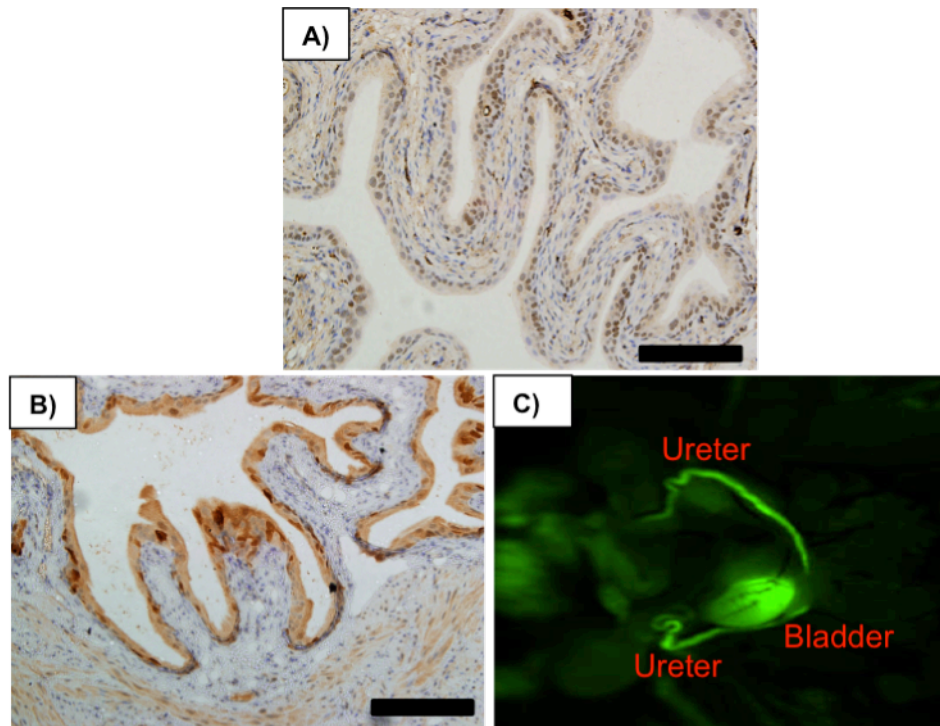


Figure 3.6: GFP expression in *AhCreER^T Z/EGFP* mice 7 days post induction

Bladders from *AhCreER^T Z/EGFP* mice reveal recombination in the bladder as evidenced by GFP signalling, identified by IHC for GFP (B) compared to wildtype (A). OV100 imaging (ex-vivo) (C).

(At least 3 samples from each cohort stained and representative images are shown above).

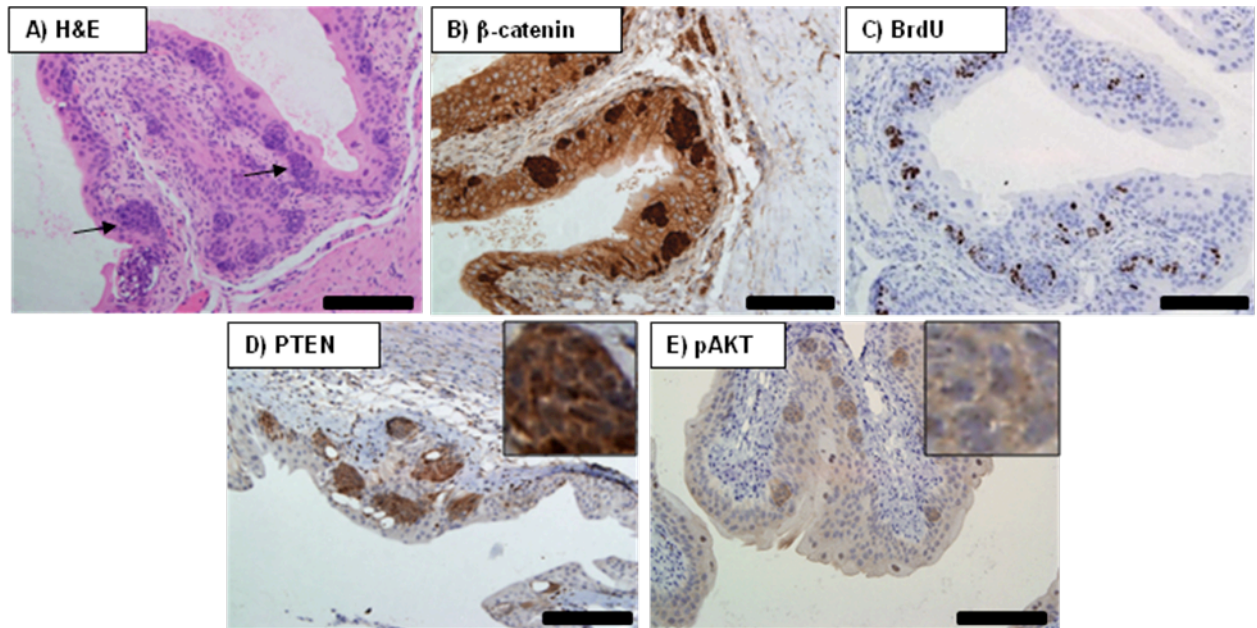


Figure 3.7: Histology of *AhCreER^T Apc^{fl/fl}* 7 days post induction

Bladders from *AhCreER^T Apc^{fl/fl}* mice reveal similar hyperproliferative lesions to our *UroICRE⁺ β-catenin^{exon3/exon3}* (A), which demonstrate proliferation (C) as well as upregulation of nuclear β-catenin and PTEN staining with minimal pAKT expression (B,D,E). Black bar measures 200μm (20x magnification).

(At least 3 samples from each cohort stained and representative images are shown above).

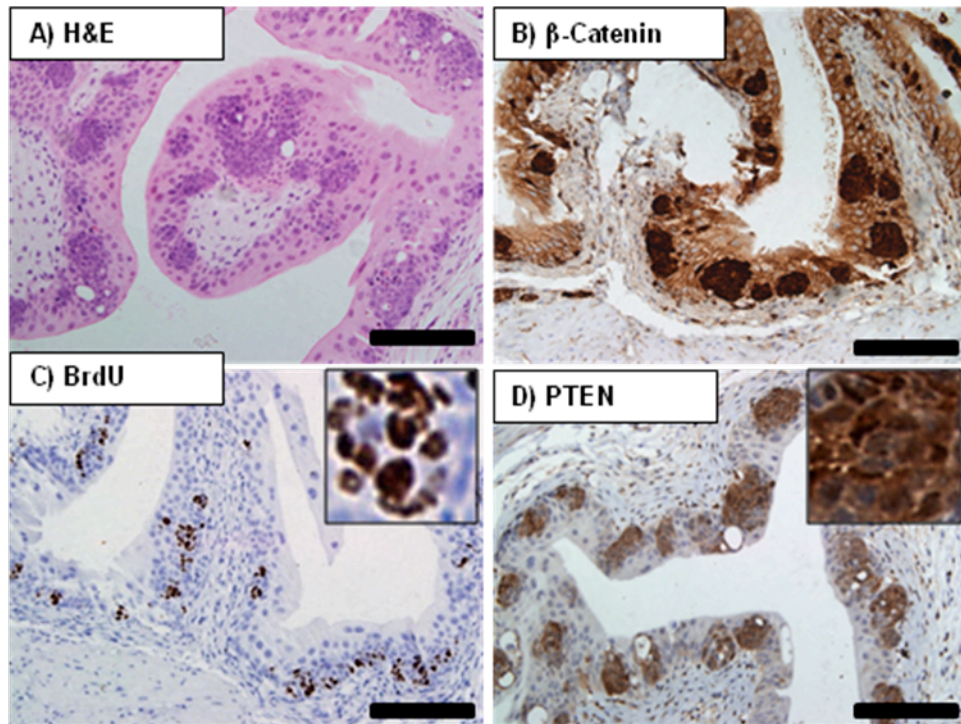


Figure 3.8: Histology of *AhCreER^T GSK3αβ^{fl/fl}* mice 7 days post induction

AhCreER^T GSK3αβ^{fl/fl} mice reveal bladder lesions (A), which demonstrate proliferation as well as accumulation of nuclear β-catenin and PTEN (B-D). Black bar measures 200μm (20x magnification).

(At least 3 samples from each cohort stained and representative images are shown above).

To test the role PTEN was having immediately following Apc loss in the urothelium I generated *AhCreER^T APC^{fl/fl} PTEN^{fl/fl}* mice. Seven days following induction, the mice again developed urothelial lesions that were much larger than in *AhCreER^T Apc^{fl/fl} Pten^{+/+}* mice (Figure 3.9 A). These lesions showed an accumulation of nuclear β -catenin, high BrdU expression and consistent with PTEN deletion, a complete absence of PTEN staining in the lesions (Figure 3.9 B-D), and showed strong pAKT(Ser473) upregulation (Figure 3.9 E) To investigate whether the reason for the enlarged lesions was due to hyperproliferation, I examined the number of BrdU positive cells per lesion in both *AhCreER^T Apc^{fl/fl}* and *AhCreER^T Apc^{fl/fl} Pten^{fl/fl}* mice and demonstrated a statistically significantly increase in proliferation when PTEN is lost ($p < 0.05$, Mann Whitney Test) (Figure 3.10). Thus PTEN accumulation following β -catenin activation is acting to limit proliferation. I was again unable to further analyse the *AhCreER^T Apc^{fl/fl} Pten^{fl/fl}* mice as these mice became ill rapidly after induction due to intestinal disease at day 8.

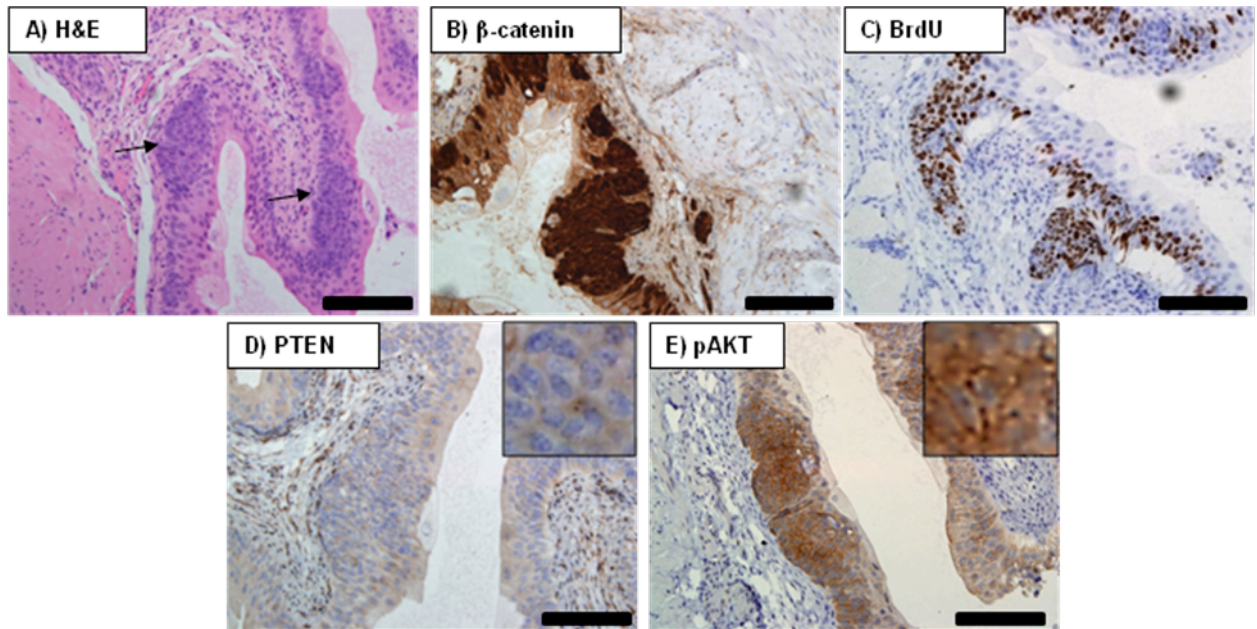


Figure 3.9: Histology of *AhCreER^T Apc^{fl/fl} Pten^{fl/fl}*

Bladders from *AhCreER^T Apc^{fl/fl} Pten^{fl/fl}* mice reveal larger lesions (A) that show further proliferation (B), nuclear β-catenin (C), but this time the absence of PTEN staining in the lesions (D). These lesions demonstrate significant upregulation of pAKT (E). Black bar measures 200μm (20x magnification).

(At least 3 samples from each cohort stained and representative images are shown above).

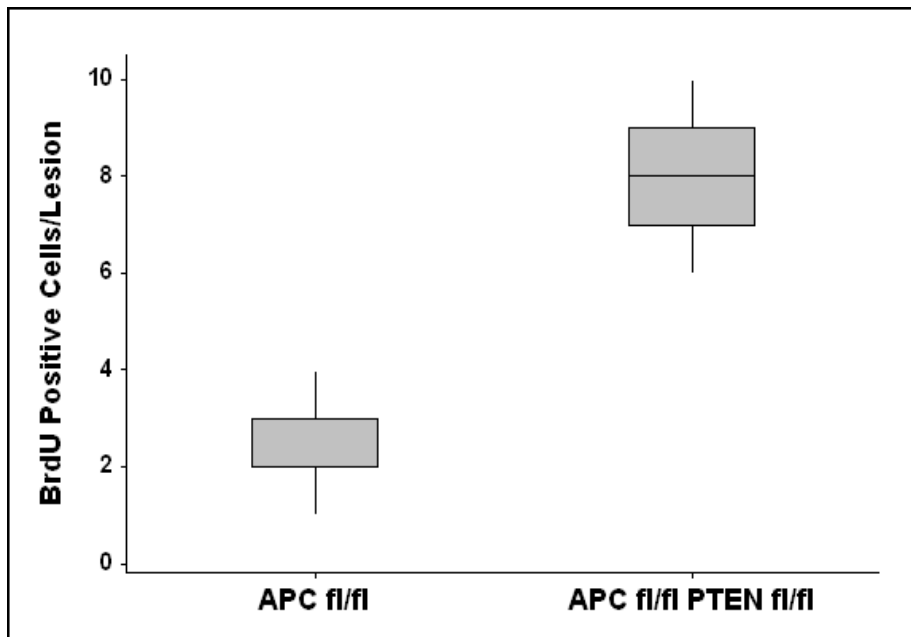


Figure 3.10: Box plot of average number of BrdU positive cells per lesion in both *AhCreER^T Apc^{fl/fl}* and *AhCreER^T Apc^{fl/fl} Pten^{fl/fl}* mice.

Urothelium assessed at 7 days after first induction (n=3) (p<0.001, Mann Whitney test). Total number of positive cells from lesions (n=3) counted from 3 mice (total lesions n=9), with median, inter-quartile range and range represented above.

3.2.4. PTEN loss cooperates with β -catenin activation to drive UCC formation

To test whether this block of proliferation by PTEN was suppressing tumourigenesis I intercrossed *UroIIICRE*⁺ *β -catenin*^{exon3/exon3} mice with mice carrying a conditional inactivatable *Pten* allele (where exon 5 is flanked by *lox p* sites) (Lesche *et al.*, 2002). A recent study using adenoviral Cre delivery to the bladder has shown that deletion of *Pten* alone in the murine urothelium is not sufficient to promote bladder cancer formation (Puzio-Kuter *et al.*, 2009). I have confirmed this result here, as neither *UroIIICRE*⁺ *Pten*^{fl/+} nor *UroIIICRE*⁺ *Pten*^{fl/fl} mice developed cancer when aged until 18 months (n=20). Indeed, no phenotypic changes (dysplasia, hyperplasia or tumourigenesis) were observed in urothelium between *UroIIICRE*⁺ *Pten*^{fl/fl} and wildtype mice (Figure 3.11 A-B). To confirm that *Pten* was deleted in these mice I stained for PTEN levels by IHC and found a downregulation of the PTEN protein in bladders from *UroIIICRE*⁺ *Pten*^{fl/fl} (Figure 3.11 C-D) and only a modest upregulation of pAKT(Ser473) staining (Figure 3.11 E-F). These data are consistent with previous studies within the intestinal epithelium where *Pten* deletion was not sufficient to drive tumourigenesis and only modestly affected the levels of pAKT (Marsh *et al.*, 2008).

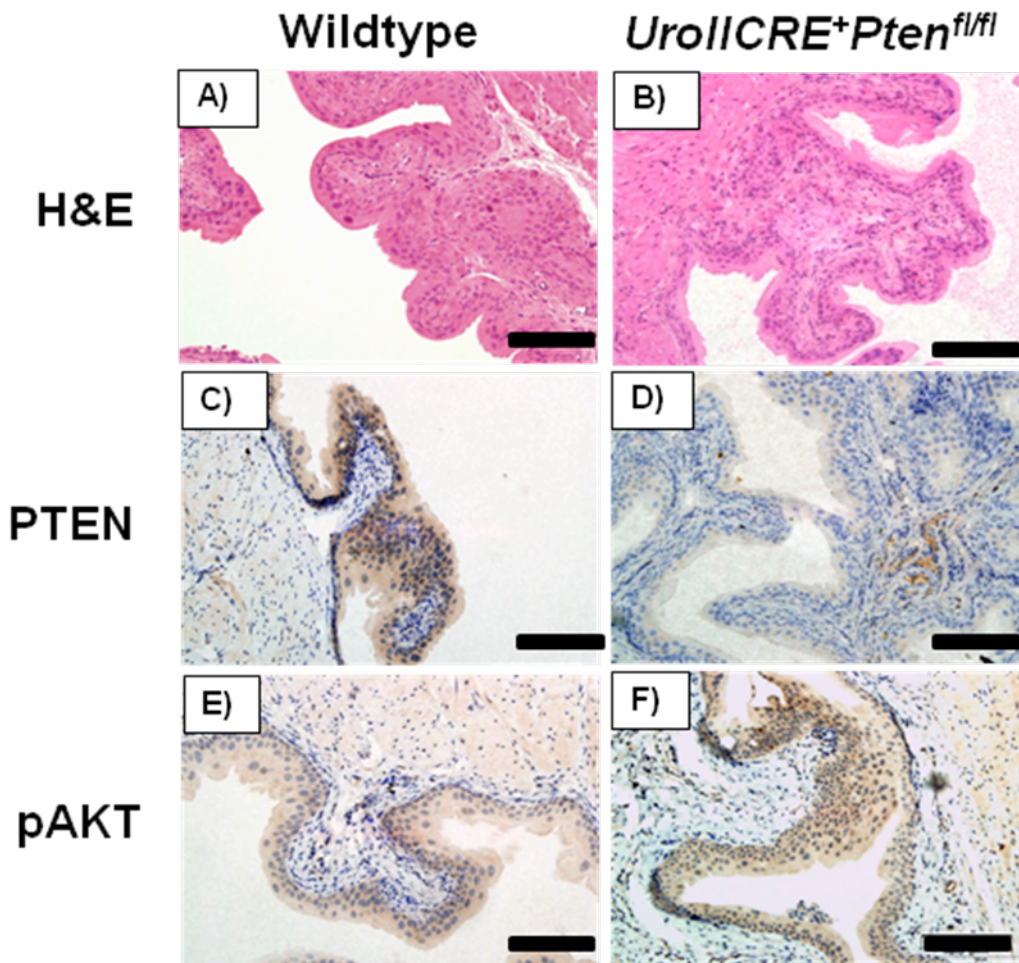


Figure 3.11: Histology of *UroII CRE⁺ Pten^{fl/fl}* mice

Comparison of 12-month-old wildtype and *UroII CRE⁺ Pten^{fl/fl}* urothelium. The H&E demonstrates that the urothelium of *UroII CRE⁺ Pten^{fl/fl}* (B) is comparable to wildtype (A) with no hyperplasia, dysplasia or tumour formation. Lower levels of PTEN in the *UroII CRE⁺ Pten^{fl/fl}* urothelium (D) when compared to wildtype (C) and slightly elevated levels of pAkt(Ser473) (E,F) were observed. Black bar measures 200µm (20x magnification).

(At least 3 samples from each cohort stained and representative images are shown above).

To study the simultaneous activation of β -catenin and PTEN loss, the following cohorts were generated: $UroIIICRE^+ \beta\text{-catenin}^{\text{exon3}/+} Pten^{\text{fl}/+}$, $UroIIICRE^+ \beta\text{-catenin}^{\text{exon3}/\text{exon3}} Pten^{\text{fl}/+}$, $UroIIICRE^+ \beta\text{-catenin}^{\text{exon3}/+} Pten^{\text{fl}/\text{fl}}$, and $UroIIICRE^+ \beta\text{-catenin}^{\text{exon3}/\text{exon3}} Pten^{\text{fl}/\text{fl}}$ (n= 20, 16, 24, 21 respectively). A cohort of these mice was harvested at 3 months of age and the bladder phenotypes were analysed. A second cohort of mice was allowed to age until clinical evidence of tumour development, or when animals were required to be sacrificed per project license guidelines. At 3 months of age, hyperplastic lesions (scored from 3 H&E cross sections of each mouse, with 3 mice in each cohort) were observed at an increased frequency in doubly mutant mice compared with mice carrying only β -catenin mutation (Figure 3.12).

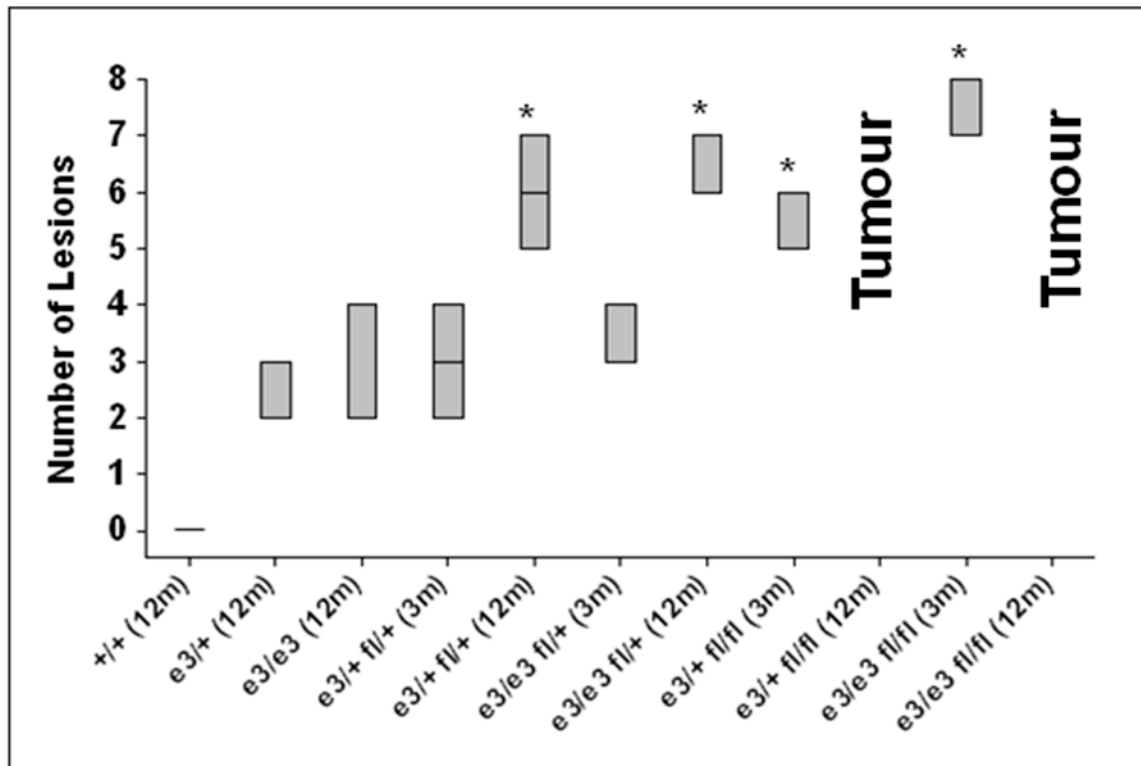


Figure 3:12 Tumour burden of *UroII CRE*⁺ *β-catenin*^{exon3/exon3} *Pten*^{fl/fl} mice

Box plot of number of lesions found in urothelium of each cohort at 3 and 12 months (n=3). Cohorts denoted by * demonstrate significantly elevated levels of lesions in comparison to 12 month old *UroII CRE*⁺ *β-catenin*^{exon3/exon3} (p<0.05, Mann Whitney Test). Abbreviations: e3/e3 (*UroII CRE*⁺ *β-catenin*^{exon3/exon3}), e3/+ fl/+ (*UroII CRE*⁺ *β-catenin*^{exon3/+} *Pten*^{fl/+}), e3/e3 fl/+ (*UroII CRE*⁺ *β-catenin*^{exon3/exon3} *Pten*^{fl/+}), e3/+ fl/fl (*UroII CRE*⁺ *β-catenin*^{exon3/+} *Pten*^{fl/fl}) and e3/e3 fl/fl (*UroII CRE*⁺ *β-catenin*^{exon3/exon3} *Pten*^{fl/fl}). Thick bar represents median, and the box represents the inter-quartile range.

In contrast to the *UroIIICRE*⁺ *β-catenin*^{exon3/+} *Pten*^{fl/+} and *UroIIICRE*⁺ *β-catenin*^{exon3/exon3} *Pten*^{fl/+} mice, the *UroIIICRE*⁺ *β-catenin*^{exon3/exon3} *Pten*^{fl/fl} mice and *UroIIICRE*⁺ *β-catenin*^{exon3/+} *Pten*^{fl/fl} mice rapidly developed symptoms of bladder tumour; abdominal swelling, haematuria (blood in the urine) and hunching (Figure 3.13 & 3.14). Mice with loss of both copies of *Pten* succumbed to bladder tumours 100 days earlier than those with single copy loss.

On necropsy, the presence of bladder tumour was confirmed, which showed histological progression to papillary carcinoma (Figure 3.15 A&B). I found no evidence of metastasis in any of the models studied (both at macroscopic and microscopic level, with multiple sections taken through the lung, liver, spleen, diaphragm, kidneys and local lymph nodes). Consistent with *Pten* deletion, the tumours that developed showed complete loss of PTEN protein and now displayed strong activation of pAKT(Ser473) (Figure 3.15 C&D). Tumours also showed a nuclear upregulation of β -catenin and Ki-67 (Figure 3.15 E&F).

These data are consistent with tumour formation in the bladder being synergistically promoted by Wnt and PI3 kinase signalling. This scenario fits with our previous studies in the intestinal epithelium where Wnt activation or *Pten* loss alone, were not sufficient to induce high levels of pAKT and presumably PI3 kinase signalling (Marsh *et al.*, 2008). However in our bladder model, combination of deregulated Wnt signalling and PTEN loss caused a dramatic increase in pAKT that presumably drives tumour formation. Of the targets downstream of pAKT, I also saw a dramatic increase in p-mTOR²⁴⁴⁸ (Figure 3.15 G), suggesting that mTOR activation is a key component of tumourigenesis in this model. A recent chemoprevention study by Puzio-Kuter has shown that mTOR inhibition using Rapamycin suppresses tumourigenesis in *Trp53/Pten* double knockout tumours (Puzio-Kuter *et al.*, 2009). Consistent with our tumours being dependent on PI3-kinase signalling, there was no upregulation of pERK1/2 in the tumours (Figure 3.15 H). There was minimal upregulation of p53 and p21

(Figure 3.15 J&K). By 12 months of age, a small subset of the *UroIIICRE+* β -catenin^{exon3/exon3} *Pten*^{fl/+} mice and *UroIIICRE+* β -catenin^{exon3/+} *Pten*^{fl/+} mice had developed tumours. This was presumably due to the loss of the remaining *Pten* allele, as staining for PTEN was absent from the tumours (Figure 3.15 I). There has been much debate over the crosstalk between the Wnt and PI3 kinase pathways and it is often proposed that the inhibitory phosphorylation of GSK3 by AKT/PKB may allow the activation of Wnt signalling. If this was the case one would argue that PTEN loss alone should be sufficient to activate Wnt signalling and numerous studies have shown that this is not the case (including our present study) (Salmena *et al.*, 2008). Moreover two key studies suggest that the phosphorylation of GSK3 by AKT does not affect Wnt signalling. First ‘knock-in’ mice where the AKT phosphorylation sites on GSK3alpha (Ser21) and GSK3beta (Ser9) were converted to alanine did not elevate Wnt signalling (McManus *et al.*, 2005). Second a recent study has shown that the Wnt pool of GSK3 is physically distinct from the AKT pool (Ng *et al.*, 2009). Our data here shows it is only in the complete genetic absence of both GSK3 α and GSK3 β that Wnt signalling is deregulated (Figure 3.8).

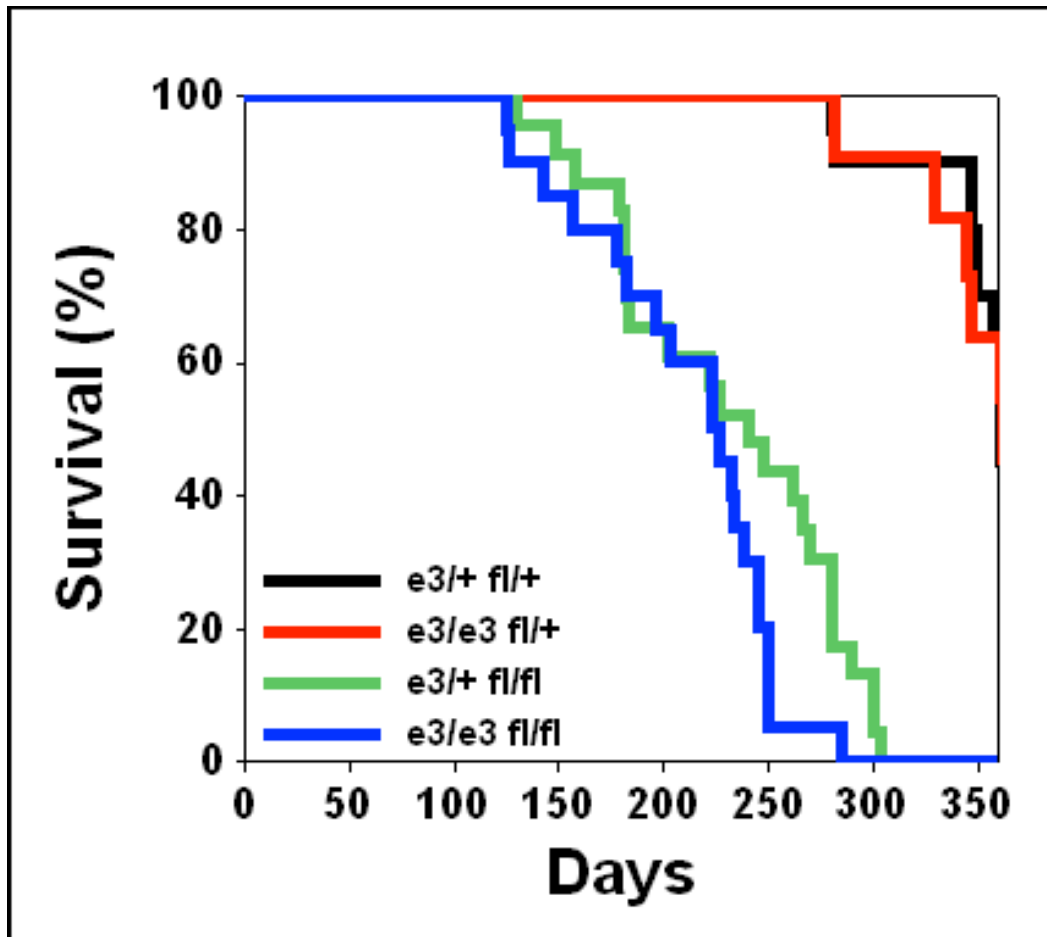


Figure 3:13 Survival of $UroIIICRE^+$ β -catenin^{exon3/exon3} $Pten^{fl/fl}$ mice

Kaplan Meier curves of tumour free survival of respective double mutant cohorts. Abbreviations: e3/+ fl/+ ($UroIIICRE^+$ β -catenin^{exon3/+} $Pten^{fl/+}$), e3/e3 fl/+ ($UroIIICRE^+$ β -catenin^{exon3/exon3} $Pten^{fl/+}$), e3/+ fl/fl ($UroIIICRE^+$ β -catenin^{exon3/+} $Pten^{fl/fl}$) and e3/e3 fl/fl ($UroIIICRE^+$ β -catenin^{exon3/exon3} $Pten^{fl/fl}$). Log rank test indicates significant difference between e3/+fl/+ / e3/e3 fl/+ and e3/+ fl/fl / e3/e3 fl/fl cohorts ($p < 0.001$).

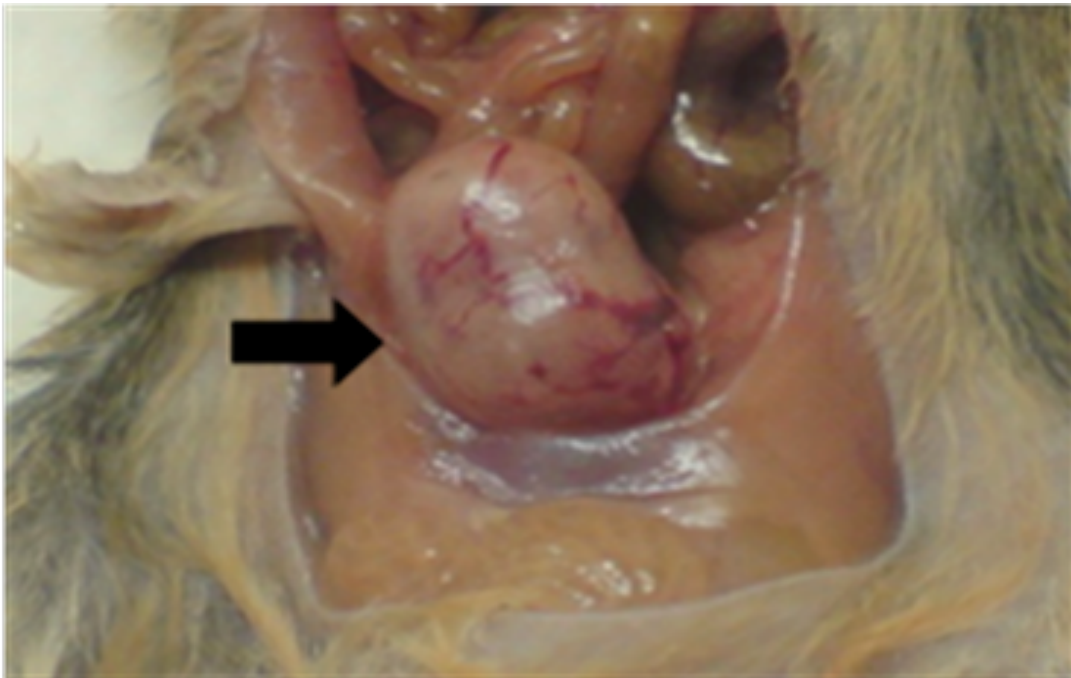


Figure 3:14 Photograph of *UroII*CRE⁺ β -catenin^{exon3/exon3} *Pten*^{fl/fl} bladder tumour

The whole bladder here has been replaced by tumour, creating the solid mass seen above.

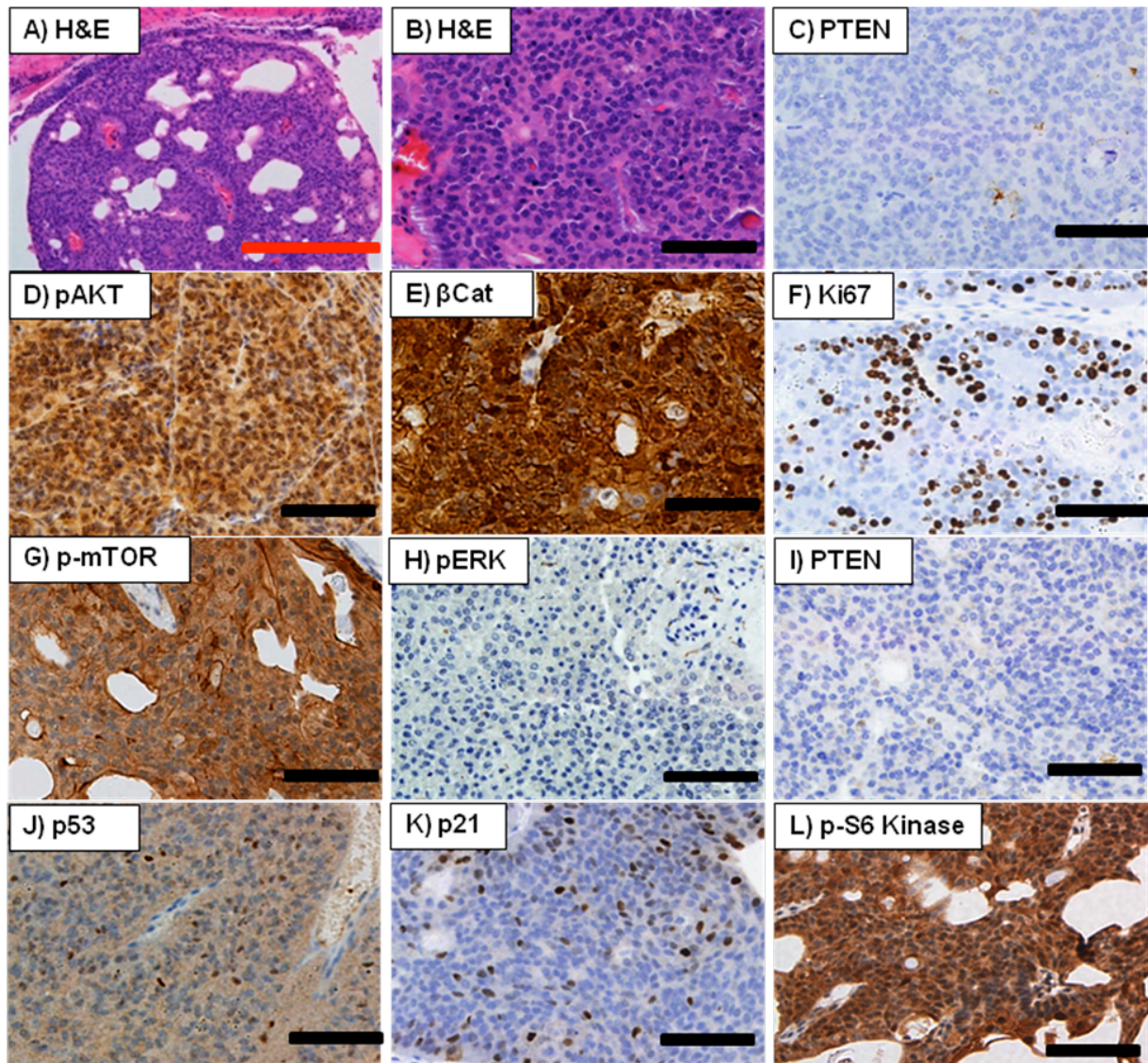


Figure 3.15: Histology of a UroII CRE⁺ β -catenin^{exon3/exon3} Pten^{fl/fl} mice

Histology of a UroII CRE⁺ β -catenin^{exon3/exon3} Pten^{fl/fl} mice reveals urothelial bladder tumour (A,B) with loss of PTEN (C) and upregulation of pAKT(Ser473) in these tumours (D). There is also upregulation of nuclear β -catenin (E), Ki67 (F) and mTOR(Ser2448) (G). I noticed no upregulation in pERK1/2 in these tumours (H). By 12 months of age, a small subset of the UroII CRE⁺ β -catenin^{exon3/exon3} Pten^{fl/+} mice and UroII CRE⁺ β -catenin^{exon3/+} Pten^{fl/+} mice had developed tumours, presumably due to the loss of the remaining Pten allele (I). Tumours demonstrate minimal upregulation of p53 (J) and p21 (K). There is significant upregulation of p-S6 Kinase (L). Red bar measures 1000 μ m (4x magnification), black bar measures 100 μ m (40x magnification).

(At least 3 samples from each cohort stained and representative images are shown above).

3.2.5. *UroIIICRE*⁺ *β-catenin*^{exon3/exon3} *Pten*^{fl/fl} UCCs are mTOR dependent

Given mTOR is one of the key tumour promoting pathways downstream of PTEN loss, I next investigated whether tumours from *UroIIICRE*⁺ *β-catenin*^{exon3/exon3} *Pten*^{fl/fl} mice would remain dependent on mTOR even if they were fully established. Therefore I treated *UroIIICRE*⁺ *β-catenin*^{exon3/exon3} *Pten*^{fl/fl} mice at 6 months of age with Rapamycin (10mg/kg i.p. daily), a potent inhibitor of mTOR, or vehicle (n=3) when mice had a detectable tumour using Visualsonic's Vevo 770 ultrasound. Remarkably I was able to demonstrate regression of tumour bulk between initiation and the end of treatment (Figure 3.16 A-D). All mice on treatment survived the 4-week experiment, however in the vehicle treated mice cohort, 2 mice had to be sacrificed early (7 and 11 days) because of tumour burden. IHC for p-mTOR²⁴⁴⁸ revealed significant upregulation of this pathway in *UroIIICRE*⁺ *β-catenin*^{exon3/exon3} *Pten*^{fl/fl} mice. However when treated with 4 weeks of Rapamycin I noticed regression of the lesions and downregulation of the protein staining, as well as downstream targets p-S6 kinase and p-4EBP1 (Figure 3.16 E&F and 3.17). I noticed a statistically significant reduction in the BrdU positive cells in the tumours from the Rapamycin treated mice compared to the vehicle controls (p<0.05, Mann Whitney Test) (Figure 3.18).

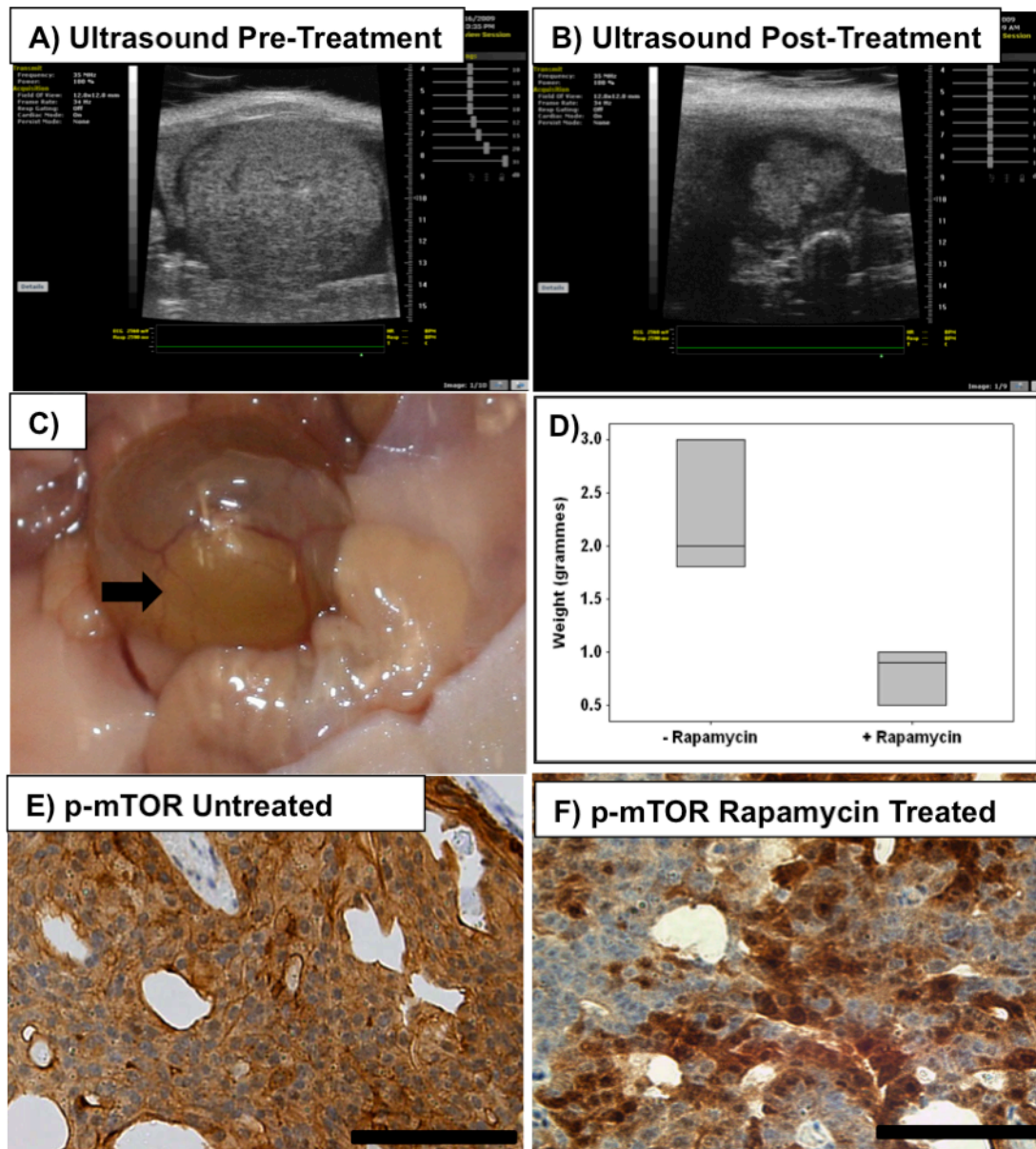


Figure 3.16: *UroICRE*⁺ *β-catenin*^{exon3/exon3} *Pten*^{fl/fl} mice treated with Rapamycin

Analysis of *UroICRE*⁺ *β-catenin*^{exon3/exon3} *Pten*^{fl/fl} mice treated with 4 weeks of daily IP injections of Rapamycin (10mg/kg). Ultrasound imaging reveals shrinking of the tumour in the treated mice bladders between initiation (A) and end of treatment (B) regimes. I saw regression of tumour formation (C) from non-treated controls. Boxplot shows that bladders of treated mice have less tumour bulk p<0.05, Mann Whitney Test) (D). IHC for p-mTOR reveals significant upregulation of this pathway in *UroICRE*⁺ *β-catenin*^{exon3/exon3} *Pten*^{fl/fl} mice (E). However when treated with 4 weeks of Rapamycin I noticed regression of the lesions and downregulation of the protein staining (F). Black bar represents 100µm (all magnifications at 40x).

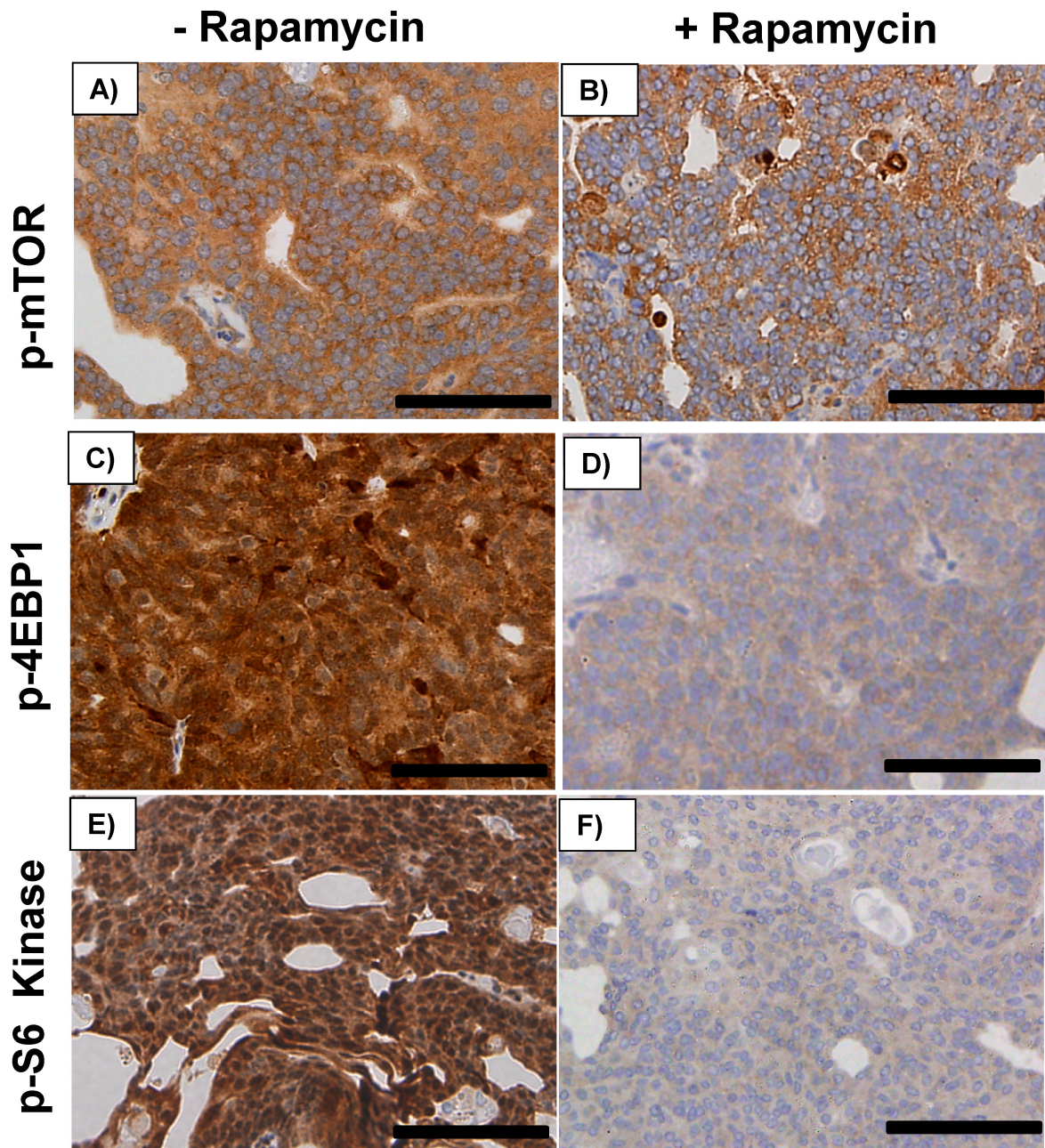


Figure 3.17: *UroII CRE⁺ β -catenin^{exon3/exon3} Pten^{fl/fl}* mice treated with Rapamycin

Additional IHC for p-mTOR reveals significant downregulation of this pathway in *UroII CRE⁺ β -catenin^{exon3/exon3} Pten^{fl/fl}* mice after treatment with Rapamycin (A,B). Similarly I also demonstrate that p-4EBP1 and p-S6 Kinase, a known target of the mTOR pathway, is downregulated after treatment (C-F). Black bar represents 100 μ m (40x objective).

(At least 3 samples from each cohort stained and representative images are shown above).

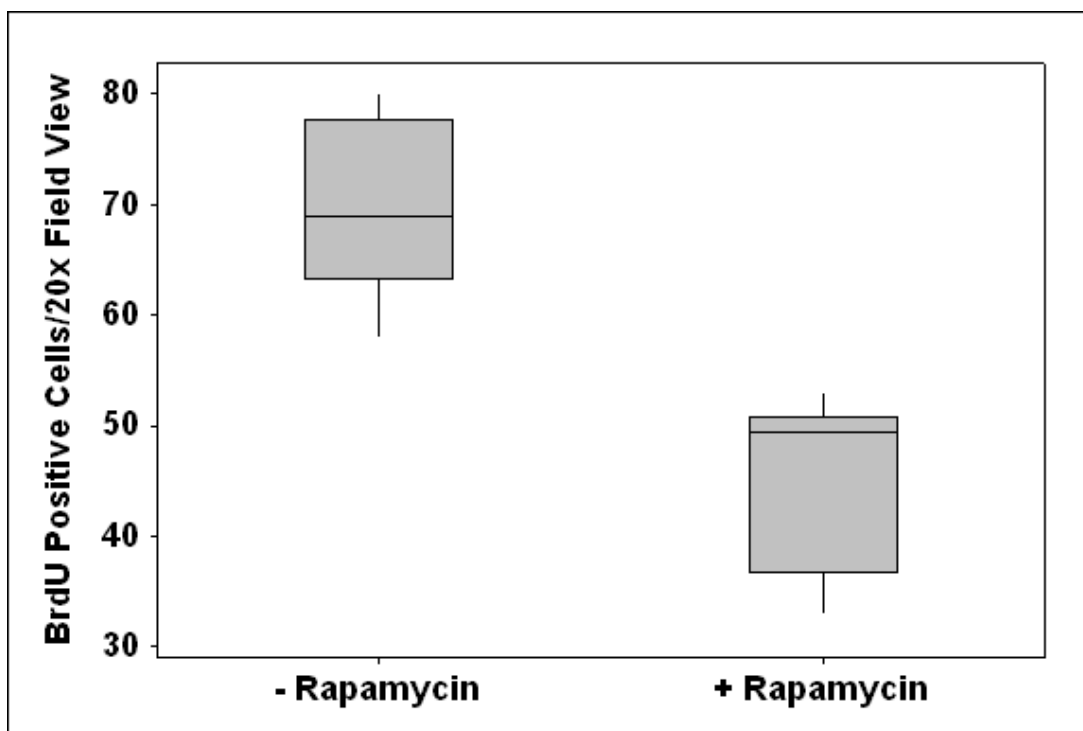


Figure 3.18: Proliferation of tumours in Rapamycin treated mice versus vehicle control

Boxplot indicating reduction of BrdU positive cells per 20x field view of bladder tumours treated with Rapamycin versus those treated with vehicle control ($p < 0.05$, Mann Whitney Test). At least 3 areas scored from each slide ($n=3$). Thick lines represents median, box represents inter-quartile range and whiskers the range.

3.2.6. Human UCC demonstrate correlation between Wnt activation and PTEN loss

In human urothelial cancer, a number of studies have suggested Wnt signalling is important. Of particular note is the demonstration that nuclear β -catenin is associated with a poor prognosis, and methylation of the genes encoding inhibitors of Wnt signalling, the SRFPs, act as markers of a bad prognosis (Marsit et al., 2005, Urakami et al., 2006a, Urakami et al., 2006b). Indeed the methylation of these genes has been suggested as a marker of invasive bladder carcinoma.

A tissue microarray of human bladder UCC containing 80 cases, 60 UCC (transitional cell carcinomas [TCC]) and 20 benign controls (Folio biosciences, OH, USA), was studied. Using the histoscore technique to quantitate immunoreactivity, upregulation of β -catenin expression and loss of PTEN signal were found to be significantly associated (n=36/56, cc=0.314, p<0.01, SPSS v15). Upregulated expression of β -Catenin and pAKT^{Ser473} were similarly associated (n=30/56, cc=0.471, p<0.001, SPSSv15) (Figure 3.19 and 3.20). Taken together, loss of PTEN and resulting upregulation of pAKT is essential for Wnt driven UCC to progress.

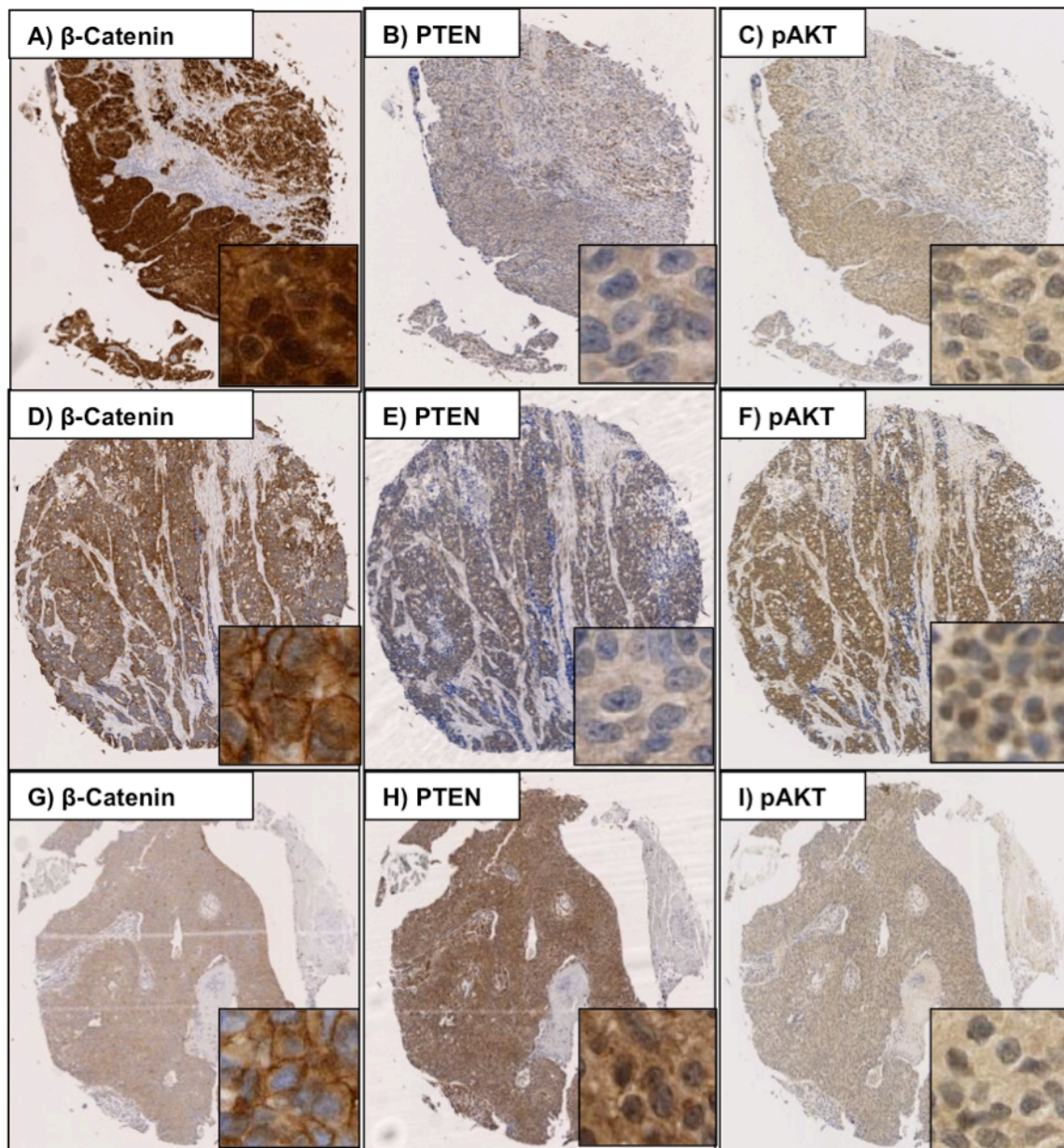


Figure 3.19: Human Bladder UCC TMA

IHC of 3 human bladder transitional cell carcinoma cases (A-C, D-F and G-I) revealing upregulation of β -catenin (A&D), loss of corresponding PTEN signal (B&E) and upregulation of $\text{pAKT}^{\text{Ser473}}$ (C&F). Conversely a few samples showed upregulation of PTEN (H) with minimal β -catenin and $\text{pAKT}^{\text{Ser473}}$ signal (G&I).

Each core size is 1.5mm

A)	Number of Cores	%	p
↑B-Catenin: ↓PTEN (p<0.01)	36	64%	<0.01
↓B-Catenin: ↑PTEN	3	5%	

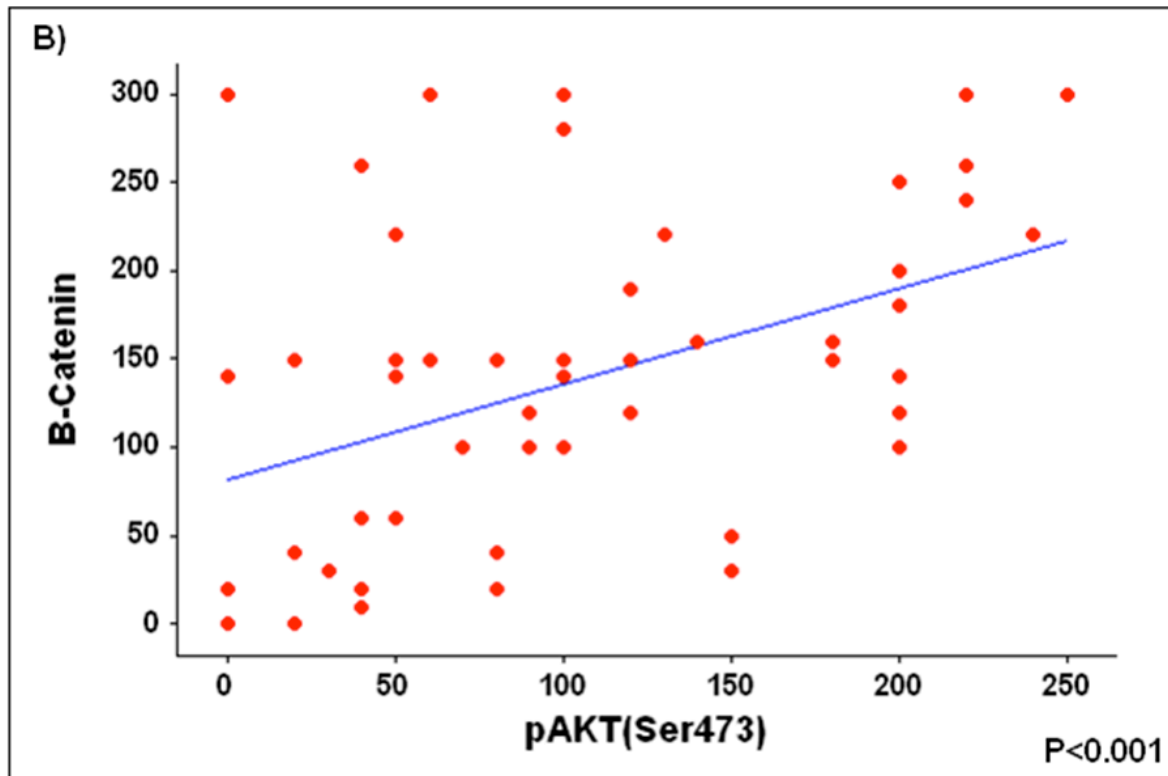


Figure 3.20: Correlation between β -catenin and PTEN/pAKT in Human Bladder UCC TMA

Table demonstrating proportions of cores that show combinations of up- and downregulation of β -catenin and PTEN/pAKT (Upregulation is classified as ≥ 100 and downregulation as < 100 using the histoscore technique) (A). Scatterplot demonstrating correlation between β -catenin and pAKT (B).

3.3. Discussion

Data presented in this chapter suggests that activation of Wnt signalling cooperates with other mutations such as loss of PTEN/activation of pAKT to drive bladder carcinogenesis. This may indicate that the significance of Wnt signalling in human bladder cancer has been underestimated, due to the relatively rare nature of *APC* and *β-catenin* mutations. Traditionally up to a quarter of bladder tumours are thought to exhibit nuclear β-catenin (Kastritis *et al.*, 2009). Instead the Wnt signalling pathway may be involved by epigenetic inactivation or mutations in other components of the pathway (e.g. secreted frizzled related proteins). Patients with Wnt dependent tumours may be identified by IHC for proteins such as β-catenin or downstream proteins such as c-Myc. Unfortunately the active epitope for β-catenin rapidly degrades unless the samples are processed and embedded within 24 hours, which is not always practical for clinical samples. Thus there is a need to identify more robust biomarkers for Wnt pathway activation that we can transfer to the clinic.

Indeed our studies would suggest in those patients where tumours had high levels of β-catenin and p-AKT, the combination of mTOR and Wnt inhibition might be an attractive combination. My TMA results are exciting, but still very preliminary, since they are carried out on a relatively small cohort of patients (n=80). I am currently repeating these studies on larger powered cohorts.

Recently, antibody-based therapies have also been developed that target molecules of the Wnt pathway (such as Wnts and Frizzleds) that are over-expressed in disease (Nagayama *et al.*, 2005, You *et al.*, 2004). These tumours may be responsive to antibodies that inhibit Wnt signalling through blocking ligand binding such as Frizzled8CRD-hFc (DeAlmeida *et al.*, 2007). These are currently being developed and tested in preclinical tumour models.

X-ray structure analysis of components of the Wnt pathway (β -catenin, Axins, APC, TCFs, Dishevelled, BCL9 and their complexes) will allow future design and testing of novel compounds targeting this pathway, and a number of high-throughput screening programmes to discover such compounds are currently underway (Klaus and Birchmeier, 2008). Future evaluation of combined inhibition of the mTOR and Wnt pathways is desirable. This would indeed be the first steps towards “personalised” medicine, in which each tumour has its molecular signature analysed and subsequent treatment regimes are based on these findings. So it would not be unreasonable to suggest our subset of UCC patients with upregulation of the Wnt and PI3K pathways may receive a combination of Wnt and PI3K inhibitors for their tumours.

Taken together, I showed original data supporting a causative role for β -catenin in the formation of UCC *in vivo* and provide definitive evidence that activating mutations in the Wnt pathway promote UCC when combined with loss of PTEN/activation of the PI3K pathway.

Chapter 4: Ras mutation cooperates with β -catenin activation to drive bladder tumorigenesis

4.1. Introduction

In the previous experimental chapter, I explored the causative role of β -catenin in the formation of UCC *in vivo*, and showed that activating mutations in the Wnt pathway promote UCC when combined with loss of PTEN/activation of the PI3K pathway.

H-Ras was the first human oncogene isolated in human UCC, being mutated most often at codon 12, 13 and 61 (Reddy et al., 1982). As well as becoming constitutively active, overexpression of the protein due to alternative splicing of the last intron can also occur. Despite the controversy regarding the reported mutation frequency rate recent studies indicate that *HRAS* mutation occurs in approximately in 30-40% of UCC (Kompier et al., 2010). Transgenic models have provided invaluable information regarding the molecular mechanisms behind HRAS activation (See section 1.6.1.1.).

Conversely few studies have looked at K-Ras mutations in human bladder cancer, although those that have suggest a wide variation in frequency (4-29%) (Ayan et al., 2001, Uchida et al., 1995, Olderoy et al., 1998). Interestingly a study by Vageli and colleagues demonstrated the K-Ras oncogene was overexpressed in 15 of the 26 (58%) samples (Vageli et al., 1996). Unfortunately, as with many of these studies there was no segregation of samples into non-invasive and muscle invasive tumours.

As I have outlined previously the human data regarding Wnt pathway activation is highly controversial. It is now becoming clear that the pathway is activated in a proportion of UCCs, but whether these are segregated to the non-invasive, papillary pathway or the muscle invasive pathway is yet to be fully elucidated.

I have previously shown that *UroIIICRE*⁺ *β -catenin*^{exon3/exon3} mice develop hyperproliferative lesions that do not progress to invasive UCC despite aging. As demonstrated the HRAS mice (low-copy) develop tumours only after a very long latency (up to 26 months) with an

incomplete penetrance (63%), despite demonstrating significant hyperproliferation at an early stage (Zhang et al., 2001). This is suggestive that additional mutations may be required to drive the non-invasive, papillary, UCC phenotype. Despite K-Ras being implicated in human UCC, there are no murine models as yet published.

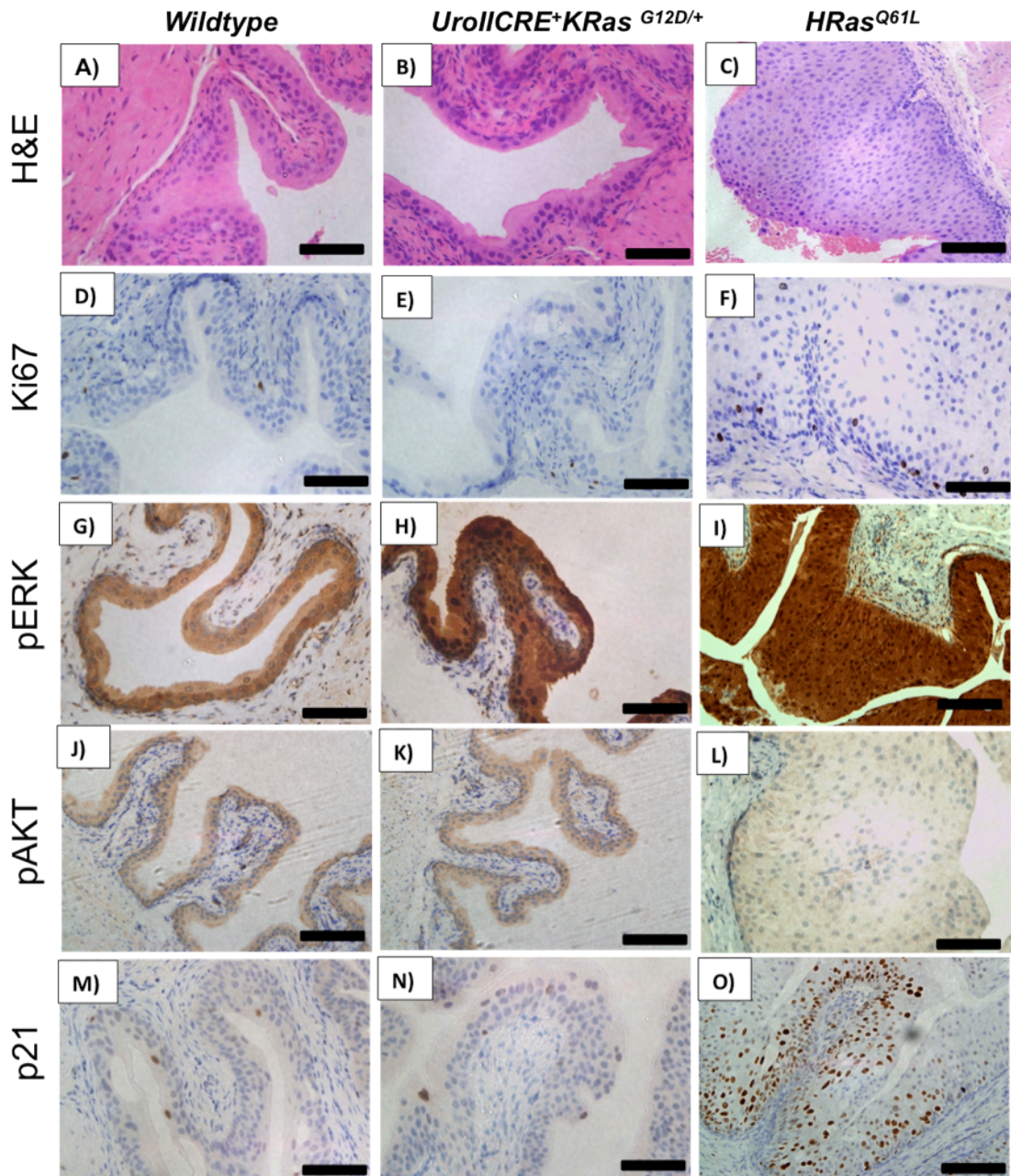
Thus the aim of this part of my project was to test the effect of Ras overexpression or its mutation on the murine urothelium *in vivo* to promote carcinogenesis, and its interaction with a background of upregulated Wnt signalling.

4.2. Results

4.2.1. Ras activation alone does not lead to UCC in the mouse

To test whether oncogenic Ras mutation would lead to UCC, *UroIIICRE*⁺ mice were intercrossed to mice carrying either oncogenic K-Ras G12D allele (Jackson et al., 2001) or constitutively active H-Ras oncogene (“low-copy”) (Zhang et al., 2001). I demonstrated that neither *UroIIICRE*⁺*K-Ras*^{G12D/+} nor *H-Ras*^{Q61L} mice developed cancer when aged to 12 months of age (n=20). Indeed, no phenotypic abnormalities were observed in the urothelium of *UroIIICRE*⁺*K-Ras*^{G12D/+} mice (Figure 4.1 A&B). There was minimal proliferation as observed by Ki67 staining (Figure 4.1 D&E), with significant upregulation of pERK1/2 compared to wildtype (Figure 4.1 G&H). I noticed no upregulation of pAKT, p21, pMEK, Active-Rac1 or β -catenin (Figure 4.1 J-K, M-N, Q-P, S-T, and V-W).

In comparison, as previously published, I noticed global hyperplasia of the 12 month old *H-Ras*^{Q61L} urothelium compared to wildtype (Figure 4.2 C) (Zhang et al., 2001). These “low copy” mice have 2 copies of the oncogenic rabbit transgene. Although Zhang et al demonstrated tumour latency from 10-26 months of age; no tumours were observed in our *H-Ras*^{Q61L} mice cohort at sacrifice (12 months of age). These aged mice again demonstrated strong upregulation of pERK1/2 with upregulation of Ki67 and p21 (Figure 4.1 F, I, O), without evidence of any upregulation of pAKT signal (Figure 4.1 L). There was minimal upregulation of pMEK and Active-Rac1, although there is some β -catenin staining, there is only the occasional sporadic cell that exhibited nuclear staining (Figure 4.1 R,U,X). This may be due to partial Wnt pathway activation by upregulation of the MAPK pathway in the *H-Ras*^{Q61L} mutant urothelium.



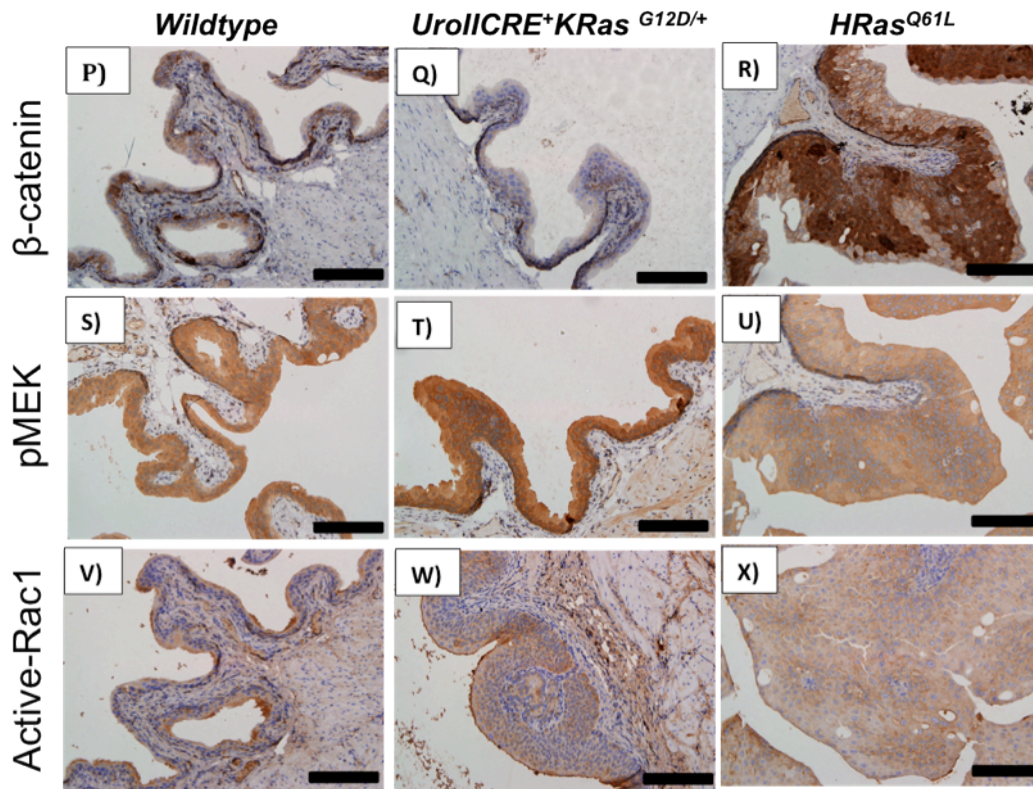


Figure 4.1: Histology from 12-month-old Wildtype, UroII CRE+K-Ras^{G12D/+} and H-Ras^{Q61L} mice

Wildtype, *UroII CRE⁺ K-Ras^{G12D/+}* (oncogenic point mutation, endogenous levels) and *H-Ras^{Q61L}* (rabbit transgene, multiple copies) urothelia H&E (A-C), Ki67 (D-F), perk (G-I), pAKT (J-L), p21(M-O), β-catenin (P-R), pMEK (S-U) and Active-Rac1 (V-X).

Black bar measures 200μm (20x magnification).

(At least 3 samples from each cohort stained and representative images are shown above).

Thus I next investigated the expression of candidate molecules from the FGFR3 and RAS oncogenic pathways within lesions from the *UroII CRE⁺ β -catenin^{exon3/exon3}* mice. Within the lesions I saw minimal levels of STAT3 signalling (Figure 4.2 C), though very high levels of pERK1/2 staining was present (Figure 4.2 D) suggesting a role of the Ras signalling pathway.

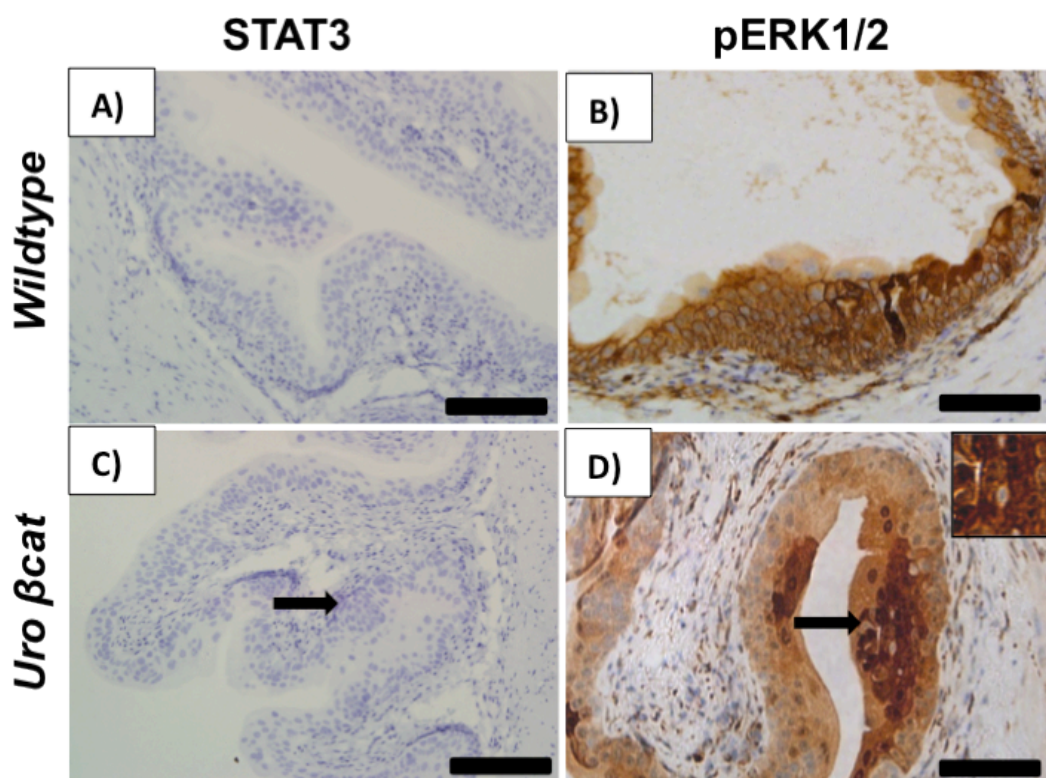


Figure 4.2: Histology from 12 month old *UroII CRE⁺ β -catenin^{exon3/exon3}* mice.

Within these urothelial lesions I see comparable (minimal) STAT3 staining to wildtype (A&C) with significant upregulation of pERK1/2 compared to wildtype (B&D) signal. Black bar measures 200 μ m (20x magnification).

(At least 3 samples from each cohort stained and representative images are shown above).

4.2.2. Ras activation cooperates with β -catenin to drive UCC formation

To test the cooperation of β -catenin and Ras activation I next generated the following cohorts: *UroIIICRE*⁺ *β -catenin*^{exon3/exon3} *K-Ras*^{G12D/+} and *UroIIICRE*⁺ *β -catenin*^{exon3/exon3} *H-Ras*^{Q61L} (n= 25 and 29 respectively). Two cohorts were studied, with mice sacrificed at 3 months of age or aged mice until tumour development, and then bladder phenotypes were characterised. In contrast to the singly mutant mice, the *UroIIICRE*⁺ *β -catenin*^{exon3/exon3} *K-Ras*^{G12D/+} (mean survival 185 days, median 200 days) and *UroIIICRE*⁺ *β -catenin*^{exon3/exon3} *H-Ras*^{Q61L} (mean survival 231 days, median 236 days) mice rapidly developed symptoms of bladder tumourigenesis, namely abdominal swelling, haematuria (blood in the urine) and hunching (Figure 4.3). On necropsy, I observed bladder tumours with histological progression to non-invasive papillary carcinomas (Figure 4.4 A&B). I found no evidence of metastasis in any of our models. Unfortunately a proportion of our *UroIIICRE*⁺ *β -catenin*^{exon3/exon3} *K-Ras*^{G12D/+} mice developed lung tumours. These mice were excluded from this analysis and will be discussed in more detail in section 5.2.3.

Tumours from both models showed a nuclear upregulation of β -catenin and Ki-67 (Figure 4.4 C-F). The numbers of proliferating cells within tumours (identified by Ki-67 and BrdU IHC) were much higher than in the *UroIIICRE*⁺ *β -catenin*^{exon3/exon3} mice (Figure 4.5), possibly explaining why lesions do not progress in the single mutant. I observed significant upregulation of pERK1/2 (Figure 4.4 G-H), with minimal levels of pAKT (Figure 4.4 I&J), similar to what was observed in the single β -catenin and Ras mutant mice. The PTEN signal is still intact in these tumours (Figure 4.4 K&L). In both sets of tumours I noticed upregulation of the tumour suppressor p21 (Figure 4.4 M&N). This upregulation is particularly marked in the *UroIIICRE*⁺ *β -catenin*^{exon3/exon3} *K-Ras*^{G12D/+} mutants since the *K-Ras* single mutants have minimal p21 staining. Interestingly when I quantified the p21 positive cells (per field view) between *H-Ras*^{Q61L} and the *UroIIICRE*⁺ *β -catenin*^{exon3/exon3} *H-Ras*^{Q61L}

mice I noticed a significant drop in positivity in the tumours compared to the hyperplastic urothelium of the single mutant (Figure 4.6).

These data are consistent with tumour formation in the bladder being synergistically promoted by Wnt and MAPK signalling.

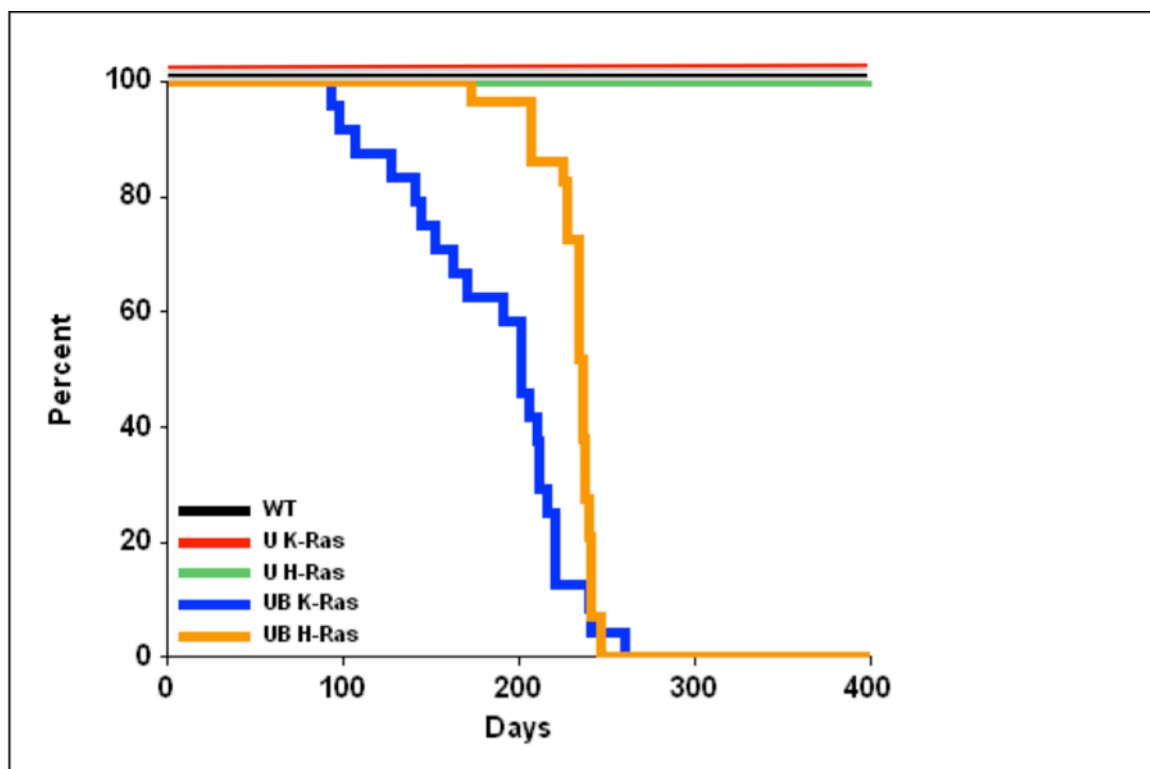


Figure 4.3: Kaplan Meier curves of tumour free survival of respective mutant cohorts

Abbreviations: WT (wildtype), U K-Ras ($UroII\text{CRE}^+ K\text{-Ras}^{G12D/+}$), U H-Ras ($H\text{-Ras}^{Q61L}$), UB K-Ras ($UroII\text{CRE}^+ \beta\text{-catenin}^{\text{exon3/exon3}} K\text{-Ras}^{G12D/+}$), UB H-Ras ($UroII\text{CRE}^+ \beta\text{-catenin}^{\text{exon3/exon3}} H\text{-Ras}^{Q61L}$). Log rank test reveals significant reduction in survival of UB K-Ras and UB-H-Ras compared to WT/U K-RAS/U H-Ras ($p < 0.001$).

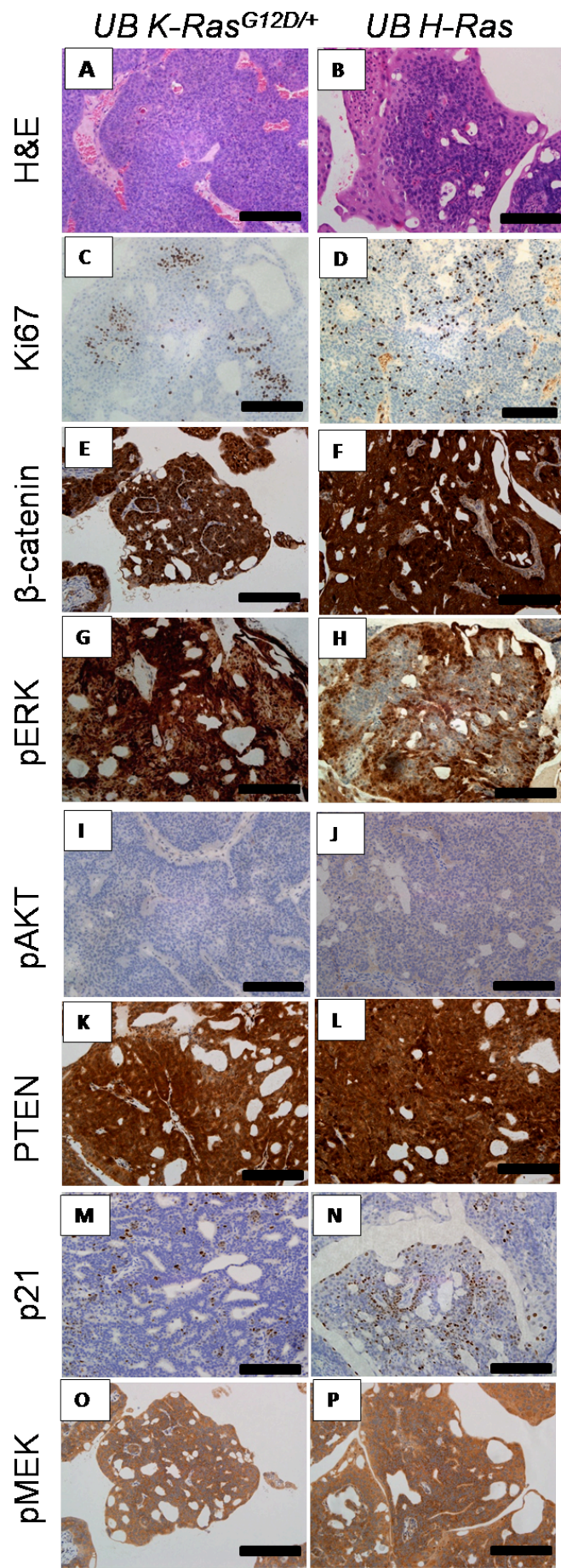


Figure 4.4: Histology of *UroII*CRE+ β -catenin^{exon3/exon3K}-*RasG12D*/+ and *UroII*CRE+ β -catenin^{exon3/exon3} *H-Ras*^{Q61L} mice:

Reveals urothelial bladder tumours (A&B). I stained for Ki67 (C&D), β -catenin (E&F), pERK1/2 (G&H), pMEK (O&P), pAKT (I&J) and PTEN (K&L). Black bar measures 200 μ m (20x magnification).

(At least 3 samples from each cohort stained and representative images are shown above).

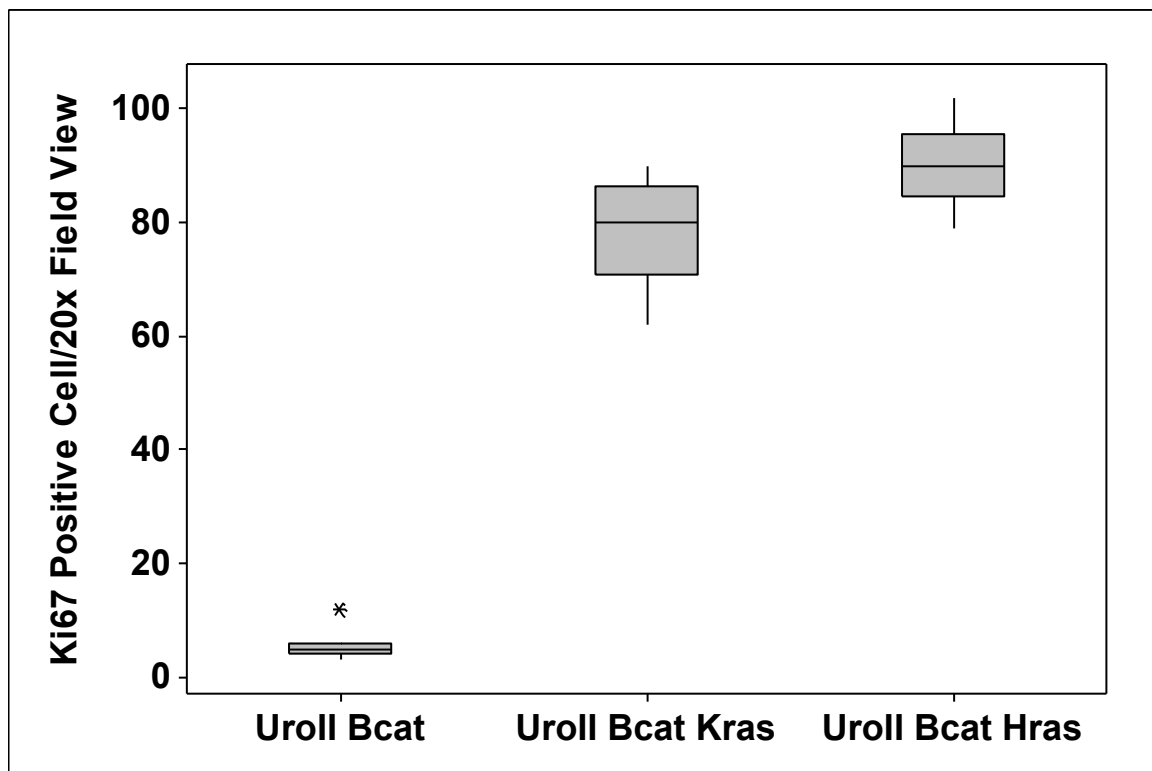


Figure 4.5: Boxplot comparing Ki67 positivity between *UroII*CRE+ β -catenin^{exon3/exon3}, *UroII*CRE+ β -catenin^{exon3/exon3} *H-Ras*^{Q61L} and *UroII*CRE+ β -catenin^{exon3/exon3} *K-Ras* mice

Boxplot indicating increase of Ki67 positive cells between the 3 cohorts of mice (p<0.001, Mann Whitney Test). At least 3 areas from each slide scored (3 mice per cohort). Thick line represents median, box represents inter-quartile range and whiskers represent range.

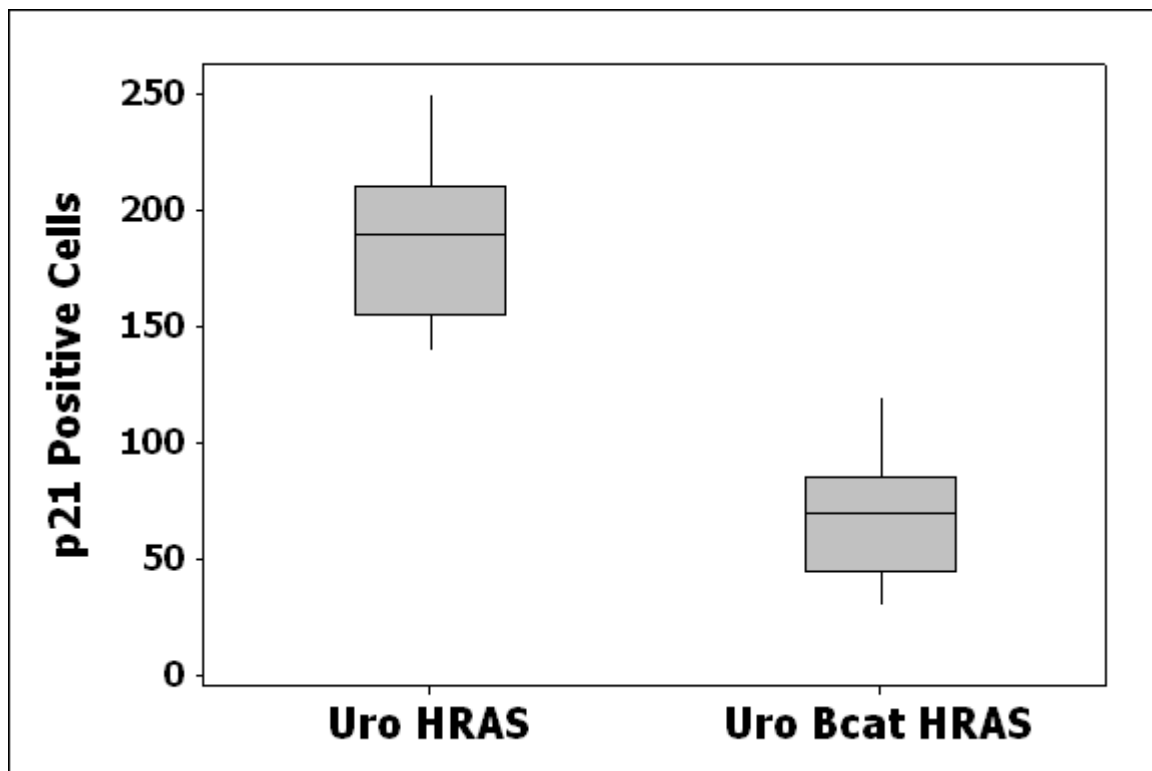


Figure 4.6: Boxplot comparing p21 positivity between *H-Ras*^{Q61L} and *UroICRE+* β -catenin^{exon3/exon3} *H-Ras*^{Q61L} mice

Boxplot indicating reduction of p21 positive cells between the 2 cohorts of mice ($p < 0.001$, Mann Whitney Test). At least 3 areas from each slide scored (3 mice per cohort). Thick line represents median, box represents inter-quartile range and whiskers represent range.

4.2.3. p21 upregulation blocks β -catenin driven UCC

As I have shown p21 levels are upregulated in the *H-Ras*^{Q61L} hyperplastic urothelium, but in the *UroII CRE*⁺ *β -catenin*^{exon3/exon3} *H-Ras*^{Q61L} tumours I noticed a significant drop in p21 positivity. This is a similar picture to the *UroII CRE*⁺ *β -catenin*^{exon3/exon3} urothelium, where I see significant upregulation of p21 in the lesions, but this disappears in the *UroII CRE*⁺ *β -catenin*^{exon3/exon3} *Pten*^{fl/fl} tumours. In both cases there appears to be a bladder-specific upregulation of p21, associated with blocked tumourigenesis of the H-Ras and β -catenin mutants. Thus, I next tested if the p21 compensatory mechanism is lost, will β -catenin activation result in progression to frank UCC.

I generated the following cohorts: *UroII CRE*⁺ *p21*^{-/-} and *UroII CRE*⁺ *β -catenin*^{exon3/exon3} *p21*^{-/-} (n= 6 and 16 respectively). I then aged mice until tumour development. The *UroII CRE*⁺ *β -catenin*^{exon3/exon3} *p21*^{-/-} mice rapidly developed urothelial tumours (mean 237, median 238 days) in comparison to the *UroII CRE*⁺ *p21*^{-/-} that were aged to 18 months with no urothelial phenotype (Figure 4.7).

Indeed consistent with previous studies these tumours demonstrated evidence of proliferation by Ki67 staining as well as high levels of nuclear β -catenin and pERK1/2 (Figure 4.8 A-D). This time the lesions did not demonstrate any significant level of nuclear p53 or p21 (Figure 4.8 E-F). This suggests that p21 plays a role in blocking β -catenin induced UCC.

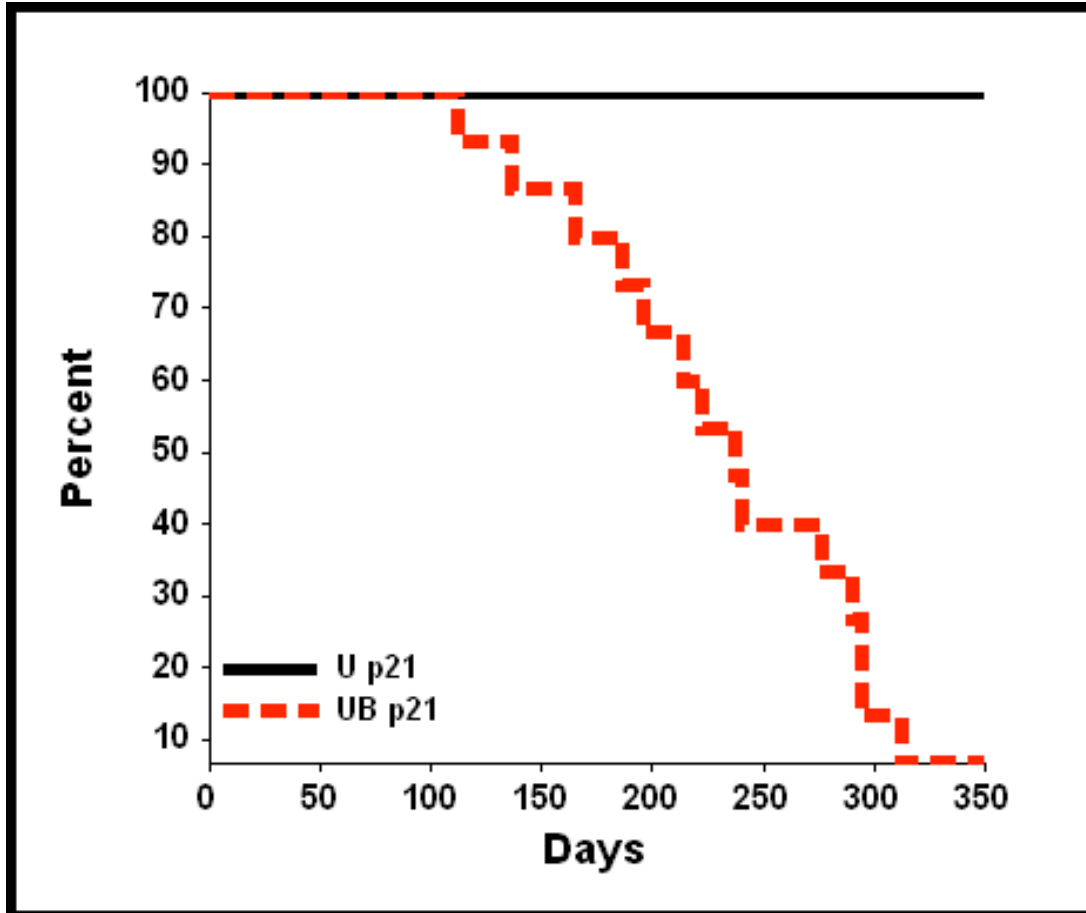


Figure 4.7: Kaplan Meier curves of tumour free survival of *UroIIICRE⁺p21^{-/-}* (U p21) and *UroIIICRE⁺ β -catenin^{exon3/exon3}p21^{-/-}* (UB p21) cohorts

Log Rank test $p < 0.0001$

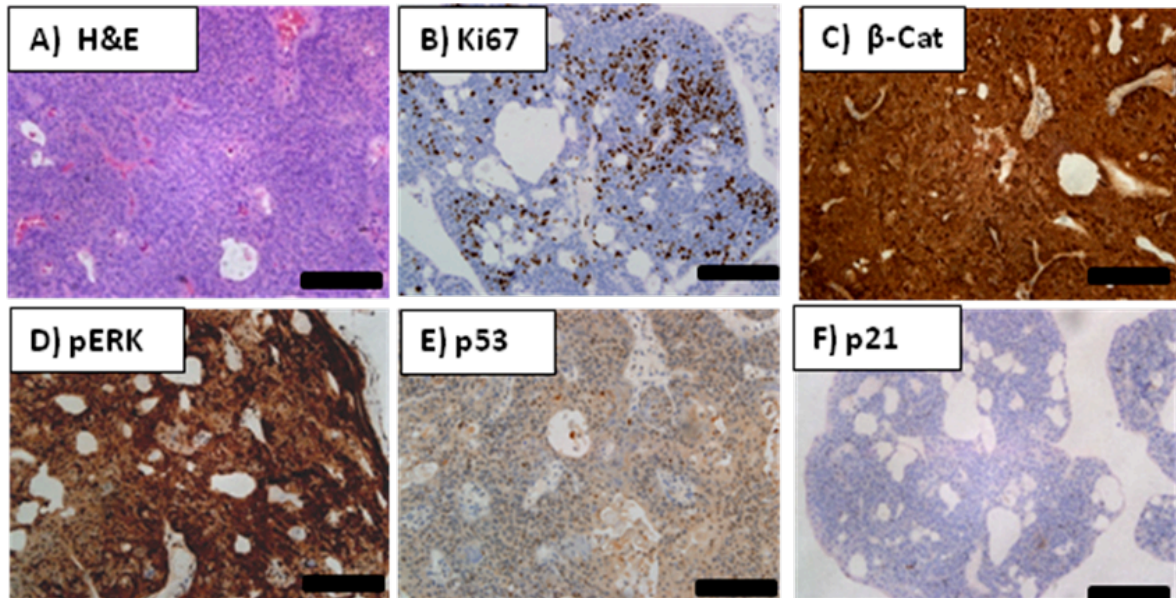


Figure 4.8: Histology of *UroII* CRE⁺ *β-catenin*^{exon3/exon3} *p21*^{-/-} mouse.

H&E reveals bladder tumour (A) with upregulation of Ki67, β -catenin and pERK1/2 (B-D). There is minimal upregulation of p53 and p21 (E&F). Black bar measures 200 μ m (20x magnification).

(At least 3 samples from each cohort stained and representative images are shown above).

4.2.4. Human UCC demonstrate correlation between Wnt and Ras activation

In human urothelial cancer, a number of studies have suggested Wnt signalling is important. Of particular note is the demonstration that nuclear β -catenin is associated with a poor prognosis, and methylation of the genes encoding inhibitors of Wnt signalling, the SRFPs, act as markers of a bad prognosis (Marsit et al., 2005, Urakami et al., 2006a, Urakami et al., 2006b). Indeed the methylation of these genes has been suggested as a marker of invasive bladder carcinoma.

I next looked at human bladder UCC using a tissue microarray of 80 cases, 60 UCC (transitional cell carcinomas [TCC]) and 20 benign controls (Folio biosciences, OH, USA). Using the histoscore technique I was able to demonstrate a significant correlation between upregulation of β -catenin and activation of pERK1/2 (n=24/56, cc=0.333, p=0.012, SPSS v15) (Figure 4.9 & Figure 4.10). This is further indication that activation of the Ras pathway is essential for Wnt driven UCC to progress.

The presence of nuclear p21 was observed in a third of the tumour samples (20 out of 60), which did not show significant association with tumour grade, probably due to the small cohort size. I next wanted to look at correlation between upregulation of β -catenin and loss of p21 (Figure 4.9). However I found no evidence for any correlation between the 2 groups (cc=0.174, p=0.199). Interestingly, there was an expected significant correlation between upregulation of pERK1/2 and p21 loss (cc=0.369, p=0.005).

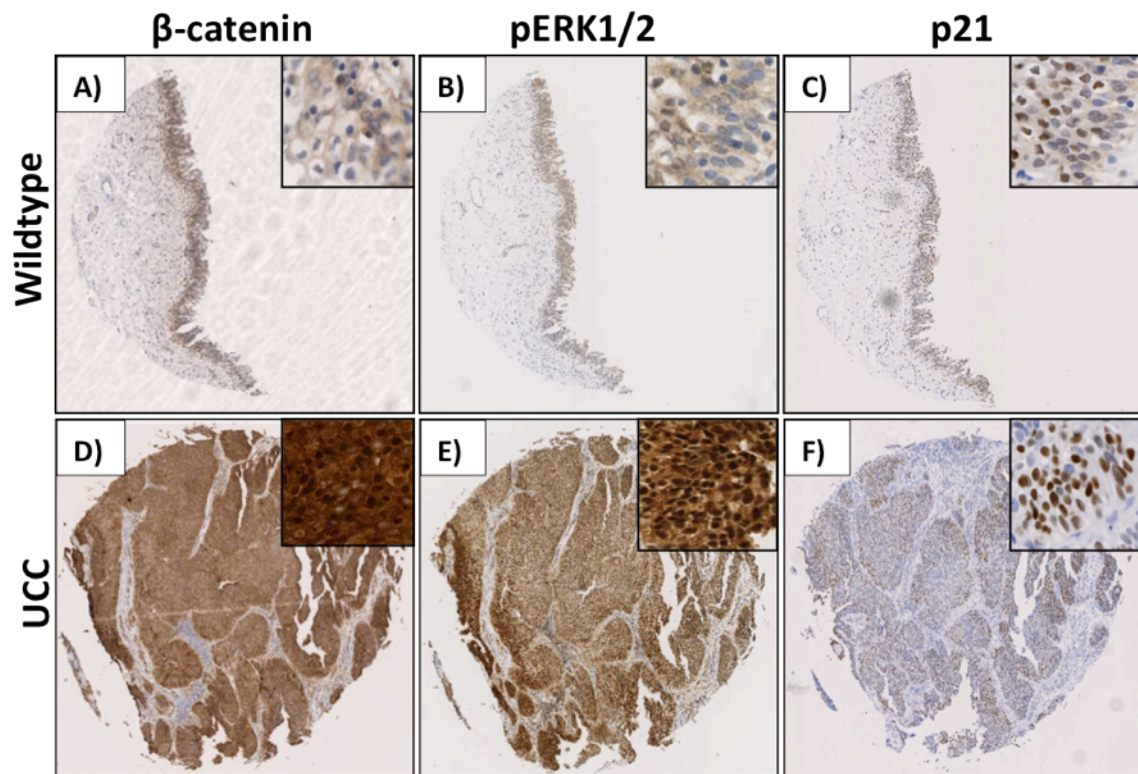


Figure 4.9: Human Bladder UCC TMA

IHC of human bladder transitional cell carcinoma revealing upregulation of β -catenin (A&D), and corresponding upregulation of pERK1/2 (B&E), with minimal expression of p21 (C&F) compared to wildtype.

Each core size is 1.5mm.

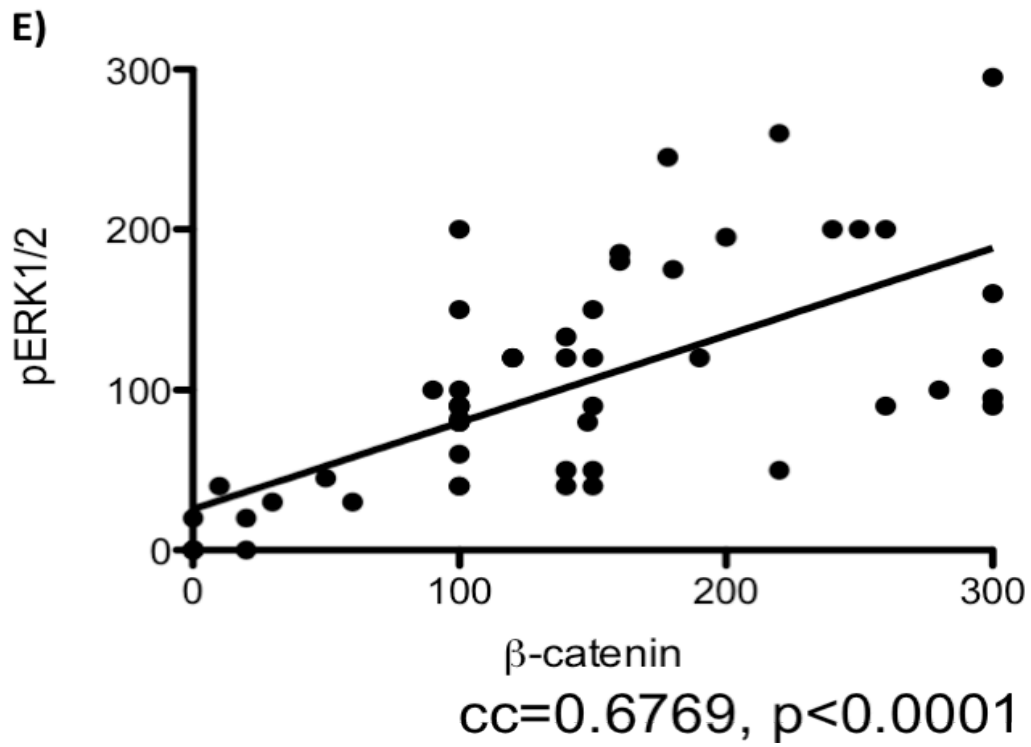


Figure 4.10: Correlation between β -catenin and pERK1/2 in Human Bladder UCC TMA

Scatterplot demonstrating correlation between β -catenin and pERK1/2.

4.3. Discussion

I have shown that activation of the Ras pathway alone is not enough to drive UCC. However, activation of Wnt signalling strongly cooperates with other genetic events that occur in bladder cancer such as activation of Ras to drive carcinoma formation. Our tumours never became invasive, suggesting co-operation of both mutations along the non-invasive/papillary UCC pathway. It must be noted that both our Ras mice are different in respect to knock-in/overexpression status. I utilised the Lox-Stop-Lox K-Ras conditional mouse strain, in which expression of oncogenic K-Ras G12D is controlled by a removable transcriptional termination Stop element (Jackson et al., 2001). Since the endogenous K-Ras locus is targeted in the K-Ras G12D strain, only endogenous levels of oncogenic K-Ras G12D are expressed (not overexpression). In contrast, the H-Ras model is an overexpression of the oncogenic rabbit transgene (point mutation at codon 61 of the second exon converting CAG (encoding glutamine) to CTG (leucine) (Zhang et al., 2001). Transgene copy number varied from 2 copies (low copy, UCC from 10-26 months of age) to 48 copies (high copy, UCC from 4 months of age). This may account for the difference in phenotypes, namely no phenotype in the *UroHICRE⁺K-Ras^{G12D/+}* and pronounced hyperplasia in the overexpression *H-Ras^{Q61L}* model. However it is difficult to make any definitive conclusions since we are dealing with different Ras alleles. In anticipation I am currently repeating these experiments with a Lox-Stop-Lox H-Ras G12V conditional mouse strain, which will allow us to make direct comparisons.

Interestingly, despite modelling all these mutations in the murine urothelium, these tumours remain non-invasive and do not metastasise despite extended follow-up. Again this may be due to our tumours not being “aggressive” enough, and by inserting p53 mutations these tumours may become locally invasive and ultimately metastatic, as has been previously outlined in the colon by our group (Muller et al., 2009). These experiments have been set up

and I am currently ageing these mice to demonstrate whether these mice develop muscle invasive UCC.

Given the experimental data from this chapter, it appears p21 acts as a bladder specific block to proliferation (and tumourigenesis) in the *UroIIICRE⁺ β-catenin^{exon3/exon3}* and *H-Ras^{Q61L}* mice. This indeed confirmed to be the case since when p21 was knocked out in these bladder lesions they rapidly progressed to UCC. The human UCC correlations of loss of p21 must be viewed with a critical eye since, as I have demonstrated that p21 is upregulated early, as a bladder specific compensatory mechanism to block proliferation and tumourigenesis. Our TMA's cohort of tumours is of varying grades and does not differentiate between non-invasive and muscle invasive disease. It will be important to interrogate a larger cohort with both early and late disease. My working hypothesis is that p21 upregulation would be observed early in precursor lesion (CIS) and low grade tumours, whilst the more aggressive and muscle invasive tumours will show loss of their compensatory mechanism and p21 will not be expressed at the protein level.

It will be interesting to treat these mice with an ERK inhibitor in order to investigate whether pERK formation is required for UCC formation in the double mutants. It will also be particularly interesting to look at the *UroIIICRE⁺ β-catenin^{exon3/exon3} H-Ras^{Q61L}* lesions to see whether the fall in pERK1/2 is accompanied by a fall in p21

Taken together, I demonstrated the causative role of β-catenin in the formation of UCC *in vivo* and provide evidence that activating mutations in the Wnt pathway promote UCC when combined with other oncogenic mutations (Ras) and loss of tumour suppressors (p21).

Chapter 5: The FGFR3 mutation cooperates with K-Ras and β -Catenin mutations to promote skin and lung but not bladder tumour formation

5.1. Introduction

In the last chapter I investigated whether Ras mutations were sufficient to drive the murine urothelium to develop non-invasive papillary UCC, as is seen with the human disease. I was able to demonstrate that in the case of K-Ras G12D point mutation no tumour forms unless this is combined with Wnt pathway upregulation. In the case of the overexpressing H-Ras oncogene, I found that Wnt pathway activation greatly reduced the tumour latency. I have also previously demonstrated that mice with β -catenin overexpression co-operates with PTEN/p21 loss to drive tumorigenesis along the non-invasive papillary pathway.

Thus the aim of this final chapter was to investigate the role of oncogenic FGFR3 mutation on the murine urothelium *in vivo*. Given our previous experiments, I also wished to test this on the background of Wnt pathway upregulation.

Somatic mutations in Fibroblast Growth Factor Receptor 3 (*FGFR3*) have been identified at a high frequency in the superficial UCC (70%) (Knowles, 2007). FGFR3 is a receptor tyrosine kinase that is known to mediate the effects of fibroblast growth factors (FGFs). Several studies have shown that mutations of FGFR3 in the bladder is strongly associated with a low tumor grade and stage (Billerey et al., 2001, Lamy et al., 2006, Jebar et al., 2005, Lindgren et al., 2006). When these activating mutations occur in the germ-line, they are known to cause several autosomal dominant human skeletal dysplasia syndromes (Muenke and Schell, 1995).

Although human studies strongly suggest the importance of FGFR3 mutations in cancer, thus far they have been uninformative on the precise mechanistic role of FGFR3 mutations in tumour formation and progression. Generation of relevant mouse model is essential not only for the investigation of mechanism but also for testing potential therapeutic approaches. In this study, I assessed the role of two potent, activating mutations of FGFR3 found in UCC in

the initiation and development of bladder cancer *in vivo* as a sole driver, and in synergy with β -catenin and K-Ras mutations.

5.2. Results

5.2.1. Targeting of the Fgfr3 mutations in the bladder

I bred *UroIIICRE*⁺ mice to lines carrying Fgfr3 K644E and Fgfr3 K644M mutations (murine equivalent of human K652E and K652M, respectively) (Iwata et al., 2000, Iwata et al., 2001). Both lines carry a neomycin resistant gene (*neo*) flanked by loxP sites in the intron 5'-upstream of the exon harboring the K644 mutations. This exogenous gene insertion was designed to suppress the expression of Fgfr3 mutant allele in the absence of Cre recombination. In the presence of Cre, the *neo* gene is excised allowing expression of the mutant Fgfr3 protein. In the offspring of *UroIIICRE*⁺*Fgfr3*^{+/K644E} and *UroIIICRE*⁺*Fgfr3*^{+/K644M}, pattern and approximate levels of the Fgfr3 protein expression were similar to those of the age matched wildtype (Figure 5.1 A,B,E & Figure 5.2). In wildtype mice, Fgfr3 expression revealed occasional scattered cells in the urothelium at P2 (Postnatal day 2) and 5 months; whilst at 12 months its expression was uniformly detected in the urothelium (Figure 5.1 D-F). I did not notice any difference in staining expression at earlier 3-month timepoint in the *UroIIICRE*⁺*Fgfr3*^{+/K644E} and *UroIIICRE*⁺*Fgfr3*^{+/K644M} mice compared to the 12-month timepoint.

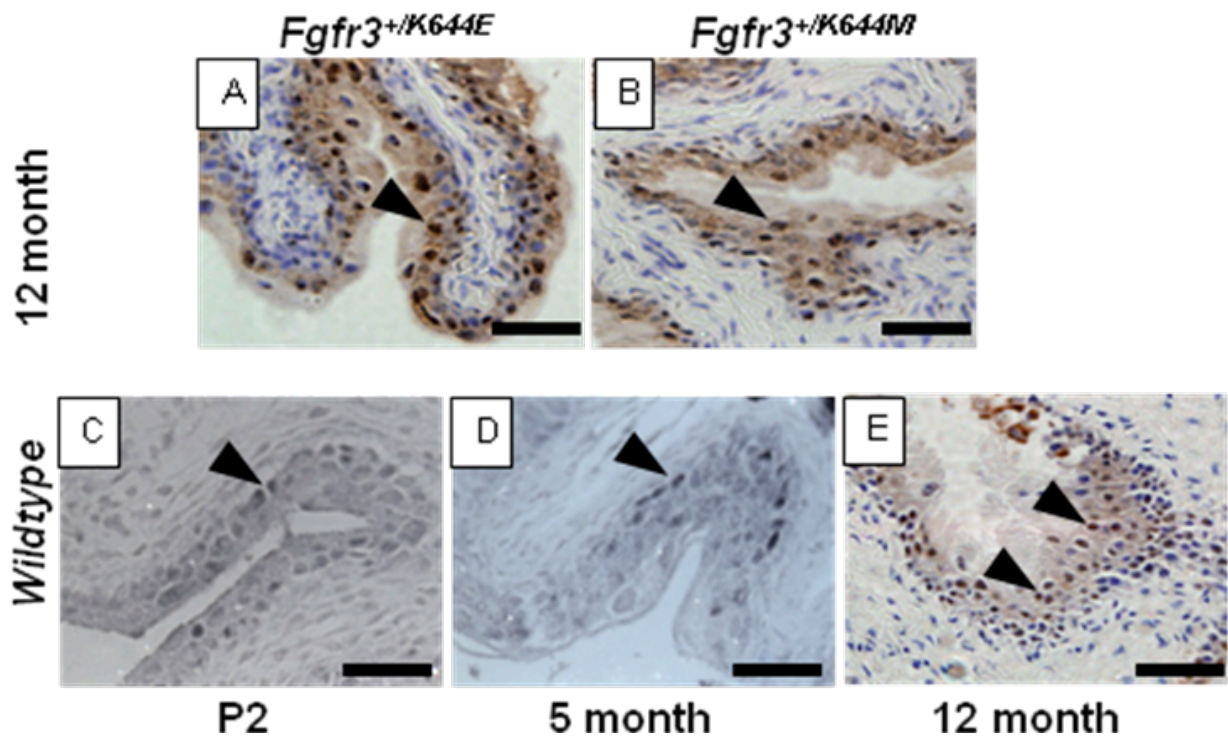


Figure 5.1 Cre recombination and expression of Fgfr3 in the urothelium

Immunohistochemistry (IHC) for Fgfr3 (arrowhead) in the urothelium of *UroII CRE⁺ Fgfr3^{+/K644E}* (A), *UroII CRE⁺ Fgfr3^{+/K644M}* (B), as well as P2 (postnatal day 2) (C), 5 month (D) and 12 month-old (E) wildtype urothelium. This revealed that expression levels and location of Fgfr3 were comparable in the mutant and wildtype at 12 month. Scale bar represents 200 μ m in B-F.

(At least 3 samples from each cohort stained and representative images are shown above).

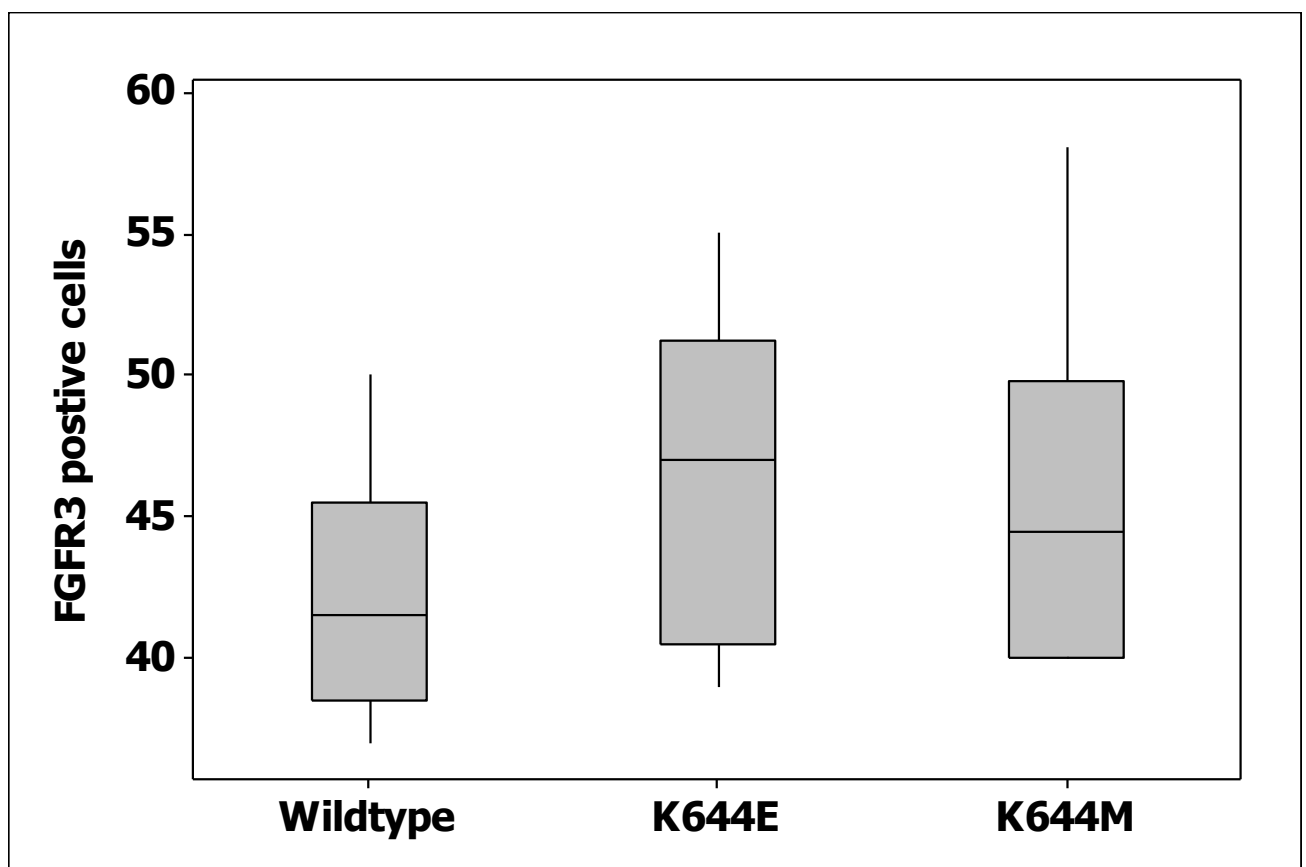


Figure 5.2 FGFR3 positive cells in 12 month old *Wildtype*, *UroIIICRE+Fgfr3^{+/K644E}* and *UroIIICRE+Fgfr3^{+/K644M}*

20x magnification, 3 fields per murine bladder, 3 mice for each cohort sampled.

Thick line represents median, box represents inter-quartile range and whiskers represent range.

5.2.2. Fgfr3 mutation alone does not drive tumourigenesis of the bladder

To investigate the role of Fgfr3 mutations as a driver of UCC, I aged the *UroIIICRE⁺Fgfr3^{+K644E}* and *UroIIICRE⁺Fgfr3^{+K644M}* mutant mice to 18 months (n=20 each genotype). No mouse developed urothelial hyperplasia, dysplasia or carcinoma when aged to 18 months of age (Figure 5.3 & 5.4 A,E,I).

Upon 2 hours of *in vivo* incorporation of BrdU in our 12 month old cohort, no apparent positivity was observed by IHC with anti-BrdU antibody, indicating that little or no cell proliferation took place in the urothelium either in the wildtype or in the mutant cohorts (Figure 5.4 B,F,J). I next examined the known core signalling pathways downstream of FGFR. A strong upregulation of pERK1/2 was observed in both *UroIIICRE⁺Fgfr3^{+K644E}* and *UroIIICRE⁺Fgfr3^{+K644M}* mutants compared to wildtype (Figure 5.4 C,J,K & Figure 5.5). This was accompanied by an upregulation of Sprouty2 levels (Figure 5.4 H,L & Figure 5.5). No significant pAKT (Ser473) or p-mTOR staining was present in the Fgfr3 mutant cohorts similar to wildtype (Figure 5.6).

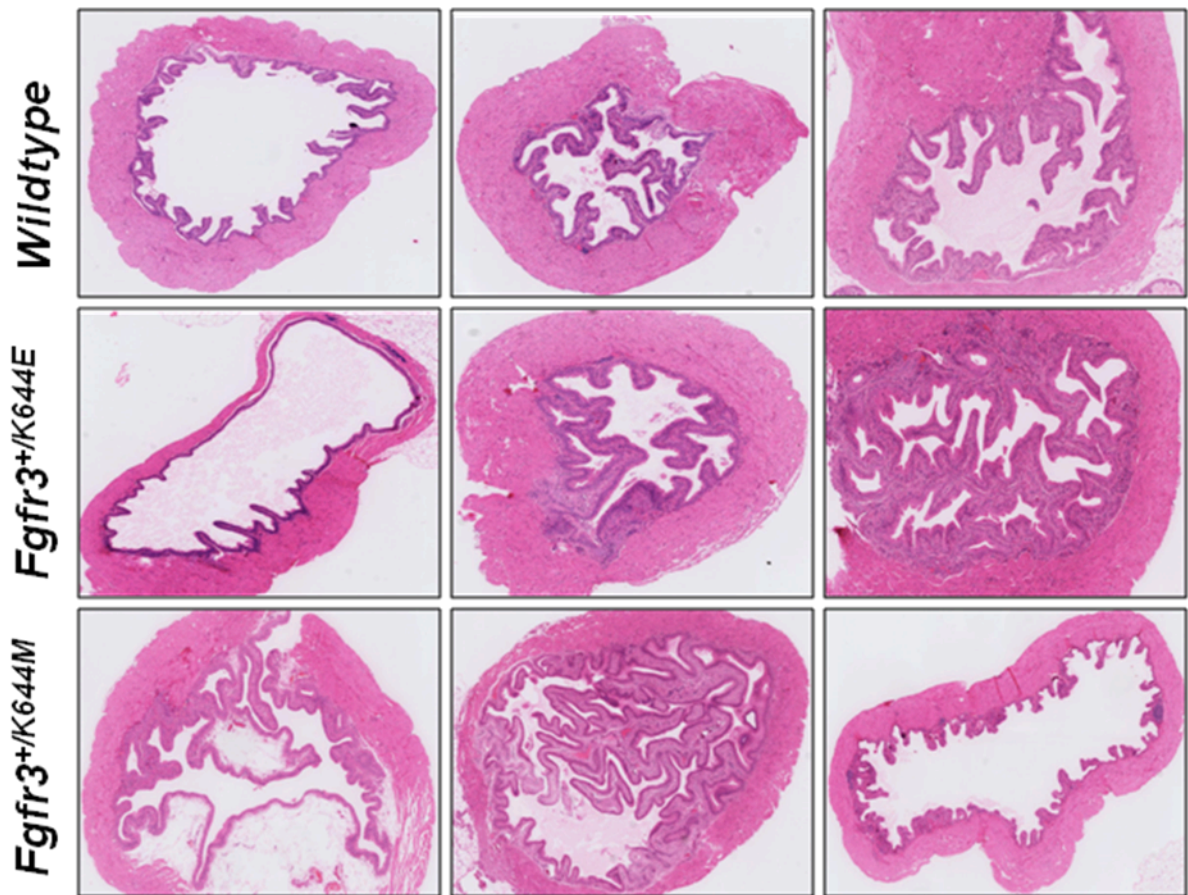


Figure 5.3 Bladder H&Es from 12 month old Wildtype, *UroII CRE⁺ Fgfr3^{+/K644E}* and *UroII CRE⁺ Fgfr3^{+/K644M}* mice

(At least 3 samples from each cohort stained and representative images are shown above).

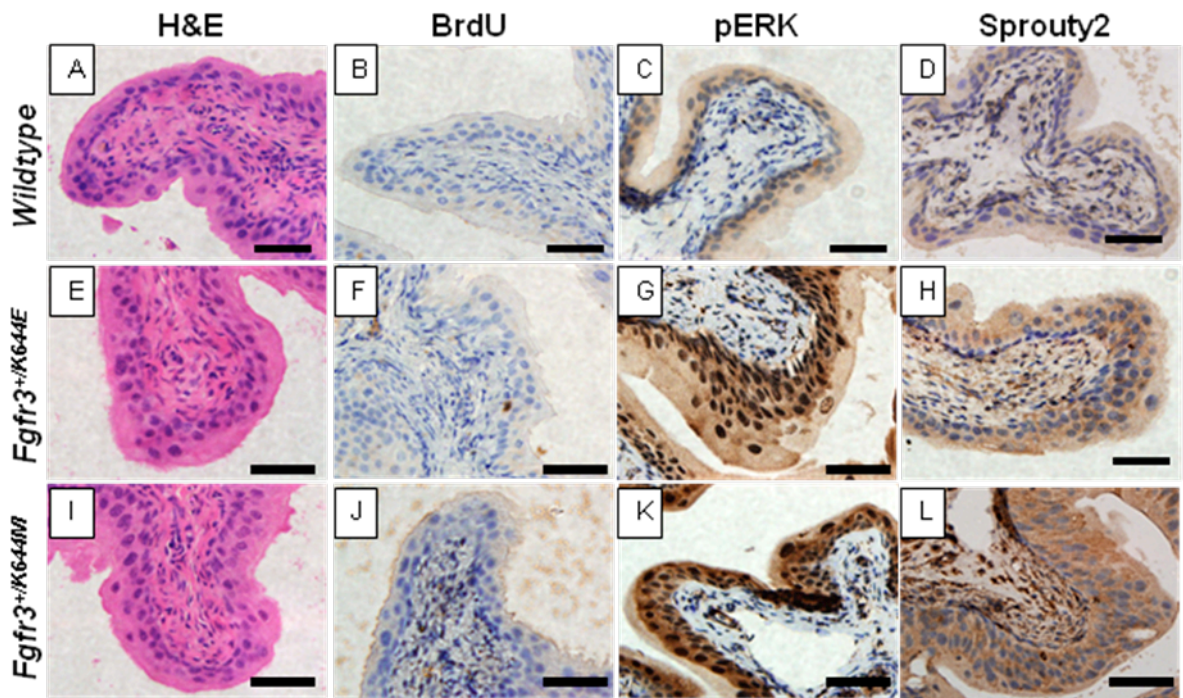


Figure 5.4 Fgfr3 mutation is not the sole driver of tumorigenesis in the bladder.

The samples are from 12-month old *Wildtype* (A-D), *UroII CRE⁺Fgfr3^{+/K644E}* (E-H) and, *UroII CRE⁺Fgfr3^{+/K644M}* (I-L). Haematoxylin and eosin (H&E) staining showed no apparent lesions in the urothelium in all Fgfr3 mutants (A,E,I). No significant cell proliferation was observed (as assessed by 2 hours of *in vivo* BrdU incorporation) (B,F,J). Upregulation of pERK1/2 (J,K) and Sprouty2 (H,L) were observed in Fgfr3 mutant mice, comparing to *Wildtype* (C,D). Scale bar represents 200 μ m in all panels.

(At least 3 samples from each cohort stained and representative images are shown above).

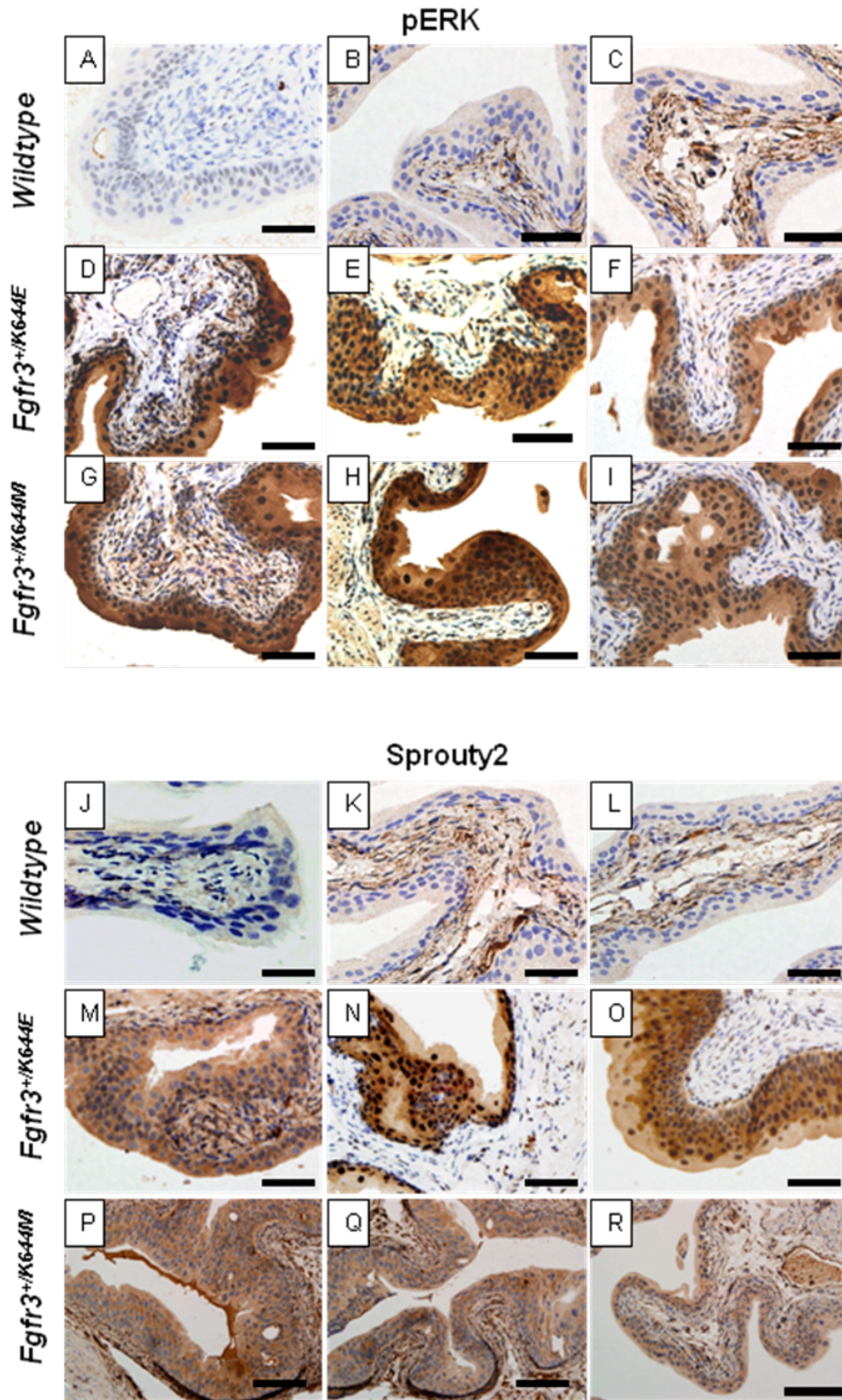


Figure 5.5 Further images showing upregulation of pERK1/2 and Sprouty2:

In 12-month-old UroIIICRE+Fgfr3^{+/K644E} (D-F, M-O), UroIIICRE+Fgfr3^{+/K644M} (G-I, P-R) compared to wildtype bladders (A-C, J-L). Scale bar represents 200 μ m in all panels.

(At least 3 samples from each cohort stained and representative images are shown above).

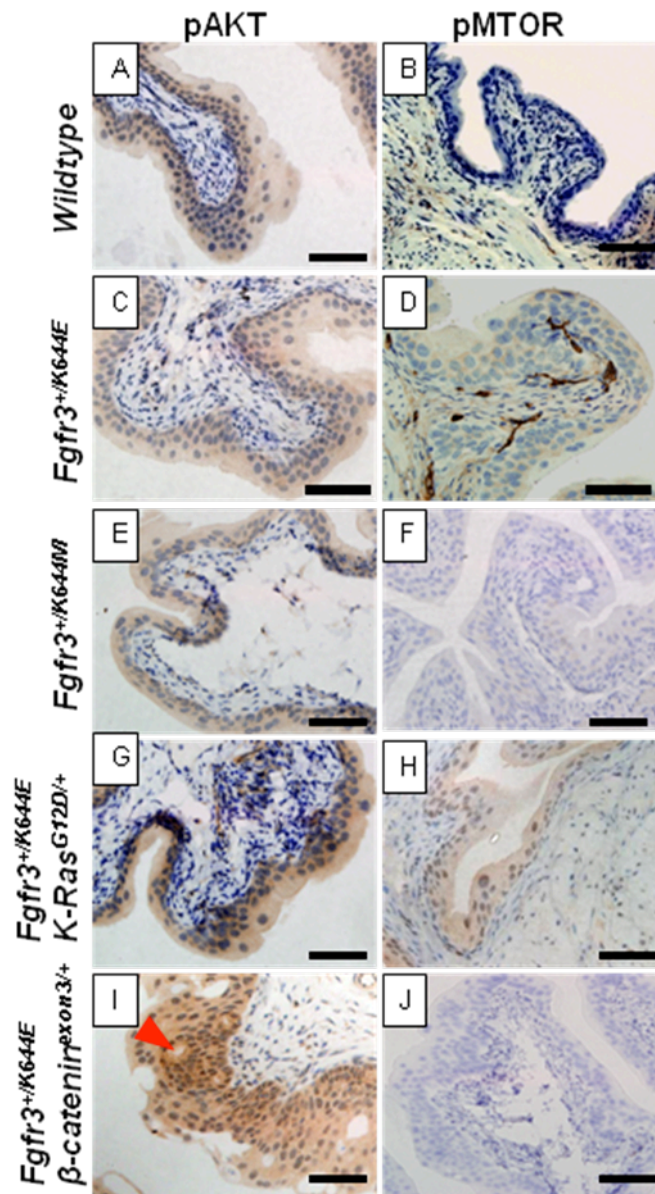


Figure 5.6 Role of the AKT-mTOR pathway in mutant models

The samples are from 12-month old *Wildtype* (A-B), *UroII CRE⁺Fgfr3^{+/K644E}* (C-D), *UroII CRE⁺Fgfr3^{+/K644M}* (E-F), *UroII CRE⁺Fgfr3^{+/K644E}K-Ras^{G12D/+}* (G-H), and *UroII CRE⁺Fgfr3^{+/K644E} β -catenin^{exon3/+}* (I-J). Minimal upregulation of pAKT and p-mTOR was observed in all mutant cohorts compared to wildtype. Red arrowhead in (I) indicates the area of hyperproliferation. Scale bar represents 200 μ m in all panels.

(At least 3 samples from each cohort stained and representative images are shown above).

Given our previous experimental work I next examined the role of β -catenin activating mutations in the context of FGFR3 mutation, $UroIIICRE^+ Fgfr3^{+/K644E} \beta\text{-catenin}^{exon3/+}$ (n=27) (Harada *et al.*, 1999). In order to drive deregulated Wnt signalling, I again used mice that carry a dominant allele of the β -catenin gene in which exon3 is flanked by *loxP* sequences (Harada *et al.*, 1999). Although areas of hyperproliferation were observed in the bladders of $UroIIICRE^+ Fgfr3^{+/K644E} \beta\text{-catenin}^{exon3/+}$ from approximately 3 months of age in 100% of mice (n=20), equivalent lesions were found in the $UroIIICRE^+ \beta\text{-catenin}^{exon3/+}$ urothelium. In both groups these lesions never progressed further upon examination up to 12 months (Figure 5.7 E); however they did show incorporation of BrdU (Figure 5.7F). Similar to above described single and double mutants, upregulation of pERK1/2 and Sprouty2 was also observed (Figure 5.7 G,H). The areas of hyperproliferation that were observed in $UroIIICRE^+ \beta\text{-catenin}^{exon3/+}$ mice had comparable levels of upregulation of BrdU, pERK1/2 and Sprouty2 in the lesions (data not shown), indicating that *Fgfr3* mutations are not contributing to urothelial hyperplasia in $UroIIICRE^+ Fgfr3^{+/K644E} \beta\text{-catenin}^{exon3/+}$ mice. I did not observe any upregulation of pAKT(Ser473) or p-mTOR (Figure 5.6). Taken together, these data suggest that FGFR3 mutation does not cooperate with activation of Wnt signaling to drive UCC.

I next examined the role of oncogenic K-Ras G12D (Jackson *et al.*, 2001) in $UroIIICRE^+ Fgfr3^{+/K644E} K\text{-Ras}^{G12D/+}$ (n=23). Upon aging to 12 months, no $UroIIICRE^+ Fgfr3^{+/K644E} K\text{-Ras}^{G12D/+}$ mice developed urothelial hyperplasia, dysplasia or carcinoma (Figure 5.7 A) and no apparent changes in BrdU incorporation were observed (Figure 5.7 B). Similar to the single mutants, a strong upregulation of pERK1/2 (Figure 5.7 C) as well as an accompanying upregulation of Sprouty2 was observed (Figure 5.7 D). Similar levels of upregulation of pERK1/2 and Sprouty2 were observed in the $UroIIICRE^+ K\text{-Ras}^{G12D/+}$

urothelium (data not shown). I observed minimal levels of upregulation of pAKT(Ser473) and p-mTOR in the $UroII\text{CRE}^+ Fgfr3^{+/K644E} K\text{-Ras}^{G12D/+}$ cohorts (Figure 5.6).

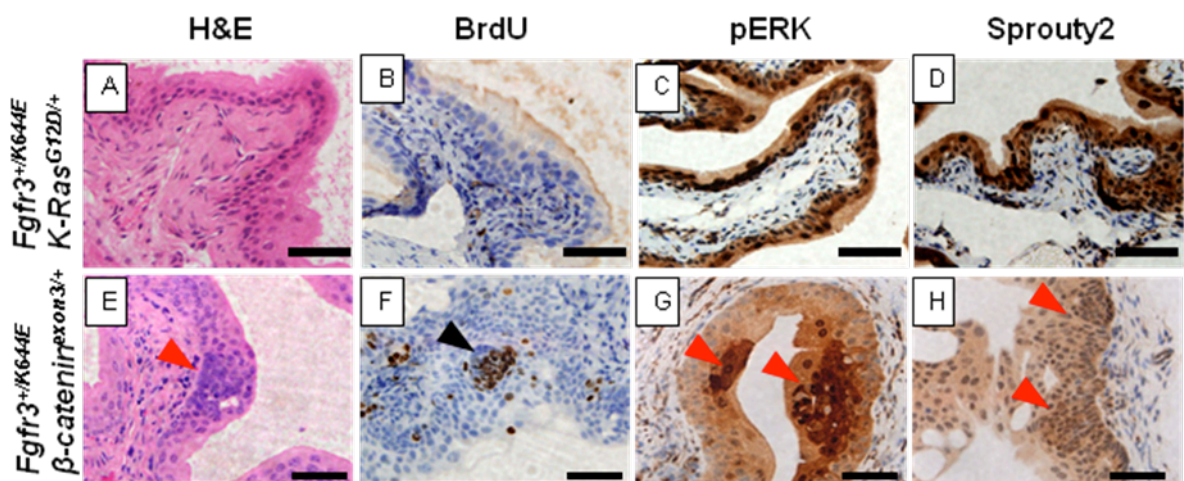


Figure 5.7 Fgfr3 mutation in combination does not lead to tumourigenesis in the bladder

The samples are from 12-month old $UroII\text{CRE}^+ Fgfr3^{+/K644E} K\text{-Ras}^{G12D/+}$ (A-D), and $UroII\text{CRE}^+ Fgfr3^{+/K644E} \beta\text{-catenin}^{\text{exon3}/+}$ (E-H). Haematoxylin and eosin (H&E) staining showed no apparent lesions in the urothelium in $UroII\text{CRE}^+ Fgfr3^{+/K644E} K\text{-Ras}^{G12D/+}$ mice (A) except for the compound model with $\beta\text{-catenin}^{\text{exon3}/+}$ (E) where hyperplasia was observed (red arrowhead, also in G,H). No significant cell proliferation was observed (as assessed by 2 hours of *in vivo* BrdU incorporation) (B) except for the area of hyperplastic lesion in $UroII\text{CRE}^+ Fgfr3^{+/K644E} \beta\text{-catenin}^{\text{exon3}/+}$ (arrowhead) (F). Upregulation of pERK1/2 (C,G) and Sprouty2 (D,H) were observed in Fgfr3 mutant mice, comparing to *Wildtype*. Scale bar represents 200 μm in all panels.

(At least 3 samples from each cohort stained and representative images are shown above).

5.2.3. Formation of lung tumors in the $UroII\text{Cre}^+ \text{Fgfr3}^{+/K644E} \beta\text{-catenin}^{\text{exon3}/+}$ mice

In contrast to observations in the urothelium, 28% (8/28) of the $UroII\text{CRE}^+ \text{Fgfr3}^{+/K644E} \beta\text{-catenin}^{\text{exon3}/+}$ mice by 1 year of age developed lung tumours (Figure 5.8). Imaging with the OV100 microscope showed a strong GFP signal in the lung tumor, indicating that the $UroII\text{CRE}$ -driven recombination occurred in these tumors (Figure 5.9 A). I did not see any signal in the normal lung tissue. These tumors resembled most closely solitary fibrous tumour (SFT) of the lung (Figure 5.9 B). Up to a third of SFTs exhibit nuclear β -catenin consistent with our murine models (Andino et al., 2006). Solitary fibrous tumours (SFTs) were termed hemangiopericytomas (HPCs) in the past. According to the World Health Organization (WHO), these tumours are mesenchymal neoplasms of subendothelial origin that can be found mostly in the pleura but also in extraserosal sites, such as lung, mediastinum, liver, head and neck, and deep soft tissues of the extremities. Most SFTs behave as slowly growing, painless masses (Kouki *et al.*, 2008). In our murine tumours strong BrdU positivity indicated rapid cell proliferation (Figure 5.9 C). In addition tumors showed high levels of nuclear β -catenin by IHC, consistent with the activation of β -catenin due to Cre mediated excision of exon 3 (Figure 5.9 D). No lung tumors were observed in the $UroII\text{CRE}^+ \beta\text{-catenin}^{\text{exon3}/+}$ mice aged up to 18 months (n=20); therefore the FGFR3 mutation is cooperating with β -catenin activation to drive lung tumourigenesis.

Increased levels of pAKT (Ser473) and p-mTOR were observed (Figure 5.9 E,F), suggesting the involvement of AKT pathway in tumourigenesis. However, I found minimal upregulation of pERK in these tumors with accompanying upregulation of Sprouty2 (Figure 5.9 G,H).

I compared these tumors to phenotypically similar lung tumours found in $UroII\text{CRE}^+ \beta\text{-catenin}^{\text{exon3}/+} K\text{-Ras}^{\text{G12D}/+}$ mice. In these tumors, I found that rather than having high levels by the pAKT pathway, they was dramatic upregulation of pERK1/2, with corresponding fall in Sprouty2 expression (Figure 5.9 I-L). When I measured staining intensity using a weighted

Histoscore technique, I found statistically significant increases in both nuclear and cytoplasmic pERK1/2 staining in the *UroII CRE⁺ β-catenin^{exon3/+} K-Ras^{G12D/+}* cohort compared to the *UroII CRE⁺ Fgfr3^{+K644E} β-catenin^{exon3/+}* mice (p<0.001, Figure 5.10 A,B) (Kirkegaard *et al.*, 2006). Conversely, I found much higher levels of pAKT(Ser473) staining in lung tumors of the *UroII CRE⁺ Fgfr3^{+K644E} β-catenin^{exon3/+}* mice in comparison to *UroII CRE⁺ β-catenin^{exon3/+} K-Ras^{G12D/+}* mice (p<0.001, Figure 5.10 C,D). Consistent with this, p-mTOR staining was also upregulated in *UroII CRE⁺ Fgfr3^{+K644E} β-catenin^{exon3/+}* mice. As observed with the IHC, when quantified I observed increased levels of membranous and cytoplasmic Sprouty2 staining in the *UroII CRE⁺ Fgfr3^{+K644E} β-catenin^{exon3/+}* mice in comparison to *UroII CRE⁺ β-catenin^{exon3/+} K-Ras^{G12D/+}* (p<0.05) (Figure 5.10 E&F).

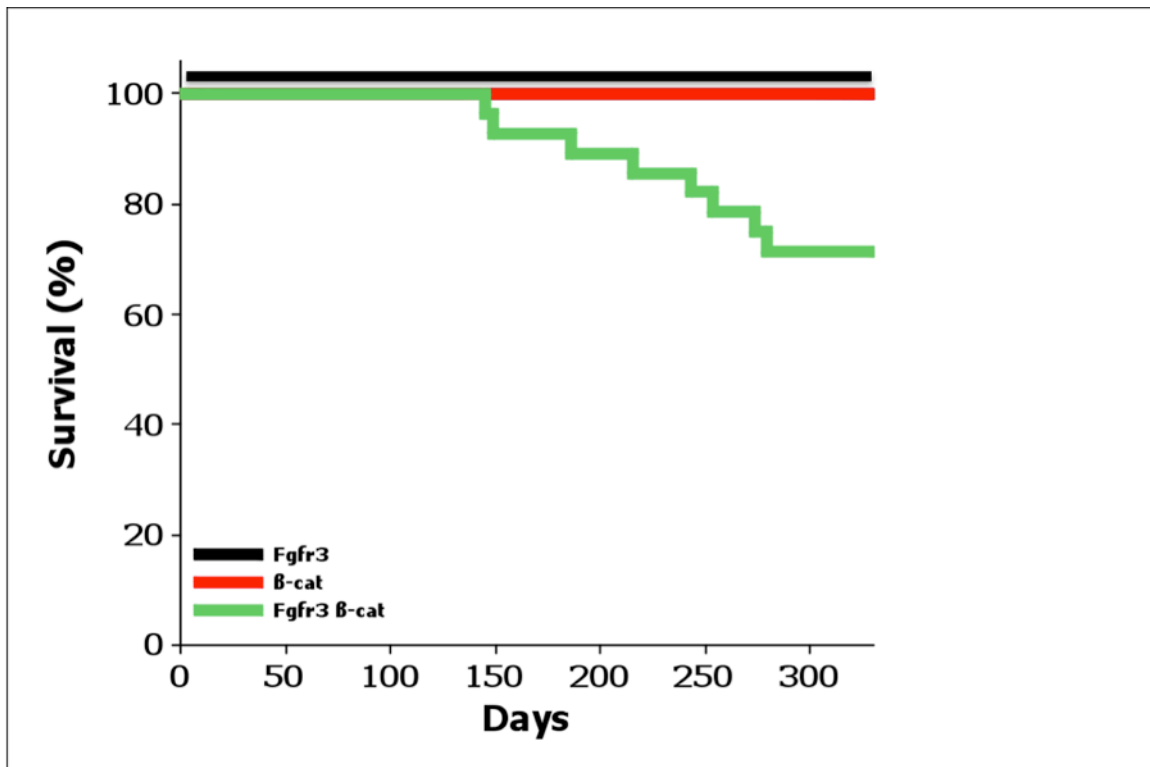


Figure 5.8 Kaplan-Meier curve of $UroII\text{CRE}^+ Fgfr3^{+/K644E} \beta\text{-catenin}^{\text{exon3}/+}$ (Fgfr3 β -Cat) mice

$UroII\text{CRE}^+ Fgfr3^{+/K644E} \beta\text{-catenin}^{\text{exon3}/+}$ (Fgfr3 β -Cat) cohorts showed accelerated lethality due to tumour formation comparing to, $UroII\text{CRE}^+ \beta\text{-catenin}^{\text{exon3}/+}$ (B-cat), and $UroII\text{CRE}^+ Fgfr3^{+/K644E}$ (Fgfr3). Long rank test reveals significant reduction in survival in Fgfr3 B-cat colony compare to Fgfr3/B-cat colonies ($p < 0001$).

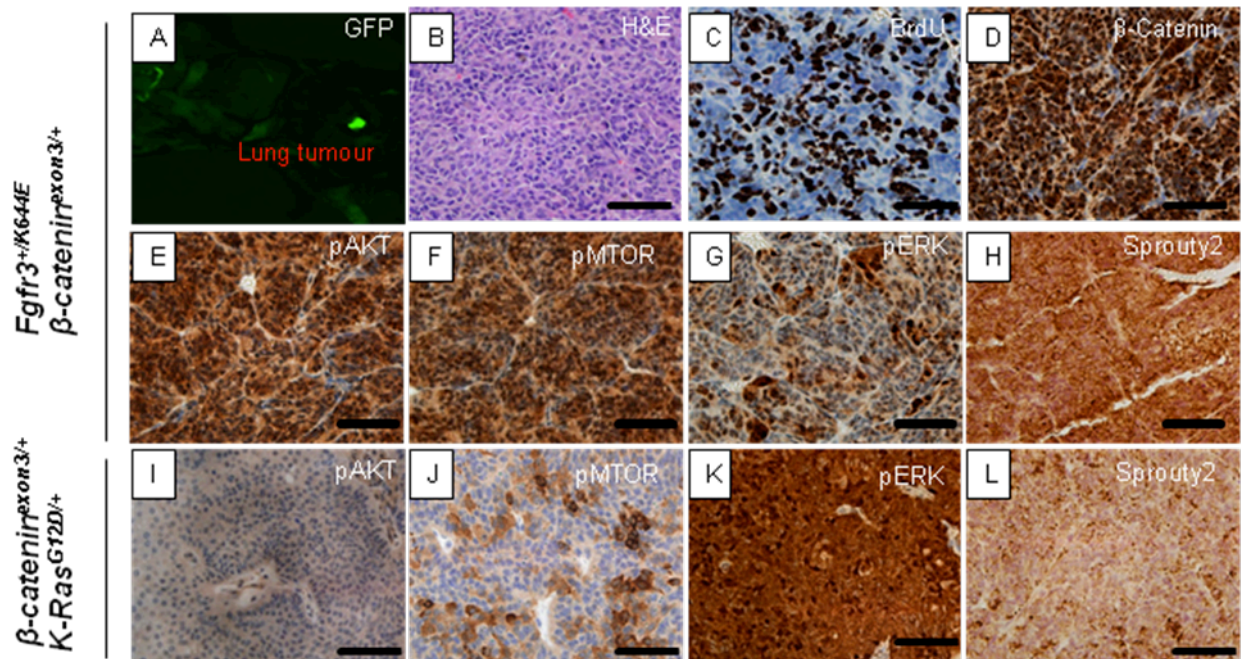


Figure 5.9 Formation of lung tumor in the *UroII CRE⁺ Fgfr3^{+/K644E} beta-catenin^{exon3/+}* model.

Ex-vivo GFP imaging by OV100 (Olympus) demonstrated Cre-mediated recombination in the lung tumors of *UroII CRE⁺ Fgfr3^{+/K644E} beta-catenin^{exon3/+}* (A). H&E staining shows the lung tumour (B), in which BrdU staining indicates high cell proliferation in the lesion (C). Strong nuclear staining indicates the activation of β -Catenin in the tumour (D). pAKT(Ser473) (E), p-mTOR(Ser2448) (F) and Sprouty2 (H) were all upregulated in the lung tumor in *UroII CRE⁺ Fgfr3^{+/K644E} beta-catenin^{exon3/+}*, with minimal pERK (G) staining. In comparison, lung tumors in *UroII CRE⁺ beta-catenin^{exon3/+} K-Ras^{G12D/+}* show minimal upregulation of pAKT (I) and p-mTOR (J), but strong upregulation of pERK (K) with very little Sprouty2 increase (L). Scale bar represents 200 μ m.

(At least 3 samples from each cohort stained and representative images are shown above).

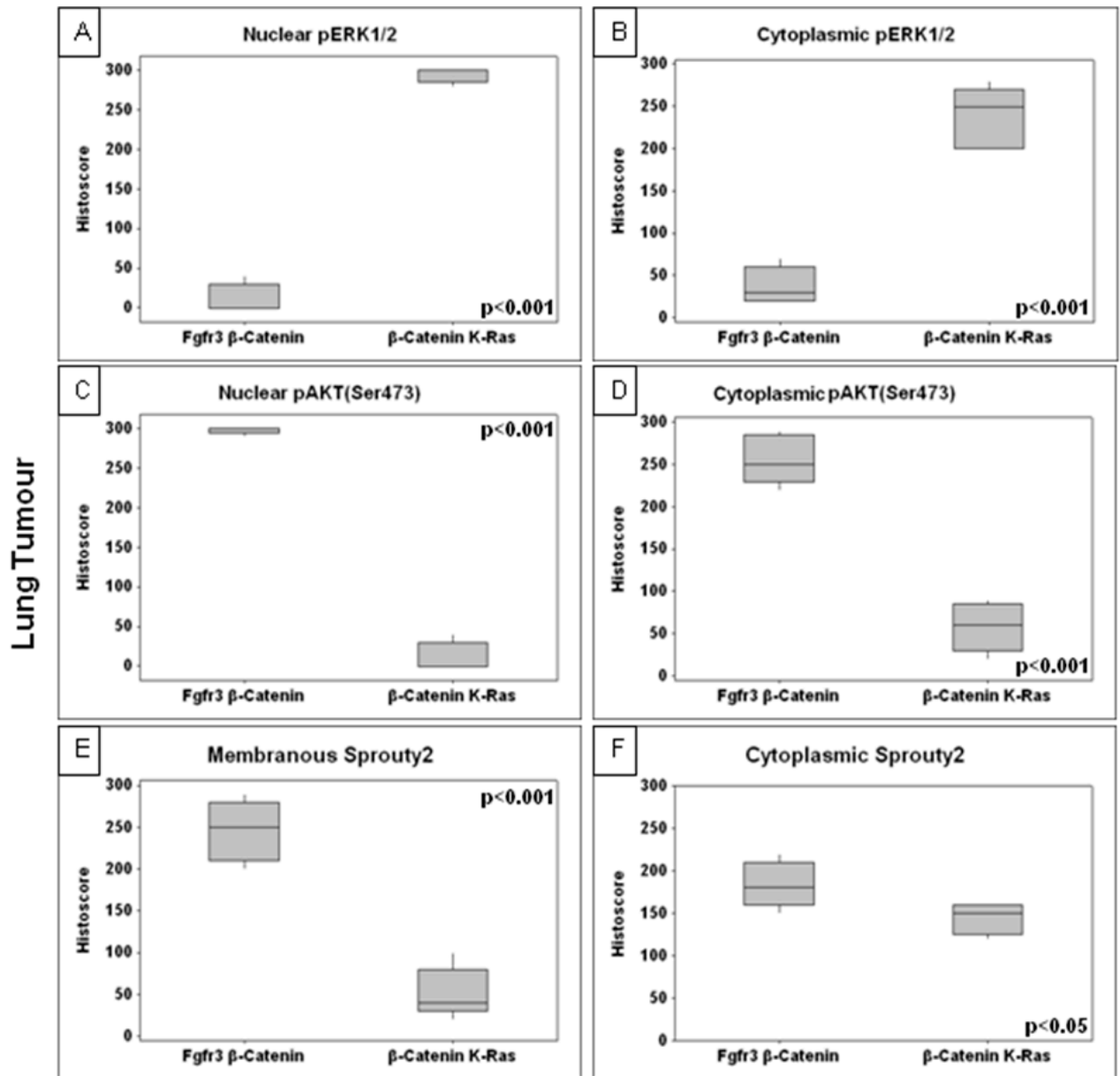


Figure 5.10 Box plots quantifying immunostaining of pERK1/2, pAKT(Ser473) and Sprouty2 in lung tumors of *UroII CRE⁺ β-catenin^{exon3/+} K-Ras^{G12D/+}* and *UroII CRE⁺ Fgfr3^{+ /K644E} β-catenin^{exon3/+}* mice

For each tissue section (n=5), the percentage of immunoreactivities in the nucleus and cytoplasm was evaluated at $\times 40$ magnification. Staining intensity was categorized into the percentage of cells with 0, 1, 2 and 3, denoting negative, weak, moderate and strong staining, respectively. The final histoscore was calculated from the sum of $(1 \times \% \text{ weakly positive tumour cells}) + (2 \times \% \text{ moderately positive tumour cells}) + (3 \times \% \text{ strongly positive tumour cells})$ positive tumour cells with a maximum histoscore of 300. Statistics were performed using the Mann Whitney test.

5.2.4. Skin Papilloma formation in $UroII\text{Cre}^+Fgfr3^{+/K644E}K\text{-Ras}^{G12D/+}$ mice

By 1 year of age, 10/21 (48%) of $UroII\text{Cre}^+Fgfr3^{+/K644E}K\text{-Ras}^{G12D/+}$ cohort developed papilloma (Figure 5.11, Figure 5.12 A,C). These tumours reached 1 cm of size by a median of 220 days (mean 249 days). To ensure the tumour formation was due to sporadic Cre recombination, I crossed the $UroII\text{Cre}^+Fgfr3^{+/K644E}K\text{-Ras}^{G12D/+}$ mice to $Z/EGFP$ reporter. I observed a strong GFP signal within these papillomas, indicating the Cre recombination (Figure 5.12 E), with no expression in normal skin. In contrast, no papilloma formation was observed in the $UroII\text{Cre}^+K\text{-Ras}^{G12D/+}$ cohort aged up to 18 months (n=20), indicating that $Fgfr3$ mutation cooperates with $K\text{-Ras}$ mutation to drive papilloma formation. The papillomas in the $UroII\text{Cre}^+Fgfr3^{+/K644E}K\text{-Ras}^{G12D/+}$ cohort incorporated BrdU (Figure 5.13 A), indicating the increase in cell proliferation. Mechanistically, tumour formation was associated with a robust activation of pERK1/2 (Figure 5.13 C). Distinct from the observation in the urothelium of these mice, an increased level of Sprouty2 was not observed (Figure 5.13 E), which either suggests that the negative feedback counteracting oncogenic MAPK pathway has not occurred in this line or that all the Sprouty2 has been lost (e.g. hypermethylation in the tumours). Levels of pAKT (Ser473) and p-mTOR were unchanged (Figure 5.13 G,I). I noticed upregulation of p21 and pMEK (Figure 5.13 K,M)

I compared this phenotype to $UroII\text{Cre}^+K\text{-Ras}^{G12D/+}Pten^{fl/+}$ mice that regularly develop papillomas (8/19 or 42%) (Figure 5.12 B,D). I found a similar increase in BrdU incorporation, but this time with much lower levels of nuclear pERK1/2 observed in the lesion (Figure 5.13 B,D). Sprouty2 was upregulated (Figure 5.13 F) similar to urothelium phenotype of $Fgfr3$ mutant models, while elevated levels of pAKT (Ser473) and p-mTOR were also observed (Figure 5.13 H,J). Similarly I observed upregulation of p21 and pMEK (Figure 5.13 L,N). I also measured staining intensity using a modified HistoScore in the papillomas from each cohort (n=5). I found statistically significant increases in both nuclear and cytoplasmic

pERK1/2 staining in the *UroII CRE⁺ Fgfr3^{+/K644E} K-Ras^{G12D/+}* compared to the *UroII CRE⁺ K-Ras^{G12D/+} Pten^{fl/+}* mice (p<0.001/0.05 respectively, Figure 5.14 A,B). Conversely, I found much higher levels of pAKT(Ser473) staining in papillomas of the *UroII CRE⁺ K-Ras^{G12D/+} Pten^{fl/+}* mice in comparison to *UroII CRE⁺ Fgfr3^{+/K644E} K-Ras^{G12D/+}* mice (p<0.001, Figure 5.14 C,D). These results indicate that although Sprouty-mediated suppression of MAPK signaling is intact, activation of AKT pathway may contribute to tumorigenesis in this model.

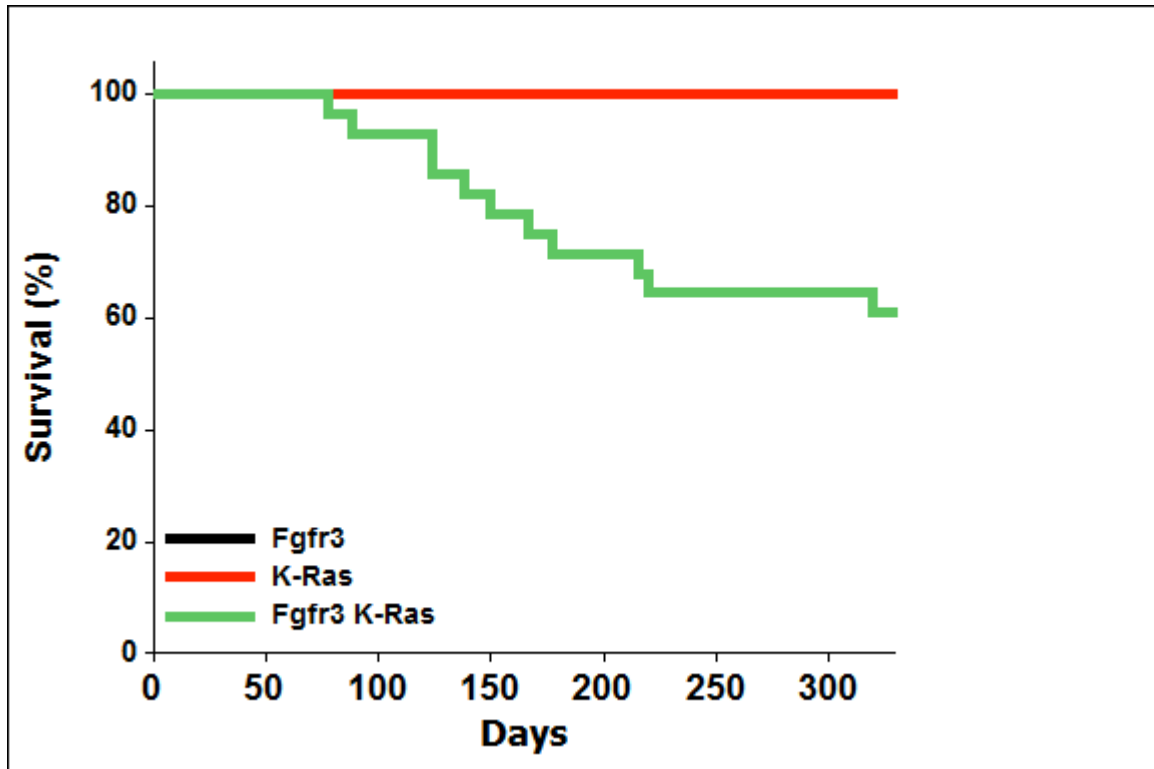


Figure 5.11 Kaplan-Meier curve of $UroIIICRE^+ Fgfr3^{+/K644E} K-Ras^{G12D/+}$ (Fgfr3 K-Ras) mice

$UroIIICRE^+ Fgfr3^{+/K644E} K-Ras^{G12D/+}$ (Fgfr3 K-Ras) cohorts showed accelerated lethality due to tumor formation comparing to, $UroIIICRE^+ K-Ras^{G12D/+}$ (K-Ras), and $UroIIICRE^+ Fgfr3^{+/K644E}$ (Fgfr3). The shorter survival of $UroIIICRE^+ Fgfr3^{+/K644E} K-Ras^{G12D/+}$ mice compared to control cohorts reflects the fact that I have sacrificed the animals when the tumor size reached 1 cm. Log rank $p < 0.001$ for Fgfr3 K-Ras vs. Fgfr3/K-Ras cohorts.

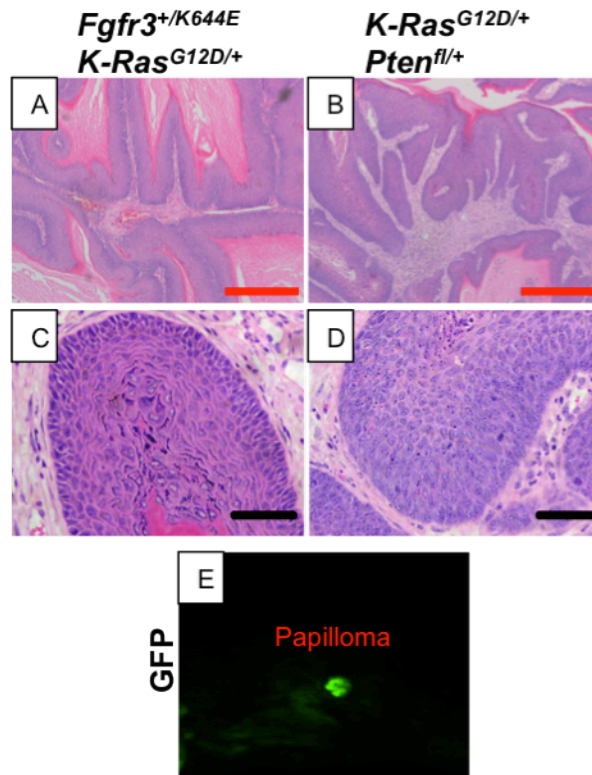


Figure 5.12 Formation of papilloma lesions in the $UroII\text{CRE}^+ Fgfr3^{+/K644E} K\text{-Ras}^{G12D/+}$ model

H&E staining of papilloma samples are from 12 month-old of $UroII\text{CRE}^+ Fgfr3^{+/K644E} K\text{-Ras}^{G12D/+}$ (A,C) and $UroII\text{CRE}^+ K\text{-Ras}^{G12D/+} Pten^{fl/+}$ mice (B,D). OV100 whole-mouse GFP imaging indicated Cre-recombined cells in papilloma (E).

Red scale bar represents 400 μm and black scale bar represents 200 μm .

(At least 3 samples from each cohort stained and representative images are shown above).

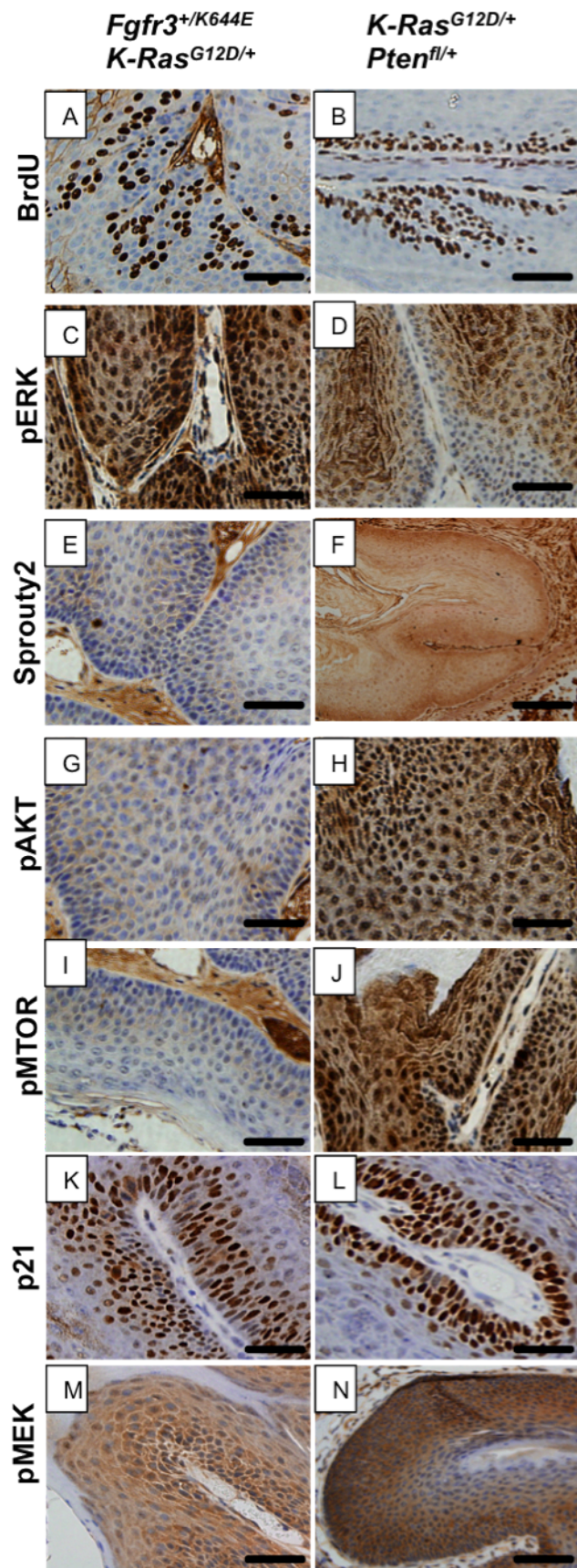


Figure 5.13 Formation of papilloma lesions in the *UroIIICRE⁺Fgfr3^{+/K644E}K-Ras^{G12D/+}* model

Papilloma samples are from 12 month-old of *UroIIICRE⁺Fgfr3^{+/K644E}K-Ras^{G12D/+}* (A,C,E,G,I,G,M) and *UroIIICRE⁺K-Ras^{G12D/+}Pten^{fl/+}* mice (B,D,F,H,J,L,N). BrdU immunoreactivity demonstrated cell proliferation (A,B). Upregulation of pERK1/2 was observed in *UroIIICRE⁺Fgfr3^{+/K644E}K-Ras^{G12D/+}* (C) as observed in the urothelium, and in the control *UroIIICRE⁺K-Ras^{G12D/+}Pten^{fl/+}* mice (D). However, upregulation of Sprouty2 was not present (E). Neither pAKT(Ser473) nor p-mTOR was upregulated in papillomas formed in *UroIIICRE⁺Fgfr3^{+/K644E}K-Ras^{G12D/+}* mice (G,I). In contrast, in *UroIIICRE⁺K-Ras^{G12D/+}Pten^{fl/+}* papillomas, Sprouty 2 (F), pAKT(Ser473) (H) and p-mTOR (J) was upregulated. I noticed significant upregulation of p21 in the papillomas (K,L), as well as pMEK (M,N)

Scale bar represents 200 μ m in all panels.

(At least 3 samples from each cohort stained and representative images are shown above).

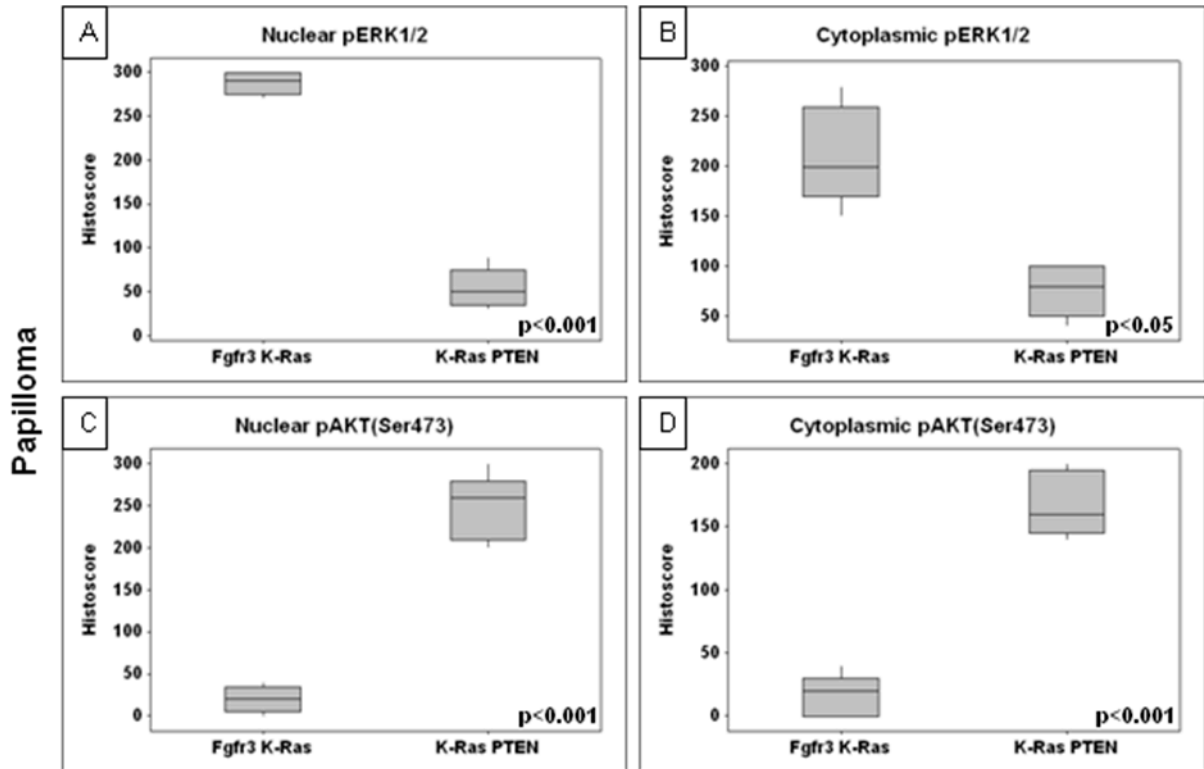


Figure 5.14 Box plots quantifying immunostaining of pERK1/2 and pAKT(Ser473) in papillomas of *UroII CRE⁺ Fgfr3^{+/K644E} K-Ras^{G12D/+}* and *UroII CRE⁺ K-Ras^{G12D/+} Pten^{fl/+}* mice

For each tissue section (n=5), the percentage of immunoreactivities in the nucleus and cytoplasm was evaluated at $\times 40$ magnification. Staining intensity was categorized into the percentage of cells with 0, 1, 2 and 3, denoting negative, weak, moderate and strong staining, respectively. The final histocore was calculated from the sum of $(1 \times \% \text{ weakly positive tumour cells}) + (2 \times \% \text{ moderately positive tumour cells}) + (3 \times \% \text{ strong of experience})$ positive tumour cells with a maximum histocore of 300. Statistics were performed using the Mann Whitney test.

5.3. Discussion

In summary, I have demonstrate here that activating mutations of FGFR3 are unlikely to be the sole initiating factor for UCC (Figure 2) and that FGFR3 does not cooperate with either Wnt or Ras signaling to drive UCC. Given that FGFR3 mutations are thought to be mutually exclusive with HRAS mutations and only rarely mutated with p53 this suggests that generating mouse models that recapitulate superficial UCC that have FGFR3 mutations will be difficult and will require greater knowledge of the genetic changes that accompany FGFR3 mutations (Puzio-Kuter et al., 2009, Wu, 2005).

The study showed that somatic FGFR3 mutations caused upregulation of the MAPK pathway in the urothelium, which accompanied upregulation of Sprouty2, one of the feedback inhibitors of the MAPK pathway. I speculate that this may be one of the mechanisms by which UCC is normally prevented. In case of lung tumours in *UroIIICRE⁺Fgfr3^{+/K644E} β -catenin^{exon3/+}* cohort, a strong upregulation of the PI3K-pAkt and Wnt- β -Catenin pathways may underlie tumourigenesis. In contrast, in papillomas in *UroIIICRE⁺Fgfr3^{+/K644E}K-Ras^{G12D/+}*, no concomitant upregulation of Sprouty2 had occurred, potentially leading to uncontrolled activation of MAPK pathway in the absence of a negative feedback mechanism. It is tempting to propose that these differential downstream signaling profiles are the basis of tumourigenesis in the presence of Fgfr3 mutations in a tissue-specific fashion (Figure 5.15). It would be interesting to assess if downregulation of Sprouty2 in our system resulted in formation of UCC. Using OncomineTM (<http://www.oncomine.org/geneModule/differential/filterStore.jsp>) Lindgren and colleagues have demonstrated that in FGFR3 mutant bladder cancer there is a downregulation of Sprouty 2 at the mRNA level (p=0.015) (Lindgren *et al.*, 2006). In the same study they find that

Sprouty2 mRNA levels are downregulated as the disease progresses from Grade 1 to 3 (p=0.015).

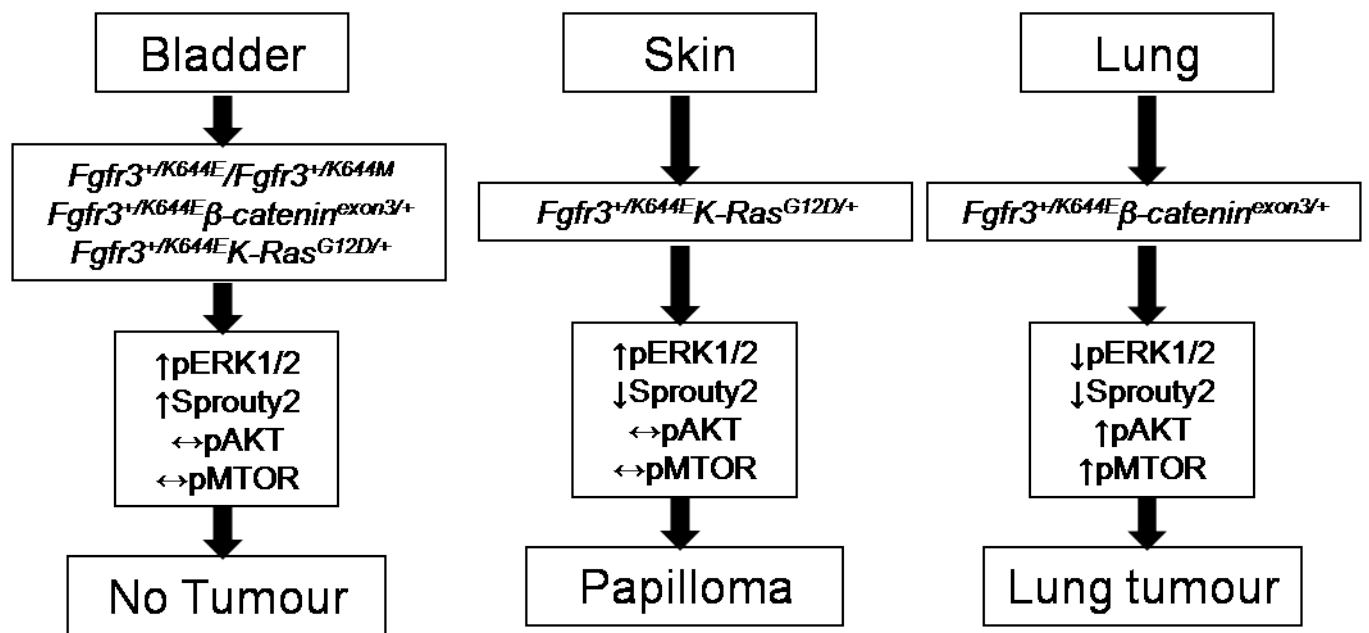


Figure 5.15 Current model of signaling pathways that could contribute to tumour formation in the presence of Fgfr3 mutations in specific organ systems

FGFR3 is a membrane tyrosine kinase that is known to mediate the effects of fibroblast growth factors (FGFs). Somatic mutations in FGFR3 have been identified at a high frequency in bladder cancer (35-41%) (Cappellen et al., 1999, Sibley et al., 2001a, Sibley et al., 2001b). In bladder, the frequency of FGFR3 mutation was higher in superficial tumours than invasive ones (Billerey et al., 2001, van Rhijn et al., 2001, Kimura et al., 2001). The mutations found in bladder cancer are specific and not found in other primary tumours and tumour cell lines (Sibley et al., 2001a, Sibley et al., 2001b, Karoui et al., 2001). However, frequent mutation has been detected in seborrhoeic keratoses and epidermal naevi (Hafner et al., 2007a, Hafner et al., 2007b, Hafner et al., 2006).

K652E and K652M (equivalent of murine K644E and K644M respectively) mutations, which I described in this thesis, are found in human UCC but are much less frequent (3%) than the S249C which account for 67% of the FGFR3 mutations in bladder cancer (Knowles 2008). Thus it is possible that S249C mutations are more oncogenic in the bladder. *In vitro*, both S249C and K652E/K652M mutations are shown to constitutively increase the FGFR3 kinase activity, albeit with different mechanisms. S249C is known to cause ligand-independent dimerization, while K652E/K652M promotes conformational change that favors the higher auto-phosphorylation and its kinase activity can be further enhanced by additional ligand stimulation (Naski et al., 1996, d'Avis et al., 1998). Upon measuring transcription-inducing activity by fos-luciferase reporter assay, K644E mutant protein was actually twice as active as S249C mutant in the absence of ligand (d'Avis *et al.*, 1998). However preliminary data suggests that, transgenic mice with human FGFR3IIIb isoform with S249C mutation did not show any tumors in the bladder up to 1 year of age (M. Knowles personal communication). This strongly indicates that UCC formation requires an additional mutation(s) to that in FGFR3.

The skin papilloma and lung tumours observed in our study with *Fgfr3* mutations are relevant in human cancer, as *FGFR3* mutations are found in such tumours (Woenckhaus et al., 2006, Hafner et al., 2007a, Cortese et al., 2008). Studies by Logie et al showed that the transgenic mice, K5-(S249C)*FGFR3*, that expresses *FGFR3* S249C mutation in the basal cells of the epidermis driven by bovine keratin 5 promoter, developed benign skin tumours (Logie *et al.*, 2005). In these mice, the skin tumours are observed from 3-4 months of age and lesions enlarged as the animals aged, without showing regression. To further this work we are investigating activation of *FGFR3* in the skin using the skin specific K14-Cre ER with and without Ras activation (Indra et al., 2000). We currently have a number of *FGFR3* inhibiting antibodies in the lab that I would wish to try in these mice to assess tumour response.

Recent work has elegantly demonstrated knockdown of *FGFR3* expression suppressed growth of bladder cell lines and mouse xenograft models (Qing *et al.*, 2009). Furthermore, *FGFR3*-specific monoclonal antibody (R3Mab) significantly inhibited growth and progression of xenograft tumors that harboured the S249C and K650E mutations (Qing *et al.*, 2009). Further studies of the *FGFR3* signaling pathway deregulated in UCC is therefore essential, firstly to allow one to stratify patients according to risk of progression/recurrence, and secondly to aid in patient selection for either single agent or combination therapy with small molecule and monoclonal antibody-based treatments in the future (Knowles, 2008, Black et al., 2007, Qing et al., 2009). Moreover identifying the cooperating molecular events that occur alongside *FGFR3* mutation to drive UCC will aid development of genetic models of UCC to test combinatorial therapies.

Chapter 6: Summary and Concluding Remarks

6.1. Summary

Manipulation of the mouse genome has allowed researchers to analyse the effect of specific genetic alterations on the development of urothelial cell cancer (UCC) *in vivo*. We are able to analyse the molecular basis of initiation, invasion and progression to metastatic disease. Transgenic mice had improved the molecular characterisation of the divergent pathways of UCC and metastasis and help examine the crosstalk among different genetic mutations. In the future one would hope that they identify new prognostic targets and novel therapeutic agents, as well as providing *in vivo* models to test these treatment regimes.

In this thesis I hope I have achieved my initial aims and have shown that deregulated Wnt signalling plays a critical role in driving UCC both in the mouse (and the human). I have demonstrated that Wnt signaling within the bladder urothelium is a progressor mutation of UCC in the background of mutations to other key oncogenic/tumour suppressor genes (PTEN, Ras p21, FGFR3). Finally I have developed better murine models of human UCC that will allow pre-clinical trialling of new drug agents and assessment of treatment response.

I showed that deregulated Wnt signalling on a background of PTEN loss leads to UCC that appears to be mTOR dependent (regression with rapamycin treatment). Similarly in our human UCC cohort we find that those patients that have high levels of Wnt signalling appear to correlate with those that have high levels of pAKT (and loss of PTEN).

I next looked at oncogenic Ras signalling on the background of deregulated Wnt signalling and discovered similar results with both H-Ras and K-Ras causing UCC in the β -catenin mutant mouse. In our human cohort I demonstrated a correlation between upregulation of β -catenin and pERK1/2. However whether the pERK1/2 upregulation is solely due to Ras mutation is unlikely, making it interesting to sequence these tumours that upregulate β -catenin to assess Ras mutational status.

I observed that in our β -catenin urothelial lesions, as well as the H-Ras induced hyperplasia an upregulation of the p21 tumour suppressor. Thus, I next decided to knock-out p21 in this mouse and demonstrated again that p21 provides an essential block to the progression of deregulated Wnt induced tumourigenesis in the urine urothelium. Although this upregulation was not confirmed by our human TMA, this is not unexpected due to the heterogenous grade and types of samples I had access to. As a result I am expanding our cohort to look at early neoplastic (CIS) and low-grade tumours, where one would expect upregulation of p21.

Similarly I attempted to test the functional significance of FGFR3 mutations as a “driver” of UCC. Thus I targeted the expression of mutated Fgfr3 to the murine urothelium using uroplakin II promoter. These FGFR3 mutations had no effect on bladder homeostasis or tumourigenesis up to 18 months of ages. Even when these mutations were combined with β -Catenin or Ras activating mutations, no urothelial dysplasia or UCC was observed. This suggests that other alterations are required that can cooperate with FGFR3 activation to cause UCC. To further investigate the role of these co-operating mutations with FGFR3, I am currently breeding these mice with a transposon based method that utilises the synthetic Tc1/mariner family transposon *Sleeping Beauty* (*SB*) to induce tumourigenesis *in vivo* (Collier et al., 2005, Dupuy et al., 2005). This synthetic *SB* transposon, called T2/Onc, can both trap upstream genes and promote downstream sequences. This allows both inactivation of tumour suppressor genes and activation of oncogenes. Since it is foreign DNA, the *SB* insertion sites can be readily cloned and rapidly characterised to implicate genes that are co-operating with FGFR3 to drive UCC *in vivo*.

Interestingly, however, due to sporadic ectopic Cre recombinase expression in the lung and skin of these mice, FGFR3 mutation caused skin papilloma and promoted lung tumourigenesis in cooperation with K-Ras and β -Catenin activation, respectively.

All these results demonstrate that deregulated Wnt signalling plays a critical role in driving bladder cancer formation, in combination with activation of proto-oncogenes such as Ras (but not Fgfr3) and loss of tumour suppressor genes such as PTEN and p21. I also demonstrated that activation of FGFR3 can cooperate with other mutations to drive tumourigenesis in a context dependent manner and support the hypothesis that activation of FGFR signaling contributes to human cancer. Interestingly there was no single mutation that drove UCC, in contrast to the intestine, where mutation to Apc is seen as the key driving tumourigenesis (Polakis, 2000a). It appears that bladder cancer is a more progressive disease, requiring combinations of mutation to drive the neoplastic phenotype.

Although these models recapitulate various aspects of UCC, no one model has yet recapitulated all stages from pre-invasive disease to metastasis. So we ask ourselves the question how we can improve these models and make them more relevant. One avenue I am currently actively pursuing is modeling loss of wildtype p53/mutation of p53 in combination with out Wnt based cancer models to observe whether this will drive metastatic disease as in other tumours. We are also considering using intravesical carcinogen treatments to investigate whether this will cooperate with the transgenic mutation found in our mice to drive muscle invasive UCC.

Recent sequencing of human UCC by the Sanger Institute in Cambridge is reassuring and demonstrates that these mutations we are modelling in the mouse are indeed relevant in human UCC.

(<http://www.sanger.ac.uk/perl/genetics/CGP/cosmic?action=byhist&ss=bladder&sn=urinaryrct&s=3>). Indeed it has demonstrated that APC mutations occur about 11% of tumour samples, confirming it is an important mutation in UCC. Further work must be done, in particular on the aggressive muscle invasive tumours and their metastasis to properly

delineate which mutations are contributing to their malignant phenotype. Then one can better model human conditions in the mouse. Since bladder tumourigenesis in humans requires genetic events in a temporal sequence, the next generation of murine models will be inducible systems, allowing us to switch on and off genes in a bladder specific manner at different time periods, in different sequences and to different levels, enabling us better understand what is occurring in the human. This in turn will allow us to better target treatment at a molecular level, initially in the murine model, and ultimately translatable into man.

The models I describe will provide ideal platforms for trialling of Wnt pathway inhibitors, most likely in combination with MAPK/PI3K inhibitors, to assess tumour response. This makes it important to be able to identify the Wnt dependents tumours. This type of preclinical trialling is essential, since in the clinic cancer patients are moving towards more personalised medicine, where their treatments will be based on the unique molecular signature of their tumours.

In summary murine models will continue to provide us with invaluable information about tumour biology, initiation and progression and ultimately identification of molecular markers, and further elucidation of molecular pathways. These models will allow for preclinical studies regarding efficacy and tolerability of various anticancer agents in isolation and in combination, as well as assessment of ultimate response. This will ultimately allows us to translate these findings to the clinical setting allowing us to prognosticate and ultimately render cancer patients disease free.

References

References

- ABBAS, T. & DUTTA, A. 2009. p21 in cancer: intricate networks and multiple activities. *Nature Reviews Cancer*, 9, 400-414.
- AHMAD, I., SANSOM, O. J. & LEUNG, H. Y. 2008. Advances in mouse models of prostate cancer. *Expert.Rev.Mol.Med.*, 10, e16.
- ANDINO, L., CAGLE, P. T., MURER, B., LU, L., POPPER, H. H., GALATEAU-SALLE, F., SIENKO, A. E., BARRIOS, R. & ZANDER, D. S. 2006. Pleuropulmonary desmoid tumors: immunohistochemical comparison with solitary fibrous tumors and assessment of beta-catenin and cyclin D1 expression. *Arch Pathol Lab Med*, 130, 1503-9.
- AVEYARD, J. S., SKILLETER, A., HABUCHI, T. & KNOWLES, M. A. 1999. Somatic mutation of PTEN in bladder carcinoma. *Br.J.Cancer*, 80, 904-908.
- AYAN, S., GOKCE, G., KILICARSLAN, H., OZDEMIR, O., YILDIZ, E. & GULTEKIN, E. Y. 2001. K-RAS mutation in transitional cell carcinoma of urinary bladder. *Int.Urol.Nephrol.*, 33, 363-367.
- BAKKAR, A. A., WALLERAND, H., RADVANYI, F., LAHAYE, J. B., PISSARD, S., LECERF, L., KOUYOUMDJIAN, J. C., ABOU, C. C., PAIRON, J. C., JAURAND, M. C., THIERY, J. P., CHOPIN, D. K. & DE MEDINA, S. G. 2003. FGFR3 and TP53 gene mutations define two distinct pathways in urothelial cell carcinoma of the bladder. *Cancer Res*, 63, 8108-12.
- BARKER, N., RIDGWAY, R. A., VAN ES, J. H., VAN DE WETERING, M., BEGTHEL, H., VAN DEN BORN, M., DANENBERG, E., CLARKE, A. R., SANSOM, O. J. & CLEVERS, H. 2009. Crypt stem cells as the cells-of-origin of intestinal cancer. *Nature*, 457, 608-U119.
- BEHRENS, J. 2008. One hit, two outcomes for VHL-mediated tumorigenesis. *Nature Cell Biology*, 10, 1127-1128.
- BEHRENS, J., VONKRIES, J. P., KUHL, M., BRUHN, L., WEDLICH, D., GROSSCHEDL, R. & BIRCHMEIER, W. 1996. Functional interaction of beta-catenin with the transcription factor LEF-1. *Nature*, 382, 638-642.
- BENTLEY, J., L'HOTE, C., PLATT, F., HURST, C. D., LOWERY, J., TAYLOR, C., SAK, S. C., HARNDEN, P., KNOWLES, M. A. & KILTIE, A. E. 2009. Papillary and muscle invasive bladder tumors with distinct genomic stability profiles have different DNA repair fidelity and KU DNA-binding activities. *Genes Chromosomes Cancer*, 48, 310-21.
- BERGGREN, P., STEINECK, G., ADOLFSSON, J., HANSSON, J., JANSSON, O., LARSSON, P., SANDSTEDT, B., WIJKSTROM, H. & HEMMINKI, K. 2001. p53 mutations in urinary bladder cancer. *Br J Cancer*, 84, 1505-11.
- BILLEREY, C., CHOPIN, D., AUBRIOT-LORTON, M. H., RICOL, D., GIL DIEZ, D. M., VAN RHIJN, B., BRALET, M. P., LEFRERE-BELDA, M. A., LAHAYE, J. B., ABOU, C. C., BONAVENTURE, J., ZAFRANI, E. S., VAN DER, K. T., THIERY, J. P. & RADVANYI, F. 2001. Frequent FGFR3 mutations in papillary non-invasive bladder (pTa) tumors. *Am.J.Pathol.*, 158, 1955-1959.
- BJERREGAARD, B. K., RAASCHOU-NIELSEN, O., SORENSEN, M., FREDERIKSEN, K., CHRISTENSEN, J., TJONNELAND, A., OVERVAD, K., CHAPELON, F. C., NAGEL, G., CHANG-CLAUDE, J., BERGMANN, M. M., BOEING, H., TRICHOPOULOS, D., TRICHOPOULOU, A., OIKONOMOU, E., BERRINO, F., PALLI, D., TUMINO, R., VINEIS, P., PANICO, S., PEETERS, P. H., BUENO-DE-

- MESQUITA, H. B., KIEMENEY, L., GRAM, I. T., BRAATEN, T., LUND, E., GONZALEZ, C. A., BERGLUND, G., ALLEN, N., RODDAM, A., BINGHAM, S. & RIBOLI, E. 2006. Tobacco smoke and bladder cancer--in the European Prospective Investigation into Cancer and Nutrition. *Int J Cancer*, 119, 2412-6.
- BLACK, P. C., AGARWAL, P. K. & DINNEY, C. P. 2007. Targeted therapies in bladder cancer--an update. *Urol.Oncol.*, 25, 433-438.
- BLACK, P. C. & DINNEY, C. P. 2007. Bladder cancer angiogenesis and metastasis--translation from murine model to clinical trial. *Cancer Metastasis Rev*, 26, 623-34.
- BOHM, M., KIRCH, H., OTTO, T., RUBBEN, H. & WIELAND, I. 1997. Deletion analysis at the DEL-27, APC and MTS1 loci in bladder cancer: LOH at the DEL-27 locus on 5p13-12 is a prognostic marker of tumor progression. *Int.J.Cancer*, 74, 291-295.
- BOORJIAN, S., COWAN, J. E., KONETY, B. R., DUCHANE, J., TEWARI, A., CARROLL, P. R. & KANE, C. J. 2007. Bladder cancer incidence and risk factors in men with prostate cancer: results from Cancer of the Prostate Strategic Urologic Research Endeavor. *J Urol*, 177, 883-7; discussion 887-8.
- BRENNAN, P., BOGILLOT, O., CORDIER, S., GREISER, E., SCHILL, W., VINEIS, P., LOPEZ-ABENTE, G., TZONOU, A., CHANG-CLAUDE, J., BOLM-AUDORFF, U., JOCKEL, K. H., DONATO, F., SERRA, C., WAHRENDORF, J., HOURS, M., T'MANNETJE, A., KOGEVINAS, M. & BOFFETTA, P. 2000. Cigarette smoking and bladder cancer in men: a pooled analysis of 11 case-control studies. *Int J Cancer*, 86, 289-94.
- BURGER, M., VAN DER AA, M. N., VAN OERS, J. M., BRINKMANN, A., VAN DER KWAST, T. H., STEYERBERG, E. C., STOEHR, R., KIRKELS, W. J., DENZINGER, S., WILD, P. J., WIELAND, W. F., HOFSTAEDTER, F., HARTMANN, A. & ZWARTHOF, E. C. 2008. Prediction of progression of non-muscle-invasive bladder cancer by WHO 1973 and 2004 grading and by FGFR3 mutation status: a prospective study. *Eur.Urol.*, 54, 835-843.
- CAIRNS, P., PROCTOR, A. J. & KNOWLES, M. A. 1991. Loss of heterozygosity at the RB locus is frequent and correlates with muscle invasion in bladder carcinoma. *Oncogene*, 6, 2305-9.
- CAMPBELL, S. C., VOLPERT, O. V., IVANOVICH, M. & BOUCK, N. P. 1998. Molecular mediators of angiogenesis in bladder cancer. *Cancer Res*, 58, 1298-304.
- CAPECCHI, M. R. 1994. Targeted gene replacement. *Sci.Am.*, 270, 52-59.
- CAPPELLEN, D., DE OLIVEIRA, C., RICOL, D., DE MEDINA, S., BOURDIN, J., SASTRE-GARAU, X., CHOPIN, D., THIERY, J. P. & RADVANYI, F. 1999. Frequent activating mutations of FGFR3 in human bladder and cervix carcinomas. *Nat.Genet.*, 23, 18-20.
- CASTELAO, J. E., YUAN, J. M., GAGO-DOMINGUEZ, M., YU, M. C. & ROSS, R. K. 2000. Non-steroidal anti-inflammatory drugs and bladder cancer prevention. *Br J Cancer*, 82, 1364-9.
- CHAN, E., PATEL, A., HESTON, W. & LARCHIAN, W. 2009. Mouse orthotopic models for bladder cancer research. *BJU Int*, 104, 1286-91.
- CHANG, B. D., BROUDE, E. V., DOKMANOVIC, M., ZHU, H. M., RUTH, A., XUAN, Y. Z., KANDEL, E. S., LAUSCH, E., CHRISTOV, K. & RONINSON, I. B. 1999. A senescence-like phenotype distinguishes tumor cells that undergo terminal proliferation arrest after exposure to anticancer agents. *Cancer Research*, 59, 3761-3767.
- CHATTERJEE, S. J., GEORGE, B., GOEBELL, P. J., ALAVI-TAFRESHI, M., SHI, S. R., FUNG, Y. K., JONES, P. A., CORDON-CARDO, C., DATAR, R. H. & COTE, R. J.

2004. Hyperphosphorylation of pRb: a mechanism for RB tumour suppressor pathway inactivation in bladder cancer. *J Pathol*, 203, 762-70.
- CHENG, J., HUANG, H., ZHANG, Z. T., SHAPIRO, E., PELLICER, A., SUN, T. T. & WU, X. R. 2002. Overexpression of epidermal growth factor receptor in urothelium elicits urothelial hyperplasia and promotes bladder tumor growth. *Cancer Res.*, 62, 4157-4163.
- CHO, J. Y., GUO, C., TORELLO, M., LUNSTRUM, G. P., IWATA, T., DENG, C. & HORTON, W. A. 2004. Defective lysosomal targeting of activated fibroblast growth factor receptor 3 in achondroplasia. *Proc Natl Acad Sci U S A*, 101, 609-14.
- CHOW, N. H., CAIRNS, P., EISENBERGER, C. F., SCHOENBERG, M. P., TAYLOR, D. C., EPSTEIN, J. I. & SIDRANSKY, D. 2000. Papillary urothelial hyperplasia is a clonal precursor to papillary transitional cell bladder cancer. *Int J Cancer*, 89, 514-8.
- CHOY, G., O'CONNOR, S., DIEHN, F. E., COSTOUROS, N., ALEXANDER, H. R., CHOYKE, P. & LIBUTTI, S. K. 2003. Comparison of noninvasive fluorescent and bioluminescent small animal optical imaging. *Biotechniques*, 35, 1022-1030.
- CHROUSER, K., LEIBOVICH, B., BERGSTRALH, E., ZINCKE, H. & BLUTE, M. 2005. Bladder cancer risk following primary and adjuvant external beam radiation for prostate cancer. *J Urol*, 174, 107-110; discussion 110-1.
- CHROUSER, K., LEIBOVICH, B., BERGSTRALH, E., ZINCKE, H. & BLUTE, M. 2008. Bladder cancer risk following primary and adjuvant external beam radiation for prostate cancer. *J Urol*, 179, S7-S11.
- CLEVERS, H. 2006. Wnt/beta-catenin signaling in development and disease. *Cell*, 127, 469-480.
- COLLIER, L. S., CARLSON, C. M., RAVIMOHAN, S., DUPUY, A. J. & LARGAESPADA, D. A. 2005. Cancer gene discovery in solid tumours using transposon-based somatic mutagenesis in the mouse. *Nature*, 436, 272-6.
- COPP, A. J. 1995. Death before birth: clues from gene knockouts and mutations. *Trends Genet.*, 11, 87-93.
- CORDON-CARDO, C. 1998. Cell cycle regulators as prognostic factors for bladder cancer. *Eur Urol*, 33 Suppl 4, 11-2.
- CORDON-CARDO, C. 2008. Molecular alterations associated with bladder cancer initiation and progression. *Scand.J.Urol.Nephrol.Suppl*, 154-165.
- CORDON-CARDO, C., DALBAGNI, G., SAEZ, G. T., OLIVA, M. R., ZHANG, Z. F., ROSAI, J., REUTER, V. E. & PELLICER, A. 1994. p53 mutations in human bladder cancer: genotypic versus phenotypic patterns. *Int J Cancer*, 56, 347-53.
- CORTESE, R., HARTMANN, O., BERLIN, K. & ECKHARDT, F. 2008. Correlative gene expression and DNA methylation profiling in lung development nominate new biomarkers in lung cancer. *Int J Biochem Cell Biol*, 40, 1494-508.
- COTTRELL, S., BICKNELL, D., KAKLAMANIS, L. & BODMER, W. F. 1992. Molecular analysis of APC mutations in familial adenomatous polyposis and sporadic colon carcinomas. *Lancet*, 340, 626-630.
- CZERNIAK, B., COHEN, G. L., ETKIND, P., DEITCH, D., SIMMONS, H., HERZ, F. & KOSS, L. G. 1992. Concurrent mutations of coding and regulatory sequences of the Ha-ras gene in urinary bladder carcinomas. *Hum Pathol*, 23, 1199-204.
- D'AVIS, P. Y., ROBERTSON, S. C., MEYER, A. N., BARDWELL, W. M., WEBSTER, M. K. & DONOGHUE, D. J. 1998. Constitutive activation of fibroblast growth factor receptor 3 by mutations responsible for the lethal skeletal dysplasia thanatophoric dysplasia type I. *Cell Growth Differ.*, 9, 71-78.

- DAHIA, P. L. 2000. PTEN, a unique tumor suppressor gene. *Endocr.Relat Cancer*, 7, 115-129.
- DEALMEIDA, V. I., MIAO, L., ERNST, J. A., KOEPPEN, H., POLAKIS, P. & RUBINFELD, B. 2007. The soluble wnt receptor Frizzled8CRD-hFc inhibits the growth of teratocarcinomas in vivo. *Cancer Res*, 67, 5371-9.
- DENG, C., ZHANG, P., HARPER, J. W., ELLEDGE, S. J. & LEDER, P. 1995. Mice lacking p21CIP1/WAF1 undergo normal development, but are defective in G1 checkpoint control. *Cell*, 82, 675-84.
- DIAZ, D. S., SEGERSTEN, U. & MALMSTROM, P. U. 2008. Molecular genetics of bladder cancer: an update. *Minerva Urol.Nefrol.*, 60, 205-216.
- DINNEY, C. P., TANGUAY, S., BUCANA, C. D., EVE, B. Y. & FIDLER, I. J. 1995. Intravesical liposomal muramyl tripeptide phosphatidylethanolamine treatment of human bladder carcinoma growing in nude mice. *J Interferon Cytokine Res*, 15, 585-92.
- DONEHOWER, L. A., HARVEY, M., SLAGLE, B. L., MCARTHUR, M. J., MONTGOMERY, C. A., JR., BUTEL, J. S. & BRADLEY, A. 1992. Mice deficient for p53 are developmentally normal but susceptible to spontaneous tumours. *Nature*, 356, 215-21.
- DULAIMI, E., DE CACERES, II, UZZO, R. G., AL-SALEEM, T., GREENBERG, R. E., POLASCIK, T. J., BABB, J. S., GRIZZLE, W. E. & CAIRNS, P. 2004. Promoter hypermethylation profile of kidney cancer. *Clinical Cancer Research*, 10, 3972-3979.
- DUNN, T. L., SEYMOUR, G. J., GARDINER, R. A., STRUTTON, G. M. & LAVIN, M. F. 1988. Immunocytochemical demonstration of p21ras in normal and transitional cell carcinoma urothelium. *J Pathol*, 156, 59-65.
- DUPUY, A. J., AKAGI, K., LARGAESPADA, D. A., COPELAND, N. G. & JENKINS, N. A. 2005. Mammalian mutagenesis using a highly mobile somatic Sleeping Beauty transposon system. *Nature*, 436, 221-6.
- EBLE JN, S. G., EPSTEIN JL, SESTERHENN I, EDS 2004. *WHO classification of classification of tumors of the urinary system and male genital organs*, Lyon, IARCC Press.
- ESRIG, D., ELMAJIAN, D., GROSHEN, S., FREEMAN, J. A., STEIN, J. P., CHEN, S. C., NICHOLS, P. W., SKINNER, D. G., JONES, P. A. & COTE, R. J. 1994. Accumulation of nuclear p53 and tumor progression in bladder cancer. *N Engl J Med*, 331, 1259-64.
- FANG, L., IGARASHI, M., LEUNG, J., SUGRUE, M. M., LEE, S. W. & AARONSON, S. A. 1999. p21(Waf1/Cip1/Sdi1) induces permanent growth arrest with markers of replicative senescence in human tumor cells lacking functional p53. *Oncogene*, 18, 2789-2797.
- FENG, Z., HU, W., ROM, W. N., BELAND, F. A. & TANG, M. S. 2002. 4-aminobiphenyl is a major etiological agent of human bladder cancer: evidence from its DNA binding spectrum in human p53 gene. *Carcinogenesis*, 23, 1721-7.
- FLETCHER, O., EASTON, D., ANDERSON, K., GILHAM, C., JAY, M. & PETO, J. 2004. Lifetime risks of common cancers among retinoblastoma survivors. *J Natl Cancer Inst*, 96, 357-63.
- FODDE, R., SMITS, R. & CLEVERS, H. 2001. APC, signal transduction and genetic instability in colorectal cancer. *Nat Rev Cancer*, 1, 55-67.
- FONG, C. W., LEONG, H. F., WONG, E. S., LIM, J., YUSOFF, P. & GUY, G. R. 2003. Tyrosine phosphorylation of Sprouty2 enhances its interaction with c-Cbl and is crucial for its function. *J Biol Chem*, 278, 33456-64.

- FUJIMOTO, K., TANAKA, Y., RADEMAKER, A. & OYASU, R. 1996. Epidermal growth factor-responsive and -refractory carcinomas initiated with N-methyl-N-nitrosourea in rat urinary bladder. *Cancer Res*, 56, 2666-70.
- GAO, J., HUANG, H. Y., PAK, J., CHENG, J., ZHANG, Z. T., SHAPIRO, E., PELLICER, A., SUN, T. T. & WU, X. R. 2004. p53 deficiency provokes urothelial proliferation and synergizes with activated Ha-ras in promoting urothelial tumorigenesis. *Oncogene*, 23, 687-96.
- GARCIA DEL MURO, X., TORREGROSA, A., MUNOZ, J., CASTELLSAGUE, X., CONDOM, E., VIGUES, F., ARANCE, A., FABRA, A. & GERMA, J. R. 2000. Prognostic value of the expression of E-cadherin and beta-catenin in bladder cancer. *Eur J Cancer*, 36, 357-62.
- GARCIA, D. M. X., TORREGROSA, A., MUNOZ, J., CASTELLSAGUE, X., CONDOM, E., VIGUES, F., ARANCE, A., FABRA, A. & GERMA, J. R. 2000. Prognostic value of the expression of E-cadherin and beta-catenin in bladder cancer. *Eur.J.Cancer*, 36, 357-362.
- GARCIA-CLOSAS, M., MALATS, N., SILVERMAN, D., DOSEMECI, M., KOGEVINAS, M., HEIN, D. W., TARDON, A., SERRA, C., CARRATO, A., GARCIA-CLOSAS, R., LLORETA, J., CASTANO-VINYALS, G., YEAGER, M., WELCH, R., CHANOCK, S., CHATTERJEE, N., WACHOLDER, S., SAMANIC, C., TORA, M., FERNANDEZ, F., REAL, F. X. & ROTHMAN, N. 2005. NAT2 slow acetylation, GSTM1 null genotype, and risk of bladder cancer: results from the Spanish Bladder Cancer Study and meta-analyses. *Lancet*, 366, 649-59.
- GARTEL, A. L. & RADHAKRISHNAN, S. K. 2005. Lost in transcription: p21 repression, mechanisms, and consequences. *Cancer Research*, 65, 3980-3985.
- GEORGE, B., DATAR, R. H., WU, L., CAI, J., PATTEN, N., BEIL, S. J., GROSHEN, S., STEIN, J., SKINNER, D., JONES, P. A. & COTE, R. J. 2007. p53 gene and protein status: the role of p53 alterations in predicting outcome in patients with bladder cancer. *J Clin Oncol*, 25, 5352-8.
- GILES, R. H., VAN ES, J. H. & CLEVERS, H. 2003. Caught up in a Wnt storm: Wnt signaling in cancer. *Biochimica Et Biophysica Acta-Reviews on Cancer*, 1653, 1-24.
- GRIPPO, P. J. & SANDGREN, E. P. 2000. Highly invasive transitional cell carcinoma of the bladder in a simian virus 40 T-antigen transgenic mouse model. *Am J Pathol*, 157, 805-13.
- GROSSFELD, G. D., GINSBERG, D. A., STEIN, J. P., BOCHNER, B. H., ESRIG, D., GROSHEN, S., DUNN, M., NICHOLS, P. W., TAYLOR, C. R., SKINNER, D. G. & COTE, R. J. 1997. Thrombospondin-1 expression in bladder cancer: association with p53 alterations, tumor angiogenesis, and tumor progression. *J Natl Cancer Inst*, 89, 219-27.
- GROSSMAN, H. B., LIEBERT, M., ANTELO, M., DINNEY, C. P., HU, S. X., PALMER, J. L. & BENEDICT, W. F. 1998. p53 and RB expression predict progression in T1 bladder cancer. *Clin Cancer Res*, 4, 829-34.
- GUILBAULT, C., SAEED, Z., DOWNEY, G. P. & RADZIOCH, D. 2007. Cystic fibrosis mouse models. *Am.J.Respir.Cell Mol.Biol.*, 36, 1-7.
- HABAS, R. & DAWID, I. B. 2005. Dishevelled and Wnt signaling: is the nucleus the final frontier? *J Biol*, 4, 2.
- HACOHEN, N., KRAMER, S., SUTHERLAND, D., HIROMI, Y. & KRASNOW, M. A. 1998. sprouty encodes a novel antagonist of FGF signaling that patterns apical branching of the Drosophila airways. *Cell*, 92, 253-63.

- HADASCHIK, B. A., BLACK, P. C., SEA, J. C., METWALLI, A. R., FAZLI, L., DINNEY, C. P., GLEAVE, M. E. & SO, A. I. 2007. A validated mouse model for orthotopic bladder cancer using transurethral tumour inoculation and bioluminescence imaging. *BJU Int*, 100, 1377-84.
- HAFNER, C., HARTMANN, A. & VOGT, T. 2007a. FGFR3 mutations in epidermal nevi and seborrheic keratoses: lessons from urothelium and skin. *J.Invest Dermatol.*, 127, 1572-1573.
- HAFNER, C., LOPEZ-KNOWLES, E., LUIS, N. M., TOLL, A., BASELGA, E., FERNANDEZ-CASADO, A., HERNANDEZ, S., RIBE, A., MENTZEL, T., STOEHR, R., HOFSTAEDTER, F., LANDTHALER, M., VOGT, T., PUJOL, R. M., HARTMANN, A. & REAL, F. X. 2007b. Oncogenic PIK3CA mutations occur in epidermal nevi and seborrheic keratoses with a characteristic mutation pattern. *Proc.Natl.Acad.Sci.U.S.A*, 104, 13450-13454.
- HAFNER, C., VAN OERS, J. M., HARTMANN, A., LANDTHALER, M., STOEHR, R., BLASZYK, H., HOFSTAEDTER, F., ZWARTHOF, E. C. & VOGT, T. 2006. High frequency of FGFR3 mutations in adenoid seborrheic keratoses. *J.Invest Dermatol.*, 126, 2404-2407.
- HARADA, N., TAMAI, Y., ISHIKAWA, T., SAUER, B., TAKAKU, K., OSHIMA, M. & TAKETO, M. M. 1999. Intestinal polyposis in mice with a dominant stable mutation of the beta-catenin gene. *EMBO J.*, 18, 5931-5942.
- HARTMANN, A., SCHLAKE, G., ZAAK, D., HUNGERHUBER, E., HOFSTETTER, A., HOFSTAEDTER, F. & KNUECHEL, R. 2002. Occurrence of chromosome 9 and p53 alterations in multifocal dysplasia and carcinoma in situ of human urinary bladder. *Cancer Res*, 62, 809-18.
- HE, F., MO, L., ZHENG, X. Y., HU, C., LEPOR, H., LEE, E. Y., SUN, T. T. & WU, X. R. 2009. Deficiency of pRb Family Proteins and p53 in Invasive Urothelial Tumorigenesis. *Cancer Res*.
- HE, T. C., SPARKS, A. B., RAGO, C., HERMEKING, H., ZAWEL, L., DA COSTA, L. T., MORIN, P. J., VOGELSTEIN, B. & KINZLER, K. W. 1998. Identification of c-MYC as a target of the APC pathway. *Science*, 281, 1509-1512.
- HICKS, R. M. 1975. The mammalian urinary bladder: an accommodating organ. *Biol Rev Camb Philos Soc*, 50, 215-46.
- HOVANES, K., LI, T. W. H., MUNGUIA, J. E., TRUONG, T., MILOVANOVIC, T., MARSH, J. L., HOLCOMBE, R. F. & WATERMAN, M. L. 2001. beta-catenin-sensitive isoforms of lymphoid enhancer factor-1 are selectively expressed in colon cancer. *Nature Genetics*, 28, 53-57.
- HOWE, L. R. & BROWN, A. M. 2004. Wnt signaling and breast cancer. *Cancer Biol Ther*, 3, 36-41.
- HUELSKEN, J. & BEHRENS, J. 2002. The Wnt signalling pathway. *J Cell Sci*, 115, 3977-8.
- INDRA, A. K., LI, M., BROCARD, J., WAROT, X., BORNERT, J. M., GERARD, C., MESSADDEQ, N., CHAMBON, P. & METZGER, D. 2000. Targeted somatic mutagenesis in mouse epidermis. *Horm Res*, 54, 296-300.
- IWATA, T., CHEN, L., LI, C., OVCHINNIKOV, D. A., BEHRINGER, R. R., FRANCOMANO, C. A. & DENG, C. X. 2000. A neonatal lethal mutation in FGFR3 uncouples proliferation and differentiation of growth plate chondrocytes in embryos. *Hum.Mol.Genet.*, 9, 1603-1613.
- IWATA, T., LI, C. L., DENG, C. X. & FRANCOMANO, C. A. 2001. Highly activated Fgfr3 with the K644M mutation causes prolonged survival in severe dwarf mice. *Hum.Mol.Genet.*, 10, 1255-1264.

- IZAWA, J. I., SLATON, J. W., KEDAR, D., KARASHIMA, T., PERROTTE, P., CZERNIAK, B., GROSSMAN, H. B. & DINNEY, C. P. 2001. Differential expression of progression-related genes in the evolution of superficial to invasive transitional cell carcinoma of the bladder. *Oncol Rep*, 8, 9-15.
- JACKSON, E. L., WILLIS, N., MERCER, K., BRONSON, R. T., CROWLEY, D., MONTOYA, R., JACKS, T. & TUVESON, D. A. 2001. Analysis of lung tumor initiation and progression using conditional expression of oncogenic K-ras. *Genes Dev.*, 15, 3243-3248.
- JEBAR, A. H., HURST, C. D., TOMLINSON, D. C., JOHNSTON, C., TAYLOR, C. F. & KNOWLES, M. A. 2005. FGFR3 and Ras gene mutations are mutually exclusive genetic events in urothelial cell carcinoma. *Oncogene*, 24, 5218-5225.
- JOHANSSON, S. L. & COHEN, S. M. 1997. Epidemiology and etiology of bladder cancer. *Semin Surg Oncol*, 13, 291-8.
- KALDOR, J. M., DAY, N. E., KITTELMANN, B., PETTERSSON, F., LANGMARK, F., PEDERSEN, D., PRIOR, P., NEAL, F., KARJALAINEN, S., BELL, J. & ET AL. 1995. Bladder tumours following chemotherapy and radiotherapy for ovarian cancer: a case-control study. *Int J Cancer*, 63, 1-6.
- KANAYAMA, H. 2001. Matrix metalloproteinases and bladder cancer. *J Med Invest*, 48, 31-43.
- KAROUI, M., HOFMANN-RADVANYI, H., ZIMMERMANN, U., COUVELARD, A., DEGOTT, C., FARIDONI-LAURENS, L., AHOMADEGBE, J. C., GAZZERI, S., BRAMBILLA, E., CLERICI, T., CHARBONNIER, P., TRESALLET, C., MITRY, E., PENNA, C., ROUGIER, P., BOILEAU, C., THIERY, J. P., NORDLINGER, B., FRANC, B. & RADVANYI, F. 2001. No evidence of somatic FGFR3 mutation in various types of carcinoma. *Oncogene*, 20, 5059-5061.
- KASHIBUCHI, K., TOMITA, K., SCHALKEN, J. A., KUME, H., YAMAGUCHI, T., MUTO, S., HORIE, S. & KITAMURA, T. 2006. The prognostic value of E-cadherin, alpha-, beta-, and gamma-catenin in urothelial cancer of the upper urinary tract. *Eur.Urol.*, 49, 839-845.
- KASTRITIS, E., MURRAY, S., KYRIAKOU, F., HORTI, M., TAMVAKIS, N., KAVANTZAS, N., PATSOURIS, E. S., NONI, A., LEGAKI, S., DIMOPOULOS, M. A. & BAMIAS, A. 2009. Somatic mutations of adenomatous polyposis coli gene and nuclear b-catenin accumulation have prognostic significance in invasive urothelial carcinomas: evidence for Wnt pathway implication. *Int.J.Cancer*, 124, 103-108.
- KEMP, R., IRELAND, H., CLAYTON, E., HOUGHTON, C., HOWARD, L. & WINTON, D. J. 2004. Elimination of background recombination: somatic induction of Cre by combined transcriptional regulation and hormone binding affinity. *Nucleic Acids Res*, 32, e92.
- KHANDELWAL, P., ABRAHAM, S. N. & APODACA, G. 2009. Cell biology and physiology of the uroepithelium. *Am J Physiol Renal Physiol*, 297, F1477-501.
- KIM, H. J. & BAR-SAGI, D. 2004. Modulation of signalling by Sprouty: a developing story. *Nat Rev Mol Cell Biol*, 5, 441-50.
- KIMURA, T., SUZUKI, H., OHASHI, T., ASANO, K., KIYOTA, H. & ETO, Y. 2001. The incidence of thanatophoric dysplasia mutations in FGFR3 gene is higher in low-grade or superficial bladder carcinomas. *Cancer*, 92, 2555-2561.
- KINZLER, K. W., NILBERT, M. C., SU, L. K., VOGELSTEIN, B., BRYAN, T. M., LEVY, D. B., SMITH, K. J., PREISINGER, A. C., HEDGE, P. & MCKECHNIE, D. 1991. Identification of FAP locus genes from chromosome 5q21. *Science*, 253, 661-665.

- KINZLER, K. W. & VOGELSTEIN, B. 1996. Lessons from hereditary colorectal cancer. *Cell*, 87, 159-170.
- KIRKEGAARD, T., EDWARDS, J., TOVEY, S., MCGLYNN, L. M., KRISHNA, S. N., MUKHERJEE, R., TAM, L., MUNRO, A. F., DUNNE, B. & BARTLETT, J. M. S. 2006. Observer variation in immunohistochemical analysis of protein expression, time for a change? *Histopathology*, 48, 787-794.
- KLAUS, A. & BIRCHMEIER, W. 2008. Wnt signalling and its impact on development and cancer. *Nat Rev Cancer*, 8, 387-98.
- KNOWLES, M. A. 2001. What we could do now: molecular pathology of bladder cancer. *Mol Pathol*, 54, 215-21.
- KNOWLES, M. A. 2007. Role of FGFR3 in urothelial cell carcinoma: biomarker and potential therapeutic target. *World J.Urol.*, 25, 581-593.
- KNOWLES, M. A. 2008. Novel therapeutic targets in bladder cancer: mutation and expression of FGF receptors. *Future.Oncol.*, 4, 71-83.
- KOGEVINAS, M., T MANNETJE, A., CORDIER, S., RANFT, U., GONZALEZ, C. A., VINEIS, P., CHANG-CLAUDE, J., LYNGE, E., WAHRENDORF, J., TZONOU, A., JOCKEL, K. H., SERRA, C., PORRU, S., HOURS, M., GREISER, E. & BOFFETTA, P. 2003. Occupation and bladder cancer among men in Western Europe. *Cancer Causes Control*, 14, 907-14.
- KOHN, A. D. & MOON, R. T. 2005. Wnt and calcium signaling: beta-catenin-independent pathways. *Cell Calcium*, 38, 439-46.
- KOMHOFF, M., GUAN, Y., SHAPPELL, H. W., DAVIS, L., JACK, G., SHYR, Y., KOCH, M. O., SHAPPELL, S. B. & BREYER, M. D. 2000. Enhanced expression of cyclooxygenase-2 in high grade human transitional cell bladder carcinomas. *Am J Pathol*, 157, 29-35.
- KOMPIER, L. C., LURKIN, I., VAN DER AA, M. N., VAN RHIJN, B. W., VAN DER KWAST, T. H. & ZWARTHOF, E. C. 2010. FGFR3, HRAS, KRAS, NRAS and PIK3CA Mutations in Bladder Cancer and Their Potential as Biomarkers for Surveillance and Therapy. *PLoS One*, 5, e13821.
- KOSS, L. G. 1969. The asymmetric unit membranes of the epithelium of the urinary bladder of the rat. An electron microscopic study of a mechanism of epithelial maturation and function. *Lab Invest*, 21, 154-68.
- KOSS, L. G. 1992. Bladder cancer from a perspective of 40 years. *J Cell Biochem Suppl*, 161, 23-9.
- KOUKI, H. S., KOLETIS, E. N., ZOLOTA, V., PROKAKIS, C., APOSTOLAKIS, E. & DOUGENIS, D. 2008. Solitary fibrous tumor of the lung. *Gen Thorac Cardiovasc Surg*, 56, 249-51.
- KRAMER, S., OKABE, M., HACOEN, N., KRASNOW, M. A. & HIROMI, Y. 1999. Sprouty: a common antagonist of FGF and EGF signaling pathways in Drosophila. *Development*, 126, 2515-25.
- KURZROCK, E. A., LIEU, D. K., DEGRAFFENRIED, L. A., CHAN, C. W. & ISSEROFF, R. R. 2008. Label-retaining cells of the bladder: candidate urothelial stem cells. *Am J Physiol Renal Physiol*, 294, F1415-21.
- LAMY, A., GOBET, F., LAURENT, M., BLANCHARD, F., VARIN, C., MOULIN, C., ANDREOU, A., FREBOURG, T. & PFISTER, C. 2006. Molecular profiling of bladder tumors based on the detection of FGFR3 and TP53 mutations. *J.Urol.*, 176, 2686-2689.

- LESCHE, R., GROSZER, M., GAO, J., WANG, Y., MESSING, A., SUN, H., LIU, X. & WU, H. 2002. Cre/loxP-mediated inactivation of the murine Pten tumor suppressor gene. *Genesis*, 32, 148-9.
- LEVINE, A. J. 1997. p53, the cellular gatekeeper for growth and division. *Cell*, 88, 323-31.
- LIN, J. H., ZHAO, H. & SUN, T. T. 1995. A tissue-specific promoter that can drive a foreign gene to express in the suprabasal urothelial cells of transgenic mice. *Proc Natl Acad Sci U S A*, 92, 679-83.
- LINDGREN, D., LIEDBERG, F., ANDERSSON, A., CHEBIL, G., GUDJONSSON, S., BORG, A., MANSSON, W., FIORETOS, T. & HOGLUND, M. 2006. Molecular characterization of early-stage bladder carcinomas by expression profiles, FGFR3 mutation status, and loss of 9q. *Oncogene*, 25, 2685-2696.
- LOGIE, A., DUNOIS-LARDE, C., ROSTY, C., LEVREL, O., BLANCHE, M., RIBEIRO, A., GASC, J. M., JORCANO, J., WERNER, S., SASTRE-GARAU, X., THIERY, J. P. & RADVANYI, F. 2005. Activating mutations of the tyrosine kinase receptor FGFR3 are associated with benign skin tumors in mice and humans. *Hum.Mol.Genet.*, 14, 1153-1160.
- LOGOTHETIS, C. J., XU, H. J., RO, J. Y., HU, S. X., SAHIN, A., ORDONEZ, N. & BENEDICT, W. F. 1992. Altered expression of retinoblastoma protein and known prognostic variables in locally advanced bladder cancer. *J Natl Cancer Inst*, 84, 1256-61.
- LU, M. L., WIKMAN, F., ORNTOFT, T. F., CHARYTONOWICZ, E., RABBANI, F., ZHANG, Z., DALBAGNI, G., POHAR, K. S., YU, G. & CORDON-CARDO, C. 2002. Impact of alterations affecting the p53 pathway in bladder cancer on clinical outcome, assessed by conventional and array-based methods. *Clin Cancer Res*, 8, 171-9.
- LUIS, N. M., LOPEZ-KNOWLES, E. & REAL, F. X. 2007. Molecular biology of bladder cancer. *Clin.Transl.Oncol.*, 9, 5-12.
- LUO, Y., CHEN, X., HAN, R., CHOREV, M., DEWOLF, W. C. & O'DONNELL, M. A. 1999. Mutated ras p21 as a target for cancer therapy in mouse transitional cell carcinoma. *J Urol*, 162, 1519-26.
- MACAULAY, K., DOBLE, B. W., PATEL, S., HANSOTIA, T., SINCLAIR, E. M., DRUCKER, D. J., NAGY, A. & WOODGETT, J. R. 2007. Glycogen synthase kinase 3alpha-specific regulation of murine hepatic glycogen metabolism. *Cell Metab*, 6, 329-37.
- MAO, J. H., WANG, J. Y., LIU, B., PAN, W. J., FARR, G. H., FLYNN, C., YUAN, H. D., TAKADA, S., KIMELMAN, D., LI, L. & WU, D. Q. 2001. Low-density lipoprotein receptor-related protein-5 binds to Axin and regulates the canonical Wnt signaling pathway. *Molecular Cell*, 7, 801-809.
- MARSH, V., WINTON, D. J., WILLIAMS, G. T., DUBOIS, N., TRUMPP, A., SANSOM, O. J. & CLARKE, A. R. 2008. Epithelial Pten is dispensable for intestinal homeostasis but suppresses adenoma development and progression after Apc mutation. *Nat Genet*, 40, 1436-44.
- MARSIT, C. J., KARAGAS, M. R., ANDREW, A., LIU, M., DANAE, H., SCHNED, A. R., NELSON, H. H. & KELSEY, K. T. 2005. Epigenetic inactivation of SFRP genes and TP53 alteration act jointly as markers of invasive bladder cancer. *Cancer Res*, 65, 7081-5.
- MASSOUD, T. F. & GAMBHIR, S. S. 2003. Molecular imaging in living subjects: seeing fundamental biological processes in a new light. *Genes Dev.*, 17, 545-580.

- MASTERS, J. R., VANI, U. D., GRIGOR, K. M., GRIFFITHS, G. O., CROOK, A., PARMAR, M. K. & KNOWLES, M. A. 2003. Can p53 staining be used to identify patients with aggressive superficial bladder cancer? *J Pathol*, 200, 74-81.
- MCGRATH, M., MICHAUD, D. S. & DE VIVO, I. 2006. Hormonal and reproductive factors and the risk of bladder cancer in women. *Am J Epidemiol*, 163, 236-44.
- MCMANUS, E. J., SAKAMOTO, K., ARMIT, L. J., RONALDSON, L., SHPIRO, N., MARQUEZ, R. & ALESSI, D. R. 2005. Role that phosphorylation of GSK3 plays in insulin and Wnt signalling defined by knockin analysis. *EMBO J*, 24, 1571-83.
- MESSING, E. M. 1990. Clinical implications of the expression of epidermal growth factor receptors in human transitional cell carcinoma. *Cancer Res*, 50, 2530-7.
- MESSING, E. M. 1992. Growth factors and bladder cancer: clinical implications of the interactions between growth factors and their urothelial receptors. *Semin Surg Oncol*, 8, 285-92.
- MIYAMOTO, H., SHUIN, T., IKEDA, I., HOSAKA, M. & KUBOTA, Y. 1996. Loss of heterozygosity at the p53, RB, DCC and APC tumor suppressor gene loci in human bladder cancer. *J.Urol.*, 155, 1444-1447.
- MIYOSHI, Y., NAGASE, H., ANDO, H., HORII, A., ICHII, S., NAKATSURU, S., AOKI, T., MIKI, Y., MORI, T. & NAKAMURA, Y. 1992. Somatic mutations of the APC gene in colorectal tumors: Mutation cluster region in the APC gene. *Human Molecular Genetics*, 1, 229-233.
- MO, L., CHENG, J., LEE, E. Y., SUN, T. T. & WU, X. R. 2005. Gene deletion in urothelium by specific expression of Cre recombinase. *Am.J.Physiol Renal Physiol*, 289, F562-F568.
- MO, L., ZHENG, X., HUANG, H. Y., SHAPIRO, E., LEPOR, H., CORDON-CARDO, C., SUN, T. T. & WU, X. R. 2007. Hyperactivation of Ha-ras oncogene, but not Ink4a/Arf deficiency, triggers bladder tumorigenesis. *J.Clin.Invest*, 117, 314-325.
- MOLENAAR, M., VANDEWETERING, M., OOSTERWEGEL, M., PETERSONMADURO, J., GODSAVE, S., KORINEK, V., ROOSE, J., DESTREE, O. & CLEVERS, H. 1996. XTcf-3 transcription factor mediates beta-catenin-induced axis formation in *Xenopus* embryos. *Cell*, 86, 391-399.
- MONSONEGO-ORNAN, E., ADAR, R., FEFERMAN, T., SEGEV, O. & YAYON, A. 2000. The transmembrane mutation G380R in fibroblast growth factor receptor 3 uncouples ligand-mediated receptor activation from down-regulation. *Mol Cell Biol*, 20, 516-22.
- MOON, R. T., KOHN, A. D., DE FERRARI, G. V. & KAYKAS, A. 2004. WNT and beta-catenin signalling: diseases and therapies. *Nat Rev Genet*, 5, 691-701.
- MOSER, A. R., PITOT, H. C. & DOVE, W. F. 1990. A DOMINANT MUTATION THAT PREDISPOSES TO MULTIPLE INTESTINAL NEOPLASIA IN THE MOUSE. *Science*, 247, 322-324.
- MUENKE, M. & SCHELL, U. 1995. Fibroblast-growth-factor receptor mutations in human skeletal disorders. *Trends Genet*, 11, 308-13.
- MULLER, P. A., CASWELL, P. T., DOYLE, B., IWANICKI, M. P., TAN, E. H., KARIM, S., LUKASHCHUK, N., GILLESPIE, D. A., LUDWIG, R. L., GOSSELIN, P., CROMER, A., BRUGGE, J. S., SANSOM, O. J., NORMAN, J. C. & VOUSDEN, K. H. 2009. Mutant p53 drives invasion by promoting integrin recycling. *Cell*, 139, 1327-41.
- NAGAYAMA, S., FUKUKAWA, C., KATAGIRI, T., OKAMOTO, T., AOYAMA, T., OYAIZU, N., IMAMURA, M., TOGUCHIDA, J. & NAKAMURA, Y. 2005. Therapeutic potential of antibodies against FZD 10, a cell-surface protein, for synovial sarcomas. *Oncogene*, 24, 6201-12.

- NAGY, A. 2000. Cre recombinase: the universal reagent for genome tailoring. *Genesis.*, 26, 99-109.
- NAKOPOULOU, L., ZERVAS, A., GAKIOPOULOU-GIVALOU, H., CONSTANTINIDES, C., DOUMANIS, G., DAVARIS, P. & DIMOPOULOS, C. 2000. Prognostic value of E-cadherin, beta-catenin, P120ctn in patients with transitional cell bladder cancer. *Anticancer Res.*, 20, 4571-4578.
- NAMBA, R., YOUNG, L. J., ABBEY, C. K., KIM, L., DAMONTE, P., BOROWSKY, A. D., QI, J., TEPPER, C. G., MACLEOD, C. L., CARDIFF, R. D. & GREGG, J. P. 2006. Rapamycin inhibits growth of premalignant and malignant mammary lesions in a mouse model of ductal carcinoma in situ. *Clin Cancer Res*, 12, 2613-21.
- NASKI, M. C., WANG, Q., XU, J. & ORNITZ, D. M. 1996. Graded activation of fibroblast growth factor receptor 3 by mutations causing achondroplasia and thanatophoric dysplasia. *Nat.Genet.*, 13, 233-237.
- NEAL, D. E. & MELLON, K. 1992. Epidermal growth factor receptor and bladder cancer: a review. *Urol Int*, 48, 365-71.
- NEGRETE, H. O., LAVELLE, J. P., BERG, J., LEWIS, S. A. & ZEIDEL, M. L. 1996. Permeability properties of the intact mammalian bladder epithelium. *Am J Physiol*, 271, F886-94.
- NG, S. S., MAHMOUDI, T., DANENBERG, E., BEJAOU, I., DE LAU, W., KORSWAGEN, H. C., SCHUTTE, M. & CLEVERS, H. 2009. Phosphatidylinositol 3-kinase signaling does not activate the wnt cascade. *J Biol Chem*, 284, 35308-13.
- NOVAK, A., GUO, C., YANG, W., NAGY, A. & LOBE, C. G. 2000. Z/EG, a double reporter mouse line that expresses enhanced green fluorescent protein upon Cre-mediated excision. *Genesis.*, 28, 147-155.
- NUSSE, R. & VARMUS, H. E. 1982. MANY TUMORS INDUCED BY THE MOUSE MAMMARY-TUMOR VIRUS CONTAIN A PROVIRUS INTEGRATED IN THE SAME REGION OF THE HOST GENOME. *Cell*, 31, 99-109.
- NUSSLEINVOLHARD, C. & WIESCHAUS, E. 1980. MUTATIONS AFFECTING SEGMENT NUMBER AND POLARITY IN DROSOPHILA. *Nature*, 287, 795-801.
- OBERMANN, E. C., JUNKER, K., STOEHR, R., DIETMAIER, W., ZAAK, D., SCHUBERT, J., HOFSTAEDTER, F., KNUECHEL, R. & HARTMANN, A. 2003. Frequent genetic alterations in flat urothelial hyperplasias and concomitant papillary bladder cancer as detected by CGH, LOH, and FISH analyses. *J Pathol*, 199, 50-7.
- OLDEROY, G., DAEHLIN, L. & OGREID, D. 1998. Low-frequency mutation of Ha-ras and Ki-ras oncogenes in transitional cell carcinoma of the bladder. *Anticancer Res.*, 18, 2675-2678.
- ORNTOFT, T. F. & WOLF, H. 1998. Molecular alterations in bladder cancer. *Urol Res*, 26, 223-33.
- OVING, I. M. & CLEVERS, H. C. 2002. Molecular causes of colon cancer. *European Journal of Clinical Investigation*, 32, 448-457.
- PASHOS, C. L., BOTTEMAN, M. F., LASKIN, B. L. & REDAELLI, A. 2002. Bladder cancer: epidemiology, diagnosis, and management. *Cancer Pract*, 10, 311-22.
- PATEL, S., DOBLE, B. W., MACAULAY, K., SINCLAIR, E. M., DRUCKER, D. J. & WOODGETT, J. R. 2008. Tissue-specific role of glycogen synthase kinase 3beta in glucose homeostasis and insulin action. *Mol Cell Biol*, 28, 6314-28.
- POLAKIS, P. 2000a. Wnt signaling and cancer. *Genes Dev.*, 14, 1837-1851.
- POLAKIS, P. 2000b. Wnt signaling and cancer. *Genes & Development*, 14, 1837-1851.
- POPOV, Z., GIL-DIEZ DE MEDINA, S., LEFRERE-BELDA, M. A., HOZNEK, A., BASTUJI-GARIN, S., ABBOU, C. C., THIERY, J. P., RADVANYI, F. & CHOPIN, C.

- D. K. 2000. Low E-cadherin expression in bladder cancer at the transcriptional and protein level provides prognostic information. *Br J Cancer*, 83, 209-14.
- POWELL, S. M., ZILZ, N., BEAZERBARCLAY, Y., BRYAN, T. M., HAMILTON, S. R., THIBODEAU, S. N., VOGELSTEIN, B. & KINZLER, K. W. 1992. APC MUTATIONS OCCUR EARLY DURING COLORECTAL TUMORIGENESIS. *Nature*, 359, 235-237.
- PUZIO-KUTER, A. M., CASTILLO-MARTIN, M., KINKADE, C. W., WANG, X., SHEN, T. H., MATOS, T., SHEN, M. M., CORDON-CARDO, C. & ABATE-SHEN, C. 2009. Inactivation of p53 and Pten promotes invasive bladder cancer. *Genes Dev*, 23, 675-80.
- QIAN, C. N., FURGE, K. A., KNOL, J., HUANG, D., CHEN, J., DYKEMA, K. J., KORT, E. J., MASSIE, A., KHOO, S. K., VANDEN BELDT, K., RESAU, J. H., ANEMA, J., KAHNOSKI, R. J., MORREAU, H., CAMPARO, P., COMPERAT, E., SIBONY, M., DENOUX, Y., MOLINIE, V., VIEILLEFOND, A., ENG, C., WILLIAMS, B. O. & TEH, B. T. 2009. Activation of the PI3K/AKT pathway induces urothelial carcinoma of the renal pelvis: identification in human tumors and confirmation in animal models. *Cancer Res*, 69, 8256-64.
- QING, J., DU, X., CHEN, Y., CHAN, P., LI, H., WU, P., MARSTERS, S., STAWICKI, S., TIEN, J., TOTPAL, K., ROSS, S., STINSON, S., DORNAN, D., FRENCH, D., WANG, Q. R., STEPHAN, J. P., WU, Y., WIESMANN, C. & ASHKENAZI, A. 2009. Antibody-based targeting of FGFR3 in bladder carcinoma and t(4;14)-positive multiple myeloma in mice. *J Clin Invest*, 119, 1216-29.
- REDDY, E. P., REYNOLDS, R. K., SANTOS, E. & BARBACID, M. 1982. A point mutation is responsible for the acquisition of transforming properties by the T24 human bladder carcinoma oncogene. *Nature*, 300, 149-52.
- REYA, T. & CLEVERS, H. 2005. Wnt signalling in stem cells and cancer. *Nature*, 434, 843-850.
- RIBEIRO-FILHO, L. A., FRANKS, J., SASAKI, M., SHIINA, H., LI, L. C., NOJIMA, D., ARAP, S., CARROLL, P., ENOKIDA, H., NAKAGAWA, M., YONEZAWA, S. & DAHIYA, R. 2002. CpG hypermethylation of promoter region and inactivation of E-cadherin gene in human bladder cancer. *Mol Carcinog*, 34, 187-98.
- RIEGER-CHRIST, K. M., LEE, P., ZAGHA, R., KOSAKOWSKI, M., MOINZADEH, A., STOFFEL, J., BEN-ZE'EV, A., LIBERTINO, J. A. & SUMMERHAYES, I. C. 2004. Novel expression of N-cadherin elicits in vitro bladder cell invasion via the Akt signaling pathway. *Oncogene*, 23, 4745-53.
- RIEGER-CHRIST, K. M., MOURTZINOS, A., LEE, P. J., ZAGHA, R. M., CAIN, J., SILVERMAN, M., LIBERTINO, J. A. & SUMMERHAYES, I. C. 2003. Identification of fibroblast growth factor receptor 3 mutations in urine sediment DNA samples complements cytology in bladder tumor detection. *Cancer*, 98, 737-744.
- RIJSEWIJK, F., SCHUERMANN, M., WAGENAAR, E., PARREN, P., WEIGEL, D. & NUSSE, R. 1987. THE DROSOPHILA HOMOLOG OF THE MOUSE MAMMARY ONCOGENE INT-1 IS IDENTICAL TO THE SEGMENT POLARITY GENE WINGLESS. *Cell*, 50, 649-657.
- ROOSE, J., HULS, G., VAN BEEST, M., MOERER, P., VAN DER HORN, K., GOLDSCHMEDING, R., LOGTENBERG, T. & CLEAVERS, H. 1999. Synergy between tumor suppressor APC and the beta-catenin-Tcf4 target Tcf1. *Science*, 285, 1923-1926.

- RUBIN, C., LITVAK, V., MEDVEDOVSKY, H., ZWANG, Y., LEV, S. & YARDEN, Y. 2003. Sprouty fine-tunes EGF signaling through interlinked positive and negative feedback loops. *Curr Biol*, 13, 297-307.
- RUBINFELD, B., SOUZA, B., ALBERT, I., MULLER, O., CHAMBERLAIN, S. H., MASIARZ, F. R., MUNEMITSU, S. & POLAKIS, P. 1993. Association of the APC gene product with beta-catenin. *Science*, 262, 1731-1734.
- SALMENA, L., CARRACEDO, A. & PANDOLFI, P. P. 2008. Tenets of PTEN tumor suppression. *Cell*, 133, 403-14.
- SANCHO, E., BATLLE, E. & CLEVERS, H. 2004. Signaling pathways in intestinal development and cancer. *Annual Review of Cell and Developmental Biology*, 20, 695-723.
- SANSOM, O. J., GRIFFITHS, D. F. R., REED, K. R., WINTON, D. J. & CLARKE, A. R. 2005. Apc deficiency predisposes to renal carcinoma in the mouse. *Oncogene*, 24, 8205-8210.
- SANSOM, O. J., REED, K. R., HAYES, A. J., IRELAND, H., BRINKMANN, H., NEWTON, I. P., BATLLE, E., SIMON-ASSMANN, P., CLEVERS, H., NATHKE, I. S., CLARKE, A. R. & WINTON, D. J. 2004. Loss of Apc in vivo immediately perturbs Wnt signaling, differentiation, and migration. *Genes & Development*, 18, 1385-1390.
- SATOH, S., DAIGO, Y., FURUKAWA, Y., KATO, T., MIWA, N., NISHIWAKI, T., KAWASOE, T., ISHIGURO, H., FUJITA, M., TOKINO, T., SASAKI, Y., IMAOKA, S., MURATA, M., SHIMANO, T., YAMAOKA, Y. & NAKAMURA, Y. 2000. AXIN1 mutations in hepatocellular carcinomas, and growth suppression in cancer cells by virus-mediated transfer of AXIN1. *Nature Genetics*, 24, 245-250.
- SAUER, B. & HENDERSON, N. 1988. Site-specific DNA recombination in mammalian cells by the Cre recombinase of bacteriophage P1. *Proc.Natl.Acad.Sci.U.S.A.*, 85, 5166-5170.
- SCHMITZ-DRAGER, B. J., GOEBELL, P. J., EBERT, T. & FRADET, Y. 2000. p53 immunohistochemistry as a prognostic marker in bladder cancer. Playground for urology scientists? *Eur Urol*, 38, 691-9;discussion 700.
- SCHROEDER, J. C., CONWAY, K., LI, Y., MISTRY, K., BELL, D. A. & TAYLOR, J. A. 2003. p53 mutations in bladder cancer: evidence for exogenous versus endogenous risk factors. *Cancer Res*, 63, 7530-8.
- SCHULZ, W. A. 2006. Understanding urothelial carcinoma through cancer pathways. *Int.J.Cancer*, 119, 1513-1518.
- SEAGER, C. M., PUZIO-KUTER, A. M., PATEL, T., JAIN, S., CORDON-CARDO, C., MC KIERNAN, J. & ABATE-SHEN, C. 2009. Intravesical delivery of rapamycin suppresses tumorigenesis in a mouse model of progressive bladder cancer. *Cancer Prev Res (Phila Pa)*, 2, 1008-14.
- SHARIAT, S. F., KIM, J., RAPTIDIS, G., AYALA, G. E. & LERNER, S. P. 2003. Association of p53 and p21 expression with clinical outcome in patients with carcinoma in situ of the urinary bladder. *Urology*, 61, 1140-5.
- SHARIAT, S. F., PAHLAVAN, S., BASEMAN, A. G., BROWN, R. M., GREEN, A. E., WHEELER, T. M. & LERNER, S. P. 2001. E-cadherin expression predicts clinical outcome in carcinoma in situ of the urinary bladder. *Urology*, 57, 60-5.
- SHIBATA, H., TOYAMA, K., SHIOYA, H., ITO, M., HIROTA, M., HASEGAWA, S., MATSUMOTO, H., TAKANO, H., AKIYAMA, T., TOYOSHIMA, K., KANAMARU, R., KANEGAE, Y., SAITO, I., NAKAMURA, Y., SHIBA, K. &

- NODA, T. 1997. Rapid colorectal adenoma formation initiated by conditional targeting of the Apc gene. *Science*, 278, 120-3.
- SHIINA, H., IGAWA, M., SHIGENO, K., TERASHIMA, M., DEGUCHI, M., YAMANAKA, M., RIBEIRO-FILHO, L., KANE, C. J. & DAHIYA, R. 2002. Beta-catenin mutations correlate with over expression of C-myc and cyclin D1 Genes in bladder cancer. *J.Urol.*, 168, 2220-2226.
- SHIINA, H., IGAWA, M., URAKAMI, S., SHIGENO, K., YONEDA, T., TERASHIMA, M., DEGUCHI, M., RIBEIRO-FILHO, L. & DAHIYA, R. 2001. Alterations of beta- and gamma-catenin in N-butyl-N-(4-hydroxybutyl)nitrosamine-induced murine bladder cancer. *Cancer Res.*, 61, 7101-7109.
- SHIMAZUI, T., SCHALKEN, J. A., GIROLDI, L. A., JANSEN, C. F., AKAZA, H., KOISO, K., DEBRUYNE, F. M. & BRINGUIER, P. P. 1996. Prognostic value of cadherin-associated molecules (alpha-, beta-, and gamma-catenins and p120cas) in bladder tumors. *Cancer Res.*, 56, 4154-4158.
- SIBLEY, K., CUTHBERT-HEAVENS, D. & KNOWLES, M. A. 2001a. Loss of heterozygosity at 4p16.3 and mutation of FGFR3 in transitional cell carcinoma. *Oncogene*, 20, 686-691.
- SIBLEY, K., STERN, P. & KNOWLES, M. A. 2001b. Frequency of fibroblast growth factor receptor 3 mutations in sporadic tumours. *Oncogene*, 20, 4416-4418.
- SLATON, J. W., KARASHIMA, T., PERROTTE, P., INOUE, K., KIM, S. J., IZAWA, J., KEDAR, D., MCCONKEY, D. J., MILLIKAN, R., SWEENEY, P., YOSHIKAWA, C., SHUIN, T. & DINNEY, C. P. 2001. Treatment with low-dose interferon-alpha restores the balance between matrix metalloproteinase-9 and E-cadherin expression in human transitional cell carcinoma of the bladder. *Clin Cancer Res*, 7, 2840-53.
- SOLOWAY, M. S. 1977. Intravesical and systemic chemotherapy of murine bladder cancer. *Cancer Res*, 37, 2918-29.
- SPRUCK, C. H., 3RD, OHNESEIT, P. F., GONZALEZ-ZULUETA, M., ESRIG, D., MIYAO, N., TSAI, Y. C., LERNER, S. P., SCHMUTTE, C., YANG, A. S., COTE, R. & ET AL. 1994. Two molecular pathways to transitional cell carcinoma of the bladder. *Cancer Res*, 54, 784-8.
- SPRUCK, C. H., 3RD, RIDEOUT, W. M., 3RD, OLUMI, A. F., OHNESEIT, P. F., YANG, A. S., TSAI, Y. C., NICHOLS, P. W., HORN, T., HERMANN, G. G., STEVEN, K. & ET AL. 1993. Distinct pattern of p53 mutations in bladder cancer: relationship to tobacco usage. *Cancer Res*, 53, 1162-6.
- STEIN, J. P., GINSBERG, D. A., GROSSFELD, G. D., CHATTERJEE, S. J., ESRIG, D., DICKINSON, M. G., GROSHEN, S., TAYLOR, C. R., JONES, P. A., SKINNER, D. G. & COTE, R. J. 1998. Effect of p21WAF1/CIP1 expression on tumor progression in bladder cancer. *J Natl Cancer Inst*, 90, 1072-9.
- STEINMAUS, C. M., NUNEZ, S. & SMITH, A. H. 2000. Diet and bladder cancer: a meta-analysis of six dietary variables. *Am J Epidemiol*, 151, 693-702.
- STOEHR, R., KRIEG, R. C., KNUECHEL, R., HOFSTAEDTER, F., PILARSKY, C., ZAAK, D., SCHMITT, R. & HARTMANN, A. 2002. No evidence for involvement of beta-catenin and APC in urothelial carcinomas. *Int.J.Oncol.*, 20, 905-911.
- SU, L. K., KINZLER, K. W., VOGELSTEIN, B., PREISINGER, A. C., MOSER, A. R., LUONGO, C., GOULD, K. A. & DOVE, W. F. 1992. MULTIPLE INTESTINAL NEOPLASIA CAUSED BY A MUTATION IN THE MURINE HOMOLOG OF THE APC GENE. *Science*, 256, 668-670.

- SUMMERHAYES, I. C. & FRANKS, L. M. 1979. Effects of donor age on neoplastic transformation of adult mouse bladder epithelium in vitro. *J Natl Cancer Inst*, 62, 1017-23.
- TAKATA, M. & SAIDA, T. 2006. Genetic alterations in melanocytic tumors. *J Dermatol Sci*, 43, 1-10.
- TANAKA, M., GEE, J. R., DE LA CERDA, J., ROSSER, C. J., ZHOU, J. H., BENEDICT, W. F. & GROSSMAN, H. B. 2003. Noninvasive detection of bladder cancer in an orthotopic murine model with green fluorescence protein cytology. *J Urol*, 170, 975-8.
- TANAKA, M., KOUL, D., DAVIES, M. A., LIEBERT, M., STECK, P. A. & GROSSMAN, H. B. 2000. MMAC1/PTEN inhibits cell growth and induces chemosensitivity to doxorubicin in human bladder cancer cells. *Oncogene*, 19, 5406-5412.
- TENG, D. H., HU, R., LIN, H., DAVIS, T., ILIEV, D., FRYE, C., SWEDLUND, B., HANSEN, K. L., VINSON, V. L., GUMPPER, K. L., ELLIS, L., EL-NAGGAR, A., FRAZIER, M., JASSER, S., LANGFORD, L. A., LEE, J., MILLS, G. B., PERSHOUSE, M. A., POLLACK, R. E., TORNOS, C., TRONCOSO, P., YUNG, W. K., FUJII, G., BERSON, A., STECK, P. A. & ET AL. 1997. MMAC1/PTEN mutations in primary tumor specimens and tumor cell lines. *Cancer Res*, 57, 5221-5.
- TRAVIS, L. B., CURTIS, R. E., GLIMELIUS, B., HOLOWATY, E. J., VAN LEEUWEN, F. E., LYNCH, C. F., HAGENBEEK, A., STOVALL, M., BANKS, P. M., ADAMI, J. & ET AL. 1995. Bladder and kidney cancer following cyclophosphamide therapy for non-Hodgkin's lymphoma. *J Natl Cancer Inst*, 87, 524-30.
- TSURUTA, H., KISHIMOTO, H., SASAKI, T., HORIE, Y., NATSUI, M., SHIBATA, Y., HAMADA, K., YAJIMA, N., KAWAHARA, K., SASAKI, M., TSUCHIYA, N., ENOMOTO, K., MAK, T. W., NAKANO, T., HABUCHI, T. & SUZUKI, A. 2006. Hyperplasia and carcinomas in Pten-deficient mice and reduced PTEN protein in human bladder cancer patients. *Cancer Res.*, 66, 8389-8396.
- UCHIDA, T., WADA, C., ISHIDA, H., EGAWA, S., AO, T., YOKOYAMA, E. & KOSHIBA, K. 1995. Infrequent involvement of mutations on neurofibromatosis type 1, H-ras, K-ras and N-ras in urothelial tumors. *Urol.Int.*, 55, 63-67.
- URAKAMI, S., SHIINA, H., ENOKIDA, H., KAWAKAMI, T., KAWAMOTO, K., HIRATA, H., TANAKA, Y., KIKUNO, N., NAKAGAWA, M., IGAWA, M. & DAHIYA, R. 2006a. Combination analysis of hypermethylated Wnt-antagonist family genes as a novel epigenetic biomarker panel for bladder cancer detection. *Clin.Cancer Res.*, 12, 2109-2116.
- URAKAMI, S., SHIINA, H., ENOKIDA, H., KAWAKAMI, T., TOKIZANE, T., OGISHIMA, T., TANAKA, Y., LI, L. C., RIBEIRO-FILHO, L. A., TERASHIMA, M., KIKUNO, N., ADACHI, H., YONEDA, T., KISHI, H., SHIGENO, K., KONETY, B. R., IGAWA, M. & DAHIYA, R. 2006b. Epigenetic inactivation of Wnt inhibitory factor-1 plays an important role in bladder cancer through aberrant canonical Wnt/beta-catenin signaling pathway. *Clin.Cancer Res.*, 12, 383-391.
- VAGELI, D., KIARIS, H., DELAKAS, D., ANEZINIS, P., CRANIDIS, A. & SPANDIDOS, D. A. 1996. Transcriptional activation of H-ras, K-ras and N-ras proto-oncogenes in human bladder tumors. *Cancer Lett.*, 107, 241-247.
- VAIDYA, A., SOLOWAY, M. S., HAWKE, C., TIGUERT, R. & CIVANTOS, F. 2001. De novo muscle invasive bladder cancer: is there a change in trend? *J Urol*, 165, 47-50; discussion 50.
- VAN RHIJN, B. W., LURKIN, I., RADVANYI, F., KIRKELS, W. J., VAN DER KWAST, T. H. & ZWARTHOFF, E. C. 2001. The fibroblast growth factor receptor 3 (FGFR3)

- mutation is a strong indicator of superficial bladder cancer with low recurrence rate. *Cancer Res.*, 61, 1265-1268.
- VAN RHIJN, B. W., VAN DER KWAST, T. H., VIS, A. N., KIRKELS, W. J., BOEVE, E. R., JOBSIS, A. C. & ZWARTHOFF, E. C. 2004. FGFR3 and P53 characterize alternative genetic pathways in the pathogenesis of urothelial cell carcinoma. *Cancer Res.*, 64, 1911-1914.
- VANDEWETERING, M., CAVALLO, R., DOOIJES, D., VANBEEST, M., VANES, J., LOUREIRO, J., YPMA, A., HURSH, D., JONES, T., BEJSOVEC, A., PEIFER, M., MORTIN, M. & CLEVERS, H. 1997. Armadillo coactivates transcription driven by the product of the Drosophila segment polarity gene dTCF. *Cell*, 88, 789-799.
- VIHINEN, P. & KAHARI, V. M. 2002. Matrix metalloproteinases in cancer: prognostic markers and therapeutic targets. *Int J Cancer*, 99, 157-66.
- WADA, Y., GOTOH, A., SHIRAKAWA, T., HAMADA, K. & KAMIDONO, S. 2001. Gene therapy for bladder cancer using adenoviral vector. *Mol Urol*, 5, 47-52.
- WAGNER, U., SAUTER, G., MOCH, H., NOVOTNA, H., EPPER, R., MIHATSCH, M. J. & WALDMAN, F. M. 1995. Patterns of p53, erbB-2, and EGF-r expression in premalignant lesions of the urinary bladder. *Hum Pathol*, 26, 970-8.
- WALKER, B. E. 1960. Renewal of cell populations in the female mouse. *Am J Anat*, 107, 95-105.
- WEISS, R. H. 2003. P21 (Waf1/Cip1) as a therapeutic target in breast and other cancers. *Cancer Cell*, 4, 425-429.
- WEISSLEDER, R. 2002. Scaling down imaging: molecular mapping of cancer in mice. *Nat.Rev.Cancer*, 2, 11-18.
- WIELENGA, V. J. M., SMITS, R., KORINEK, V., SMIT, L., KIELMAN, M., FODDE, R., CLEVERS, H. & PALS, S. T. 1999. Expression of CD44 in Apc and Tcf mutant mice implies regulation by the WNT pathway. *American Journal of Pathology*, 154, 515-523.
- WILLIAMS, P. D., LEE, J. K. & THEODORESCU, D. 2008. Molecular credentialing of rodent bladder carcinogenesis models. *Neoplasia*, 10, 838-46.
- WILLIAMS, S. G. & STEIN, J. P. 2004. Molecular pathways in bladder cancer. *Urol Res*, 32, 373-85.
- WOENCKHAUS, M., KLEIN-HITPASS, L., GREPMEIER, U., MERK, J., PFEIFER, M., WILD, P., BETTSTETTER, M., WUENSCH, P., BLASZYK, H., HARTMANN, A., HOFSTAEDTER, F. & DIETMAIER, W. 2006. Smoking and cancer-related gene expression in bronchial epithelium and non-small-cell lung cancers. *J Pathol*, 210, 192-204.
- WU, X., OBATA, T., KHAN, Q., HIGHSHAW, R. A., DE VERE, W. R. & SWEENEY, C. 2004. The phosphatidylinositol-3 kinase pathway regulates bladder cancer cell invasion. *BJU.Int.*, 93, 143-150.
- WU, X. R. 2005. Urothelial tumorigenesis: a tale of divergent pathways. *Nat Rev Cancer*, 5, 713-25.
- WU, X. R., KONG, X. P., PELLICER, A., KREIBICH, G. & SUN, T. T. 2009. Uroplakins in urothelial biology, function, and disease. *Kidney Int*, 75, 1153-65.
- YANAGAWA, S. I., VANLEEUEWEN, F., WODARZ, A., KLINGENSMITH, J. & NUSSE, R. 1995. THE DISHEVELLED PROTEIN IS MODIFIED BY WINGLESS SIGNALING IN DROSOPHILA. *Genes & Development*, 9, 1087-1097.
- YE, D. W., ZHENG, J. F., QIAN, S. X. & MA, Y. J. 1993. Correlation between the expression of oncogenes ras and c-erbB-2 and the biological behavior of bladder tumors. *Urol Res*, 21, 39-43.

- YOO, L. I., LIU, D. W., LE VU, S., BRONSON, R. T., WU, H. & YUAN, J. 2006. Pten deficiency activates distinct downstream signaling pathways in a tissue-specific manner. *Cancer Res.*, 66, 1929-1939.
- YOU, L., HE, B., XU, Z., UEMATSU, K., MAZIERES, J., FUJII, N., MIKAMI, I., REGUART, N., MCINTOSH, J. K., KASHANI-SABET, M., MCCORMICK, F. & JABLONS, D. M. 2004. An anti-Wnt-2 monoclonal antibody induces apoptosis in malignant melanoma cells and inhibits tumor growth. *Cancer Res*, 64, 5385-9.
- ZHANG, X., MA, X., ZHU, Q. G., LI, L. C., CHEN, Z. & YE, Z. Q. 2003. Association between a C/A single nucleotide polymorphism of the E-cadherin gene promoter and transitional cell carcinoma of the bladder. *J Urol*, 170, 1379-82.
- ZHANG, Z. T., PAK, J., HUANG, H. Y., SHAPIRO, E., SUN, T. T., PELLICER, A. & WU, X. R. 2001. Role of Ha-ras activation in superficial papillary pathway of urothelial tumor formation. *Oncogene*, 20, 1973-1980.
- ZHANG, Z. T., PAK, J., SHAPIRO, E., SUN, T. T. & WU, X. R. 1999. Urothelium-specific expression of an oncogene in transgenic mice induced the formation of carcinoma in situ and invasive transitional cell carcinoma. *Cancer Res.*, 59, 3512-3517.
- ZHOU, M. I., FOY, R. L., CHITALIA, V. C., ZHAO, J., PANCHENKO, M. V., WANG, H. M. & COHEN, H. T. 2005. Jade-1, a candidate renal tumor suppressor that promotes apoptosis. *Proceedings of the National Academy of Sciences of the United States of America*, 102, 11035-11040.
- ZHU, X., KANAI, Y., SAITO, A., KONDO, Y. & HIROHASHI, S. 2000. Aberrant expression of beta-catenin and mutation of exon 3 of the beta-catenin gene in renal and urothelial carcinomas. *Pathol.Int.*, 50, 945-952.

Appendix 1: Funding Sources



Mr R C McKail
The Beatson Institute for Cancer Research
Garscube Estate
Switchback Road
Bearsden
Glasgow
G61 1BD

Our Ref: G0802141

06/04/2009

ID: 89716

PROTECT - RESEARCH

Dear Mr McKail,

I am pleased to confirm that the Council has approved the award of a Fellowship to your Research Organisation as detailed overleaf. Standard 'Terms and Conditions of MRC FEC Fellowships' apply to this award

(<http://www.mrc.ac.uk/Fundingopportunities/Applicanthandbook/Fellowships/Termsconditions/index.htm>) and both the Research Organisation and the Fellow must read and accept these before the award can be activated. In particular, may I draw your attention to the sections on the general responsibilities of the Research Organisation, and, where applicable, to responsibilities relating to clinicians and MRC's commitment to the Concordat on Contract Research Staff Careers.

If the award of this MRC fellowship is contingent upon local research ethics committee (LREC) approval (or multi-centre research ethics committee [MREC] approval) for the research proposed in the original application and reviewed by the Council, it is the responsibility of the Fellow and the Research Organisation to ensure that LREC/MREC approval is granted for this study and adhered to, and that no research requiring LREC/MREC approval is initiated until it has been granted. The Fellow/ Research Organisation must be prepared to furnish the MRC with a copy of the LREC/MREC approval, and any correspondence with the LREC/MREC, if requested by the Council.

When an award of an MRC Fellowship is contingent upon the fellow obtaining a PhD, DPhil or MD prior to commencement, this must be achieved within the published take-up dates for the scheme. Failure to do so will cause the offer of a fellowship to be withdrawn.

Documentary evidence of the qualification must be sent to Awards Management Team prior to starting the fellowship.

There are a number of enclosures with this letter:

- **Award Details** - this document outlines the details of the Fellowship award and the agreed level of the award;
- **Award Acceptance letter** – this should be completed and returned (to your named contact overleaf) **within 14 days** to the MRC AMT Payments Team at Head Office, 20 Park Crescent, London W1B 1AL; failure to do so may result in the award being withdrawn;

- **Starting Certificate** – this should be completed and returned to the AMT Payments Team once documentary evidence is available that expenditure has been incurred on the fellowship (i.e. staff have actually started working on this research). Receipt of the starting certificate will initiate payments to your Research Organisation. No payments can be made until a starting certificate has been received. Submission of the starting certificate is required within 42 days of the actual start date. Failure to do so will result in delayed payments to your Research Organisation;
- **Payment Schedule** - this details the profiled payments which will be made over the lifetime of the award; (this may differ slightly from the Indexed Cash Limited total on the award letter – the award letter has the correct total). The account start date on the payment schedule may be later than the from the proposed start date on the award letter.

Research funds may be used, without reference to Council in such a way that is considered to be most beneficial to the research. Transferring of funds is only permitted between the Directly Incurred and Exceptions headings. Under no circumstances may Directly Incurred costs and Exceptions Funds be used to meet the costs of any other project headings.

Please note that the enclosed payment schedule has been indexed and therefore includes an element for anticipated future pay awards and inflationary increases and is made on the understanding that its value will not be increased except in the exceptional circumstances stated below. Any funds unspent at the end of a fellowship will be retained/reclaimed by the Council.

MRC will not supplement a Fellowship financially once it has been awarded apart from circumstances of maternity/paternity or sick leave where a member of staff has been replaced by a temporary staff member in their absence and an extra salary has therefore been paid. Any additional funds will only be paid at the end of the Fellowship. They should be claimed as Exceptional Items within the Final Statement of Expenditure.

The Fellow may start the fellowship within the take-up period for this scheme without reference to the MRC. This award will lapse if the research has not started within the take-up period and the MRC has not received the completed starting certificate.

It is the responsibility of the Research Organisation to ensure that a final statement of expenditure and final scientific report are submitted, together, to AMT within 90 days of the end date of the Fellowship. The final payment will be withheld until the final report and final statement of expenditure are received and failure to submit or delayed submission of the reports may result in financial sanctions. Final report forms are available from our website (<http://www.mrc.ac.uk/Fundingopportunities/Applicanthandbook/Grantcalls/Finalreport/index.htm>)

Any publicity material associated with the research undertaken as part of this award should be discussed with the MRC Press Office prior to issue.

If you have any queries please do not hesitate to contact us. All queries relating to this award should be addressed to robert.goodall@headoffice.mrc.ac.uk.

Yours sincerely

Ann Holt (Mrs)
 Team Manager
 Awards Management Team
 direct line 020 7670 5462
 direct fax 020 7636 3427
 email robert.goodall@headoffice.mrc.ac.uk

PROTECT - RESEARCH

AWARD DETAILS

G file ref :	G0802141	ID no.:	89716
Fellow :	Dr I Ahmad		
Research Organisation :	The Beatson Institute for Cancer Research		
Department :	The Beatson Institute for Cancer Research		
Supervisor/sponsor:	Professor H Leung		
Head of Department:	Professor K Vousden		
Title of project (in months):	Synergistic interactions between PTEN, HER and Sprouty signalling in prostate cancer		
Tenure:	30		
Proposed Start Date :	01/04/2009	End Date :	30/09/2011
Type of award :	Clinical Training Fellowship		
Co-Funder(s):			

GRANT VALUE					
Funds Awarded	FEC Award		MRC Contribution		% FEC
	Net	Indexed	Net	Indexed	
Directly Incurred					
Investigators	110,001	119,088	110,001	119,088	100%
Staff	0	0	0	0	100%
Travel and Subsistence	6,000	6,527	6,000	6,527	100%
Other Costs	100,972	109,860	100,972	109,860	100%
Equipment	0	0	0	0	100%
Overseas / Industrial Training	0	0	0	0	100%
Sub-total	216,973	235,475	216,973	235,475	
Directly Allocated					
Investigators	0	0	0	0	80%
Staff	0	0	0	0	80%
Estates Costs	0	0	0	0	80%
Other Directly Allocated	0	0	0	0	80%
Sub-total	0	0	0	0	
Indirect Costs					
Indirect Costs	0	0	0	0	80%
Sub-total	0	0	0	0	
Exceptions					
Staff	0	0	0	0	100%
Other Costs	0	0	0	0	100%
Equipment	0	0	0	0	100%
Travel and Subsistence	0	0	0	0	100%
Overseas \ Industrial Training	0	0	0	0	100%
Sub-total	0	0	0	0	
Total	216,973	235,475	216,973	235,475	

STAFF				
Summary	Authorised FEC net	RC contribution net	Number of months	Number of posts
Research	0	0	0	0
Technician	0	0	0	0
Other	0	0	0	0
Investigator	110,001	110,001	30	1
Total	110,001	110,001	30	1

Staff Details (Directly Incurred / Exceptions)								
Name (if known)	Grade	Spine Point	Date of Scale	Number of Months	Number of Posts	Start Date	Increment Date	Staff Effort (FTE)
Dr I Ahmad	CRF	4		30	1		01.08.09	30 months is 100%

Staff Details (Directly Allocated)						
Role	Number of Months	Start Date	Total Hours	Average Hours /week	Staff Effort (FTE)	Name

Equipment Details		
Description	Expected Delivery Date	Total

PROTECT-RESEARCH



Our Reference: G0802141

DATE: 06/04/2009

Agreement ID: 89716

AWARD ACCEPTANCE LETTER – PROTECT-RESEARCH

The **Research Organisation**, The Beatson Institute for Cancer Research and the **Fellow**, Dr I Ahmad, agree to:

- undertake the responsibilities outlined in, and comply with, the MRC grants and fellowships terms and conditions (as detailed on the MRC Web site) (<http://www.mrc.ac.uk/Fundingopportunities/Applicanthandbook/Fellowships/Termsconditions/index.htm>);
- accept the awarded fellowship (as detailed in the accompanying award letter);
- conduct the research, as approved by Council, within the budget awarded and the time frame agreed by Council.

The Research Organisation, The Beatson Institute for Cancer Research, agrees to accommodate the research detailed in the award letter. For research involving NHS Patients, their organs, tissues or data, and which falls within the scope of the UK Health departments Research Governance Framework for Health and Social Care, **The Research Organisation**, The Beatson Institute for Cancer Research, agrees to accept responsibility for ensuring that:-

- The **research undertaken by the organisation itself under this award is managed and monitored** so as to comply with (a) MRC Terms and Conditions, including MRC's ethical and good practice guidance, and (b) the requirements of the Employing Organisation set out in the Research Governance Framework;
- The **agreements and systems are in place with NHS Trusts and other Partner Organisations, including Commercial Organisations**, so as to comply with MRC Terms and Conditions and the Research Governance Framework;
- It, or a Partner Organisation, **systematically documents regulatory and ethical submissions, approvals and amendments** and that it and they **will not permit work that requires such approvals to be undertaken without the necessary approvals**.

Research Organisation The Beatson Institute for Cancer Research

Name Signature Date

Position within the Research Organisation

Fellow

Name Dr I Ahmad Signature Date

Please return a copy of this signed acceptance letter **within 14 days** to Robert Goodall at MRC Awards Management Team, Head Office, 20 Park Crescent, London, W1B 1AL.

Note: This document is to confirm the acceptance of MRC's Terms and Conditions relating to this Award – **it DOES NOT activate payments to the Research Organisation.**

Payments to the Research Organisation will only be activated by completion and submission of the Starting Certificate. This must be submitted within 42 days of the actual start date.

G0802141

PROTECT-RESEARCH



FELLOW STARTING CERTIFICATE – PROTECT-RESEARCH

This Certificate should be completed and signed by the Finance Officer as soon as documentary evidence is available that the first member of staff has started work. This will be the actual start date of the grant. The completed certificate should then be returned, within 42 days of the above date, to the AMT Payments Team, Medical Research Council, 20 Park Crescent, London W1B 1AL, who will then initiate payments to the Research Organisation via the payment profiling system.

If the award is not activated within six months of the proposed start date detailed on the award letter, the award will lapse.

MRC REFERENCE G NUMBER	G0802141
AGREEMENT ID (5 digit number)	89716
RESEARCH ORGANISATION	The Beatson Institute for Cancer Researc
AWARD HOLDER(s)	Dr I Ahmad
RESEARCH TITLE	Synergistic interactions between PTEN, HER and Sprouty signalling in prostate cancer
PROPOSED START DATE	01/04/2009
ACTUAL START DATE (date on which the first member of staff starts work).	Please insert actual start date
RESEARCH ORGANISATION REFERENCE	
NAME (BLOCK CAPITALS)	
POSITION HELD	
DATE	
SIGNATURE OF RESEARCH ORGANISATION FINANCE OFFICER (CONTACT EMAIL ADDRESS /TELEPHONE NUMBER)	

PAYMENTS

When the **ACTUAL START DATE** (as specified by the Research Organisation below) is entered on our payments system, the profile of quarterly payments issued within the award letter will be adjusted, if necessary, to reflect the actual start date and payments will commence. If a grant starts during the first half of a quarter then a payment will be made at the end of that quarter. If a grant starts during the second half of a quarter then the first payment will be made at the end of the following quarter.

FOR RESEARCH COUNCILS USE

Date recorded:

Signature:

Date

Appendix 2: Home Office Licenses

Re-issue



Home Office

No. PIL 60/11372

ANIMALS (SCIENTIFIC PROCEDURES) ACT 1986

PERSONAL LICENCE

to

carry out regulated procedures on living animals.

In pursuance of the powers vested in him by the above Act, the Secretary of State hereby licenses

Mr I Ahmad
Beatson Institute of Cancer Research
University of Glasgow
Garscube Estate, Switchback Road
Glasgow
G61 1BD

to apply the techniques specified in column a of paragraph 15 of the attached Schedule to the kinds of animals in column b of the same paragraph at the place or places specified in paragraph 14 of this Schedule, subject to the restrictions and provisions contained in the Act, and subject also to the limitations and conditions contained in this licence and to such other conditions as the Secretary of State may from time to time prescribe.

This licence shall be in force until revoked by the Secretary of State and shall be periodically reviewed by him.

Home Office
2 Marsham Street
London SW1P 4DF

For the Secretary
of State



19 August 2009

NB. This licence does not authorise the licensee to perform any of the procedures specified in it unless they are carried out in the course of a project for which there is a project licence in force under the Act.

Re-issue



No. PIL 60/11372
19 August 2009

Personal Licence - Additional Conditions

This licence is subject to the following additional conditions -

The performance of all techniques in the attached schedule shall be given the appropriate level of supervision by the project licence holder or an experienced personal licensee deputed by him/her for such time as may be needed to achieve competence.



PERSONAL LICENCE APPLICATION FORM

FOR OFFICE

ONLY

15 NOV 2007

<p>13</p> <p>Is this application submitted with a project licence application?</p>	<p style="text-align: center;">YES NO</p> <p style="text-align: center;"> <input type="checkbox"/> <input checked="" type="checkbox"/> </p> <p style="text-align: center;">(tick appropriate box)</p>	
<p>a. If YES please state the TITLE of the project</p>		<p style="text-align: center;">PPL No</p>
<p>b. If NO for which projects (identify if possible) or area of work do you require this licence? (First-time applicants must specify the project(s) on which they intend to work)</p>	<p>60/3530</p>	<p style="text-align: center;">PPL No</p>

<p>14</p> <p>a. Title and address (including department) of the designated establishment at which you wish your licence to be primarily available to carry out procedures on living animals subject to the Act.</p>	<p>TITLE University of Glasgow</p> <hr/> <p>ADDRESS CRC Beatson Institute Garscube Estate, Switchback Road, Glasgow.</p> <hr/> <p>SUPERVISOR. Owen Sansom</p>	<p>PRIMARY AVAILABILITY</p>
<p>b. If you intend to carry out procedures at more than one establishment please give the names and addresses of the additional establishments and supervisors' names if applicable (Please attach an additional sheet if necessary)</p>	<p>ADDRESS.</p> <hr/> <p>SUPERVISOR</p> <hr/> <p>TITLE</p> <hr/> <p>ADDRESS</p> <hr/> <p>SUPERVISOR</p>	<p>CODE</p> <hr/> <p>DEPT</p> <hr/> <p>CODE</p> <hr/> <p>DEPT</p>
<p>c. If you intend to carry out procedures at a place other than a designated establishment, please specify the location</p>		<p>CODE</p>

15 The techniques and animals for which you seek authority (Please continue on additional sheets if necessary)			FOR OFFICE USE ONLY
Number	a. Technique Please use codes S and NS respectively to indicate surgical and non-surgical techniques	b. Animal(s)	c. Anaesthesia Please use codes given in note
1.	Administration of substances by the following routes: a) oral by gavage or admixture with food and or water b) intravenous injection c) subcutaneous injection d) intraperitoneal injection e) intramuscular injection (NS).	Mouse Mouse Mouse Mouse Mouse Mouse	AA AA, AB, AC AA, AB, AC AA, AB, AC AA, AB, AC
2.	Withdrawal of blood by superficial venepuncture/ venesection (NS).	Mouse	AA, AB, AC
3.	Tissue Biopsy (NS).	Mouse	AA
4.	Breeding and Maintenance of genetically altered animals (NS).	Mouse	AA
5.	Induction and maintenance of general anaesthesia using volatile and/or injectable agents suitable for the species and duration of the procedure (NS).	Mouse	AA AB AC
6.	Variation in the composition of the diet and the quantity and/or availability of food or water (NS).	Mouse	AA
7.	Exposure to ionising radiation (NS).	Mouse	AA

RECEIVED
15 NOV 2007

PERSONAL LICENCE APPLICATION FORM

15 The techniques and animals for which you seek authority (Please continue on additional sheets if necessary)			FOR OFFICE USE ONLY
Number	a. Technique Please use codes S and NS respectively to indicate surgical and non-surgical techniques	b. Animal(s)	c. Anaesthesia Please use codes given in note
8	Injection in to the prostate after laparotomy S	Mouse	AB
9	Bilateral surgical orchidectomy S	Mouse	AB

RECEIVED
12/15/2009